DESIGN, DEVELOPMENT AND EVALUATION OF SHAPE TRANSFORMABLE FOUR-DIMENSIONAL PRINTED POLYMER-TEXTILE COMPOSITES

TIN CHUN CHEUNG

PhD

The Hong Kong Polytechnic University

2025

The Hong Kong Polytechnic University

School of Fashion and Textiles

Design, Development and Evaluation of Shape Transformable Four-dimensional Printed Polymer-textile Composites

Tin Chun Cheung

A thesis submitted in partial fulfilment of the requirements for the Degree of Doctor of Philosophy

August 2024

CERTIFICATE OF ORGINALITY

I hereby declare that this thesis is my own work and that, to the best of my knowledge and belief, it reproduces no material previously published or written, nor material that has been accepted for the award of any other degree or diploma, except where due acknowledgement has been made in the text.

_____ (signed)

<u>Tin Chun Cheung</u> (Name of student)

TO MY MOTHER AND FATHER

ABSTRACT

Four-dimensional printed materials refer to a class of advanced materials that can shape transform with the help of a stimuli. Such materials have broad applications including fashion and textiles products, biomedical devices, manufacturing, robotics and more. However, the results have historically been inconsistent and often shows poor performance, difficult to fully reverse/re-program and lacking in mechanical performance (i.e., bursting, tensile strength), thus making it incompatible for wearables and other textile products that requires consistent performance. Such factors have hindered its application into real-world functional products.

In recent years, practitioners have investigated the extrusion of polymers onto textile substrates resulting in polymer-textile composites (PTCs). Its novelty lies in its high customisability and distinct mechanical properties owing to its multi-material composition. Whilst considerable progress has been made in both four-dimensional printing and PTC fields independently, existing theoretical and practical contributions in 4D printed polymer-textile composites (4DP PTC) research are insufficient and limited.

This research bridges together four-dimensional printing and PTC techniques with aims to establish a systematic process involving the design, development, and evaluation of 4DP PTCs via using fused deposition modelling and polyurethane-based materials with textile substrates. The direct extrusion of thermo-responsive shape-memory polymers (SMPs) onto textile substrates opens new opportunities to develop highly adaptable and customisable textile-based materials for wearables and other textile products. 4DP PTC's versatility also promises new opportunities for embedding programmability with high customizability into non-electronic textile materials. Based on design experiments and lab-based work, a systematic design and

decision-making process for 4DP PTC is also established. In this study, 4DP PTC prototypes are designed, produced, and analysed using this concept model.

The theoretical and practical investigation of 4DP PTCs is systematised into three phases. Phase one identifies the design requirements, challenges, materials, and technologies forming a conceptual model for 4DP PTCs. Phase two offers room for creative exploration of PTCs and 4DP PTCs design, development, and evaluation via practice-led and lab-based experiments. Subsequently, the quantitative data deriving from the experiments are comparatively analysed to identify variables that influence 4DP PTC's mechanical properties and shape performance. This analysis help refine the design process and optimise material performance. In the final phase, 4DP PTCs were implemented in various textile-based design applications based on the findings from prior theoretical and practical experiments.

This study delivers a new design approach for 4DP materials that bridges together two key disciplines. It results in efficient shape transformative materials that possess unique mechanical properties. Moreover, under this design concept, the creative potential of additive technologies is demonstrated, and furthers works on adaptable and shape transformative material design. The results highlight the aesthetics and functionality of 4DP PTCs and how its innate shape fixity properties can be exploited to develop highly adaptable and re-shapable textile-based products ranging from personal protective equipment to textile-based lampshade. In contrast with the current literature's use of shape recovery primarily as an eye-catching novelty, it further demonstrates the possibility for post-manufacture customisation by utilising 4DP PTC's innate shape fixity. Overall, this study provides a solid foundation for the further development and application of 4DP PTCs into practical and functional textile products.

LIST OF PUBLICATIONS

Journal Publications

Cheung, T. C., Choi, S. Y., & Jiang, S. X. (2024). Manipulation of Printing Direction and Temperature on the Mechanical and Shape Performance of Thermoplastic Polyurethane 4D-printed Polymer-textile Composites. Journal of Applied Polymer Science. (Accepted/In Press)

Cheung, T. C., Choi, S. Y., & Jiang, S. X. (2024). Influence of Thermoplastic Polyurethane and Elastomer Polymers on Self-folding Behaviour of 4D-printed Polymer-textile Composites. Additive Manufacturing.

Cheung, T. C., & Choi, S. Y. (2023). Evaluation of the Influence of Three-dimensional Printing Conditions on Peel Resistance and Surface Roughness of Flexible Polymer-textile Composites. Textiles Research Journal.

Conference Papers and Oral Presentations

Cheung, T. C., & Choi, S. Y. (2023). Evaluating the Transformation Performance of 4D-printed polymer-Textile Composites. International Textile and Apparel Association 2023 Conference, Baltimore, Maryland, USA.

Cheung, T. C., & Choi, S. Y. (2022). Comparative Study on the Adhesion Strength of 3D-printed Flex Polymers on Natural and Synthetic Textiles Substrates. International Textile and Apparel Association 2022 Conference, Denver, Colorado, USA.

Cheung, T. C., & Choi, S. Y. (2022). Characterizing the Adhesion Strength of 3D-printed Flex on Knit/Woven Textiles via T-peel tests. ITC-KSCT Joint Symposium Programme, ICCT 2022 Conference.

Awards and Achievements

Cheung, T. C., & Choi, S. Y. (2023). Distinction Award for "*Comparative Study on the Adhesion Strength of 3D-printed Flex Polymers on Natural and Synthetic Textiles Substrates*". International Textile and Apparel Association Conference, 2022.

ACKNOWLEDGEMENTS

Table of Contents

LIST OF FIGURES

LIST OF TABLES

LIST OF ABBREVIATIONS

2D   Two-dimensional

3D   Three-dimensional

3DP   3D printed

4D   Four-dimensional

4DP   4D printed

4DP PTC   4D printed polymer-textile composite

AM   Additive manufacturing

CAD   Computer-aided design

CAM   Computer-aided manufacturing

CTE   Coefficient of thermal expansion

DMA   Dynamic mechanical analysis

FDM   Fused deposition modelling

FFF   Fused filament fabrication

HY   Hysteresis

PTC   Polymer-textile composite

PU   Polyurethane

RI   Bending rigidity

SD   Standard deviation

SEM   Scanning electron microscope

SM   Shape memory

SMA   Shape memory alloy

SME   Shape memory effect

SMM   Shape memory materials

SMP   Shape memory polymer

TPE   Thermoplastic elastomer

TPU   Thermoplastic polyurethane

Chapter 1: INTRODUCTION

1.1 Background of research

The global pandemic of 2019 has shifted the interest of designers towards adaptable, modular, and multi-functional design. The transformable nature of adaptable products befits our increasingly multidimensional life. WGSN has likewise forecasted adaptable design as one of the key fashion and design trends of the next decade (WGSN, 2022). However, the static nature of existing materials has impeded its assimilation into the mainstream (Khamkar, 2021). Designers and researchers have made attempts to create active materials and designs via construction methods (Tibbits, 2014), physical mechanisms (Vivanco et al., 2020; Yamamura & Iwase, 2021), or with complex devices (Wang & Li, 2021). Though results have historically been poor, limited in scale and extent of change, and inconsistent in performance (Koch et al., 2021).

Four-dimensional printing or 4D printing, is an advanced 3D printing method that has made it possible to develop materials that can alter its shape, size, or texture with a programmable stimuli (Schmelzeisen et al., 2018). This additional fourth dimension refers to the time in which a surface and/or structural transformation takes place after the printing process (Schmelzeisen et al., 2018). 4DP components can transform between static to dynamic structures with some materials allowing programming to different dynamic structures (Biswas et al., 2021). Both static and dynamic states can be exploited to design products. The fundamental difference between 4DP and other programmable matter is that additive processes are used which can assist in developing mass-produced personalised parts with high repeatability ranging from garments to robotics (Schmelzeisen et al., 2018).

Existing studies have highlighted 4DP material's advantages i.e., high customisability, does not require electronic activation, and design and manufacturing process is sustainable and environmentally conscious (Cheung et al., 2024; Loh, 2021; Naficy et al., 2017; Tibbits et al., 2014). Scholars have elaborated on the future applications of 4DP materials if the technology and materials further developed. The possibilities include programmable products that adapt and respond to different environments and scenarios, garments that can self-assemble and disassemble, textiles that can be re-shaped, architectural features that adapt to fluctuating environments and products that can be flat packed for easier shipping and storage that can later be activated back to its designed shape (Cheung et al., 2024; Koch et al., 2021; Loh, 2021; Schmelzeisen et al., 2018; Tanaka et al., 2020; Tibbits et al., 2014).

Fused deposition modelling/fused filament fabrication (FDM/FFF) are prevalently used in 4D printing due to its flexibility and wide variety of material compatibility (Ngo et al., 2018). Common 4D printing practices include pre-stressed fabric and multi-material printing methods. In the pre-stressed fabric method, polymers i.e., polylactic acids are extruded atop a pre-stretched fabric resulting in a PTC. The transformation occurs when the mechanical energy stored in the pre-stretched fabric is released (Cheung et al., 2024; Koch et al., 2021). However, no further shape transformation can take place once released from the printing bed as such materials are single-driven and non-reversible (Cheung et al., 2024). The latter method often involves the printing of polymers that are embedded with a shape-memory element that reacts to a stimulus. Such materials can be programmed to alternative forms post manufacture, though often have poor mechanical and dimensional performance due to the polymer's properties.

Whilst considerable progress has been made in 4DP fields existing contributions are fragmented and limited. They often lack exploration into identifying appropriate material

combinations or processing requirements to fine-tune 4DP materials for specific applications. Existing frameworks are also mostly theoretically based and lacks practical experimentation that evaluates the material's mechanical or shape performance (Biswas et al., 2021; Schmelzeisen et al., 2018; Tanaka et al., 2020). This is often caused by the miniature sized prototypes limited by the types of materials used resulting in difficulty trying to evaluate under ISO, ASTM and other industry standards which have strict testing requirements.

In existing 4D printing studies, the extrusion of SMPs onto textile surfaces has not been scientifically investigated due to difficulty finding the appropriate material combinations to achieve adhesion and shape performance (Koch et al., 2021). This is particularly the case for wearables or textile-based products that require the materials to have specific mechanical properties whilst also achieving adequate adhesion with the SMPs. Fortunately, in recent years, a thermo-responsive polyurethane-based SMP was developed for FDM/FFF printers. This SMP enjoys greater dimensional accuracy and has excellent covalent bond with synthetic substrates in comparison with existing SMPs. It has also opened up new opportunities to create novel 4DP composites, first coined as 4DP PTC (Cheung et al., 2024). Though, there is a lack of literature associated with this subject.

4DP PTC's shape transformation capabilities and fine-tuneable mechanical properties shows potentials for a diverse range of uses. Through using FDM/FFF technologies, different polymers can be extruded on various substrates to create composite materials with unique surface aesthetics, specific mechanical performance, and reduce material and production time. However, existing contributions in 4DP PTCs are fragmented and largely theoretically based calling for further investigation. In this study, a systematic 4DP PTC theory, a novel design principle, 4D printing processes, and scientific evaluation methods are proposed to investigate

the creative potential of shape transformable materials via FDM/FFF technologies to produce 4DP PTC. The exploration of 4DP PTC is built on the understanding of the integration of textiles in textile-based wearables and product design as well as the use of FDM/FFF extrusion technologies.

1.2 Study aim and objectives

The research scope is categorised into four main research areas shown in **Figure 1-1**. **Table 1-1** denotes themes that were investigated to determine the appropriate additive manufacturing (AM) techniques, materials, and evaluation methods for thermo-responsive 4DP PTCs.
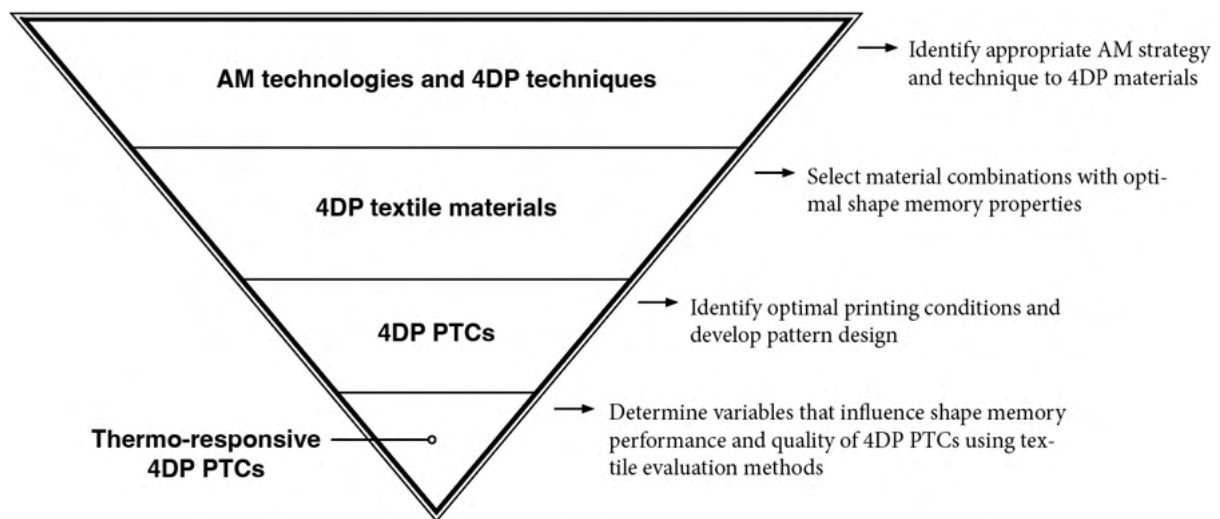
Figure 1-1 Research scope

Table 1-1Research scope and topics

Research Scope	Topics
i) AM technologies and 4D printing techniques	o *Background and concept* o *Design framework* o *Technologies, processes, materials, and evaluation methods* o *Potential applications* o *Research gaps, difficulties, and limitations*
ii) 4DP materials	o *Propose and develop a 4DP design framework* o *Conduct experiments with various material combinations (polymer and textiles) to identify optimal combinations for developing 4DP PTC*

	o	*2D/3D evaluation: methods and tools to evaluate material performance i.e., T-peel tests, tensile strength tests, surface quality evaluation, bursting strength tests, and cross-sectional microscopic analysis*
	o	*Framework validation*
iii) 4DP PTCs	o	*Design and develop 4DP PTC patterns with optimal shape recovery and flexibility*
	o	*4D evaluation: material flexibility evaluation, thermomechanical programming, and shape recovery experiments*
iv) Thermo-responsive 4DP PTCs	o	*Determine factors that influence shape performance of 4DP PTCs*
	o	*Methods and tools to optimise 4DP PTC performance*
	o	*Shape recovery results and discussions*
	o	*Potential applications*

1.3 Research methods
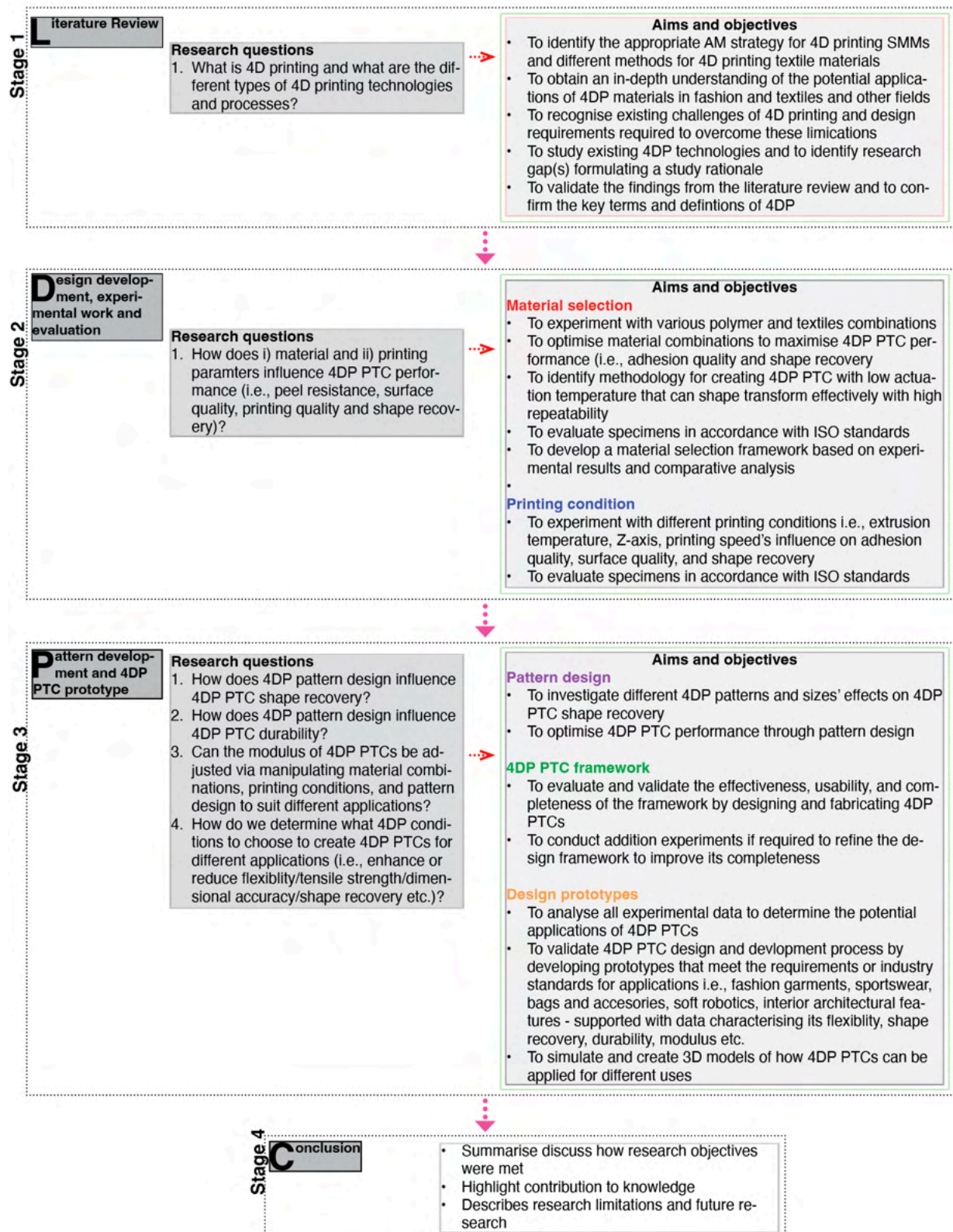
Figure 1-2 Research methods and stages

A mixed-methods approach (practice-led and data-driven) was used to collect and analyse quantitative and qualitative data (**Figure 1-1**, **1-2**, and **Table 1-2**). Content analysis was used to examine qualitative data (literature review), while comparative methods were used to compare and identify quantitative data trends and anomalies. In-depth exploration of related 4D printing and Additive Manufacturing processes, technologies, and methods were conducted using qualitative methods which led to the generation of ideas and identification of research gaps (Stage 1) (**Figure 1-2**).

Stage 2 commenced with design experiments which explored 4DP variables (i.e., material selection and printing conditions) on 4DP PTC performance resulting in quantitative data. The data generated through these tests and was analysed comparatively to ascertain the ideal conditions for fabricating optimal performing specimens. Similarly in stage 3, quantitative data was also acquired by examining the effects of 4DP pattern designs with various geometry, scale, and profile on 4DP PTC performance. Comparative data analysis and Nielsen's Heuristic Analysis (Kohli & Krishnamurti, 1987) or Heuristic Design Analysis was also used to evaluate the effectiveness, usability, and completeness of the 4DP PTC design framework. Through Heuristic Analysis, design decisions can be made based on trial and error through design experiments and additional experiments may be introduced to refine the design cycle for specific applications. **Table 1-3** illustrates the fundamental design heuristics (modified to be applicable for textiles design).

Table 1-2 Research methodology

Research method	Advantages	Disadvantages
Content analysis	Attain a clear understanding of the data including qualitative and quantitative analysis.	Time-consuming process
Design experiments	Engaged in practice-based and practice-led research leading to new knowledge through making.	Based on experience of researcher
Textile evaluation	Evaluation of specimens in accordance with an industry recognised standard for textiles.	Different countries use different standards and some evaluation methods have not yet been standardised
Comparative analysis	Data-led method that deals with facts which helps us identify the correlations and differences between items. Comparison can also be used to discover new hypotheses and to build theories.	Focuses on a single cause only
Nielsen's Heuristic Analysis or Heuristic Design Analysis (Kohli & Krishnamurti, 1987)	Fix usability issues during design process through trial and error by providing an overview of a product/service usability without relying on user testing/feedback	Can be subjective and bias

Table 1-3 Fundamental design heuristics (modified to be applicable for textile design)

Understanding	Action	Feedback
Consistency: Consistent and standardised design language – set of design principles that provides a feeling of continuity	**User freedom and flexibility:** Easy and efficient to use for users of different experience levels	**Show status:** Immediate feedback on what is going on
Familiar design language: Matches existing real-world design concepts and conventions	**Recognition:** Making designs easier to use by providing visible options to minimise user's memory load	**Error prevention:** Eliminate error-prone conditions through design development
Aesthetic and functional design: Streamlined to only shows relevant information while diminishing anything irrelevant		**Help and documentation:** Easy guide instructions

1.4 Significance and value
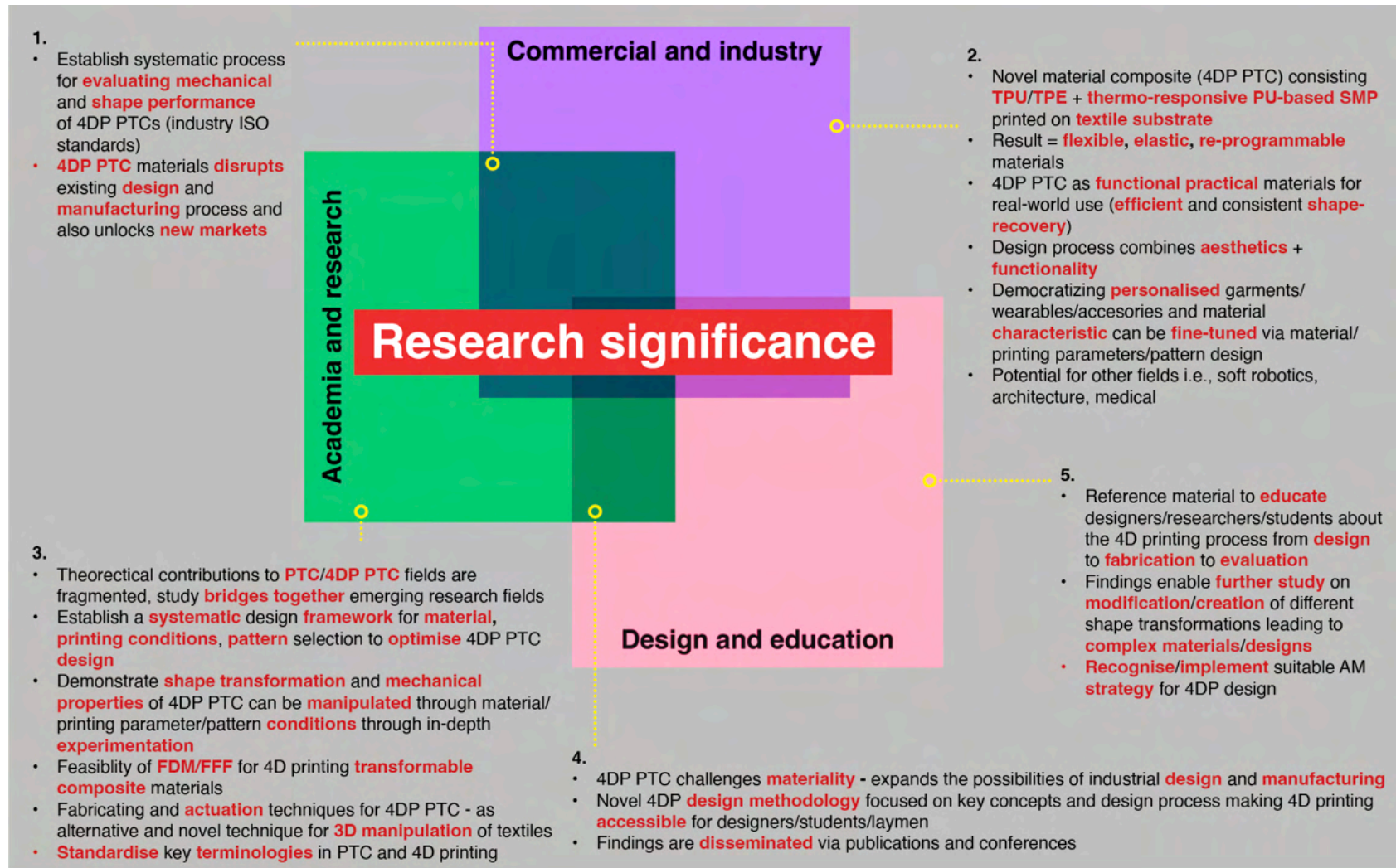
Figure 1-3 Research significance

This study will help bring attention and contribute new knowledge to 4D printing fields (specifically 4DP PTCs) with a focus on designing, developing, and evaluating highly customisable, functional, and practical textiles (**Figure 1-3**). 4DP PTCs' unique features pertains to fields not limited to fashion and textiles, medical applications, soft robotics, architecture, and other applications that require customisable and flexible active materials. Through multidisciplinary research methods, a systematic design, development, and evaluation process was established for 4DP PTCs. This study outcome provides important knowledge for individuals including i) academic researchers, ii) practitioners in engineering and fashion and textile manufacturing industries, iii) students perusing engineering and design degrees. This study serves as groundwork for further 4DP research and the development of new applications. Moreover, this study serves as a reference to assist practitioners when developing 4DP PTCs. The detailed contributions are specified below:

1. This study bridges together two emerging AM research fields (4D printing and PTCs) where existing theoretical contributions are fragmented and limited. The assemblage of information derived from the critical reviews will enable the understanding of key concepts, the design process of 4D printing from design, manufacturing, to evaluation, and to discussing further capabilities and potentials.

2. There is an inherent lack of a general classification for 4DP PTC in 4D printing research, and this study will help define and elucidate key terminologies in 4D printing fields through publishing in peer-reviewed articles to instigate researchers and practitioners to adopt a standard vocabulary.

3. This study contributes to new theoretical and practical knowledge by identifying in 4D printing and PTC development that impede the design and development of 4DP PTCs. Through study of 4D printing and PTC, the commonalities and differences are recognised. This enables designers and researchers to identify and implement suitable AM strategies for a specific design or application.

4. Existing 4DP textile research relies on experimental characterisation methods which lacks consistency and reliability. In this study, textile evaluation methods in accordance with industry standards (ISO) are used for assessing textile performance which vastly improves the reliability of the results. And under rigorous mechanical behaviour testing, the correlation between the mechanical performance and shape performance of 4DP PTCs can be determined.

5. This research also examines three key variables which can affect 4DP PTC's performance i.e., material combinations, printing parameters, and pattern design. The results will provide a fundamental understanding of how a different combination of conditions can influence mechanical and shape performance. Designers and researchers can use the results as a reference to modify and create different shape transformations or to develop further complex patterns through manipulating these variables.

6. This study aims to expand the purpose and demonstrate the potentials of multi-material 4DP processes to develop new design process and highly personalised textiles and garments through direct to digital manufacturing disrupting the current design and manufacturing process of garments and wearables The results of this study will be

disseminated through journal article publications, conference presentations, exhibitions, and academic books.

7. Commercially, 4DP PTC will provide i) a new design solution that is both wearable and practical for real-world use, ii) using 4DP technology to create a novel textile that can be actively manipulated by the user to different arrangements for aesthetic and functional purposes, iii) high customisability during the design process democratizing personalised garments and adoption of 3D scanning, v) mechanical properties of the 4DP textiles can be personalised during the design process through various conditions i.e., polymer type, printing parameters, structure design and fabric selection, iv) offers high shape-recovery with repetitive results and gives users the ability to re-configure the textiles to a new shape or form through a straightforward process (no need for complex devices to stimulate actuation).

1.5 Outline of thesis

This thesis consists of seven chapters and is organised into three principal research phases: 1) review and exploration, 2) experimentation - design, development, evaluation, and revision and 3) conclusion.

1) *Review and exploration:*

This phase consists of the collecting and reviewing of theoretical knowledge from sources i.e., scientific articles, academic books, and discussions from academics, practitioners, and other industry experts in AM, 4D printing, and PTC fields.

Chapter 1. *Introduction*

Chapter one presents a general introduction to the study, the aims and objectives, an organisation of the thesis, various approaches to this research, and different methods implemented to answer the research questions.

Chapter 2. *Literature Review*

Chapter two reviews relevant literature to establish and outline the key concepts of SMMs, its applications, and techniques used to design and synthesise SMMs. In addition, an overview of the technologies, processes, and potentials of using AM as a technology to produce SMMs, different 4D printing methods, and materials are also reviewed. Furthermore, the primary mechanism and shape memory effect (SME) of 4DP materials are also studied. An in-depth analysis on different design and fabrication methods are conducted to examine how these conditions can be fine-tuned to induce different shape transformative behaviours. This chapter concludes by pinpointing existing design obstacles and identifies limitations of 4D printing as a strategy for producing SMMs. Through the literature review, an appropriate strategy is identified which will be used to answer the research questions.

2) *Experimentation - design, development, evaluation, and revision*

Chapters three to six presents the methods, results, discussion of results, and ends with a conclusion.

Chapter 3. *Methodology*

Chapter three proposes a 4DP PTC design process which considers the diverse aspects of 4D material design. The basic requirements of 4DP materials and appropriate evaluation methods are identified. Subsequently a systematic model for developing 4DP PTCs was designed to

characterise and evaluate 4DP materials quantitatively in accordance with ISO textile industry standards, resulting in the development of functional SMMs for real-world applications. This chapter also outlines the fundamental practical and theoretical knowledge towards the development of thermo-responsive 4DP PTCs, including material selection process, design preparation, experimental procedure, 2D/3D/4D evaluation methods, pattern design and development, and prototyping. In addition, the functional and aesthetics considerations of 4DP PTCs will also be described. The chapter concludes with a summary of the methods used.

Chapter 4. *Polymer-textile Composite Development*

In chapter four, the design process of PTCs using FFF/FDM processes with various flexible filaments printed on different textile substrates is highlighted. Through these experiments, the optimal material and printing conditions are identified which assists in the enhancement of the peel resistance between substrates and improvement on the surface quality of the printed polymers. Such experiments reveal the combability of the materials and is used as the groundwork for further experiments in Chapter five. Detailed descriptions of the whole design and fabrication process are presented in this chapter. In addition, the experiments, equipment, testing standards, and observations made during the tests are also described in detail. The top performing material combinations and printing parameters in terms of peel resistance and surface quality are applied for the development of 4DP PTCs in Chapter five. The chapter ends with a summary of the experiments and results.

Chapter 5. *4DP Shape-Transformative Thermo-Responsive Polymer-textile Composite*

The top-performing material combinations and printing parameters discovered in Chapter Four were applied for the 4D printing of 4DP PTCs. This chapter outlines the design, fabrication, evaluation, programming, and characterisation of thermo-responsive shape-transformative

4DP PTCs. Equipment, methods, and testing standards are also described in detail. The further analysis of material, printing parameters, and pattern design are investigated as conditions which can facilitate the producing of different types of shape-transformative behaviours in 4DP PTCs. The findings present the three conditions as fundamental influences on the performance of 4DP PTCs. And through manipulating these conditions, 4D printing researchers and practitioners can produce designs or materials with specific mechanical properties and relevant shape transformations which will result in the development of new applications and further active material development. The chapter concludes with a summary of the 4DP PTC development and evaluation process.

Chapter 6. *Comparative Analysis of Results*

Chapter six corroborated all the experimental results for examination. Through comparatively analysing all findings alongside one and other, several objectives are realised: 1) determine optimal performing material combinations, 2) identify which conditions (i.e., material, printing parameter, and pattern design) has the strongest influence on the performance of 4DP PTCs, 3) determine whether the material's mechanical property influences the shape recovery of 4DP PTCs, and 4) decide what conditions to manipulate when developing 4DP PTCs for different applications. The findings presented the opportunity to establish a systematic 4DP PTC design model for 4DP PTCs. A visual mapping system was created to facilitate the development of 4DP PTCs aimed at 4D printing designers and researchers. The user-friendly mapping system serves as a guide for practitioners of 4D printing to fine-tune the mechanical properties or shape recovery performance of their designs to target specific applications or to produce specified results. Via a combining different condition together, unique mechanical behaviours can also be achieved.

3) *Conclusion*

Chapter 7. *Conclusion*

Chapter seven summarises the research work by describing how the research aims and objectives were met. The chapter also highlights the knowledge contributions made. Furthermore, it also outlines the limitations of research and suggests further potentials in 4DP PTC research.

Chapter 2: LITERATURE REVIEW

2.1 Introduction

In this chapter, a review of existing approaches towards the design and manufacturing of shape-memory materials and four-dimensional printed materials will be discussed. Part one will review the application of smart (shape-memory alloys and polymers) materials for designing active textile materials with shape recovery capabilities. The following part will probe into the basic principles of additive manufacturing (AM) technologies, its practice in fashion and textile fields, and how it can be used to develop novel materials that overcomes the limitations of existing active textiles. Moreover, advanced three-dimensional printing techniques and its materials (polymer composites/polymer-textile composites), four-dimensional printing design process (design structures, techniques), an outline the principles of two, three, and four-dimensional fashion and textiles, and methods of evaluation (mechanical and shape performance) will also be discussed. And to conclude this chapter, a summary and identification of research gaps and limitations of existing research will help formulate the research questions of this study.

2.2 Shape-memory materials

Existing shape memory material (SMM) are limited by the availability of pre-existing materials and manufacturing processes. To enhance the transformation capabilities of such materials, new types of materials and processes will need to be developed. Related research has demonstrated the shape transformation capabilities of SMMs and if used appropriately can add aesthetic value to a garment (further discussed in this chapter). SMMs i.e., shape-memory alloys (SMAs), shape-memory polymers (SMPs) and shape-memory ceramics (SMC), hydrogels, memory foams and liquid crystal elastomers (LCE) have been extensively studied

in various disciplines. Such materials respond to environmental stimuli and can be identified as smart or intelligent materials (Gandhi & Thompson, 1992). Particularly in fashion and textile fields, designers and practitioners have recognised the potentials of SMA/SMPs owing to their ability to return from a deformed state to their permanent shape when triggered by an external stimulus. Through using SMMs, researchers have been able to develop smart textiles with shape transformation capabilities (Schwarz & Kovačević, 2017). However, the studying of such materials is fragmented and limited. Further investigation is essential to bridge these emerging research fields together which will enable practitioners to identify and implement appropriate strategies for developing specific materials and applications.

SMMs have been vastly investigated in a wide range of disciplines including biomedical, engineering and aircraft industries. Fashion & textiles practitioners have likewise recognised the potentials of smart materials. SMA and SMPs are commonly used by practitioners to develop shape transformable materials and products. SMAs and common SMPs i.e., PLA and ethylene-vinyl acetate (EVA) are used in favour over hydrogels/LCE because they can be programmed whereas the latter are non-programmable or unable to produce stable shape memory effects (Zhao et al., 2015). In the past decades, there has been immense interest in developing wearables with shape-memory characteristics. SMPs were first developed in the 1980s in Japan as materials that have dual-shape capability (Tadaki et al., 1988). When exposed to an appropriate stimulus (i.e., heat, stress, pH) it returns to a predefined form (Behl & Lendlein, 2007). For example, a temperature responsive SMM assumes a structural change at a "transitional" temperature (Tr). This transformation in shape triggered by temperature is identified as a thermally induced shape memory effect (Gandhi & Thompson, 1992).

Figure 2-1 Transformation process in SMA (Christopher, 2018)

Shape-memory alloys

Common SMAs i.e., nickel-titanium and copper-aluminium-nickel-alloys often come in wired or thin sheeted forms, are some of the foremost smart materials used in SME textile research. SMAs can return (remember) to its initial form after deformation via a shift in temperature or through other stimuli. This shape changing phenomenon is caused by the two crystal structures in SMAs (austenite/martensite phases) – austenite phase (high temperature) and martensite phase (low temperature) (**Figure 2-1**). This transition between the phases triggers the memory behaviour in SMAs (Otsuka & Ren, 1999).

Shape-memory polymers

Alike SMAs that changes form when triggered by a stimuli, SMPs also possess the ability to shape recover to a permanent form after contact with a stimulus (i.e., heat, pH, moisture) (Mather et al., 2009). Common SMPs for manufacturing smart textiles include shape memory polyurethane, hydrogels and poly-hydroxyproline (Thakur, 2017). The structure of SMPs is

altered when heated above glass transition temperature (T_g) meanwhile deformation can be fixed below T_g, and once heated above T_g, the original programmed shape is recovered.

2.2.1 SMA and SMP comparison

Both SMAs and SMPs have been extensively studied in fashion & textiles research, however both materials have their advantages & limitations and are thus chosen according to the requirements of the application (**Table 2-1.**). Based upon existing literature, it was identified that SMPs are more favoured due to its mechanical properties particularly for wearable applications (Kong & Xiao, 2016; Strzelec et al., 2020). In comparison with SMAs, SMPs possesses numerous advantages including lower costs, broader range of temperature, easy to process, low stressed required for deformation (easy to re-configure material), high plasticity (easy to mould), highly flexible programming, lower density than alloys, biocompatible & biodegradable and capability for elastic deformation (Liu et al., 2007). Moreover, SMPs are often biocompatible and biodegradable making it a cost-effective solution for commercial products. With its superior mechanical properties (rigid to soft rubber) compared with SMAs, SMPs have been able to revolutionise how products are designed & manufactured and have broadened the purpose of SMP materials i.e., smart fabrics that can regulate heat/moisture, intelligent wearable devices, anti-crease textiles and other advance textiles (Gök et al., 2015). In addition, SMPs highly tuneable properties, lightweight and adjustable modulus parallel to conventional fabrics engender the possibility to engineer SMPs to textile surfaces to produce polymer-textile composite materials. Furthermore, SMPs can occur in both crystalline (rigid uniform structure) and amorphous (flexible scattered structure) state concurrently within a typical room temperature environment (BritishPlasticsFederation, n.d.) that is easily activated making it more versatile for real-world applications for the development of active wearable textiles with shape transformation capabilities for smarter design.

Table 2-1 Comparison of SMAs and SMPs

SMA	SMP
Pros ■ Faster recovery speed ■ Complete reversal to original shape ■ Better mechanical properties (i.e., stronger, durability) ■ Can be woven, knitted, stitched into textiles (Lagoudas, 2008) **Cons** ■ Must be programmed before embedding into textile structure due to high programming temperatures ■ Expensive ■ Heavier compared with polymers (Lagoudas, 2008) *Applications – require stronger/quicker shape-memory recover or garments/materials that require more structure i.e., intimate apparel, assistive garments, interior design*	**Pros** ■ Easy processing conditions (low pressure and temperature compared with SMAs) ■ Low stress required for deformation (MPa) ■ Easy plasticity (easily moulded) ■ Can be used with 3D printing ■ Can be melted into fabrics ■ Lightweight ■ Lower costs ■ Highly transformable shapes (can increase in size a lot more) ■ Complex geometries ■ Good recovery ■ Wider temperature options (lower transitional temperatures) ■ Biodegradable & biocompatible suited for medical applications ■ Can deform elastically ■ Lower density ■ Self-healing properties (Shin et al., 2017) **Cons** ■ Lower tensile strength ■ Slower shape-memory behaviour (Mu et al., 2018) *Applications – dynamic, transformable & lightweight requirements i.e., athleisurewear, sportswear, daily wear (shirts, dresses etc.)*

2.2.2 Application in fashion and textiles

SMMs seen in fashion and textiles research are predominantly moisture sensitive or stimulated by heat with dual-shaped effects (Hu, 2007). Coating, lamination, knitting, and weaving are common approaches towards the integration of SMMs into textile materials (Hu et al., 2012). Existing SMM research have primarily focused on developing functional materials i.e., anti-crease materials (Hu & Lu, 2014), self-adaptable textiles (intimate apparel/compression garments) (Satami, n.d.), and thermal/moisture regulating fabrics (breathable fabrics) (Yao, Ou, Wang, et al., 2015). Such materials have demonstrated its versatility in skin-care, wound-dressing products, soft robotics, on-body actuators, deodorant fabrics, damping fabrics, finishing fabrics and smart energy storage textile applications (Thakur, 2017). In design fields, researchers have investigated the use of SMMs to develop smart textiles that incorporate aesthetics with function. These smart materials can often sense, adapt, and react to its

environment making it suitable for various applications shown in **Figure 2-2** Researchers have demonstrated the feasibility of applying SMA to develop kinetic garments for self-expression (Berzowska & Coelho, 2005), textiles that can pleat itself for various wearables including garments (Leenders, 2011), and for compression and assistive garments (Foo et al., 2019). Other studies have also investigated SMP for garments with practical functions i.e., anti-wrinkle fabrics (Hu & Lu, 2014), sportswear with smart vents that open up to ensure optimal cooling (Nike sphere macro react) (TIME, 2006) and similarly bioLogic (responds to sweat and moisture and opens up to ensure proper ventilation) (Yao, Ou, Cheng, et al., 2015; Yao, Ou, Wang, et al., 2015). In precedent research, SMMs has demonstrated itself as the most advanced and versatile material for developing shape transformative textiles and wearables (multi-functional smart garments) with various shape-changing capabilities not limited to fashion, performance wear, interior design, intimate apparel applications etc.
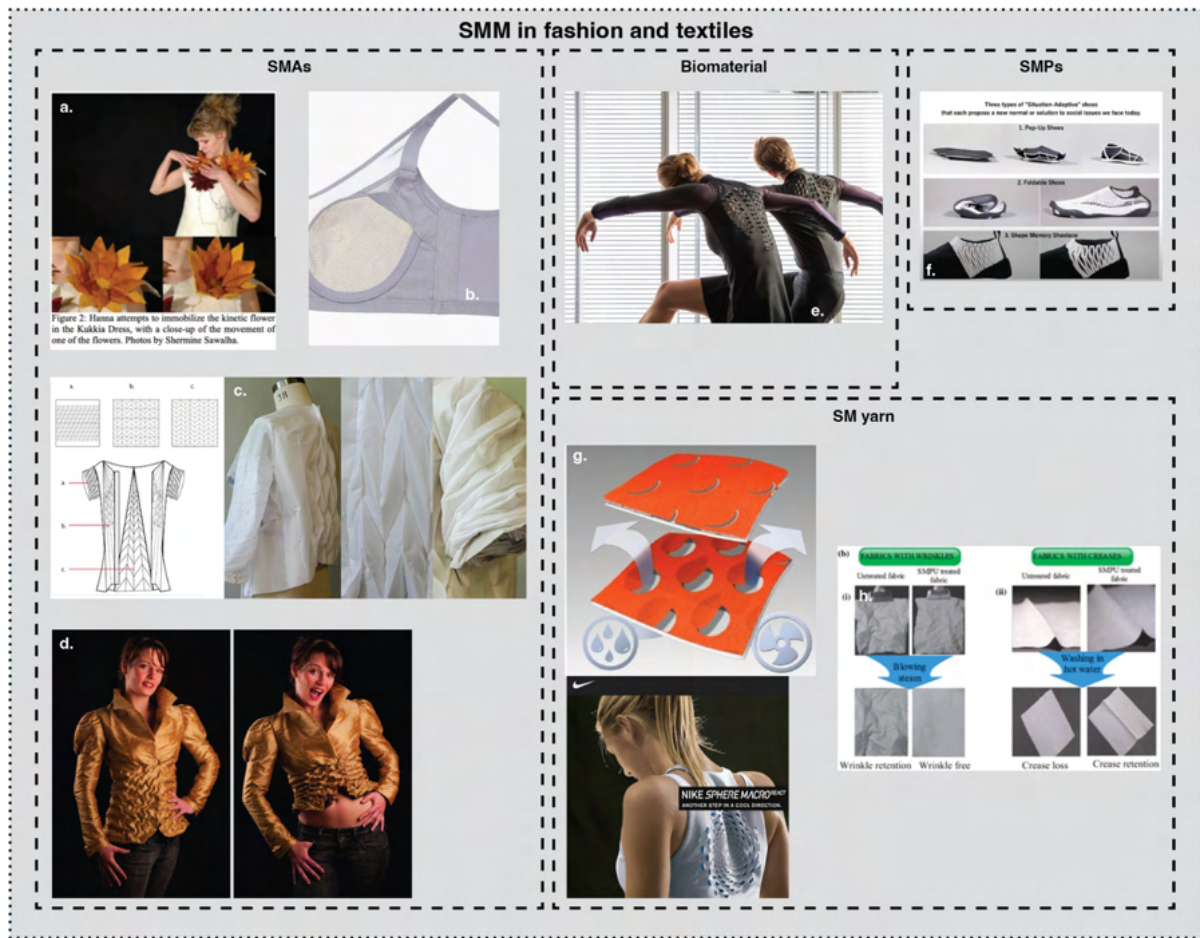
Figure 2-2 SMM in fashion and textiles a. Berzowska and Coelho (2005), b. Satami (n.d.), c. Lin et al. (2015), d. Leenders (2011), e. Yao, Ou, Cheng, et al. (2015), f. Tanaka et al. (2020), g. TIME (2006) and h. Hu and Lu (2014)

2.2.3 Dimensionality of textile materials and manufacturing process

In fashion and textiles, textile materials can be manufactured as two-dimensional (2D), three-dimensional (3D) or four-dimensional (4D) structures through various methods i.e., knitting, weaving, braiding, nonwoven, or with AM processes (3DP) (Chen, 2015). 2D textiles are fabricated on two planes where the weave in 2D textiles are perpendicular and the yarn is fed in two directions – length (x-axis) and width (y-axis) (Chen, 2015). 3D textiles differ in that they are produced with a three planar geometry (x and y-axis with an additional perpendicular weave and additional z-axis feed of yarn creating thickness) (Gokarneshan & Alagirusamy, 2009). Such textiles have widespread use including composite material manufacturing,

performance materials, and technical materials (Paul, 2019). Examples of 3D textile processes include 3D weaving/knitting/braiding/pleating/composites/3DP and auxetic materials which when stretched becomes thicker vertically to the applied force (Grimmelsmann et al., 2016). Smart garments that can transform between 2D to 3D sculptural forms are also by definition 3D fashion (i.e., Issey Miyake's 132.5 collection). Furthermore, 4D textiles are materials that can shape transform over a 4th dimensional element when influenced by a stimulus (Tibbits, 2014). Such textiles are typically manufactured by using 3DP processes with textile materials. Conditions not limited to geometry design, polymer materials and fabrics can be manipulated to achieve different shape transformation effects (Koch et al., 2021). Through reviewing existing definitions of 2D, 3D and 4D, we can summarise these terminologies as follows:

- *Two-dimensional (2D)* – textiles and garments that are manufactured on two planes (x and y-axis) (Chen, 2015)
- *Three-dimensional (3D)* – textiles and garments that are produced with a three planar geometry (x, y, and z-axis) i.e., 3D knitting, woven, pleats, auxetic materials, 3DP composites (Gokarneshan & Alagirusamy, 2009), and smart garments that can transform between 2D to 3D sculptural forms
- *Four-dimensional (4D)* – textiles and garments that were made using 3DP technologies and possess the ability to perform shape transformation over time (time as 4th dimension) (Tibbits, 2014)

2.3 Four-dimensional printing

2.3.1 Introduction

With growing interest in 3D printing (3DP) and 3DP polymer-textile composites (PTCs) (Cheung & Choi, 2022), practitioners have explored the potentials of developing PTCs that

responds to an external stimulus and changes with time (4th dimension). Four-dimensional printing also known as 4D printing is manufactured by means of 3D printing technologies whereby a computer controlled process enables the fabrication of three-dimensional forms through the deposition of materials in layered form (Ngo et al., 2018). 4D materials can be pre-programmed to shape-shift, evolve, adapt, and reconfigure depending on environmental stimulus within a given timeframe (Schmelzeisen et al., 2018) otherwise challenging with conventional sewing, knitting or coating methods. Four-dimensional printed textiles are hybrid composites that consists a minimum of two materials that are combined additively (Sitotaw et al., 2020). Therefore, the fabrics placed onto the build platform becomes the new build surface (Koch et al., 2021). This ability to transform has posed countless possibilities for 4D printing to be applied into designing real-world products including smart garments and active textiles.

2.3.2 3D printing and 4D printing

4D printing was first coined by Tibbits to define programmable materials with the ability to change its physical properties over time (fourth dimension) (Tibbits, 2014; Tibbits et al., 2014). The key difference between 4D printing and other programmable matters is that it uses additive manufacturing (AM) technologies which can efficiently mass-produce personalised components with repetitive results (Schmelzeisen et al., 2018). **Figure 2-3** illustrates the dissimilarities between 3D printing and 4D printing. In 4D printing, the printed objects can transform from a static to a dynamic structure and can repeatedly be re-programmed to a different dynamic structures (Biswas et al., 2021). 4D printing has prompted practitioners to focus on user-centred design thinking to design products that are personalised to the user with the capability to adapt to the differing lifestyles of their target audiences (Tanaka et al., 2020). Though adaptive and personalised wearables and other textile-related products have been extensively studied under other design and manufacturing methods, further improvements are

necessary for these designs to be functional in real-life scenarios and to be truly inclusive (Ayachit & Thakur, 2017; Kars, 2021; Rahman & Gong, 2016; Zaytseva et al., 2021). Precedent 4D printing research has demonstrated its potentials to substitute existing methods through direct digital manufacturing and by developing personalised active materials for application in adaptive and configurable clothing (Guberan, n.d.; Schmelzeisen et al., 2018; Tanaka et al., 2020).
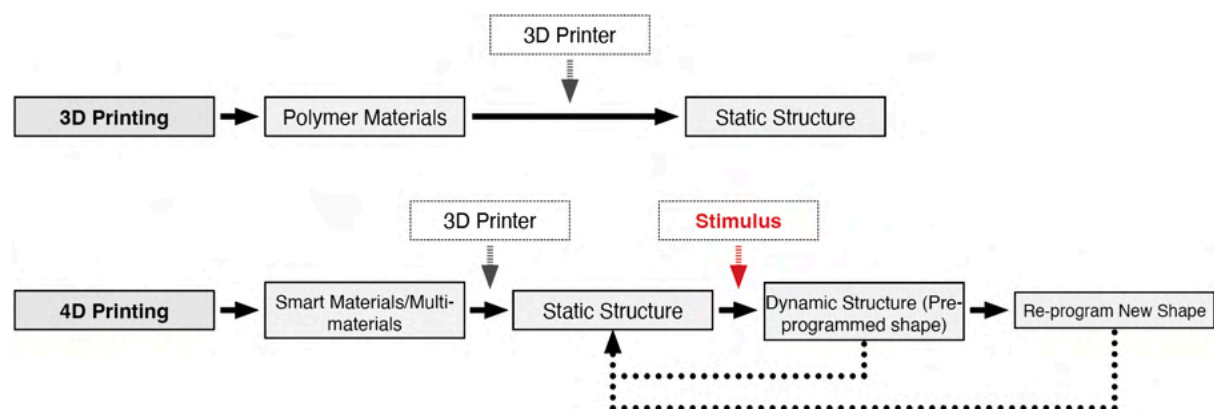
Figure 2-3 Comparison of 3D printing and 4D printing, adapted and modified from (Biswas et al., 2021)

2.3.3 4D printing technologies and processes

Material extrusion processes are currently the most prevalent methods used in the additive manufacturing industry i.e., fused deposition modelling/fused filament fabrication (FDM/FFF) printing (Koch et al., 2021). In comparison with other 3D printing technologies i.e., stereolithography, selective laser sintering, FDM/FFF technologies possess numerous advantages including direct extrusion of polymers on different materials, has a wide range of material compatibility allowing experimentation with different combinations, has relatively fast printing speeds, uses less hazardous filament or pellet materials instead of resins or powders and does not require post-processing curing (Cheung & Choi, 2022; Ngo et al., 2018). With progresses made in AM technologies and materials, the 3D printing process has further

progressed into the development of printing with a fourth-dimension element. 4D printing is an advanced technique that utilises 3D printing technologies but results in materials with the ability to change their physical properties over a time element. The fourth dimension is defined as the time in which a transformation of structural properties might occur after the 3D printing process is completed (Schmelzeisen et al., 2018). Often the change can be triggered by the influence of an external stimulus or from energy stored in the material itself (Tibbits et al., 2014).

In 4D printing's digital manufacturing process, the standard workflow consists of 3D modelling on CAD programs → slicing on slicer software → 3D printing (Lipson & Kurman, 2013). **Figure 2-4** illustrates a design framework for operating 4D printing. In 4D printing, polymers, smart polymers, hydrogels, and biomaterials are typically printed using FDM/FFF processes – materials are chosen based upon its final application (Tanaka et al., 2020). Geometrical pattern design in 4D printing can take inspiration from textile structures, biomimicry, auxetic and origami patterns. And such patterns can offer aesthetic value but more importantly enhance or alter the mechanical properties of the printed material (Kabir et al., 2020b). Furthermore, depending on the materials used for printing, the printed outcome can be stimulated by a stimulus to transform to a pre-configured form. 4D printing research have demonstrated its potentials to be applied in fashion and sportswear, medical-related wearables, product and industrial design, architecture and automobile design (Tanaka et al., 2020).
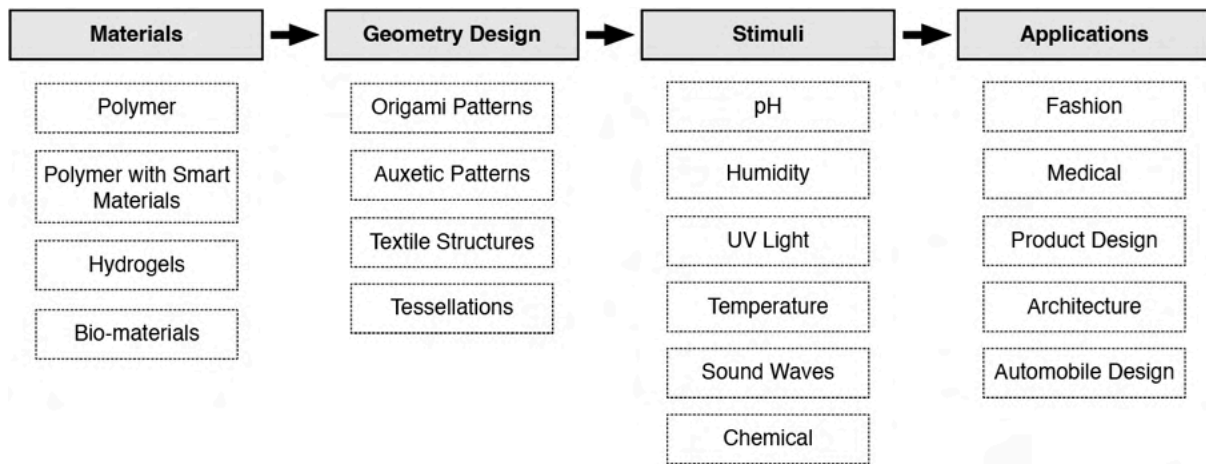
Figure 2-4 4D printing framework adapted and modified from (Tanaka et al., 2020)

2.3.4 4D printing methods

2.3.4.1 pre-stressed fabric 4D printing method

Figure 2-5., illustrates the concept behind using pre-stressed elastic fabrics to achieve shape change. The fabric is initially stretched and secured onto the 3DP platform. The polymer materials are subsequently extruded directly onto the fabric surface producing a polymer-textile composite (PTC). Due to the elastic nature of the pre-stretched fabric, it can store and transmit energy which enables the polymer-textile composite to transform from a 2D to 3D prescribed form when released from the machine (Schmelzeisen et al., 2018). The shape transformation performance of 4DP textiles is affected by factors i.e., i) pattern design and arrangement of polymer layer, ii) thickness of polymer and fabrics, iii) mechanical properties polymers used (shore hardness, elasticity), iv) peel resistance (adhesion between polymer/textile layer) and v) printing parameters (Koch et al., 2021).
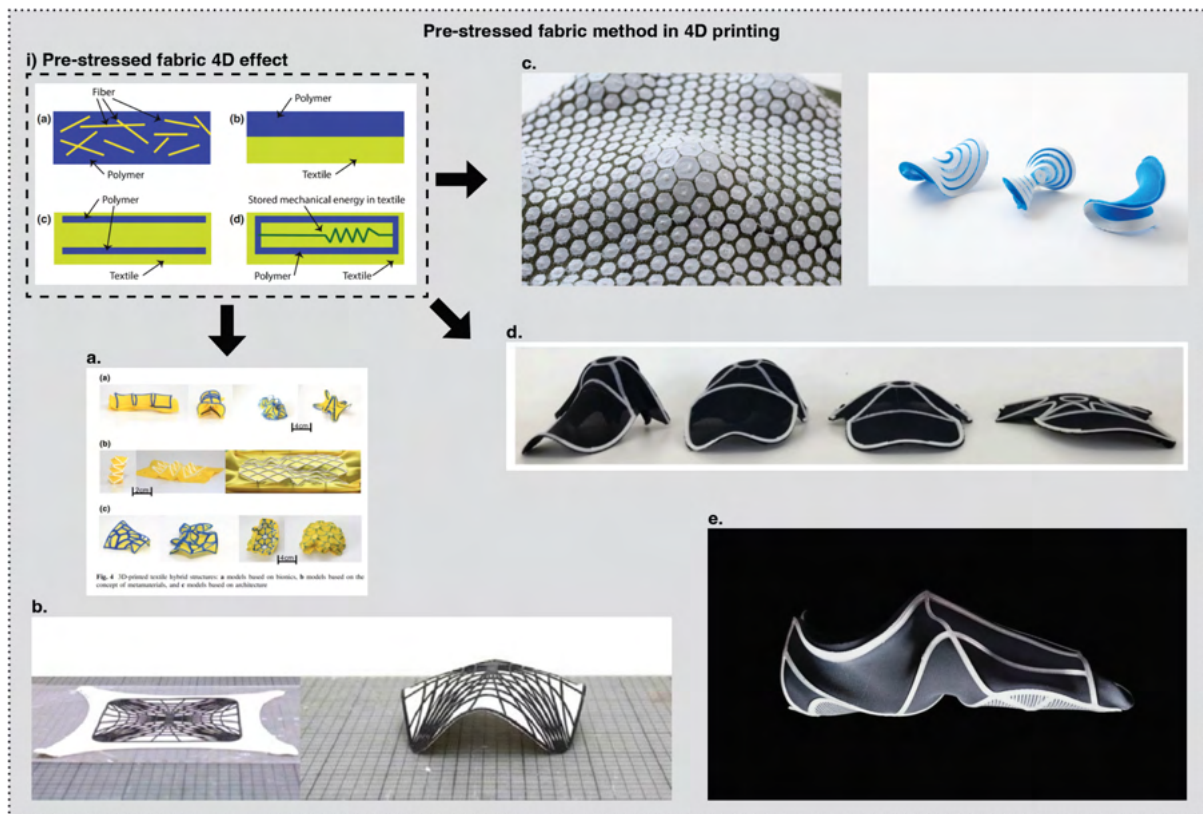
Figure 2-5 Pre-stressed fabric method in 4D printing i) and a. Schmelzeisen et al. (2018), b. Kycia (2022), c. Fields (2018), d. Vivanco et al. (2020), e. Guberan (n.d.)

Various examples of 4D printing using FDM/FFF are shown in **Figure 2-5**., Tibbits from MIT's self-assembly lab explored the production of shoes by printing a 2D shoe pattern at varying layer thickness onto pre-stretched textiles which jumped into a programmed shoe form when released (Guberan, n.d.). Through a combination of pattern design, elastic fabric and Polylactic acid (PLA) polymers, he demonstrated a novel method of shoe production by producing a self-forming shoe form. Schmelzeisen et al. (2018) explored this method into developing hybrid structures inspired by architectural forms, bionics, and meta materials. Fields (2018) furthered this concept by using 3D scanning technologies to develop a pattern for printing. Their aims were to create shape change by utilising the mechanical energy storage and release from elastic fabrics. Other research utilised this concept to digitally simulate anticlastic shapes to predict how 4DP prototypes would transform (Vivanco et al., 2020).

2.3.4.2 multi-material 4D printing method
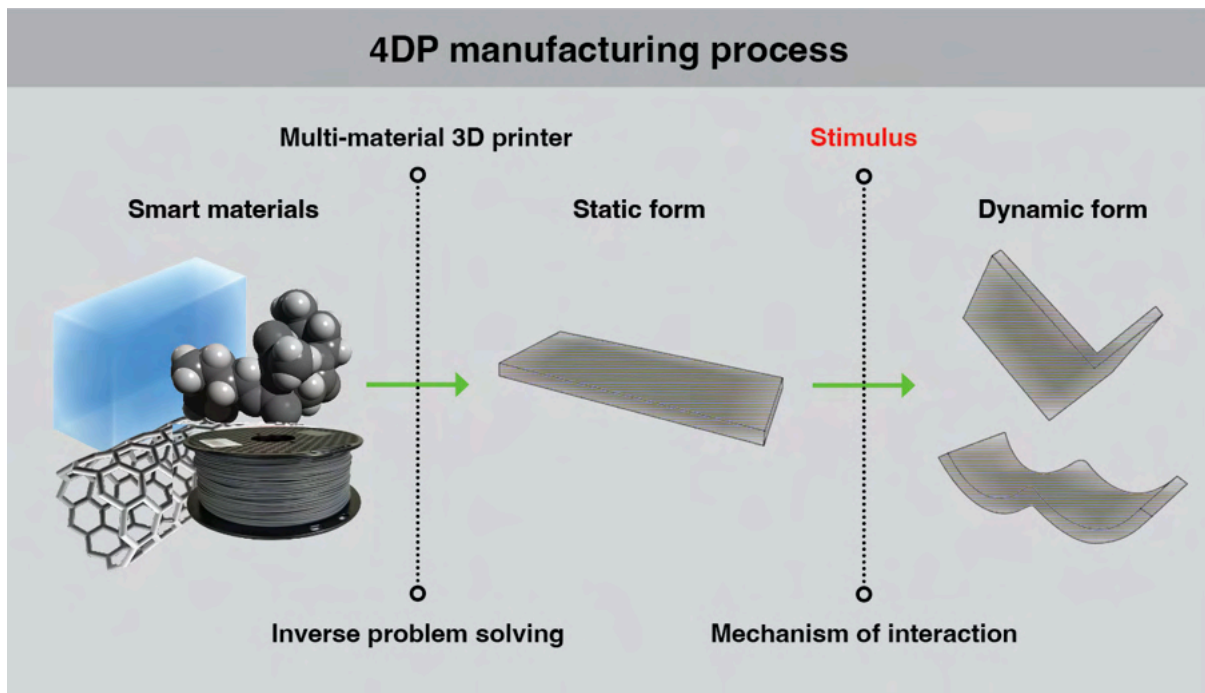
Figure 2-6 4D printing manufacturing process (Cheung et al., 2024)

In multi-material 4D printing, polymers used are often embedded with a SME component that reacts to different stimuli meaning the printed materials can be re-configured to transform its physical properties rather than in pre-stressed fabric methods where the transformation relies purely on the energy of the elastic textiles. The 4DP materials can exist in a static form and when exposed to a stimulus transforms to a pre-programmed dynamic form (**Figure 2-6**). When designing the 4DP materials, inverse problem solving can be used to pre-determine how the material will transform (Biswas et al., 2021; Sydney Gladman et al., 2016). The ability to be re-configured is particularly valuable for creating environmental responsive design (Tanaka et al., 2020). Smart sensing polymers in 4D printing are not limited to pH, humidity (Tibbits, 2014) and temperature (Ge et al., 2016) sensing materials (**Figure 2-7**).
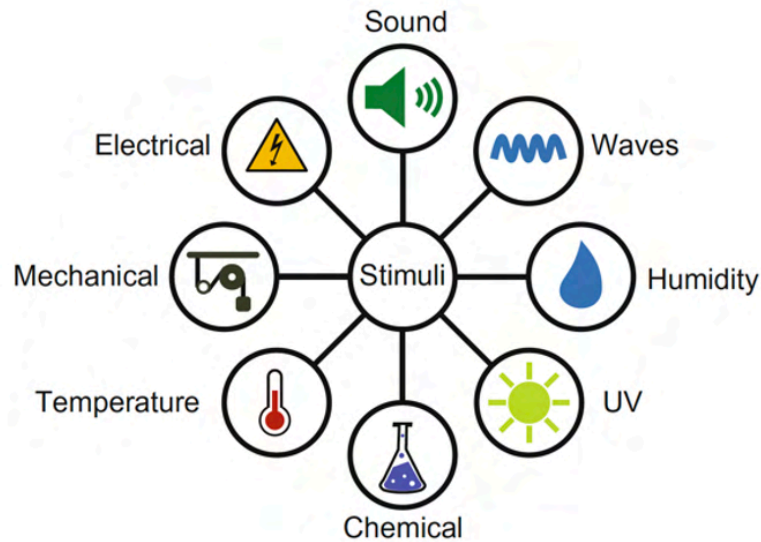
Figure 2-7 Examples of environmental stimuli in smart materials (Schmelzeisen et al., 2018)

Examples of multi-material 4D printing methods are shown in **Figure 2-8**., Initial studies explored the potentials of 4D printing and its materials with latter research more focused on its applications. NervousSystem (2013) developed a computational folding method which enabled the printing of objects that were much larger than actual printer size. The compressed object could be unfolded manually to a secondary form enabled by geometrical design (NervousSystem, 2013). Tibbits (2014) furthered this idea by developing programmable polymers, woods and carbon materials that can self-assemble into a pre-configured form. Ge et al. (2016) printed objects with thermal responsive polymers that were programmed to perform gripping, expansion and contraction and bending actions using multi-material printing. Likewise, Sydney Gladman et al. (2016) printed transformable architectural assemblies that mimicked plants with hydrogels which reacts to humidity. Ding et al. (2017) also explored a two-component composite material which consisted of an elastomeric hydrogel which changed in shape when heated. Wagner et al. (2017) explored 4DP assemblies which were programmed to expand when pressure was asserted. Furthermore, Tanaka et al. (2020) demonstrated by integrating 4D printing processes with user-centred design thinking, practitioners are able to

use 4D printing to develop practical applications i.e., collapsible shoes. Through such techniques, he has demonstrated the potential of 4D printing in developing environmental responsive design that performed folding and expanding actions.
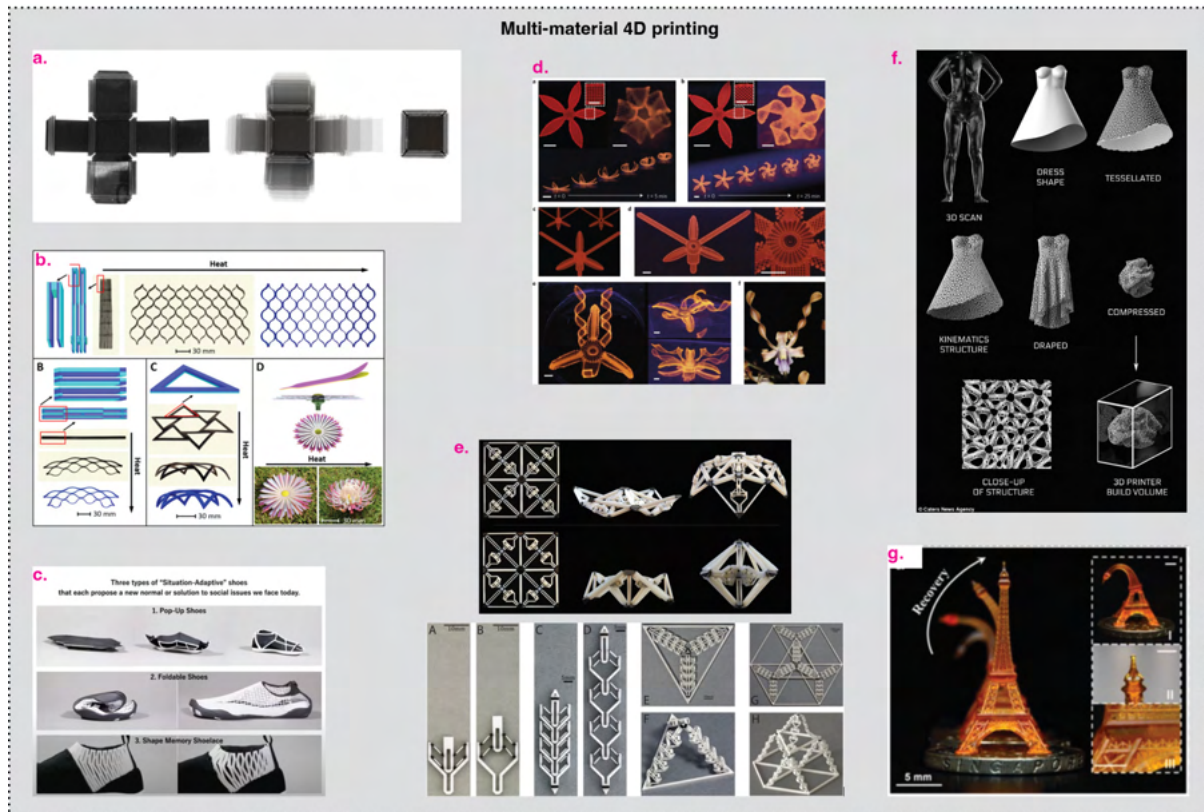
Figure 2-8 Multi-material 4D printing a. Tibbits et al. (2014), b. Ding et al. (2017), c. Tanaka et al. (2020), d. Sydney Gladman et al. (2016), e. Wagner et al. (2017), f. NervousSystem (2013), and g. Ge et al. (2016)

2.4 Materials in 4D printing

Precedent PTC and 4D printing studies have reported on a wide range of polymers including polylactic acid (PLA) (Grimmelsmann et al., 2016), thermoplastic elastomer (TPE) (Cheung & Choi, 2022), thermoplastic polyurethane (TPU) (Cheung & Choi, 2022), nylon, and acrylonitrile butadiene styrene (ABS) (Pei et al., 2015) to adhere on various types of fabrics of different textile structures and fibre content at varying levels of peel resistance. Due to the varying mechanical properties of the polymer types, the decision on which materials to use

depends highly on the requirements and purpose of the application with a focus on the end-user (Cheung & Choi, 2022). In 4DP, the additive (polymer), must be sufficiently dominant to influence the fabric to perform a shape transformation effect (Schmelzeisen et al., 2018). Though there are reports of 4D printing with smart materials i.e., SMP (Ge et al., 2016; Tanaka et al., 2020) and hydrogels (Sydney Gladman et al., 2016), the printing of smart materials onto textiles has not yet been scientifically investigated (Koch et al., 2021). Further exploration is required to enable direct printing of SME materials onto textile substrates.

2.4.1 4DP material's shape behaviour

Shape transformation or recovery behaviour can be divided into various movements: contraction/expansion, folding/bending (perform gripping), and surface changes (pleated effects) alike the behaviours seen in smart actuators (Persson et al., 2018). Complex shape transformations can be created by combining different shape changing behaviours which are unachievable via existing fabric manipulation techniques i.e., combination of bending with surface changes. Existing literature have emphasised on the importance of producing folding, and bending actions in 4D printing before moving onto developing more complex shape transformation behaviours (Groeger et al., 2016). **Figure 2-9.**, illustrates fundamental shape transformation behaviours in 4DP textiles.
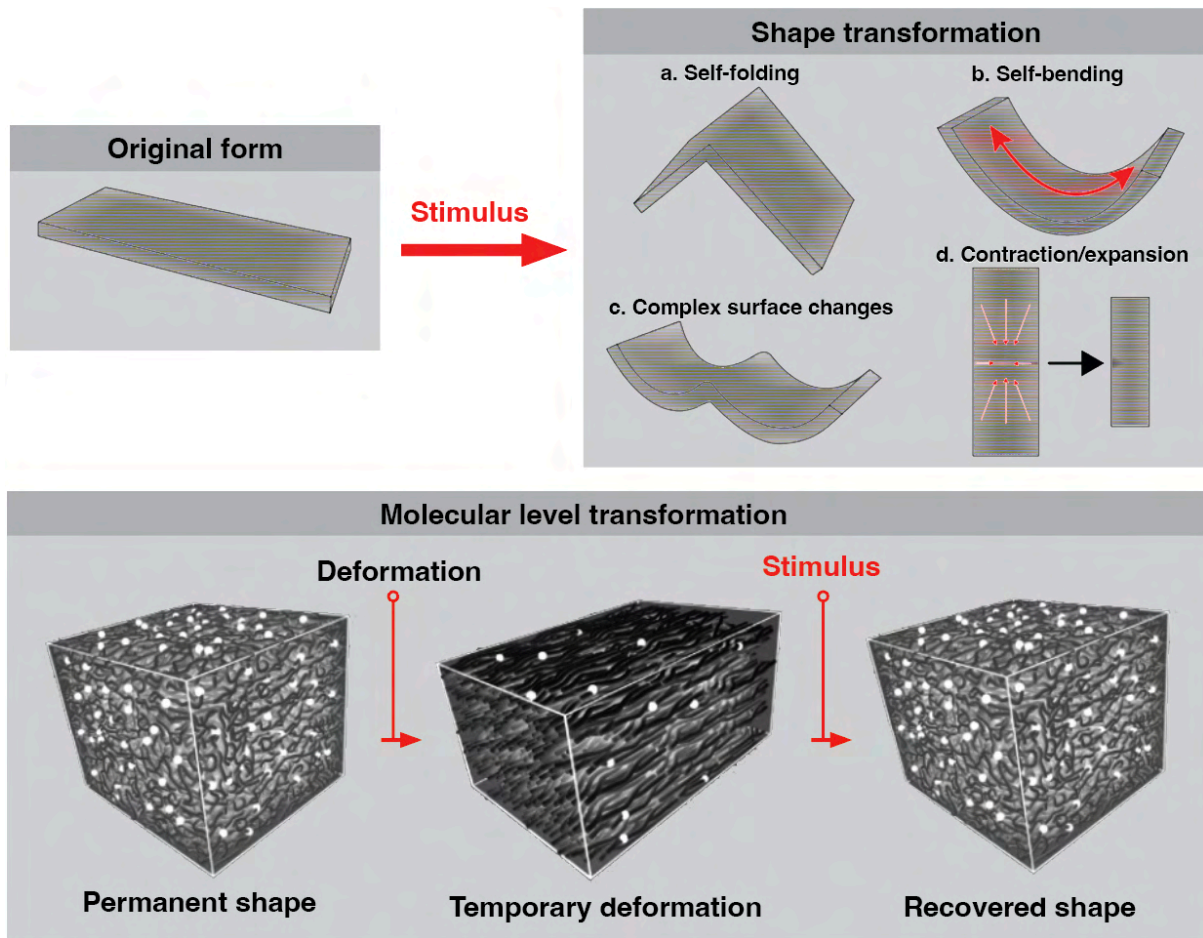
Figure 2-9 Shape transformation behaviours in 4DP textiles (Cheung et al., 2024)

- *Folding* – a local shape transformation (hinge) in which results in a change of position of the structures connected to the functional material fold.

- *Bending* – a universal change in structure which influences on the change in shape, position, and properties of all connected structures.

- *Surface changes* – a surface geometry transformation which influences connected structures in shape, properties, and positioning, may resemble fabric manipulation techniques i.e., pleated surfaces in fashion and textiles.

- *Contraction/expansion* – a scaling of the structure which can happen between/within dimensions (Koch et al., 2021)

The transformation behaviours can be further manipulated through selective adhesion and stiffening. Stiffening is achieved via part application of a polymer onto a textile and adhesion is realized by partial contact of a polymer with a textile (Koch et al., 2021). Furthermore, due to the temporal shape changing behaviours and characteristics, the load capacity of a 4DP structure and the mechanical stiffness of the polymers, a 4DP material's shape recovery speed and behaviour, and ability to perform asymmetrical shape transformations can be strategically designed by manipulating the material structure by varying the position of the materials (i.e., lattice structures) and printing parameters (i.e., fill pattern/density) (Nam & Pei, 2020). Thus, the shape changing behaviours of 4DP materials enable the possibility for the development of active textiles that can adapt to different situations, environments, and usages (Tanaka et al., 2020).

2.4.2 Design obstacles in 4DP materials

Though existing 4DP textile materials, garments, and products have shown great potential, they do not exist in realms beyond lab-scaled prototypes. Such materials and design have failed to integrate into mainstream products due to a lack of a standardised design, development, and evaluation process. In addition, existing technologies, materials, and processes also possesses limitations. Furthermore, existing studies have also neglected the practicality and functionality of such materials. Thus, to improve the practicality of 4DP materials, one must focus on the requirements of the applications and the needs of the end-users, understand the performance requirements of similar products in the current market, recognise the fundamental elements that makes a design successful i.e., application of scale, texture, colour (Ellinwood, 2021), and also apply design thinking that ensures desirability, technical feasibility, and possible market viability. By recognising such requirements, one can optimize 4DP material design that emphasises on functionality, usability, and aesthetics resulting in textile-based materials and

products that suits specific purposes and facilitates the development of adaptable materials and designs.

The key components of this study include i) the design of textile materials that considers aesthetics and functionality, ii) demonstrate the technical feasibility of using FDM processes for 4D printing materials, iii) identify optimal performing material combinations and printing parameters, iv) evaluate mechanical and shape performance under rigorous industry standard tests to validate its functionality and practicality, iv) consider the potentials of integrating personalised aesthetics with functions through print and pattern designs, and v) demonstrate the potentials of 4DP PTCs in different design concepts i.e., re-pleatable textile materials, flexible sizing facemasks, and re-shapable lampshade. The resulting designs anticipates the end-user to modify such products to adapt to their needs (users become a part of the design process post-manufacture).

2.5 Textile analysis and evaluation

2.5.1 Introduction

To meet the basic requirements of 4DP PTCs, specimens must be subjected to material evaluation using quantitative methods. Quantitative data can provide objective and accurate data for analysis (Lerche, 2012). In various design disciplines, material selection is foremost driven by design constraints and the final application. And in textiles-related design fields, the material's characteristics i.e., fibre content and combination, structure, weight, and drape all contribute to the mechanical behaviour of the material (Sinclair, 2014) and must thus be assessed. In the PTC discipline, additional conditions to consider include material compatibility and printing parameters which has been shown to influence peel resistance between substrates (Agkathidis & Varinlioglu, 2022).

2.5.2 Textile characterisation methods

For 4DP PTCs, further conditions to investigate include pattern design, structure, density, scale, thermomechanical programming, and shape recovery experiments. Through altering material, printing parameter, and pattern design conditions, the functionality of 4DP PTCs can be customised (Cheung et al., 2024). As knowledge on these topics are limited and fragmented in 4D printing fields, a systematic material selection, printing parameter, and pattern design selection process was developed to evaluate the influence of these factors on 4DP PTC performance and to determine the optimal material and processing parameters. **Table 2-2** illustrates standard methods used to characterise 3DP and 4DP materials and SMMs.

Table 2-2 Textile material characterisation methods

Reference	Type	Application	Type	Method(s)	Testing Standard
(Tibbits et al., 2014)	*4D printing (Smart material)*	Architecture	Shape-memory evaluation	o Timed transformation response (submerged in water bath)	*N/a*
(Neuß et al., 2016)	*3DP PTC/4D printing (Single driven/non-reversible)*	Design and technology	Shape-memory evaluation	o Measurement with ruler/protractor	*N/a*
(Kuang et al., 2018)	*4D printing (Smart material)*	Biomedical	Shape-memory evaluation	o Uniaxial tension tests and DMA tester to identify thermomechanical properties o 4DP object heated with a heat gun then deformed to desired configuration by using external force then fixed to shape by cooling to room temperature with water o Recovery: achieved by using heat gun or submerged into hot water	*N/a*
(Jose et al., 2020)	*SMM*	SMM principles	Shape-memory evaluation	o Shape fixity, response, and life cycle	*N/a*
(Kabir et al., 2020a)	*3DP PTC*	Garment	PTC evaluation	o Microscopic analysis o Weighing fabric o Fabric stiffness – KS K 0539 o Tensile strength – KS K 0521 o Poisson's ratio o Bursting strength – ASTM D 774	*ASTM, KS K*
(Loh et al., 2021; Loh, 2021)	*3DP PTC/4D printing (Single driven/non-reversible)*	Garment	PTC evaluation/ Shape-memory evaluation	o Peel resistance – ISO 11339: 2010 (ISO, 2010) o Geometrical dimensions – influence of geometrical dimensions, thickness, width, and length of printed structure – studies addition variable – shape recovery temperature 60°C/65°C (Tr) to investigate	*ISO*

				difference in response rate and shape-change effect to determine optimal Tr ○ Structural arrangement – testing structural widths (1/2/3mm) to determine optimal parameter for shape transformation	
(Cheung & Choi, 2022)	*3DP PTC*	Garment	PTC evaluation	○ Peel resistance – ISO 11339: 2022 (ISO, 2022b) ○ Surface quality – KES-FB4-A (KatoTech, n.d.-a) ○ Cross-sectional microscopic analysis and measurement	*ISO*
(Cheung et al., 2024)	*4DP PTC*	Garment and textile-based applications	Shape-memory evaluation	○ Peel resistance – ISO 11339: 2022 (ISO, 2022b) ○ Tensile strength and modulus – ISO 9073-18:2008 (ISO, 2008a) ○ Shape fixity, response, and life cycle	*ISO*
(Staszczak et al., 2022)	*SMM*	SMP characterisation	Shape-memory evaluation	○ SEM to investigate the cross-sectional morphology of 4D printed sample ○ DMA tester to identify thermomechanical properties	*N/a*

Notes: - 3DP PTC = 3D printed polymer-textile composite; *4DP PTC* = 4D printed polymer-textile composite; and *SMMs* = shape memory materials

Existing literature has suggested the evaluation of a textile material's resistance properties using industry standard tensile and bursting strength tests (Cheung et al., 2024; Kabir et al., 2020a). Peel resistance tests may be applied to evaluate the adhesive quality of material composites (Loh et al., 2021). Studies have also recommended the use of cross-sectional microscopic analysis to identify the depth of polymer penetration into a material structure (Kabir et al., 2020a). In addition, KES systems can be used to evaluate surface quality, friction and roughness of the material's surface (Cheung & Choi, 2022). For programming thermo-responsive SMMs, studies have used various thermomechanical methods ranging from heat regulated water baths to vacuum ovens (Agbakoba et al., 2022; Cheung et al., 2024; Loh, 2021). Dynamic mechanical analysis (DM) have also been used to identify the thermomechanical properties of SMMs (Kuang et al., 2018; Staszczak et al., 2022). In addition, scanning electron microscope (SEM) can be used to investigate the morphology of 4D printed samples (Staszczak et al., 2022). Furthermore, rigidity and hysteresis tests can be applied to study the influence of material bending ability on shape performance (Cheung et al., 2024). The above methods used in related studies can be used as a guide for establishing the evaluation process for 4DP PTC materials.

2.6 Summary

Through reviewing existing literature, three key directions in 4D printing have been identified i) material science (developing materials with SME), ii) development of geometries and structures for 4D printing and iii) further development of 4DP materials for the design of practical adaptive products where research is still insufficient and limited. Existing research has been limited by i) difficulty scaling up due to machine size and material properties, ii) not possible to re-configure 4DP pre-stressed textiles to new shape – limiting its use as an active material iii) 4DP multi-material materials too rigid/inelastic for wearables, iv) lack of research that demonstrates the feasibility and practicality of adopting 4D printing in designing wearable or textile-based products, v) transformation of 4DP material can be slow when scaled up and vi) not possible to print complex structures with materials like hydrogel (too soft and SME unstable).

Due to insufficient studies on 4DP materials, we anticipate further 4D printing research to be focused on investigating multi-material printing methods, extrusion of smart polymers directly onto textile substrates, developing a standardised design framework, and employing the use of industry testing standards for evaluating material performance. Existing studies have shown the possibilities to develop highly customisable active textile materials with shape transformation capabilities that can be activated with a stimulus. Such materials have manifested itself in wearable applications and have led to new designing thinking and the concept user-centred products that can be personalised post-manufacturing. Existing literature have also listed the potential for 4D printing to be applied in other fields i.e., architectural (Yi, 2022), medical (Khamkar, 2021), and flat storage and shipping (Tibbits et al., 2014). Further research should pay attention to the mechanical and shape performance of the 4DP materials

to identify potential applications. Particular attention should also be paid to developing full scaled prototypes and not just lab-scaled samples.

Chapter 3: METHODOLOGY

3.1 Introduction

Chapter three introduces the methodology which includes the design and decision-making process for 4DP PTC research. The overall concept of 4DP PTC is first identified. Based upon this concept of creating novel material composites using FDM/FFF processes with shape transformation capabilities, the basic requirements of 4DP PTCs are identified. This includes material performance and design requirements deriving from the analysis of existing 4D printing materials and applications. Having identified the design issues, suitable evaluation methods are determined. In addition, existing 4D printing theoretical frameworks are also reviewed to identify issues and gaps that require addressing. This methodical process helps with the formulation of a new design process that combines theoretical, practice-led, and lab-based experimentation. The design process subsequently leads to a decision-making process for 4D printing. Lastly, an overall summary and research questions are established to help fill the research gaps.

3.2 4DP PTC concept

The word *textile* is a collective terminology that includes a wide range of yarns, fibres, threads, filaments, and fabrics (Sinclair, 2014). Traditionally, it referred exclusively to woven materials. However this later included all types of textile structures as different technologies were developed (Kadolph, 2012). In the contemporary context, textiles are materials that fulfil the necessities of a wide range of applications, from garments and interior furnishings to medical and robotic applications.

AM i.e., FDM/FFF printing is an example of an advanced technology used for developing textiles owing to its wide material compatibility with various polymers and substrates, it can be used to combine several materials to create composite materials with unique properties. Material and processing parameters are frequently used to adjust a textile's fitness for purpose (Elsasser, 2010). As such, these novel materials can be engineered to fulfil the needs of consumer textiles for domestic purposes and/or technical textile's requirements for functionality.

This study on 4DP PTC exploits the advantages of FDM/FFF printing to create novel materials that can be fined-tuned via material, processing, and pattern design variables. Related literature has indicated its suitability for 4D printing textile materials owing to its high efficiency, material handling capability, high customisability, and potential for fabricating complex structures. In 4DP PTCs, the 4D printing element adds value to existing PTCs due to its efficient and consistent shape transformation capabilities which can advance the development of adaptable and functional textile-based materials and applications. Considering these advantages, using FDM/FFF technologies to 4D printing can contribute to the development of innovative shape transformative materials (**Figure 3-1**).

Figure 3-1 4DP PTC concept

3.3 Textile design and development model

A design model is a necessary tool that links together methods within a common structure that can be applied to various design fields (LaBat & Sokolowski, 1999). LaBat and Sokolowski (1999) discussed design methods used in different research fields and demonstrated the use of a design process to undertake a textile design problem. Clothing, textile, and product design commonly adheres to a three-stage design process – i) defining a problem and research on topic(s), ii) creative exploration, and iii) implementation of processes. **Figure 3-2** illustrates the design stages in clothing and textile design. The figure was edited and adapted for the design of 4DP PTC and in keeping with developments in contemporary society. In stage 1, an initial design problem was identified, followed by research on the target audience, users' requirements, and design criteria. Creative exploration (stage 2) takes place after the development of preliminary design ideas. The design concept is refined from the perspective of the type of application, and production feasibility. During the textile development and evaluation process, the aesthetic and function of textiles are considered and refined in accordance with relevant testing standards. In fashion, the aesthetics, functions, and target price range are often considered from the perspective of the end-users. And finally in the third stage, production costs, time to produce, and methods are refined to optimize its potential in the market.
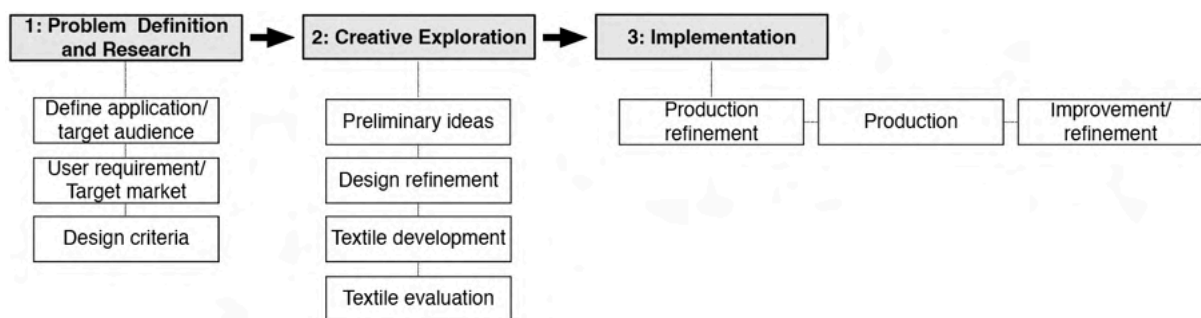
Figure 3-2 Clothing and textile design model edited and adapted from (LaBat & Sokolowski, 1999)

3.4 Identification of design problems

3.4.1 Introduction

In recent years, we have witnessed an upsurge of interest into developing 4DP structures (Sydney Gladman et al., 2016; Tanaka et al., 2020; Tibbits, 2014) and PTCs with FDM/FFF methods (Grimmelsmann et al., 2016). Yet there is an inherent lack of research into developing PTC with SME abilities due to material and technological constraints. The literature review has already discussed the advantages of extruding directly onto textile substrates. However, groundwork studies have been limited to investigating rigid materials such as PLA which fail to emulate the behaviours of conventional textiles. With the commercialization of flexible 3D printing polymers, we are presented with new opportunities for the development of flexible polymer-textile composites which are more focused on the end-user i.e., flexibility, mobility, and tactile comfort. According to existing literature, the key challenges of printing polymers on textiles can be summarised as follows – achieving high levels of peel resistance while maintaining flexibility, elasticity, weight, and mobility for wearability and aesthetic design.

3.4.2 Performance requirements for textile-related applications
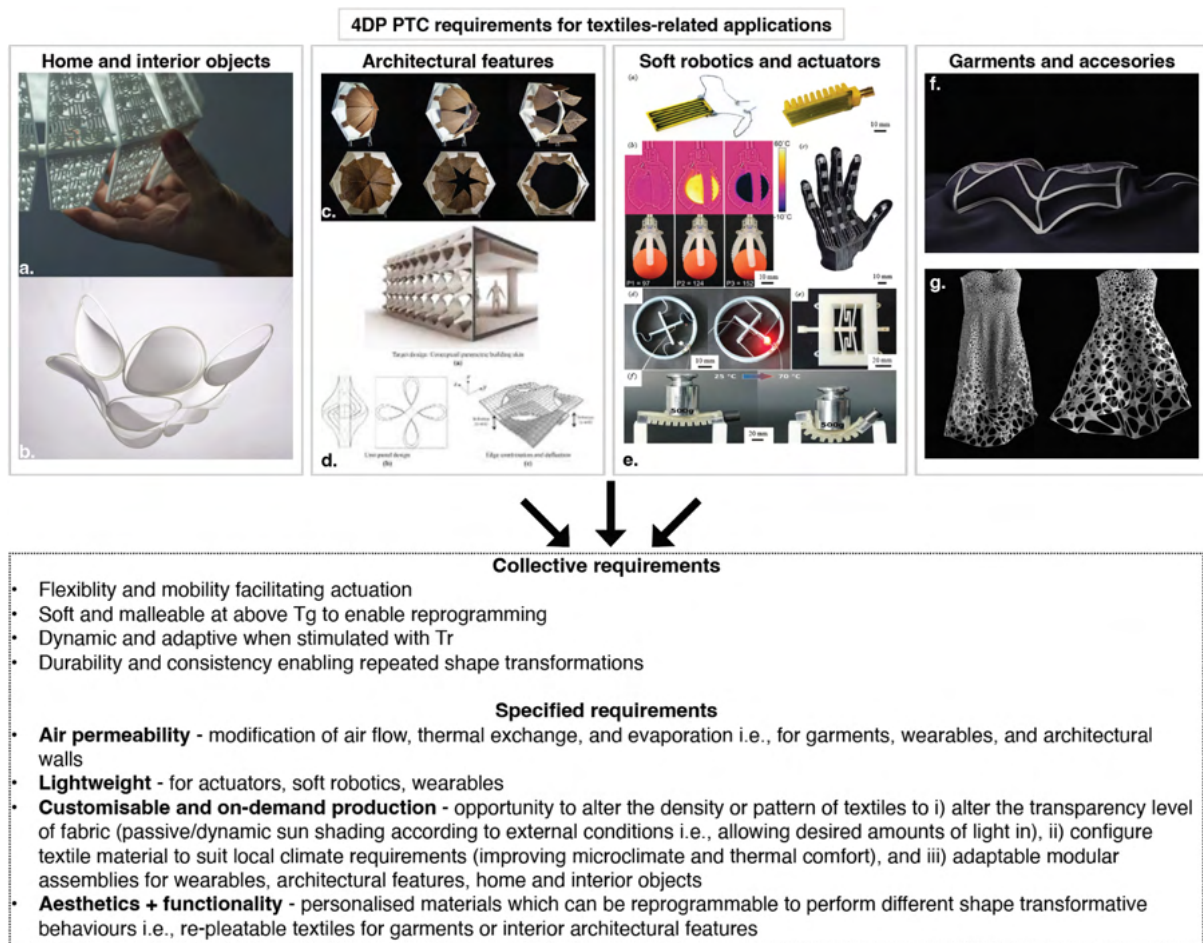
Figure 3-3 4DP PTC requirements for textile-related applications a. Goehrke (2015), b. Tibbits et al. (2014), c. Correa et al. (2017), d. Yi (2022), e. Zolfagharian et al. (2020), f. Guberan (2016), and g. NervousSystem (2013)

Figure 3-3 illustrates the basic requirements for 4DP PTCs aimed for textile-related applications i.e., home, and interior objects, architectural features, soft robotics and actuators, and garments and accessories. The collective requirements of these applications include i) a level of flexibility and mobility facilitating actuation, ii) soft and malleable when subject to above Tg which enables shape reprogramming, iii) dynamic shape transformation when stimulated with Tr, and iv) consistency and durability supporting repeated shape transformations (Kuang et al., 2019). Other specific requirements include i) air permeability for wearable applications or architectural walls (Biswas et al., 2021; Yi, 2022), ii) customisable

and on-demand production – offering the opportunity to alter the transparency level of fabrics targeted according to external conditions (Yi, 2022) i.e., different climates or to improve the thermal comfort of wearables , iii) aesthetics + functionality – enabling the personalisation of textile materials which can be reprogrammable i.e., re-pleatable/shapable fabric (Tanaka et al., 2020), and iv) lightweight materials with customisable mechanical properties (Tibbits, 2014).

3.4.3 Design requirements

Apart from considering the effects of material distribution and arrangement on shape transformation capabilities, the overall aesthetics of the garments and fabrics are equally as important. Therefore, when designing 4DP PTC, one needs to strike a balance between aesthetics and functionality – existing literature have discussed the importance of this equilibrium in various design fields (Seymour, 2019). With the intent of developing 4DP PTC modular garments for real-world use, the aesthetics and functionality of the garment components will have to be novel enough to draw the attention of potential consumers but also appeal to them by following the basic principles of design i.e., line, space, shape, form, texture, and colour (Roueche & Shirley, 2012). This can be achieved by taking cues from recognizable design elements adopted from timeless trends in fashion i.e., patterns, colour combinations, etc. By providing consumers an array of design options to choose from, one can communicate their personal style, taste, and mood and adapt their garments to achieve a desired look for specific scenarios in their lives. **Table 3-1** shows elements of design to consider when developing 4DP PTC surface patterns.

Table 3-1 4DP PTC design requirements

Design element	Details
Line	▪ Lines can suggest movement/rhythm and directs eyes from one part of the body to another ▪ Can draw attention/emphasize specific body part or garment detail i.e., topstitch draws attention to seams focusing attention to length of leg or pocket of jeans (Roueche & Shirley, 2012) ▪ **Types of lines** – 1) straight, 2) curved, 3) jagged ▪ **Directions of lines** – 1) vertical, 2) horizontal, 3) diagonal – can be used to create illusion. – vertical lines = illusion of added height/slimness/slenderness, strength, poise, sophistication = vertical lines ▪ Horizontal lines = shorter/wider also calm/relaxed look suggesting rest and gentleness ▪ Diagonal lines = action/strength/dramatic/eccentric/movement ▪ Application of lines = 1) structurally, 2) decoratively: ▪ Structurally = seams, darts, pleats, tucks, edges – garment construction – 4DP fastening ▪ Decorative = surface details on garment i.e., ruffles, braid, fringes, appliques, buttons, accessories – 4DP PTC pattern (Wolfe, 2016)
Space	▪ Use of positive/negative space to create surface design/pattern ▪ Use of other design elements to define contrast between negative/positive space found on fabrics in clothing

Shape/form	▪ Silhouette/overall outline of garment or item (Wolfe, 2016)
	▪ Typically dictated by designer – how they cut/construct garment impacts final shape/form – but modular garments can be manipulated by wearer – new silhouette/purpose/purpose
	▪ Recognised from a distance considered shape/form/silhouette
	▪ Draws attention or away to different body parts
	▪ Larger shape/silhouette = more visible vice versa
	▪ Fundamental silhouettes in history – 1) tubular, 2) bell, 3) back fullness:
	   ○ tubular – slimming body using vertical line structure/decoration
	   ○ bell silhouette – fitted waist and full skirt
	   ○ back fullness – puffed out skirt in front but not back

Texture	▪ Normally determined by fibre content, yarn, method of construction – 4dp ptc down to polymer type and fill quality
	▪ Finishes to change overall texture/feel
	▪ **2 texture types:** 1) structural texture, 2) added visual texture
	   ○ *structural texture* – describe weight/visual size of garment i.e., bulky wool sweater to increase body size
	   ○ *added visual texture* – surface design integrated to garment – intarsia, prints, logos etc – change overall motif of garment – important for comfort/appearance and generating interest

Colour	▪ Express feelings/create illusions/bring excitement ▪ Colours – symbolize moods/feelings/cultural practices/communication tool/gender (Funk & Ndubisi, 2006; Mahnke, 1996) ▪ For example, blue is often seen as a calming colour associated with comfort and security, red communicates excitement, passion, or anger, yellow is cheerful, representing prosperity and a bright or sunny disposition, and purple can be used to showcase loyalty, power, or even mysteriousness (Ballast, 2002; Wexner, 1954) ▪ Colour – influence how other respond to them – communication **Hue, value, intensity:** ▪ Hue – separates one colour from another – name of each colour-on-colour wheel ▪ Value – lightness/darkness ▪ Intensity – brightness/dull ness of colour

3.5 Research materials and equipment

This section outlines the materials and equipment used to carry out the experiments in this study. The 4D printing experiments were conducted using the same FDM printer in a regulated environment to ensure the consistency of the results. In addition, the filaments were also kept

in a dry box to maintain print quality. Moreover, all the 4DP PTC characterisation experiments were conducted in an environment that adheres to the constant atmospheric conditions outlined in ISO 291:2008 (ISO, 2008b). Whensoever necessary, an iphone7 camera was used to document the experimental processes.

3.5.1 Materials

There are a total of seven different textile substrates composed of synthetic or natural fibres with woven or knitted structures. In addition, there were three types of flexible filaments with a shore hardness ranging from 70A to 40D (90A equivalent). Furthermore, there was one type of thermo-responsive polyurethane-based shape-memory filament with a shore hardness of 57A. Detailed specifications of the materials are shown in chapters four and five in the experimentation sections. The range of materials used in this study were specifically chosen to exemplify the different material types with distinct properties that are readily available in the market.

3.5.2 Equipment

3.5.2.1 FDM printer

All the specimens were printed with an Original Prusa I3 MK3S+. The detailed specifications and parameters of the machine is shown in chapter four. To design and develop 4DP materials, the standard consists of 3D modelling on CAD → slicing on software → 4D printing (**Figure 3-4**). AM technologies have a competitive edge in comparison with traditional manufacturing processes owing to that fact that it can i) facilitate mass individually customised designs, ii) enhance the efficiency of the global supply chain from cost distribution to assembly, iii) reduce costs in design and labour and iv) introduce new supply chain models (Attaran, 2017; Vanderploeg et al., 2017). Moreover, AM technologies also enable the manufacturing of highly

complex designs at relatively low costs making it ideal for manufacturers (Lipson & Kurman, 2013).
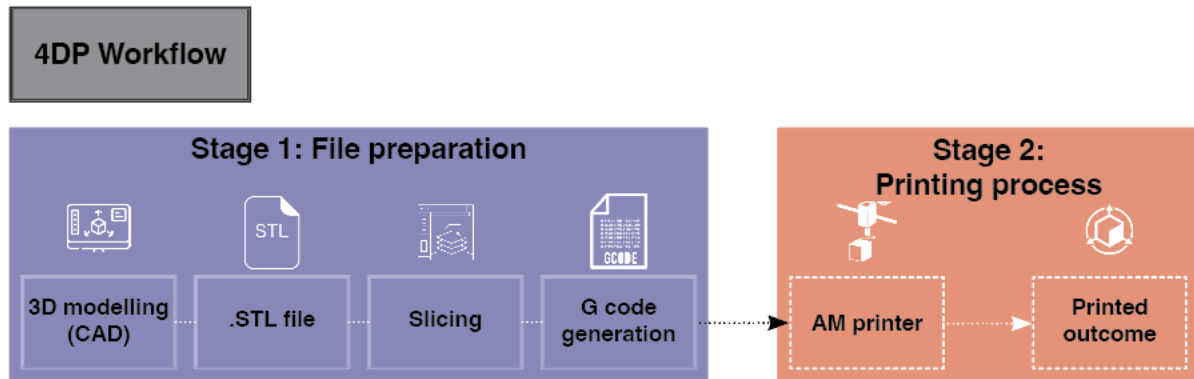
Figure 3-4 4D printing workflow

3.5.2.2 Textile characterisation equipment

Various types of instruments were used to evaluate textile performance (**Figure 3-5**). This included the use of an Instron 4411 testing system for evaluating peel resistance, tensile strength, and modulus (Instron, 1996), a Kawabata Evaluation System surface tester for evaluating surface quality (Kawabata & Niwa, 1991), a Leica M165C digital microscope for microscopic analysis (Microsystems, n.d.), a Hitachi TM3000 tabletop scanning electron microscope (SEM) for analysing surface information (Hitachi, 2011), a TruBurst 610 tester for evaluating bursting strength (Heal, 2019), and a Lab Companion OV4-30 vacuum oven for thermomechanical and shape performance experiments (LabCompanion, 2023). All of the equipment were operated in accordance with the manufacturer's requirements and in an environment that adheres to the constant atmospheric conditions outlined in ISO 291:2008 (ISO, 2008b).

Figure 3-5 Textile characterisation equipment

3.6 4D printing framework

3.6.1 Introduction
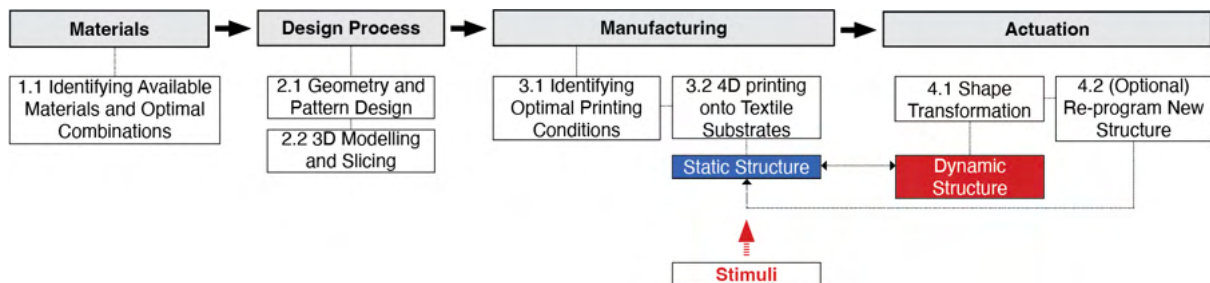
Figure 3-6 Conventional 4DP design framework (adapted and modified from (Biswas et al., 2021; Schmelzeisen et al., 2018)

Theoretical contributions in 4D printing and PTC fields are currently limited and often fragmented. Moreover, there are currently no standardised design framework established for 4DP materials. Though, the 4D printing process shares similar steps with 3D printing. However, in 4D printing, the process is more complex owing to the additional steps of

identifying material compatibility during the PTC stage and at the latter stage when a SMP is added resulting in a 4DP PTC. In addition, the dynamic properties of SMPs also makes the design process more intricate in comparison with 3D printing. Nonetheless, relevant literature has suggested basic design models for developing 4DP PTCs (Biswas et al., 2021; Schmelzeisen et al., 2018; Tanaka et al., 2020) (**Figure 3-6**). However, many of propositions are merely theoretical and has not been implemented in the real-world to prove its functioning. Moreover, these design frameworks only provide a rough outline of the process and does not specify detailed methods or steps required for the designing or evaluation of 4DP PTC materials. Thus, in **Figure 3-7**, a new and comprehensive 4DP PTC design process has been established which incorporates a systematic material selection process, identification of optimal printing conditions, design, and evaluation process.

3.6.2 4DP PTC design process
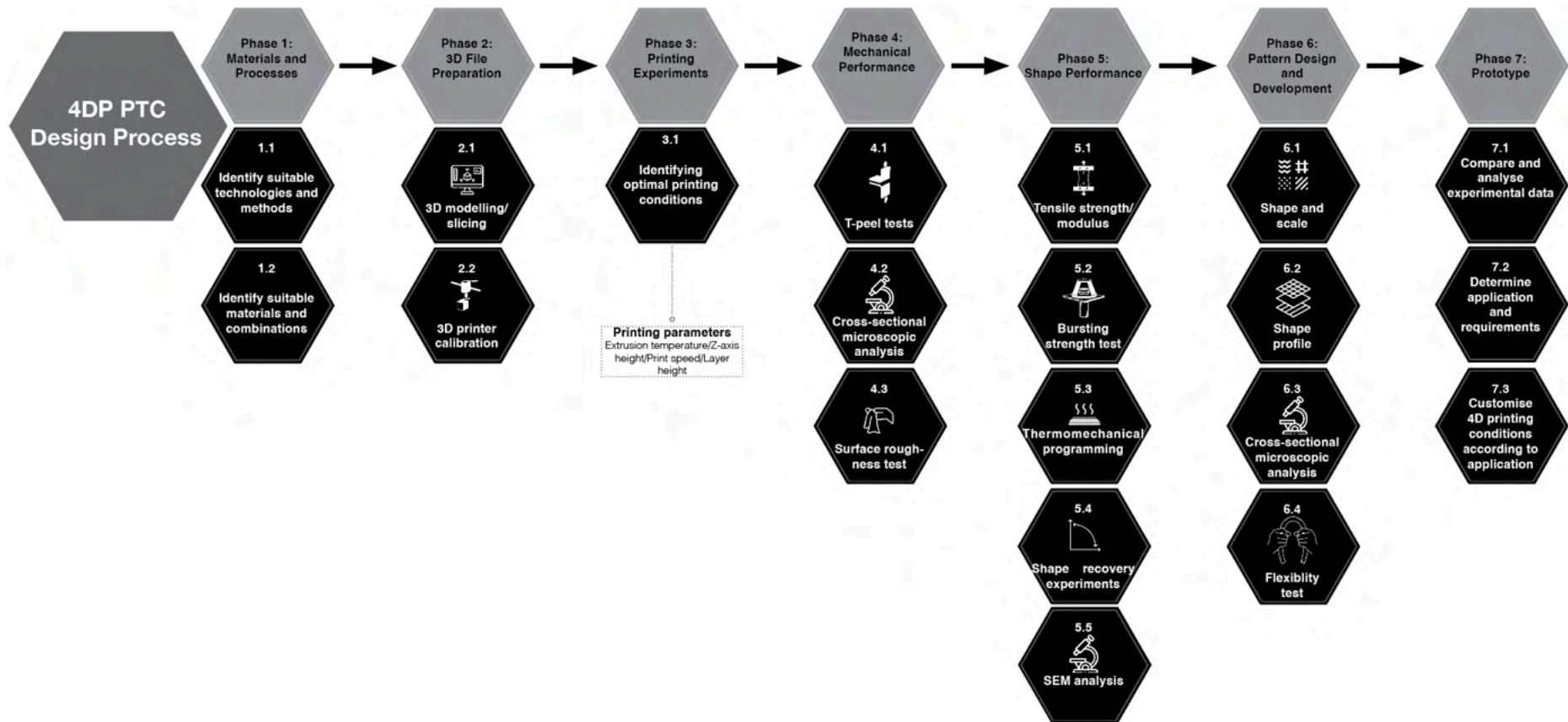
Figure 3-7 4DP PTC design process developed in this study

The 4DP PTC design process is based on the key study variables identified in existing studies i.e., materials, printing parameters, and pattern design. The design process established for this study consists of seven phases (**Figure 3-7**). Phase one is concerned with the identification of suitable technologies, methods, and material combinations. Phase two consists of 3D modelling, slicing, and printer calibration. Phase three is the conducting of printing experiments using different printing parameters i.e., temperature, print speed etc. Phase four evaluates the mechanical performance of the specimens developed in phase three to determine the optimal printing parameters for producing PTCs. Both PTCs and 4DP PTCs undergo phase four to characterise its mechanical performance. Phase five is solely for the testing of 4DP PTC's shape performance. Phase six studies the effects of design and structure of patterns on 4DP PTC performance (primarily its flexibility which dictate its actuation capability). Phase seven is about the comparative analysis of all experimental findings which will assist in determining which conditions to manipulate when designing 4DP materials for specific applications.

3.6.3 Material selection process

The material selection process is centred on the study variables (materials/printing parameters/pattern design) and its influence on the mechanical and shape performance of PTCs and 4DP PTCs (**Figure 3-8**). It also illustrates the key design steps and its connection with each other. Under a Yes/No decision-making model one can effectively identify and tackle challenges and then systematically progress to further steps (Akiyama et al., 1979). When selecting the appropriate material partners, a design variable is first selected, followed by the type of specimen (PTC/4DP PTC). For PTC development step three consists of mechanical performance evaluation methods that identifies PTC adhesion, evaluates surface quality, and characterises its mechanical performance. Poor performing materials are eliminated and tested

with an alternative condition. Due to PTCs being a multi-material composite encompassing polymers and textile substrates, the adhesion quality between components greatly influences the composite's structural properties which also affects its shape transformation efficiency (Schmelzeisen et al., 2018). The overall test results are comparatively analysed to determine the optimal conditions for developing PTCs.

4DP PTCs undergo a similar process but with additional characterisation methods i.e., bending hardness/recoverability in stage three. Such tests help gain insight into how bending rigidity and hysteresis influence the latter shape fixity and recovery experiments. Bending rigidity performance is also particularly important for materials that are aimed for applications that require movement or adaptable shaping. In stage four, 4DP PTCs undergo a shape performance evaluation process consisting of thermomechanical programming and shape recovery experiments. Loh (2021) have suggested the use of chart systems to measure a material's SME capabilities (Loh, 2021). The experimental data are computed using a formula resulting in shape fixity (R_f) and recovery (R_r) rates, and response results which will help identify the optimal conditions for developing 4DP PTCs. In SMMs research, the key aspects to consider are shape fixity, recovery rate, and life cycle (Jose et al., 2020). Shape fixity describes the capability of switching segments to fix the mechanical deformation (Tobushi et al., 1998), recovery rate is the time required for a material to shape transform into a pre-configured shape when stimulated (Tobushi et al., 1998), and the life cycle refers to the successive cycles a material can complete before a visible decline in shape fixity and recovery is found (Kong & Xiao, 2016).
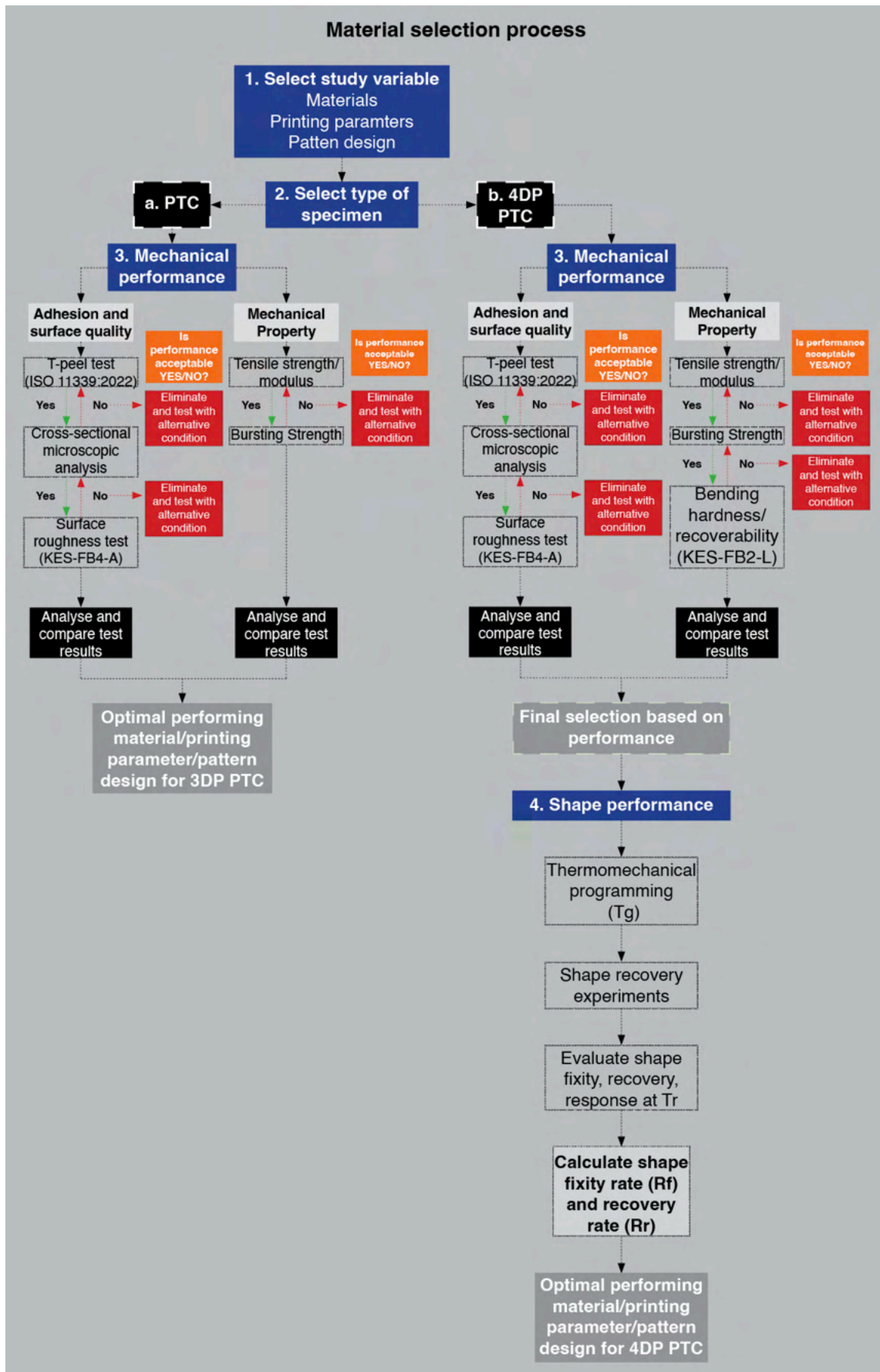
Figure 3-8 Material selection process flowchart

3.7 Summary and research questions

Precedent studies are primarily based upon identifying parameters that tackle adhesive challenges of polymers onto fabric in PTC (Grimmelsmann et al., 2016; Loh et al., 2021). However, there is an inherent lack of investigation into i) developing a systematic 4DP PTC design process, ii) exploring direct printing of PU-based SMPs onto fabrics, iii) identification of evaluation methods for 4DP PTCs to determine its performance, iv) consideration of pattern design and scale which influences aesthetics and functionality, and v) development of hinge mechanisms that can enhance the shape transformability of materials. Thus, in chapters four and five, the experiments will be designed to fill these research gaps.

Though much progress has been made in 4D printing fields, existing literature has revealed theoretical contributions to be fragmented and limited. In addition, there is a lack of exploration into 4D printing smart polymers directly onto textile substrates leading to 4DP PTCs. Related studies have too shown a lack of consistency and reliability when designing, fabricating, and assessing 4DP material performance. This has resulted in a lack of awareness on how 4D printing conditions influences the performance of materials. Moreover, 4DP materials have remained lab-scaled and have not shown feasibility for real-world applications. By reviewing existing literature, the merits, limitations, and research gaps of precedent 4DP material research have been recognised. The research questions are formulated with the aim to address these problems in 4D printing. This research aims to propose and establish a design, development, and evaluation process for 4DP PTCs using FDM/FFF technologies. The research questions are divided into three groups, with each group defined to accomplish the research aims.

PTC experiments group (adhesion and surface quality)

RQ1: What are the optimal material combinations and printing parameters for maximising peel resistance between TPU/TPE and textile substrate?

RQ2: What the optimal material combinations and printing parameters for maximising surface quality of polymers?

PTC experiments group (mechanical property)

RQ3: What the optimal material combinations and printing parameters for maximising tensile strength of 4DP PTCs?

RQ4: What the optimal material combinations/printing parameters for maximising bursting strength of 4DP PTCs?

RQ5: How does material and pattern design influence bending rigidity and recoverability?

4DP PTC experiments group (shape performance evaluation)

RQ6: What do we have to consider when making design decisions for fabricating 4DP PTCs?

RQ7: What processes and equipment are used to program a permanent shape into 4DP PTCs?

RQ8: How does bending rigidity and recoverability influence the shape recovery of 4DP PTCs?

RQ9: How can we fine-tune 4D printing conditions to manipulate the performance (i.e., fixity, recovery, and response rate) of 4DP PTCs?

RQ10: What are the potentials and limitations of 4DP PTCs using FDM/FFF printing technologies? What applications would benefit from thermo-responsive 4DP PTCs?

Chapter 4: POLYMER-TEXTILE COMPOSITE

4.1 Introduction
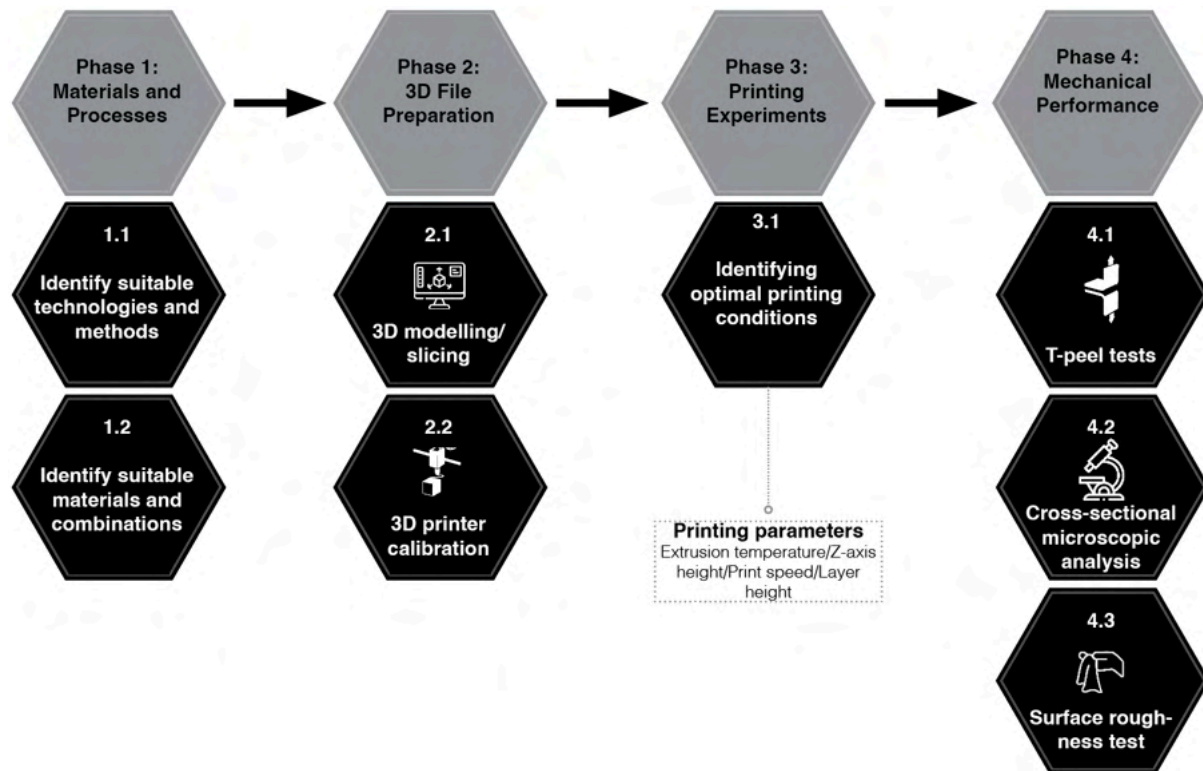
Figure 4-1 4DP PTC design process (showing chapter 4 experiments)

This study aims to explore the feasibility and potentials of 4D printing on conventional textiles using FDM printing processes to develop novel 4DP PTC. **Figure 4-1** illustrates the experiments conducted in chapter 4. At this stage of the study, printing experiments were conducted using Thermoplastic polyurethane (TPU) and elastomer (TPE) polymers on a wide array of textile substrates composed of various textile structures and fibre content. Small test swatches were printed to determine the optimal z-axis distance for various types of fabric. Other printing parameters not limited to temperature and print-speed were investigated to pinpoint optimal peel resistance performance. To characterize how polymer and fabric structure type and printing parameters can influence the adhesive performance between flexible-to-flexible assemblies, a T-peel test was conducted on the textile prototypes under strict conditions set by ISO 11339:2022 (ISO, 2022b). A KES-FB4-A surface tester was also used to analyse the effects of printing parameters on polymer surface quality and whether surface quality of fabrics influenced adhesion between polymer and textile substrate. Furthermore, cross-sectional microscopic analysis was also used to identify the depth of polymer penetration into a textile structure. These experiments provided a basis for further research steps.

4.2 Experiment design

4.2.1 Design parameters and specimen development

4.2.1.1 FDM/FFF printer settings

In this study, an Original Prusa I3 MK3S+ machine (FDM/FFF technology) with a single extruder head was used to conduct the printing experiments. FDM/FFF printers builds models in layer by layered form and obeys a system of X, Y, and Z-axis coordinates to determine the position of the extrusion nozzle when printing (Lipson & Kurman, 2013). The minimum printing layer height of 0.05 mm enables this machine to achieve higher levels of precision

compared with market alternatives (FastRadius, n.d.). **Table 4-1** indicates the technical parameters of the Prusa I3 MK3S+ machine provided by Original Prusa (Prusa, 2021a).

Table 4-1 Technical specifications of Prusa I3 MK3S+ machine (Prusa, 2021a)

Prusa I3 MK3S+ technical specifications	
Build volume	250 x 210 x 210 mm
Layer height	0.05 – 0.35 mm
Nozzle size	0.4 mm default (option for range of other diameters)
Filament diameter	1.75 mm
Max speed	200+ mm/s
Max nozzle temperature	300°C / 572°F
Max bed temperature	120°C / 248°F
Extruder type	Direct drive
Extruder(s)	1
Supported materials	PLA, PETG, ABS, PC, TPU, TPE, Nylon

To identify the proper printing parameters for the different material combinations, we initiated by printing small test swatches. Z-axis, temperature, and material partners were all variables that were considered during the printing tests. By referring to the temperature settings advised by filament manufacturers and the Prusa slicer software, we have set the baseline printing temperature for TPU/TPE at 240°C. The bed platform heating was unnecessary as we were not printing directly onto the platform. 20 mm/s was the default recommended setting for print speed by the Prusa3D slicer (Prusa, 2021a). A rectilinear fill pattern at 100% density was used across samples. FDM/FFF printers follow a system of X, Y, and Z-axis coordinates to determine the position of the extrusion nozzle when printing (Lipson & Kurman, 2013). This study used an Original Prusa I3 MK3S+ machine with a single-extruder head. **Table 4-2** illustrates printing parameters used in precedent PTC research that we should take into consideration.

Table 4-2 Parameters to consider in FDM/FFF printing of textile composites

Parameter	Variables	Calibration
Printer calibration	*X, Y, Z coordinates*	▪ *To identify X, Y, Z coordinates for printing and determine the optimal z-axis distance through first layer calibration*

Extrusion temperature & bed temperature	*Temperature of extruder nozzle*	• *230°C – 240°C for TPU (Korger et al., 2020)* • *240°C for TPE/TPU – higher than recommended setting by 5°C to 10°C (Loh et al., 2021)*
	Bed temperature	• *According – default setting for flex by Prusa3D (Prusa, 2021a)*
Fabric thickness & Z-axis height	*Z-axis adjustment depending on the thickness of the fabric*	• *Conduct preliminary swatch printing tests by increasing or decreasing z-height depending on fabric thickness (Loh et al., 2021; Spahiu et al., 2020)*
Print speed	*First layer*	• *20 mm/s – default setting for flex by Prusa3D (Prusa, 2021a)*
Layer height	*First layer/subsequent layer*	• *0.05 mm and 0.05 mm subsequent layers – default setting for flex by Prusa3D (Prusa3d, 2022)*
Infill	*Pattern/density*	• *Rectilinear/15% – default setting for flex by Prusa3D (Prusa, 2021a)*

Print settings have been shown to influence the adhesion & surface quality and the visual appearance of a final print (Pei et al., 2015). Z-axis distance has been extensively covered by previous studies as one of the principal factors contributing to the quality of adhesion between polymer-textile (Korger et al., 2020; Loh et al., 2021; Sanatgar et al., 2017; Spahiu et al., 2017). Z-axis tuning is required depending on the thickness of the fabric used. For raise-textured fabrics, an increase in Z-axis is necessary to compensate for the fabric's thickness to prevent the nozzle from digging into the fabric, causing damage to the textile. However, on the other hand, it must be close enough to deposit polymers with no gaps in-between layers to achieve optimal adhesion. Studies have suggested layer heights or no greater than 0.2 mm to achieve dimensional accuracy and surface finishing (Hsiang Loh et al., 2020). We printed at 0.10 mm quality in this study. Printing temperature is also understood to have considerable effects on adhesion (Sanatgar et al., 2017). Previous research has suggested using higher temperature ranges within the recommended settings because it can reduce the viscosity of the polymers, which will lead to stronger penetration into the fabric's pores (Spahiu et al., 2017). Moreover, as we were not printing directly onto the printer bed, the build platform temperature does not affect the adhesion between polymer-textile (Sanatgar et al., 2017). We adhered to the default flex printing settings provided by Prusa3D for considerations such as fill, pattern, and speed – existing studies had shown no substantial effect on adhesion when print speed was increased (Spahiu et al., 2017).

4.2.1.2 3D modelling and G-code generation
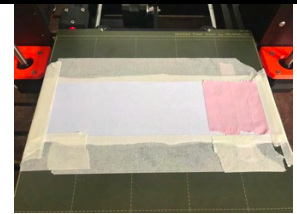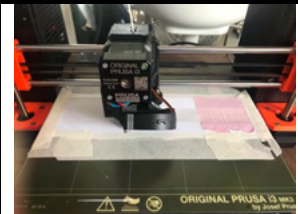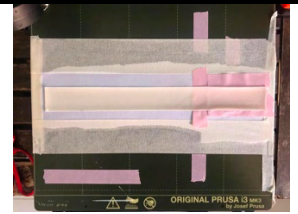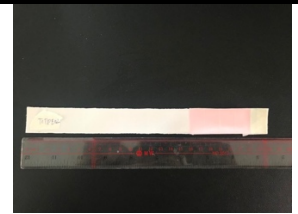
To fabricate the PTC through 3D printing, a flat drawing of the test strip with dimensions specified by ISO was created using Rhino – Rhinoceros 3D version 8 (Rhinoceros, 2024), a computer-aided design (CAD) software used commercially in the design, rapid prototyping, and computer-aided manufacturing (CAM) industries. and exported as an STL file which was then imported into Prusa Slicer for remodelling & slicing and generated as a G-code for printing (G-code contains printing commands including infill, speed, temperature, etc.) (shown in **Figure 3-4**). The printing process was done via an Original Prusa I3 MK3S+ FFF printer with a nozzle diameter of 0.4 mm.

4.2.1.3 Extrusion of polymers onto textile substrates

To identify the proper printing parameters, we referred to the temperature settings advised by filament manufacturers and Prusa. The default printing temperature for TPU/TPE was set at 240°C (other temperature ranging from 220 to 260°C were also tested) by the Prusa software and as we were not printing directly onto the platform, bed platform heating was unnecessary. 20 mm/s was the default print speed suggested by Prusa3D slicer (Prusa, 2021a). A rectilinear fill pattern at 100% density was used across samples. To determine the optimal Z-axis for printing, a first layer calibration was conducted to identify the ideal distance between the nozzle tip and printing surface. The purpose of this process was to fine-tune the nozzle height until the extruded polymers stuck onto the print surface with no ridges or gaps between lines (Prusa, 2021b). The optimal Z-axis height is unique to each machine subject to the position of the SuperPINDA sensor. And through repetitive trials, a Z-axis distance of -1.600 mm was identified as optimal for printing directly onto the platform. Therefore, when printing on fabrics we must consider the thickness of the fabric and increase the Z-axis distance accordingly. For example, fabric T1 that has a thickness of 0.5 mm, a Z-axis of -1.100 mm was identified as the

optimal distance and for fabric T2 that has a thickness of 0.1 mm, a z-axis of -1.500 mm would provide optimal adhesion. When printing with Z-axis heights of less than -1.100 mm (T1) and -1.500 mm (T2), the nozzle would dig into the fabrics, leave burn marks and cause under extrusion due to the retraction of filament materials which will lead to clogging in the extruder. On the other hand, the polymer layer could be peeled off with ease in samples that were printed at above optimal distance. **Table 4-3** depicts the printing process for T-peel test specimens.

Table 4-3 Printing process for T-peel test specimens (Cheung & Choi, 2022)

▪ Contact Z-distance calibration performed to identify the optimal distance between platform and extruder nozzle ▪ Masking tape is used to secure the fabric onto the printing platform ▪ Pink washi tape is applied onto areas of fabric that we do adhesion to happen (polymers do not adhere to washi tape due to its irregular surface) ▪ Unbonded areas (pink) are necessary for the T-peel tests	▪ Extruder head printing TPU filament	▪ Print process completed – polymer is adhered onto the textile substrate, but no bonding has occurred in areas with washi tape	▪ Textile composite sample is removed from the print platform, and the sample is trimmed off and measured in accordance with ISO 11339:2022 standards

4.2.2 3D printing materials

4.2.2.1 Polymers

Previous challenges associated with flex polymer printing have been resolved with the introduction of direct-drive extruders and more sophisticated flex filament materials of different shore hardness. In direct extrusion, polymer materials are directly pushed through the hot end facilitating steady control and calibration of polymer retraction (Recreus, 2021). In this study, TPU and TPE polymers were used to experiment with direct printing onto textiles. TPU

and TPE are typically available in various shore hardness, and in this study the TPU filaments has a shore hardness of 70A and 82A which is comparable to elastic bands and soft mousepads meanwhile, the TPE has a shore of 40D akin to stiffer rubbers commonly seen in sneaker soles or phone cases. The polymers were chosen due to their high level of elasticity making them well-suited for wearables that quire flexibility and mobility consistent with the mechanical properties of the textile substrates used in this study (other examples of applications are shown in **Table 4-4**).

Table 4-4 Overview of TPU/TPE pros/cons & applications

Filament	Pros	Cons	Applications
Flex (TPU/TPE) (Filatech, 2022; NinjaTek, 2022; Recreus, 2022a)	**TPU** - Flexible & elastic - Shock absorption - Abrasion resistance - Crack resistance - Adhere to fabric (Kabir et al., 2020a; Tadesse et al., 2018)	- Some are too soft to print - Risk of clogging extruder leading to under extrusion - TPE does not adhere to polyamide/polyester (Goncu-Berk et al., 2020)	**TPU** - Wearables, LED diffusers, - Insulation, phone cases, grips, pipes, airbags, interior trims, sport shoe soles, sport equipment **TPE** - Cables, sole material, wearables, protective coatings, special-shaped materials, decorative strips, production line machine parts

Table 4-5 reports on the specifications of the polymer filaments used. The filaments were sourced from Recreus Filaflex (TPU) (Recreus, 2022a) and Filatech FilaFlexible (TPE) (Filatech, 2022). There were two TPU filaments with shore hardness of 70A and 82A, both with a diameter of 1.75 mm, and an elastic limit of up to 900% (70A) and 650% (82A). Meanwhile, the TPE filament has a shore hardness of 40D, a diameter of 1.75 mm, and an elastic limit of up to 400%. 70A shore has a similar hardness as a rubber band and 82A shore has a comparable hardness with soft mousepads. Meanwhile, 40D has a hardness akin to stiffer rubbers, i.e., phone cases or shoe soles. The TPUs were chosen because it possessed high levels of elasticity aimed for wearables that require flexibility and mobility, i.e., casual wear and

sportswear consistent with the mechanical properties of our textile substrates. Likewise, the TPE, while relatively flexible, can provide additional support well-suited for applications, i.e., compression garments or intimate wear. Furthermore, though lower shore hardness filaments are currently available, these ultra-soft filaments are still at their trial stages and are not ensured to be printable by the manufacturers; hence we had to find an equilibrium between usability and shore hardness.

Table 4-5 TPU/TPE filament specifications

Property	Filaflex 70A (TPU) (Recreus, 2022b)	Filaflex 82A (TPU) (Recreus, 2022a)	FilaFlexible40 (TPE) (Filatech, 2022)
Shore hardness	70A	82A	40D (approx. 90A equivalent)
Diameter [mm]	1.75 mm -/+ 0.03 mm	1.75 mm -/+ 0.03 mm	1.75 mm -/+ 0.03 mm
Density [g/cm³]	1.08	1.12	1.22
Elongation at break [%]	900%	650%	400%
Melting temperature [°C]	84°C	113°C	160°C
Extrusion temperature [°C]	215 - 235°C	215 - 250°C	220 - 240°C
Printing bed temperature [°C]	40°C if required	Not required	50°C if required

4.2.2.2 Textile substrates

In this study, the fabrics considered in this study were chosen on the basis that they are some of the most universally used fabrics for consumer textiles aimed for athleisurewear, ready-to-wear, sportswear, interior furnishings, and crafts due to their lightweight, air permeability and affordability (Venkatraman, 2015). The selection included synthetic/natural compositions, different thicknesses, colour, elasticity, surface roughness and textile structure and were sourced from Whaley's Bradford Ltd in United Kingdom (WBLFabrics, 2022). Precedent studies have suggested fabric type, structure, weight and density to influence adhesion with

rigid polymers (PLA/nylon) (Loh et al., 2021). Thus, in this study a thorough investigation is essential to determine if this is the same case for flex polymer composites.

4.2.2.2.1 Knitted fabrics

Knitted structures are typically constructed by the interlocking/inter-meshing of yarns and distinct itself from woven fabrics due to its flexible, elastic, and easier construction into smaller wearables (Spencer, 2001). Advantages of knit include quicker fabrication process compared with woven and with lower costs, light in weight, comfortable to wear, garments can be fully fashioned, requires little maintenance to keep its appearance, can resist wrinkling, and are thus suited for sportswear and other applications where mobility or comfort is required (Banerjee, 2014). In this study, three fabrics composed of two common knitted structures – single-knitted jersey and warp knit was examined. The properties of the knitted fabrics are shown in **Table 4-6**.

Table 4-6 Properties of knitted fabrics

Fabric ID	Type	Composition	Construction	Thickness
T1	Knitted jersey (k)	80% NY 20% EA	Single-knitted jersey	0.10 mm
T6	Warp knit (k)	100% PL	Warp knit	0.50 mm
T7	Knitted jersey (k)	100% PL	Single-knitted jersey	0.10 mm

T = textiles; EA = elastane; NY = nylon; PL = polyester; k = knit

4.2.2.2.2 Woven fabrics

Woven fabrics refers to any textile that is fabricated through weaving on a loom. Threads are interlaced in warp and weft directions at right angles (Banerjee, 2014). Woven fabrics though lack the elastic capability of knitted structures makes it more durable and keeps better shape than knitted structures. In this study, four types of woven fabrics were examined including plain woven, ripstop weave and twill weave. The properties of the woven fabrics are shown in **Table 4-7**.

Table 4-7 Properties of woven fabrics

Fabric ID	Type	Composition	Construction	Thickness
T2	Polyamide 6,6 (plain weave)	100% NY	Plain woven	0.10 mm
T3	Ripstop (*w*)	100% NY	Ripstop weave	0.10 mm
T4	Twill (*w*)	100% CO	Twill weave	0.20 mm
T5	Plain woven (*w*)	100% CO	Plain woven	0.30 mm

T = textiles; CO = cotton; NY = nylon; *w* = woven

Natural & synthetic fibres

Fabrics are commonly characterized as natural, synthetic or a blend of both. Natural fibres i.e., cotton is sourced from nature and are either cellulose, protein or mineral based. Advantages of natural fibres include durability, strength, comfort, insulation, absorbent, hypoallergenic and eco-friendly (less chemical use, breaks down quicker than synthetics) (Mondal, 2021). On the other hand, synthetic fibres are generally artificially manufactured fibres but there are exceptions i.e., rayon that are man-made fibre alike synthetic fibres but is regenerated from cellulose. The advantages of synthetics include resistance to stains, waterproof & resistance and cheaper compared with natural fibres (McIntyre, 2005). In this study, an assortment of natural and synthetic fabrics is investigated to identify whether textile composition influences adhesion in flexible polymer printing.

4.2.2.3 Surface roughness and coefficient of friction

The mean coefficient of friction (MIU) and surface roughness deviation (SMD) (Kawabata & Niwa, 1991) of all textile substrates were evaluated using a Kawabata Evaluation System, KES-FB4-A surface tester, which enabled the predictions of tactile sensations perceived by human touch (KatoTech, n.d.-b). The module sensor for measuring the fabric's surface roughness consisted of a 0.5 mm diameter single wire and worked at a contact force of 10 ± 0.5 g, meanwhile surface friction was measured with a piano-wire sensor that applied a compression force of 50 g to the fabric surface (Capdevila et al., 2020). The sensors were designed to mimic

a human fingertip enabling the quantification of a fabric's texture similar to human touch (KatoTech, n.d.-b). During the measurement process, the fabric specimen was moved by 2 cm (in each test) at a constant speed of 0.1 cm/s over a horizontal platform subjected to a force of 20 g/cm. MIU determined a mean coefficient of friction at values between 0 and 1 (a higher value corresponds to greater friction) (WilsonCollegeofTextiles, n.d.). Though friction coefficient can occur at values much larger than 1 for particular materials i.e., aluminium on aluminium (Matmatch, n.d.), it is highly unlikely for conventional garment fabrics to possess such quantities of friction with human touch (KES-FB4-A module was designed to mimic the human fingertip) (Zhang & Mak, 1999). Meanwhile, SMD revealed the surface roughness at micron levels, where higher values represented geometrically rougher surfaces.

4.2.2.3.1 Fabric surface roughness and coefficient of friction

The tests were repeated three times on each fabric in warp and weft directions with an aggregated average reported (**Table 4-8**).

Table 4-8 Average surface roughness & coefficient of friction of textiles in (warp/weft)

ID	MIU (μ)		SMD (μm)	
	Warp	*weft*	*Warp*	*weft*
T1	0.39	0.41	1.05	5.53
T2	0.18	0.15	7.79	11.57
T3	0.24	0.17	3.10	3.54
T4	0.27	0.20	2.01	1.51
T5	0.22	0.16	2.03	8.41
T6	0.30	0.18	2.00	0.17
T7	0.25	0.24	0.72	1.90

MIU – mean coefficient of friction; SMD – surface roughness deviation

4.2.2.3.2 Summary

Our results indicated T1 to have a lower SMD but higher MIU than T2, thus suggesting T1 to have a smoother tactile sensation; however, the surface has a higher resistance to touch caused by slight irregularities in the knitted structure (**Table 4-8**). These irregularities are caused by

the interlocking of the knitted structures, which creates friction, and the larger the irregularities are, the more resistance is caused (Bertaux et al., 2007).

4.2.2.3.3 Polymer surface roughness and coefficient of friction

Polymer layers printed at various temperature settings were also evaluated for their coefficient of friction and surface roughness using a KES-FB4-A surface tester. The samples for testing surface friction and roughness were sized at 200 mm x 200 mm in line with the build platform dimensions of the KES surface tester, with the layer thickness consistent with the T-peel test specimens at 0.5 mm. TPU/TPE samples of 4 temperature groups were printed (220/240/250/260°C), and tests were completed over three different regions (each 2 cm area) of the polymer in both warp/weft directions with an aggregated averaged result (**Table 4-9**).

Table 4-9 Surface friction and roughness results (warp/weft directions)

Sample	SMD (μm)		MIU (μ)	
	Warp	*weft*	*Warp*	*weft*
220 - TPU 70A (warp/weft	0.86	0.90	1.43	1.44
240 - TPU 70A (warp/weft	0.96	0.91	1.25	1.34
220 - TPU 82A (warp/weft)	0.41	0.52	1.63	1.78
240 - TPU 82A (warp/weft)	0.46	0.50	1.36	1.66
250 - TPU 82A (warp/weft)	0.46	0.51	3.45	3.38
260 - TPU 82A (warp/weft)	0.30	0.47	3.85	4.35
220 - TPE 40D (warp/weft)	0.38	0.33	2.30	2.11
240 - TPE 40D (warp/weft)	0.45	0.46	3.70	3.37
250 - TPE 40D (warp/weft)	0.48	0.51	2.80	2.72
260 - TPE 40D (warp/weft)	0.49	0.50	2.00	2.22

MIU – mean coefficient of friction; SMD – surface roughness deviation
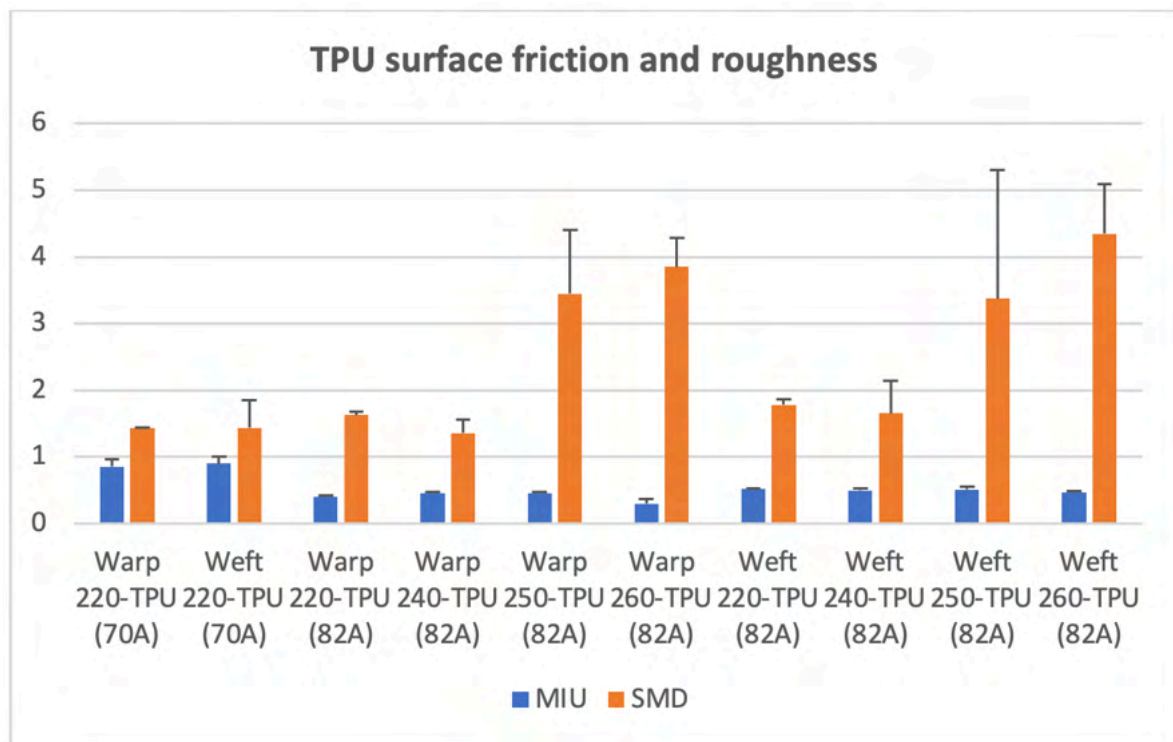
Figure 4-2 TPU surface friction and roughness results

For TPU polymers, the lowest MIU and SMD were recorded on specimens printed at 240 (**Figure 4-2**). 70A polymers also recorded relatively lower MIU and SMD than 82A polymers. Similar results of surface friction and roughness were also recorded for TPU samples in warp/weft directions apart from the 260°C sample. On the whole, at higher temperature settings 250/260 °C, a rougher surface was observed caused by over extrusion at higher temperatures (also observed in microscopic measurements) (Shaqour et al., 2021). A higher SD was also found at 250°C and 260°C suggesting an inconsistency in polymer surface quality.
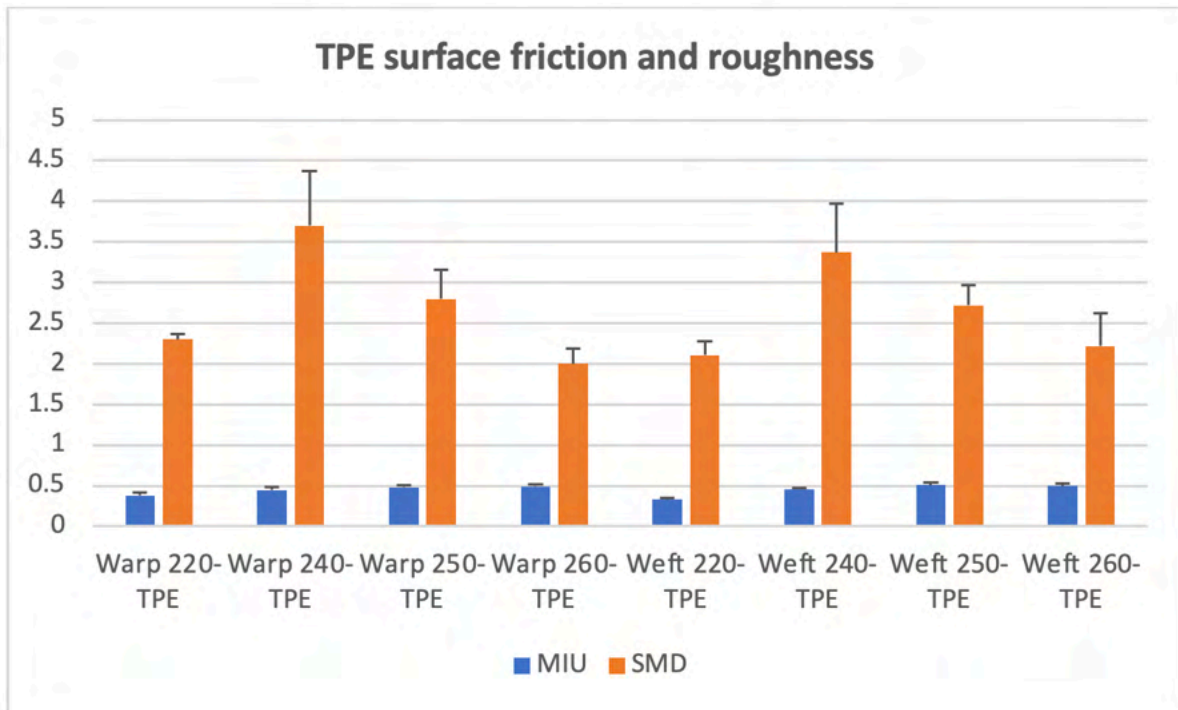
Figure 4-3 TPE surface friction and roughness results

Similar results of surface friction and roughness were recorded for TPE samples in warp/weft directions (**Figure 4-3**). 220°C measured the lowest coefficient of friction at meanwhile, 250°C and 260°C samples recorded the highest surface friction. This phenomenon was caused by the likelihood of over extrusion caused by higher temperatures which caused materials to flow unevenly from the nozzle (also observed in microscopic measurements) (Shaqour et al., 2021). A higher SD was found at 240°C suggesting an inconsistency in polymer surface quality.

4.2.2.3.4 Summary

Overall, TPU recorded lower MIU and SMD than TPE polymers with 70A measuring the lowest MIU/SMD at 240°C printing temperatures followed by 82A at 240°C. 70A 240°C also recorded the highest peel resistance among all polymers printed at 240°C. Meanwhile a higher peel resistance can be achieved when printing 82A polymers at 250/260°C, the adhesion quality compromised the surface quality and consistency of the print. Furthermore, 70A 240°C was

also able to provide comparable adhesion quality with 82A 250°C specimens. Therefore, to maximize peel resistance while maintain print surface quality, 70A 240°C and 82A 240°C can both be used to further develop 4DP PTC.

4.2.3 Characterisation and evaluation

4.2.3.1 T-peel test for peel resistance

PTCs are advantageous over polymer only 3DP textiles because it possesses the flexibility, elasticity and characteristics of conventional fabrics (Goncu-Berk et al., 2020) but with the added potential for the customisation of a fabric's tensile strength, stiffness or embed smart sensors that is not attainable with traditional knitting or weaving (Kabir et al., 2020a). Due to the nature of 4DP textiles and PTC being a multi-material composite, the adhesion between materials highly influences its structural properties. Studies have compared AM processes with welding in which the polymers are melted into molten material enabling the penetration of polymers into fabric pores (Sanatgar et al., 2017). Conditions that influence the quality of adhesion include polymer and shore hardness (Korger et al., 2020; Loh et al., 2021; Mpofu et al., 2019; Uysal & Stubbs, 2019), printing temperature and speed (Gorlachova & Mahltig, 2021), fabric treatments (Kozior et al., 2018; Störmer et al., 2021), z-axis height (Rivera et al., 2017), shape and size of polymer (Goncu-Berk et al., 2020) and environmental conditions (Korger et al., 2020). Though, results from existing studies have been inconsistent due to the lack of standardized testing. Thus, Goncu-Berk et al. (2020) have suggested testing of specimens with at least five repetitions to improve the reliability of the results.
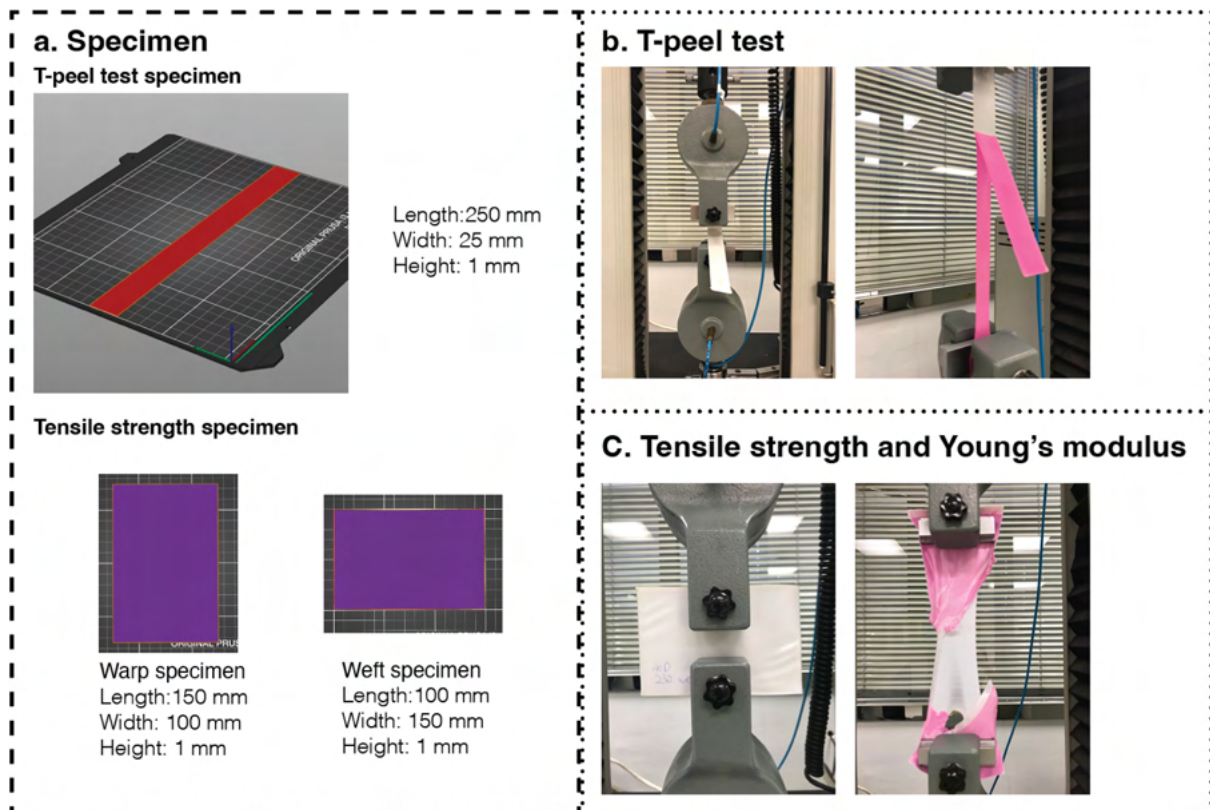
Figure 4-4 a. T-peel test specimen and tensile strength specimen specifications, b. T-peel test setup, c. tensile strength and Young's modulus test setup (Cheung & Choi, 2022; Cheung et al., 2024)

The 3DP test strip was designed in accordance with ISO 11339:2022 standards (**Figure 4-4**). According to ISO, the specimens can be prepared individually or cut from bonded laminates and are standardized at 25 mm ± 0.5 mm width, ≥ 150 mm length (bonded areas), and an additional ≥ 50 mm (unbonded ends) with a total length of ≥ 200 mm. ISO also recommends flexible adherends to have thicknesses of 0.5 mm ± 0.02 mm (ISO, 2022b). Our samples were prepared to utilize the width of the machine's build platform (250 mm) with a bonded length of ≥ 200 mm. By testing longer bonded lengths, we can collect data at higher levels of precision (i.e., disregarding the first & last 25 mm and allowing the average force curve to reach a smooth level before taking data) and note the type of failure according to ISO 10365:2022 (ISO, 2022a). This test was developed to test the relative peel resistance of bonded assemblies of flexible adherend (ISO, 2022b). ISO defines flexible adherend as specimens that have physical

properties that allow bending up to 90° without cracking or breaking. The general principle is that a force is applied to the unbonded ends of the sample in opposite directions until both ends are perpendicular to form a T-shape. The adherend were separated uniformly along the bonded strip at a steady rate of 100 mm/min.

To test for material combination's influence on adhesion three polymers TPU 70A, 82A and TPE 40D were tested on seven different textile substrates composed of natural and synthetic fibres with different textile structures and thicknesses. The experiment was set up according to ISO 11339:2022 (ISO, 2022b) and the samples were fabricated to adhere to ISO's standards. **Table 4-10** indicates the various processing parameters for this experiment. To identify whether material partners influenced adhesion in PTC, extrusion temperature, print thickness of the polymer layer, and speed were kept constant (Z-axis varied according to fabric thickness). Through studying material partners independently while keeping printing parameters constant we were able to identify whether i) polymers or textile substrates affected adhesion, ii) surface roughness and friction of textile substrates affected adhesion and whether iii) polymer penetration depth led to stronger peel resistance. For this experiment, a total of 105 samples were printed constituting three types of polymers printed on seven different textile substrates each with five repetitions to test for the influence of material partners (polymer and textile substrate) on peel resistance.

Table 4-10 3DP specimens on various textile substrates under default flex printing conditions

ID	Fibre	TPU (70A/82A)				TPE (40D)			
		Extrusion temperature	*Print thickness*	*Z-axis [mm]*	*Speed*	*Extrusion temperature*	*Print thickness*	*Z-axis [mm]*	*Speed*
T1	*Synthetic*	*240°C*	0.50 mm	-1.500	20 mm/s	*240°C*	0.50 mm	-1.500	20 mm/s
T2	*Natural*	*240°C*	0.50 mm	-1.500	20 mm/s	*240°C*	0.50 mm	-1.500	20 mm/s
T3	*Natural*	*240°C*	0.50 mm	-1.500	20 mm/s	*240°C*	0.50 mm	-1.500	20 mm/s
T4	*Natural*	*240°C*	0.50 mm	-1.200	20 mm/s	*240°C*	0.50 mm	-1.200	20 mm/s

T5	_Natural_	_240°C_	0.50 mm	-1.000	20 mm/s	_240°C_	0.50 mm	-1.000	20 mm/s
T6	_Synthetic_	_240°C_	0.50 mm	-0.800	20 mm/s	_240°C_	0.50 mm	-0.800	20 mm/s
T7	_Synthetic_	_240°C_	0.50 mm	-1.500	20 mm/s	_240°C_	0.50 mm	-1.500	20 mm/s

The results were expressed as (N) and to calculate the peel strength, the average peel force (N) was divided by the specimen width (25 mm) and expressed as (N/mm). And the T-peel tests were conducted in a controlled environment on an Instron 4411 tensile testing machine with a maximum load capacity of 5KN (Instron, 1996). The laboratory was regulated to a temperature of 23°C with a relative humidity of 65% adhering to the constant atmospheric conditions set by ISO 291:2008 (ISO, 2008b). An iPhone 7 camera was used to monitor the process.

4.2.3.2 Cross-sectional microscopic analysis

Cross-sectional Microscopic analysis was used to analyse the depth of penetration of polymers on textile substrates. The samples were analysed at a scale of 500 μm using a Leica M165c digital microscope. The images were further examined using Leica Application Suite V4.13.0 (Microsystems, n.d.). To evaluate the penetration depth of the polymers and its thickness consistency, three points within the microscopic region were measured – minimum/maximum depth of polymer layer and total thickness of polymer with textile substrate.

In previous experiments, peel resistance was observed to increase as i) extrusion temperature was increased, ii) knitted structure textile was used as base material for PTC, and iii) polymers with lower shore hardness tended to create stronger adhesion with textiles substrates. To understand these phenomena, textile specimens were examined under cross-sectional microscopic analysis. The samples were analysed under a scale of 500 μm using a Leica M165c digital microscope and images were further analysed on Leica Application Suite V4.13.0 (Microsystems, n.d.). To evaluate the depth of penetration and polymer thickness consistency,

three points within the microscopic area were measured (minimum/maximum depth of polymer layer and the total thickness of polymer and textile substrate).

4.3 Results and discussion

4.3.1 Influence of material on peel resistance

4.3.1.1 Peel resistance

For the evaluation of optimal material combinations, a total of 75 samples (5 per material combination) were printed under default flex printing settings and tested in accordance with ISO 11339:2022. 82A TPU and 40D TPE were printed on all textile substrates meanwhile 70A was only printed on T1 as the polymer did not adhere to any of the other substrates through repetitive trials which often led to the clogging of the extruder head caused by the poor polar interaction between 70A TPU with the fabrics. **Table 4-11** shows the results that were collected during the T-peel tests. As advised by ISO, the data collected during the first and last 25 mm of the tests were disregarded when determining from the recorded curve for more precise data. The minimum, maximum, and average value were recorded in newtons (N) and the peel strength was presented as N/mm. **Figure 4-5** illustrates the maximum peel resistance and averaged peel strength of the material combinations. In addition, **Figure 4-6** shows the peel force/distance for all material combinations.

Table 4-11 Average peel forces and strengths of polymer-textile composite samples

ID	Peel force (N)						Minimum load (N)	Peel strength (N/mm)		
	Maximum load (N)			Average value (N)						
	TPU 70A	TPU 82A	TPE 40D	TPU 70A	TPU 82A	TPE 40D		TPU 70A	TPU 82A	TPE 40D
T1	95.70	46.80	22.10	69.00	34.10	16.50		2.80	1.36	0.70
T2		13.30	2.80		10.80	2.10			0.43	0.08
T3		10.90	4.69		3.70	3.18	0		0.15	0.13
T4		3.35	5.63		2.41	3.53			0.10	0.14
T5		6.57	3.75		1.36	3.19			0.05	0.13
T6		10.60	39.59		9.16	33.82			0.37	1.60
T7		63.80	13.28		47.6	10.84			1.90	0.43

Note: - N = newton; load values are rounded to nearest digit
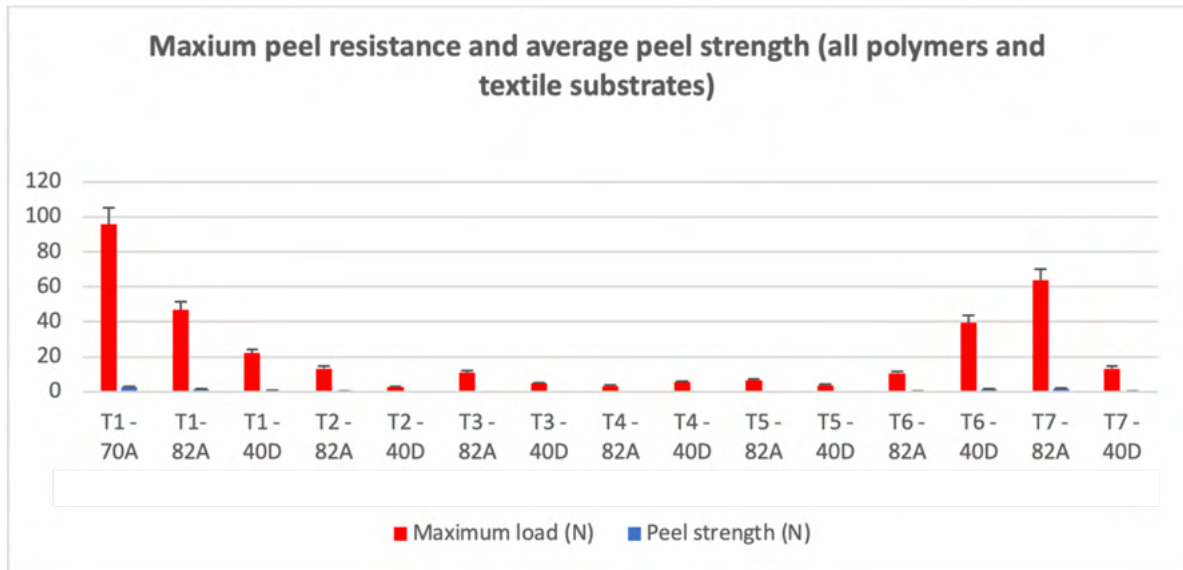
Figure 4-5 Maximum peel resistance and average peel strength for all polymer and textile substrate combinations at default printing temperature

Textile structure and polymer type were found to influence peel resistance in 3DP PTC. The results indicate textile substrates T1, T2, and T7 (synthetic knitted fabrics) to yield significantly higher maximum load and averaged peel strength than woven substrates (T3, T4, and T5) (**Figure 4-5**). In addition, the polymers with lower shore hardness (70A and 82A TPU) was also able to yield much higher peel resistance than 40D TPE combinations. T1-70A combinations were able to yield a maximum peel resistance of 95.70 N with an average peel strength of 2.89 N/mm followed by T7-82A with a maximum resistance of 63.80 N and 1.90 N/mm average peel strength and T1-82A combinations at 46.80 N maximum resistance with an average peel strength of 1.36 N/mm. On the other hand, in woven 3DP PTC combinations, T2-TPU highest maximum load of 13.30 N with an average peel strength of 0.43 N/mm. Overall, the results suggest softer polymers with synthetic knitted textile substrate combinations to produce significantly higher peel resistance than harder polymer and woven textile combinations.
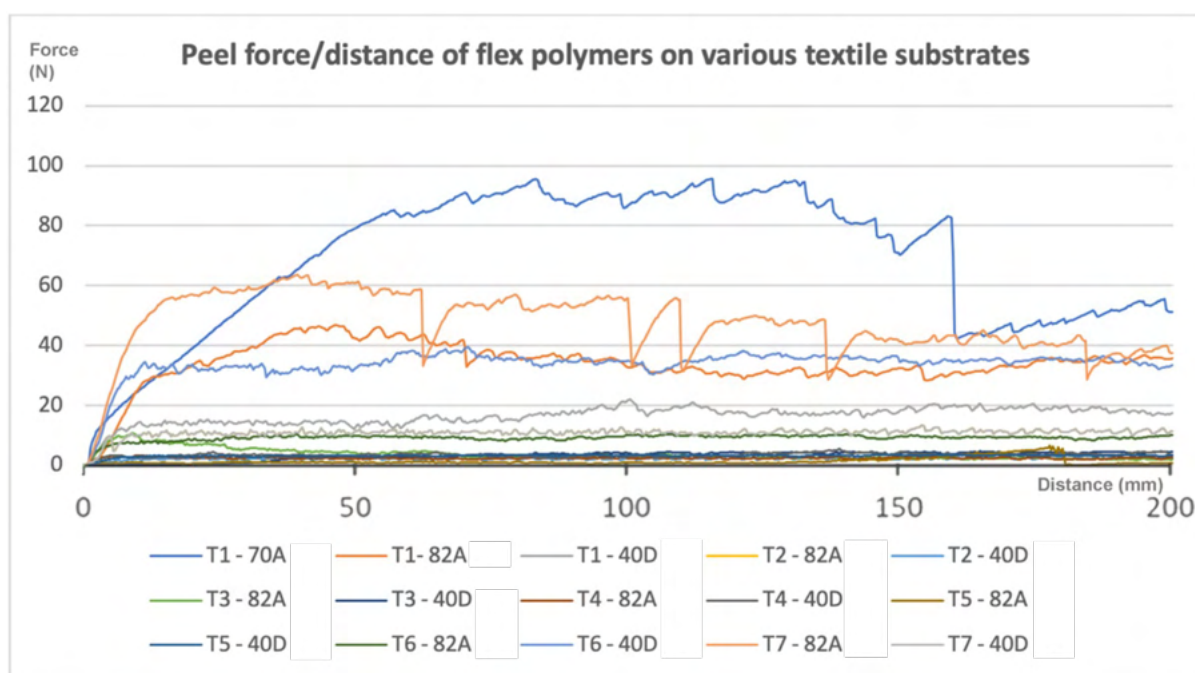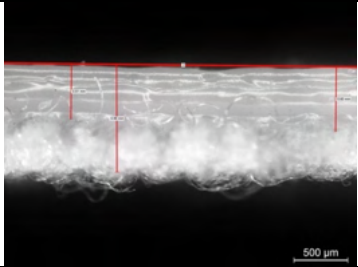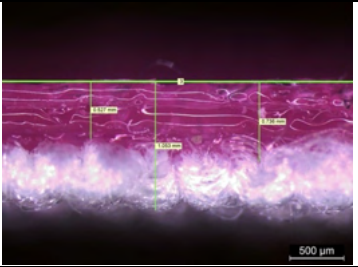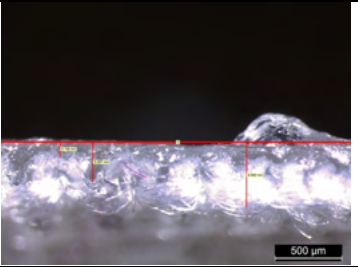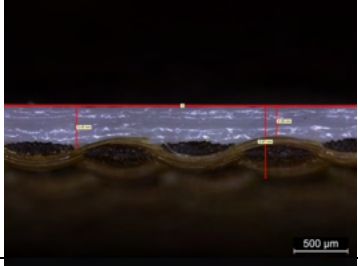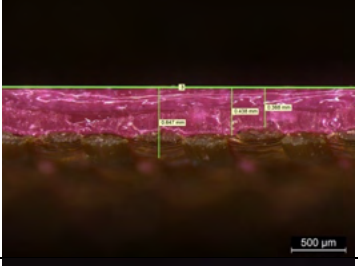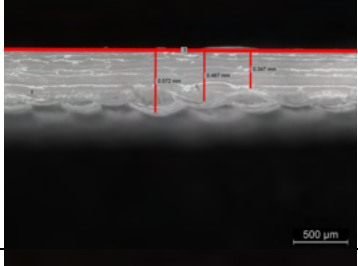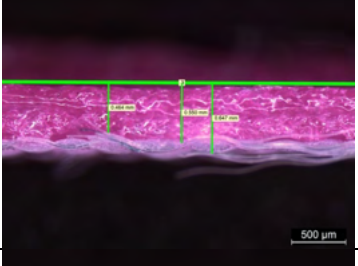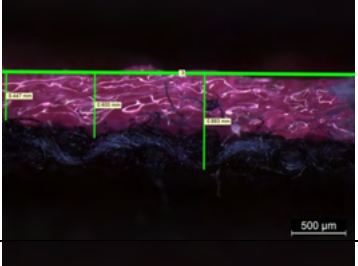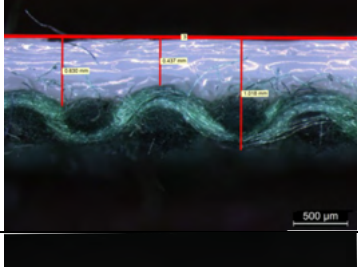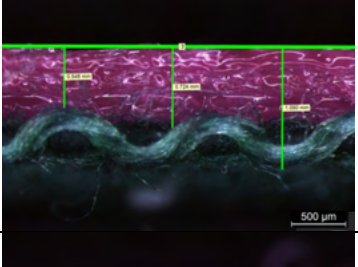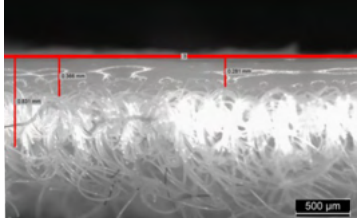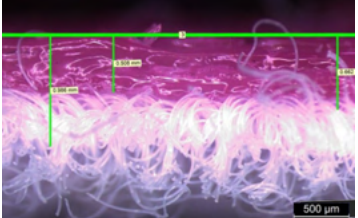
Figure 4-6 Peel force/distance comparison for all polymers and textile substrate combinations at default printing temperature
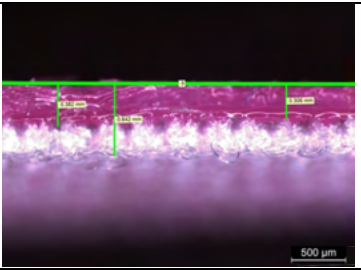
Figure 4-6 illustrates the peel force/distance comparison for all polymer and textile substrate combinations printed at default flex settings. All 3DP PTC specimens demonstrated a consistent peel resistance reflecting the gradual separation of the polymer layer from the textile substrate. In addition, there was also no damage found on either material apart from T1-70A and T7-82A where there was a cohesive failure caused by the fracture of the adherend (textile substrate) causing a sudden dip in peel resistance. Overall, the specimens recorded peel resistance of > 20 N apart from combinations T1-70A, T1-82A, T6-40D, and T7 82A.

4.3.1.2 Cross-sectional microscopic analysis

The first series of microscopic analysis shown in **Table 4-12** corresponds to the experiments where various polymers were printed on a wide array of textile substrates (T1 to T7) at default settings.

Table 4-12 Cross-sectional microscopic analysis of PTC samples

Fabric	TPE (40D)	TPU (82A)	TPU (70A)
T1			
T2			
T3			
T4			
T5			
T6			

Fabric	MAX	MIN	Total	MAX	MIN	Total	MAX	MIN	Total
T7 (images)									
T1	0.61 mm	0.58 mm	0.99 mm	0.74 mm	0.53 mm	1.05 mm	0.30 mm	0.11 mm	0.50 mm
T2	0.34 mm	0.21 mm	0.67 mm	0.44 mm	0.37 mm	0.65 mm			
T3	0.47 mm	0.35 mm	0.57 mm	0.55 mm	0.46 mm	0.65 mm			
T4	0.63 mm	0.45 mm	0.92 mm	0.60 mm	0.45 mm	0.88 mm			
T5	0.63 mm	0.44 mm	1.02 mm	0.72 mm	0.55 mm	1.09 mm			
T6	0.37 mm	0.28 mm	0.83 mm	0.66 mm	0.51 mm	0.97 mm			
T7	0.47 mm	0.28 mm	0.59 mm	0.38 mm	0.31 mm	0.64 mm			

MAX – maximum polymer depth; MIN – minimum polymer depth; Total – total thickness of polymer and fabric

The results in **Table 4-12** indicate TPE polymers to have a further depth of penetration than TPU polymers across all textile substrates. The variance between minimum/maximum depth across TPU samples ranged from 0.03 mm to 0.19 mm. And the variance between minimum/maximum depth across TPE samples ranged from 0.07 mm to 0.21 mm. For TPE polymers, the difference between minimum/maximum depth was lowest at 0.03 mm for T1, indicating a polymer thickness consistency. Meanwhile, T5 and T7 specimens had the highest difference between depth measurements caused by the uneven surface roughness of the textile substrates.

On the other hand, among TPU, T2 and T7 measured with the lowest variance between penetration depth at 0.07 mm indicating a polymer thickness consistency. Meanwhile, T1 recorded the highest depth variation at 0.21 mm caused by the rougher surface of the textile structure in the weft direction. The variance in surface roughness between warp/weft directions in textile substrates is seen to increase polymer penetration into the uneven surface crevices of the fabrics. T4/T5 samples (woven/natural) though have similar depth of penetration with T6/T7 (knit/synthetic) yielded inferior peel resistance. Thus, the depth of penetration alone

cannot be accounted for the quality of adhesion, other factors like fibre content and structure are also variables that affect adhesion.

4.3.1.3 Summary

The results from the experiments suggest both polymer type and textile structure to influence peel resistance in 3DP PTC. Synthetics fabrics typically have greater polar interactions with polyester based TPU than natural fibres due to the forming of covalent links with polyester fibres (Schollenberger, 2000). During printing, TPU's backbone chain containing polar/nonpolar substances are moulded repeatedly under heat during printing to form tight polymer chains with the textiles without the need of a coupling agent for adhesion. Moreover, the results also indicated knitted structures to yield stronger adhesion than wovens due to the likelihood for polymers to penetrate the knitted pores yielding better adhesion between polymer and textile which was also suggested in previous studies (Sanatgar et al., 2017). All specimens demonstrated a consistent peel resistance reflecting the gradual separation of the polymer layer from the textile substrate. No damage to the specimens was found apart from T1-70A and T7-82A as aforementioned.

Existing studies have suggested a stronger interpenetration of PLA polymer into fabric to improve peel resistance (Gorlachova & Mahltig, 2021). However, this was not the same case for TPE polymers, in our experiments, this variance between depths which indicate a further depth of polymer penetration did not always increase the peel resistance. The results suggest that depth of penetration only improved peel resistance if the fabric was a i) knitted structure, ii) synthetic, or iii) a synthetic knitted fabric). Therefore, depth of penetration measurements alone cannot be used to determine the peel strength for TPE PTC. Regardless of penetration

depth, knit, synthetics, or knitted synthetic combinations remain superior in adhesion strength in both TPU and TPE specimens.

4.3.2 Influence of extrusion temperature on peel resistance

4.3.2.1 Peel resistance

The results from the first set of experiments using default flex printing conditions have established a baseline for comparing with further experiments. To identify whether 3DP parameters influenced adhesion between textile and polymer, further experiments investigated processing parameters i.e., extrusion temperature. **Table 4-13** shows PTC specimens printed under various temperature conditions ranging from 220°C to 260°C. During such experiments, 82A TPU and 40D TPE were printed at above-recommended extrusion temperatures to see if it can further enhance adhesion in PTC. Meanwhile 70A TPU was printed only at 220°C and 240°C because the polymer was unprintable at temperatures beyond 240°C (higher temperature causing over extrusion which clogged the printer nozzle). Existing studies lack exploration into testing how different extrusion temperatures can influence peel resistance in PTC (Goncu-Berk et al., 2020; Korger et al., 2020; Loh et al., 2021) and whether polymers extruder at various temperatures affected its surface quality. Through comparing the peel resistance results from different printing temperatures will help identify its effects on peel resistance and which material combinations are shown to achieve the highest peel resistance. Textile substrates T1 to T7 used in this study encompasses an array of knitted and woven structures composed of synthetic and natural fibres which are commonly used in ready-to-wear, athleisurewear and sportwear garments.

Table 4-13 Polymer-textile composite samples under other temperature parameters

Textile substrate	Extrusion temperature	TPU (70A)			TPU (82A) and TPE (40D)		
		Z-axis [mm]	*Print thickness* [mm]	*Speed* [mm/s]	*Z-axis* [mm]	*Print thickness* [mm]	*Speed* [mm/s]
T1	*220°C - 260°C*	-1.500	0.50	20	-1.500	0.50	20
T2	*220°C - 260°C*				-1.500	0.50	20
T3	*220°C - 260°C*				-1.500	0.50	20
T4	*220°C - 260°C*		**n/a**		-1.200	0.50	20
T5	*220°C - 260°C*				-1.000	0.50	20
T6	*220°C - 260°C*				-0.800	0.50	20
T7	*220°C - 260°C*				-1.500	0.50	20

All polymer types (70A, 82A TPU, and 40D TPE) along with the top performing knitted and woven fabrics (T1 and T2) were carried forward in this part of the experiment. In this experiment the objective was to examine and identify printing temperature's effects on adhesion. Temperature settings ranging from 220°C to 260°C in increments of 20°C (apart from the 250°C samples which was the maximum recommended temperature for 82A TPU and 40D TPE). Previous research has suggested higher temperatures to affect adhesion force in PLA-textile combinations (Spahiu et al., 2017) and yet to explore beyond recommended temperatures fearing that it might cause damage to the textile substrate (Loh et al., 2021). However, textile substrates (T1, T2) used in this experiment is highly resilient with a melting point of 268.8°C (Craftech, 2013). Therefore, in this study, temperatures beyond recommended settings were also experimented with to identify whether further temperature increase can enhance peel resistance in PTC. However, the 70A TPU was only tested from 220°C to 240°C temperatures due to its lower melting point and recommended settings (the polymer also over extruded at temperatures above 240°C making it difficult to print accurately and caused clogging to the extruder). **Table 4-14** shows the results from fine-tuning temperature settings to achieve optimal adhesion.

Table 4-14 Results from T-peel tests in accordance with ISO 11339:2022

ID	Peel force (N)									Minimum load (N)	Peel strength (N/mm)		
	Maximum load (N)			Average value (N)			SD (N)						
	TPU 70A	TPU 82A	TPE 40D	TPU 70A	TPU 82A	TPE 40D	TPU 70A	TPU 82A	TPE 40D		TPU 70A	TPU 82A	TPE 40D
T1 (220°C; -1.100 mm)	59.00	42.10	24.80	29.40	32.20	6.40	11.90	7.33	2.67		1.18	1.30	0.26
T1 (240°C; -1.100 mm)	95.70	46.80	22.10	69.00	34.10	16.50	22.94	7.38	3.00		2.80	1.36	0.70
T1 (250°C; -1.100 mm)		89.30	50.20		77.20	41.80		18.00	6.71			3.10	1.70
T1 (260°C; -1.100 mm)		120.30	62.00		82.00	43.10		14.08	8.81	0		3.28	1.72
T2 (220°C; -1.500 mm)		8.50	2.40		6.30	1.90		1.22	0.42			0.25	0.08
T2 (240°C; -1.100 mm)		13.30	2.80		10.80	2.10		1.44	0.35			0.43	0.08
T2 (250°C; -1.500 mm)		34.20	3.40		20.20	2.50		5.31	0.64			0.81	0.10
T2 (260°C; -1.500 mm)		84.00	4.20		53.80	2.90		19.20	0.56			2.15	0.12

Note: - N = newton; load values are rounded to nearest digit; SD = standard deviation

The results shown in **Table 4-14** and **Figures 4-7** indicate printing temperature to have significant effects on adhesion quality in T1 PTC. At lower temperature ranges for T1 composites (220°C and 240°C), 70A TPU measured significantly higher maximum peel resistance (up to 200% and 496% respectively) than 82A TPU and 40D TPE. However, 82A TPU recorded marginally higher averaged peel strength than 70A TPU. Though both TPUs had significantly better adhesion than 40D TPE at 454% (70A TPU) and 500% (82A TPE). Meanwhile, at 240°C printing temperature, 70A TPU outperformed all polymers in maximum peel resistance by 204% (82A TPU) and 433% (40D TPE) and averaged peel strength by 206% (82A TPU) and 400% (40D TPE) with comparable peel resistance with 82A TPU at 250°C settings. Moreover, at 250°C, 82A TPU measured 178% higher maximum peel resistance than

40D TPE with 182% higher averaged peel strength. And at 260°C, 82A TPU measured 194% higher maximum peel resistance than 40D TPE with 191% higher averaged peel strength.
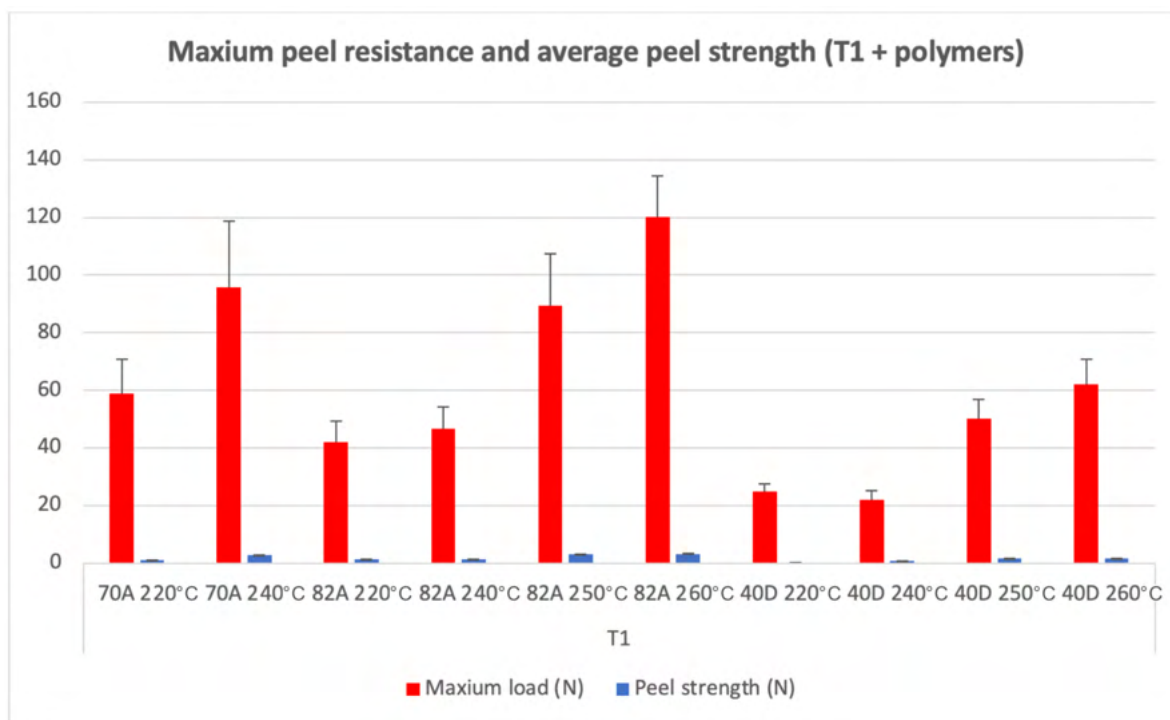
Figure 4-7 Maximum peel resistance and average peel strength (T1 + polymers)

Table 4-14 and **Figure 4-8** also indicate printing temperature to have significant effects on adhesion quality in both T2 PTC. Overall, 82A TPU measured significantly higher peel resistance than 40D TPE PTC. At 220°C 82A TPU yielded 354% higher maximum peel resistance and 313% higher averaged peel strength. And at 240°C settings, 82A TPU measured 475% higher peel resistance than 40D TPE PTC with 538% higher averaged peel strength. Moreover at 250°C, 82A TPU measured over 10 times higher peel resistance than 40D TPE PTC with over 810% higher averaged peel strength. Furthermore, at 260°C, 82A TPU measured over 20 times higher peel resistance than 40D TPE PTC with over 17.9 times higher averaged peel strength.
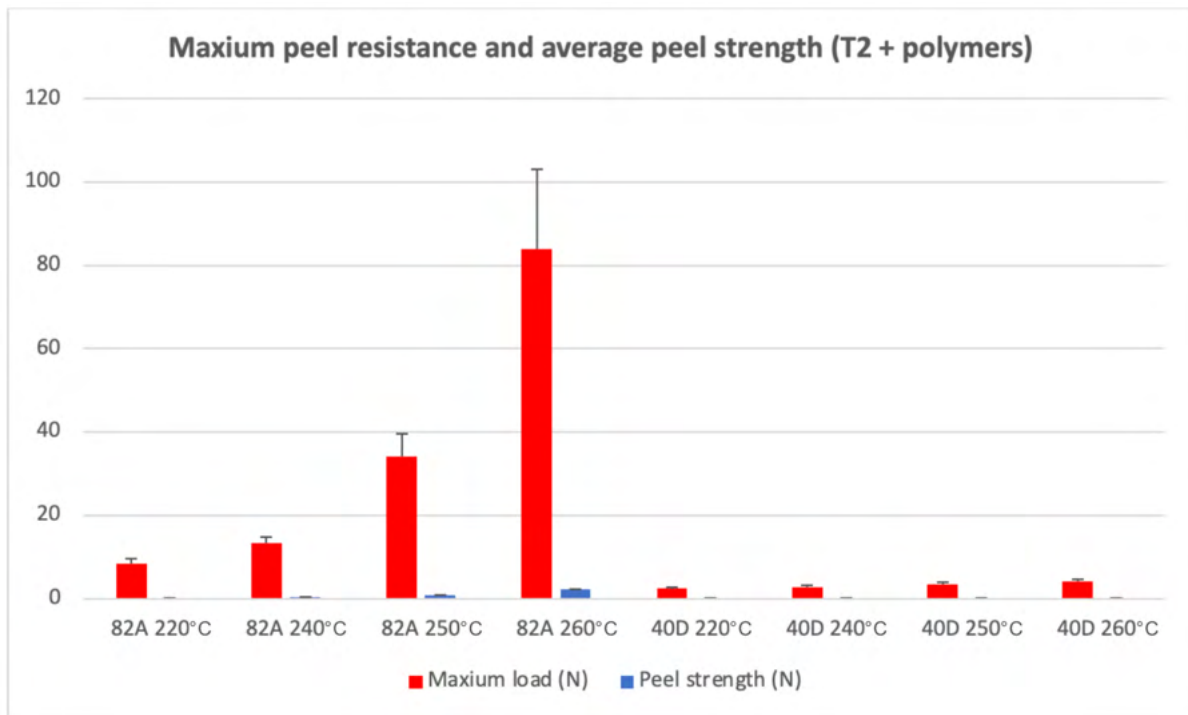
Figure 4-8 Maximum peel resistance and average peel strength (T2 + polymers)

Figure 4-9 and **4-10** illustrates the peel force/distance comparison for T1-70A, T1-82A, T1-40D, T2-82A, and T2-40D at various temperatures ranging from 220°C to 260°C. All specimens demonstrated a consistent peel resistance reflecting the gradual separation of the polymer layer from the textile substrate. In addition, there was also no damage found on either material apart from T1-70A at 240°C where there was a cohesive failure caused by the fracture of the adherend (textile substrate) causing a sudden dip in peel resistance. Overall, for T1 specimens 82A at 250°C and 260°C yielded significantly higher peel resistance compared with other specimens, however 70A was also able to yield comparable results at 240°C. On the other hand, for T2 specimens, 82A at 260°C achieved significantly higher peel resistance compared with other temperature settings which was followed by 82A at 250°C and 240°C.
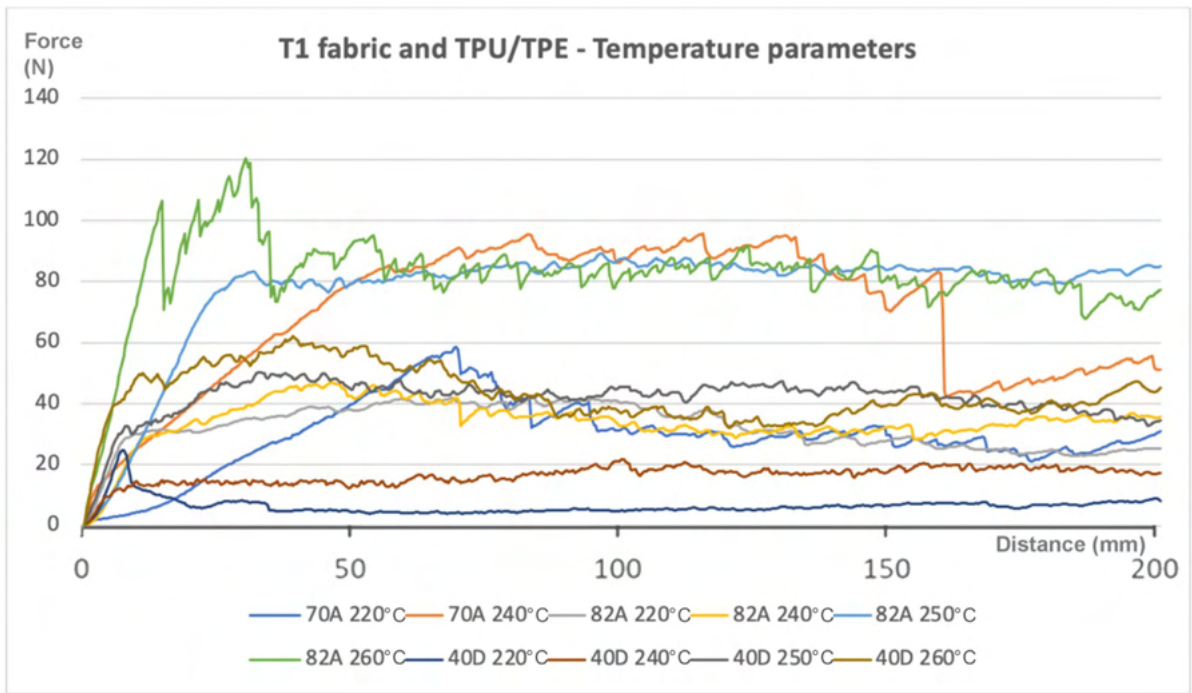
Figure 4-9 Peel force/distance comparison under different temperatures (T1 + polymers)
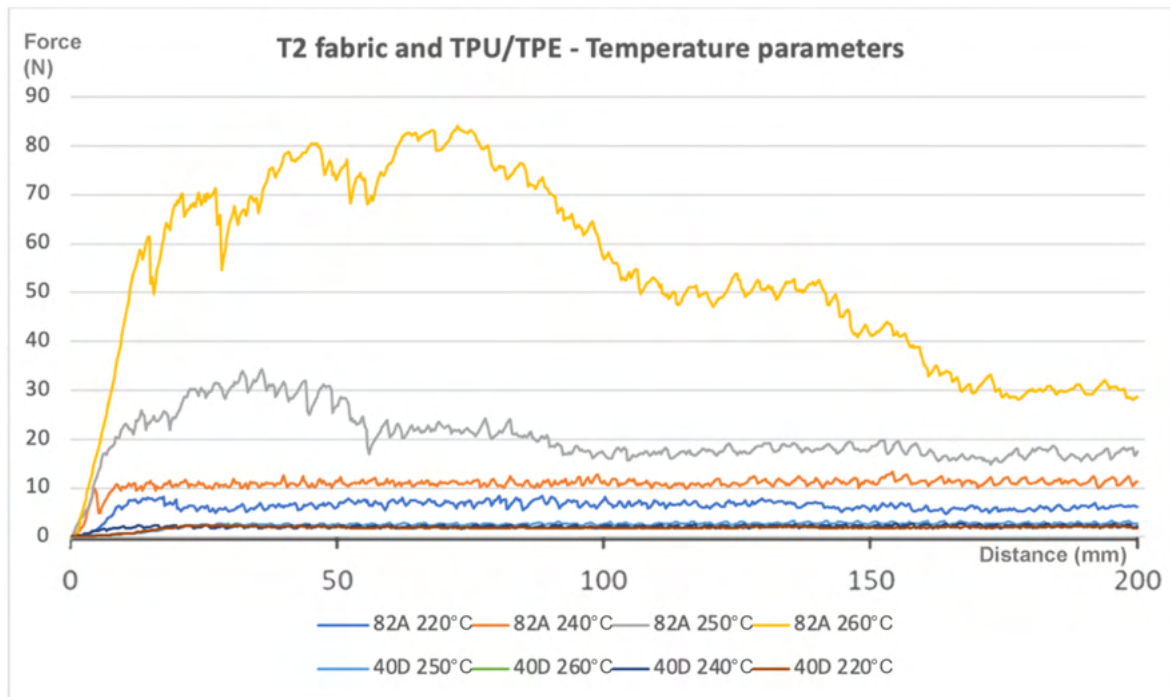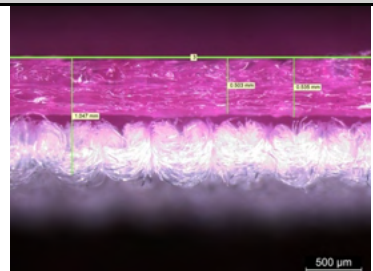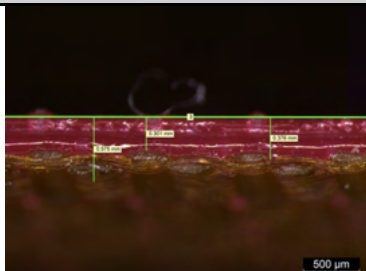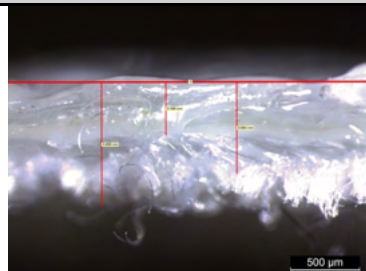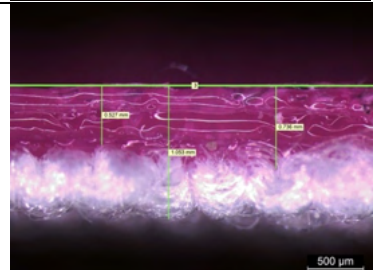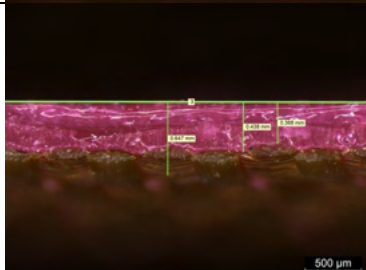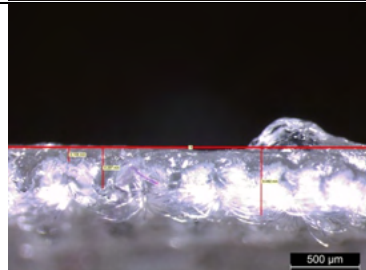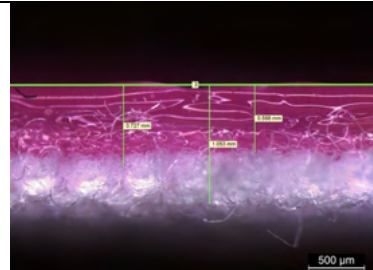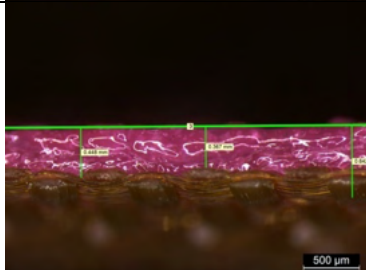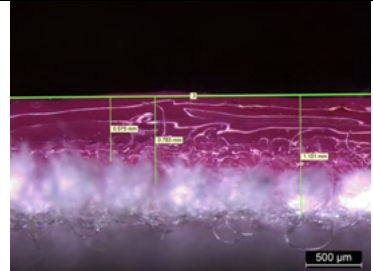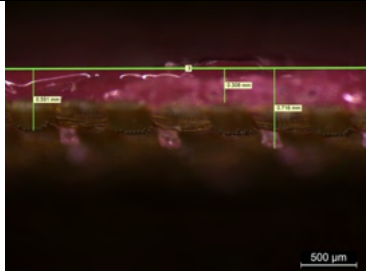
Figure 4-10 Peel force/distance comparison under different temperatures (T2 + polymers)

4.3.2.2 Cross-sectional microscopic analysis

Table 4-15 and **4-16** shows cross-sectional microscopic images from the experiments where polymers were printed on a knitted (T1) and woven (T2) textile substrate at temperatures ranging from 220°C to 260°C. **Table 4-15** contains images of TPU-T1/T2 (70A and 82A) combinations and **Table 4-16** contains images of TPE-T1/T2 combinations.

Table 4-15 Cross-sectional microscopic analysis of PTC samples (TPU)

Extrusion temperature	T1-TPU (knit 82A)	T2-TPU (woven 82A)	T1-TPU (knit 70A)
220°C			
240°C			
250°C			
260°C			

Extrusion temperature	MAX	MIN	Total	MAX	MIN	Total	MAX	MIN	Total
220°C	0.54 mm	0.50 mm	1.05 mm	0.38 mm	0.30 mm	0.58 mm	0.66 mm	0.37 mm	0.90 mm

240°C	0.74 mm	0.53 mm	1.05 mm	0.44 mm	0.37 mm	0.65 mm	0.30 mm	0.11 mm	0.50 mm
250°C	0.74 mm	0.60 mm	1.05 mm	0.45 mm	0.37 mm	0.64 mm			
260°C	0.78 mm	0.58 mm	1.10 mm	0.72 mm	0.31 mm	0.55 mm			

MAX – maximum polymer depth; MIN – minimum polymer depth; Total – total thickness of polymer and fabric
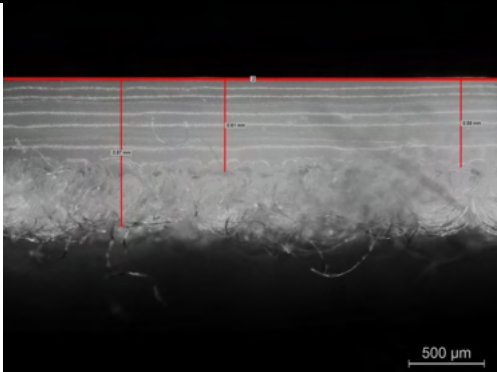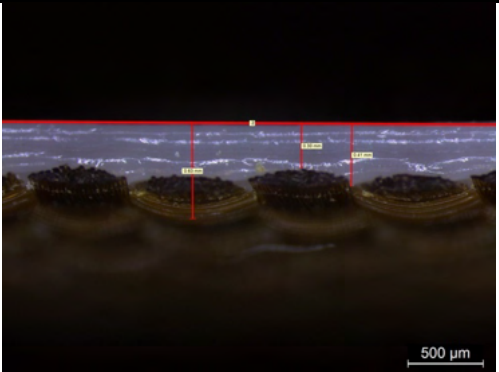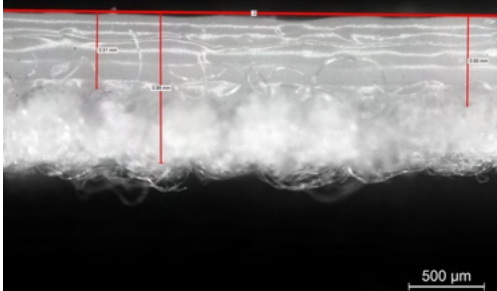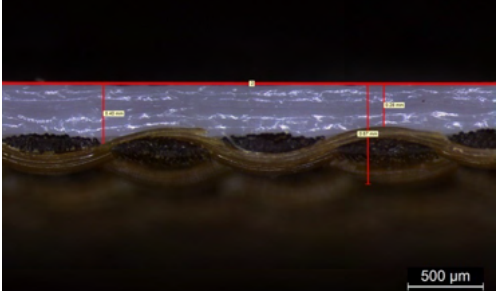
Table 4-15 indicated an increase in maximum polymer depth as the extrusion temperature was increased for 82A TPU, meanwhile the opposite was found in 70A TPU. The variance between minimum/maximum depth across T1 samples ranged from 0.04 mm to 0.29 mm. At 220°C, the difference between minimum/maximum depth was the lowest at 0.04 mm, suggesting a print thickness consistency for 82A TPU, meanwhile for 70A TPU a difference of 0.29 mm was found. For the 70A TPU a lower difference in depth was found at 240°C. Moreover, the 260°C sample (82A TPU) measured with the highest maximum depth at 0.78 mm for 82A TPU, while the lowest maximum depth was shown on the 220°C sample at 0.54 mm. This difference in maximum depth was partly caused by greater penetration of the polymer into the pores of the knitted structure but also due to the CTE of the TPU layer (total thickness from 1.05 mm to 1.10 mm).
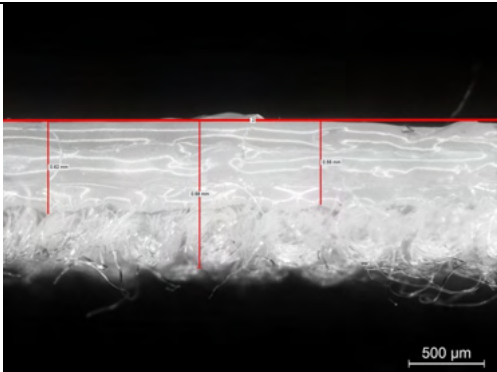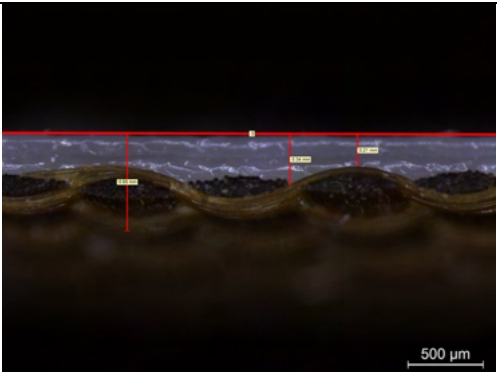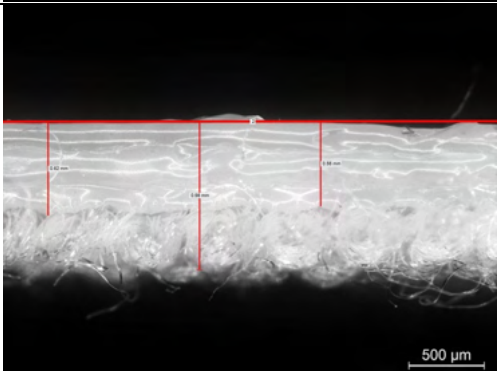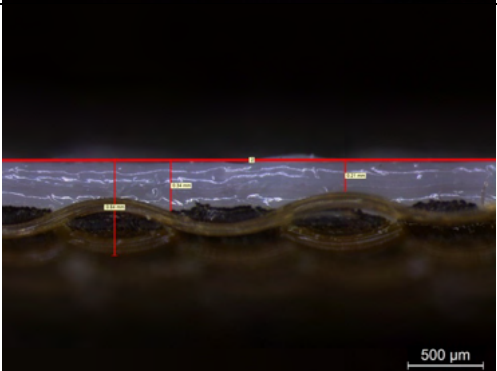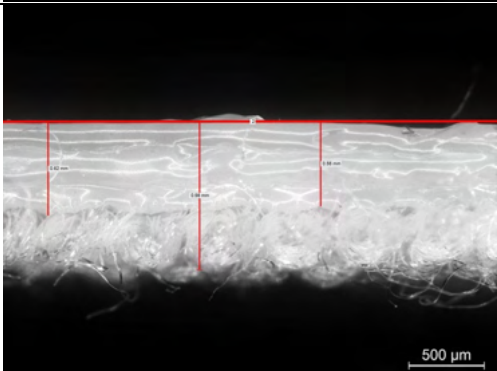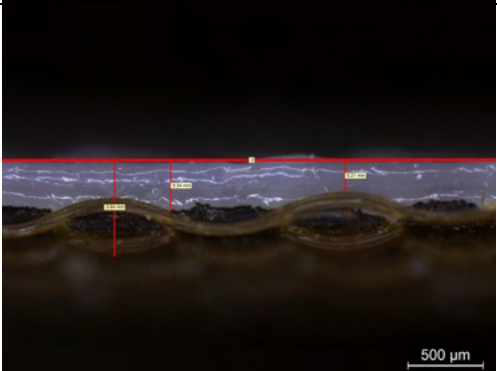
At 220°C, the 82A TPU layer sits atop the knitted loops, and a crevice between the polymer and textile substrate can be observed, while the 70A TPU is able to penetrate the knitted pores. This gap between polymer-textile was not observed in the T1-TPE 220°C sample (**Table 4-16**), even though our T-peel results suggested T1-TPU poses a higher peel resistance compared with T1-TPE samples. This phenomenon was caused by TPU being an ionomer, made up of small ionic groups along its backbone chain containing both polar/nonpolar substances and can be processed and moulded repeatedly to form tight polymer chains (Drobny, 2014). With nylon which happens to be highly polar, TPU-nylon can interact well even without the presence of a coupling agent for adhesion (Miachalovic, 2022), forming covalent bonds under heat. And at 240/250/260°C, both the 82A and 70A TPU were fully merged into the knitted pores.

On the other hand, T2 samples (with 82A TPU) displayed a difference between minimum/maximum depth of polymer ranging from 0.07 mm to 0.41 mm. As aforementioned the 70A TPU was not printable onto T2. The difference between the minimum/maximum depth was the lowest at 0.07 mm on the 240°C sample suggesting a more consistent print thickness. Meanwhile, the 260°C sample showed a significantly higher maximum depth of polymer at 0.72 mm. TPE polymers managed to penetrate through the woven structure at 260°C forming globules below the surface of the textile substrate (causing the significant peel resistance in comparison with other temperatures).

Table 4-16 Cross-sectional microscopic analysis of PTC samples (TPE)

Extrusion temperature	T1-TPE (knit)	T2-TPE (woven)
220°C		
240°C		

Extrusion temperature	MAX	MIN	Total	MAX	MIN	Total
220°C	0.60 mm	0.51 mm	0.97 mm	0.34 mm	0.21 mm	0.63 mm
240°C	0.61 mm	0.58 mm	0.99 mm	0.34 mm	0.21 mm	0.67 mm
250°C	0.62 mm	0.56 mm	0.98 mm	0.40 mm	0.28 mm	0.65 mm
260°C	0.64 mm	0.53 mm	0.99 mm	0.41 mm	0.30 mm	0.64 mm

MAX – maximum polymer depth; MIN – minimum polymer depth; Total – total thickness of polymer and fabric

Similarly, **Table 4-16** (TPE results) indicated an increase in maximum polymer depth as the extrusion temperature was increased in both T1 and T2 textile substrates. However, from the cross-sectional images, no significant increase in penetration depth was observed, and there was a negligible difference in the total thickness of the polymer-textile across samples with a maximum difference of 0.02 mm. The variance between the maximum and the minimum depth of polymer across T1 samples ranged from 0.03 mm to 0.11 mm. At 240°C, the minimum/maximum depth difference was the lowest at 0.03 mm, suggesting a polymer thickness consistency. Furthermore, the 260°C sample measured the highest maximum depth at 0.64 mm, while the lowest maximum depth was shown in the 220°C sample at 0.60 mm. This increase in the polymer layer was caused by a CTE, where polymers expanded at higher temperatures (Drobny, 2014).

On the other hand, T2 samples showed a difference between minimum/maximum depth of polymer ranging from 0.11 mm to 0.13 mm. Among T2 samples, the difference in total thickness across samples was also insignificant, with a maximum difference at 0.04 mm. The difference between the minimum/maximum depth was the lowest at 0.11 mm on the 260°C sample suggesting a more consistent polymer layer thickness. The highest maximum depth was shown on the 260°C sample at 0.41 mm; meanwhile, at 220°C and 240°C, a 0.34 mm depth was recorded. Again, this increase in polymer thickness was caused by CTE of the polymer at higher temperatures. However, from the cross-sectional images, we do not observe the same irregularity of the surface seen in the T1 samples.

4.3.2.3 Summary

In this experiment, the results have shown extrusion temperature to have significant effects on peel resistance in T1 and T2 PTC. PTC with TPU polymers tended to measure significantly higher maximum peel resistance and averaged peel strength than TPE polymer combinations. Higher temperatures (250/260°C) also tended to measure significantly higher peel resistance than lower temperature ranges (220/240°C). And at default flex printing temperature (240°C), 70A TPU recorded significantly higher resistance than 82A TPU and 40D TPE for T1 PTC. Meanwhile for T2 PTC 82A TPU recorded significantly higher peel resistance (up to 20 times stronger) than 40D TPE PTC (though 70A TPU did not adhere to T2 in preliminary tests therefore not further experimented with). T1 knitted fabrics also demonstrated superior peel resistance compared with T2 woven fabrics. Overall, the results suggest T1-TPU combinations and higher temperature ranges to yield superior peel resistance, however further tests are required to evaluate higher temperature extrusion and its effects on polymer surface quality and form accuracy which will be further discussed. Moreover, cross-sectional analysis indicated that to achieve a more consistent minimum/maximum depth for 82A TPU, our results

indicate that a 220°C setting should be used on T1 fabrics, and a lower 240°C setting should be used on T2 fabrics. And for 70A TPU, a 240°C setting should be used. Moreover, to achieve a more consistent minimum/maximum depth with 40D TPE, our results indicate that a 240°C setting should be used on T1 fabrics, and a higher 260°C setting should be used on T2 fabrics.

Chapter 5: 4DP THERMO-RESPONSIVE POLYMER-TEXTILE

COMPOSITE

5.1 Introduction
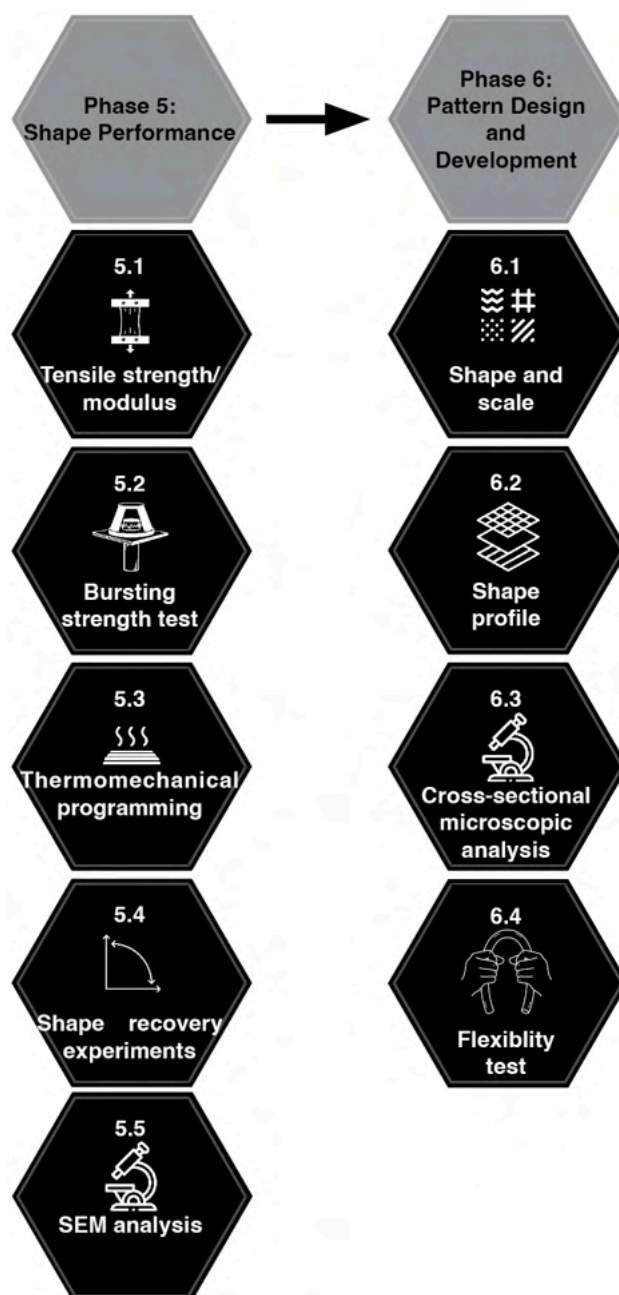
Figure 5-1 4DP PTC design framework (showing chapter 5 experiments)

Figure 5-1 illustrates the experiments conducted in chapter five. Chapter five consists of characterisation of 4DP PTCs, shape performance evaluation, pattern development, and evaluating the shape performance of 4DP PTCs with various patterns to determine the overall functionality of 4DP PTCs.

5.2 Experimental design

5.2.1 Design parameters and substrates

5.2.1.1 4DP PTC printing parameters

To achieve an efficient and repetitive SME, an additional PU-based thermo-responsive SMP filament was introduced and used in conjunction with the flexible polymers. The SMP filament is a TPU with added shape-memory polymers. Though less elastic than conventional flex polymers, the SMP filament can provide comparable flexibility. Furthermore, the SMP filament has a lower Tr (45°C) and Tg (55°C) in comparison with existing SMMs giving it potential in a wider range of applications. An overview of the SMP filament is shown in **Table 5-1**.

Table 5-1 PU-based SMP filament specifications

Property	TPU (SMP) (KatoTech, n.d.-c)
Shore hardness	57A
Diameter [mm]	1.75 mm -/+ 0.05 mm
Density [g/cm³]	1.24
Elongation at break [%]	31%
Maximum strain [%]	400%
Melting temperature [°C]	55°C
Extrusion temperature [°C]	200°C
Printing bed temperature [°C]	0 - 45°C if required

Experimental results from Chapter four informed the optimal conditions to fabricate 4DP PTCs (SMP layer at 200°C, TPU/TPE layer at 230/240°C) (**Table 5-2**). The print speed, layer height, z-axis height, infill pattern and density and bed temperature were identical across specimens.

Table 5-2 4DP PTC printing parameters

Printing parameter	F1-SMP 4DP PTC	F2-SMP 4DP PTC	F3-SMP 4DP PTC
Extrusion	TPU (240°C) SMP (200°C)	TPU (240°C) SMP (200°C)	TPU (230°C) SMP (200°C)
Bed temperature	n/a	n/a	n/a
Z-axis height	TPU (-1.500 mm)/SMP (-1.400 mm)	TPU (-1.500 mm)/SMP (-1.400 mm)	TPU (-1.500 mm)/SMP (-1.400 mm)
Print speed	20 mm/s	20 mm/s	20 mm/s
Layer height	0.10 mm	0.10 mm	0.10 mm
Infill pattern	Rectilinear	Rectilinear	Rectilinear
Infill density	15%	15%	15%
Textile substrate	80% NY 20% EA	80% NY 20% EA	80% NY 20% EA

For 4DP PTC specimens, the textile substrate had a thickness of 0.1 mm which meant the z-axis had to be increased to -1.500 mm for optimal adhesion. And to print the SMP layer atop the TPU-textile composite, the z-axis had to be further increased to -1.400 mm which accounts for the 0.1 mm textile substrate and 0.1 mm TPU layer thickness. All specimens contain the same SMP and nylon substrate (80% NY and 20% EA), except for a TPU/TPE printed layer of 70/82A/40D Shore hardness.

5.2.1.2 4DP PTC structural composition

Studies have shown pattern arrangement i.e., scale, thickness, and placement of polymers to have great influence on the shape deformation of 4DP materials (Khoo et al., 2015). The change in shape and direction can be predicted and controlled via calculated material distribution and arrangement (Choi et al., 2015). Moreover, the mechanical properties of 4DP materials i.e., bending rigidity, tensile properties can be fine-tuned via patten design for specific applications. In addition to pattern arrangement, the profile of 4DP materials is also of importance. Multi-material 4DP PTCs are often composed of two or more polymers in addition to a textile

substrate which delivers more opportunities for further engineering the material's mechanical properties and performance by reorganising the existing material profiles within the composite. The polymer layers can be printed with homogenous or varied pattern size configurations ensuing materials with interesting surface designs and dynamic structures with unique mechanical properties. 4DP PTCs can be a juxtaposition of different types of materials, patterns, scales, and polymer thickness resulting in complex material structures.

To avoid overcomplicating 4DP PTC design and to maintain material fineness, this study explores multi-material 4D printing with a bi-layer configuration. 4DP PTCs will be composed of a textile substrate (base layer), TPU/TPE (mid-layer), and polyurethane (PU) based (top layer) (**Figure 5-2**). The purpose of the mid-layer is to enhance the interfacial bond between the substrates without interfering with the thermo-responsive SME of the SMP. In 4DP PTCs, free areas of textiles with no polymers applied has been reported to have a major influence on shape transformation in 4DP materials (Schmelzeisen et al., 2018). Thus, whilst designing 4D printing patterns, it is important to avoid the overfilling of textile substrates with polymers.
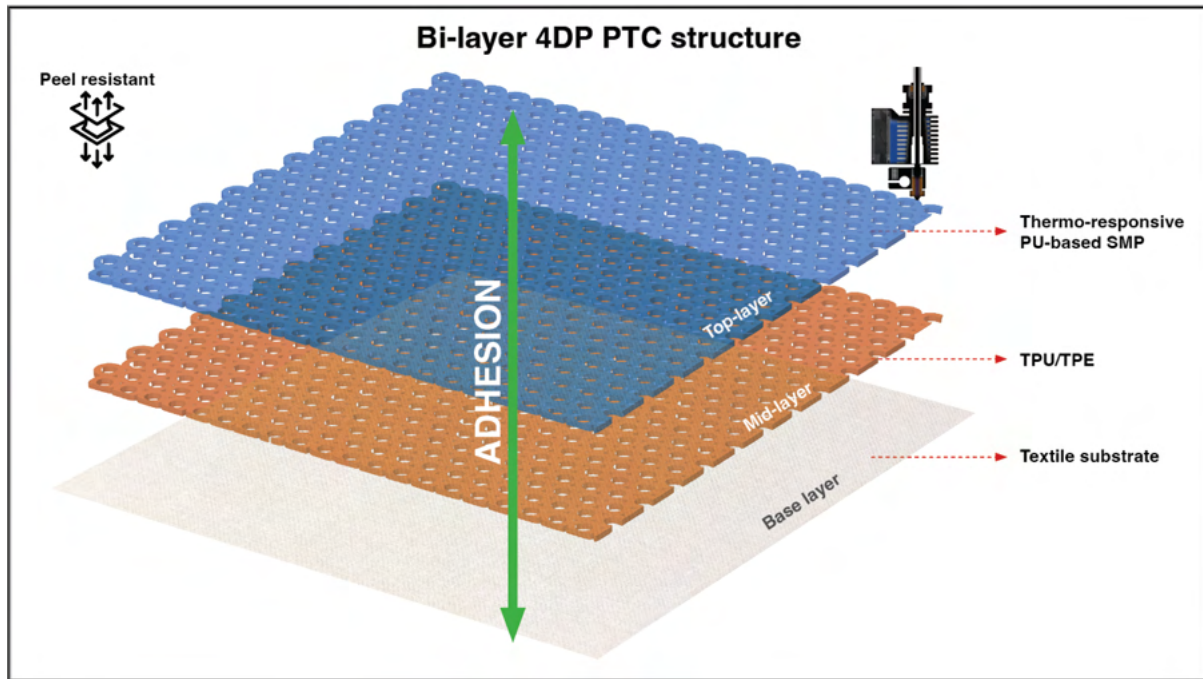
Figure 5-2 Schematic of bilayer 4DP PTC structure

5.2.2 Pattern development

5.2.2.1 Patterns and structures in textile design

Studies have demonstrated the use of bioinspired patterns to maximise material performance in various fields i.e., wearable technology (Da-Silva-Júnior et al., 2018), soft robotics (Chi et al., 2022), fashion and textiles (McKnight, 2016), high-performance sportswear (Kapsali, 2015) and architectural design (Fernandes et al., 2021). Existing literature have classified common 4D printing shapes and structures as tessellation, membrane, or compliant mechanism (Koch et al., 2021) (**Figure 5-3**).
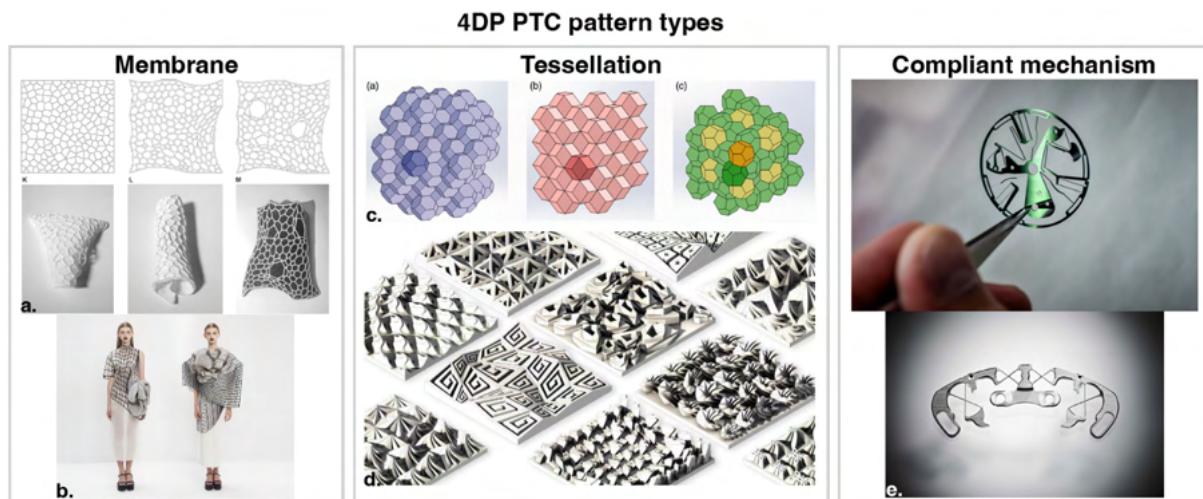
Figure 5-3 4DP PTC pattern types a. Agkathidis and Varinlioglu (2022), b. Hosmer (2014), c. Dragoni and Ciace (2021), d. Watkin (2016), e. Markl (2017)

- *Tessellation* – can be combined with membrane structures to create repeated patterns. Patterns are commonly designed as auxetics (Grimmelsmann et al., 2016), Voronoi (Agkathidis et al., 2019), and other geometrical tessellations (Schmelzeisen et al., 2018).

- *Membrane* – structures with large areas of textiles with no polymer applied and are bounded by beams.

- *Compliant mechanism* – are flexible in nature with the ability to transmit force through elastic deformation and can also work in combination with membranes. Studies have suggested that the transformation behaviour depends on the design of the joints in i) textiles, ii) textile/polymer combinations, or iii) textiles and two different polymers (Schmelzeisen et al., 2018).

By integrating nature inspired structures in micro and macro scales, designers can develop functional materials that forms the intersection between aesthetics and technology resulting in smart and intelligent material solutions (Imani et al., 2018). Nature-driven designs are regularly used for the design of more durable and resilient structures (i.e., designing skeletal structures)

(Fernandes et al., 2021), for varying material stiffness, flexibility, or deformation behaviour (i.e., mimicking plants) (Alshebly et al., 2022), and for the design of high-performance wearables that enhances human performance i.e., offering freedom of movement, easily don/off, comfort, wicks moisture from skin, textiles with varying permeability, or smart materials that can adapt to its environment (Kapsali, 2015). Such factors are vital for the development of 4DP materials, specifically when it comes to 4DP PTCs whereby repeated shape transformations may be performed. Thus, by studying bioinspired geometrical patterns, we can acquire a better understanding on how different pattern configurations can influence the performance of 4DP PTCs. Typical examples of bio-inspired shapes include hexagons (honeycomb), triangular (Widmanstatten pattern), rectangular (membrane structures), circular (polyhedral foam structure), and squares (sponge structures) (**Figure 5-4**).
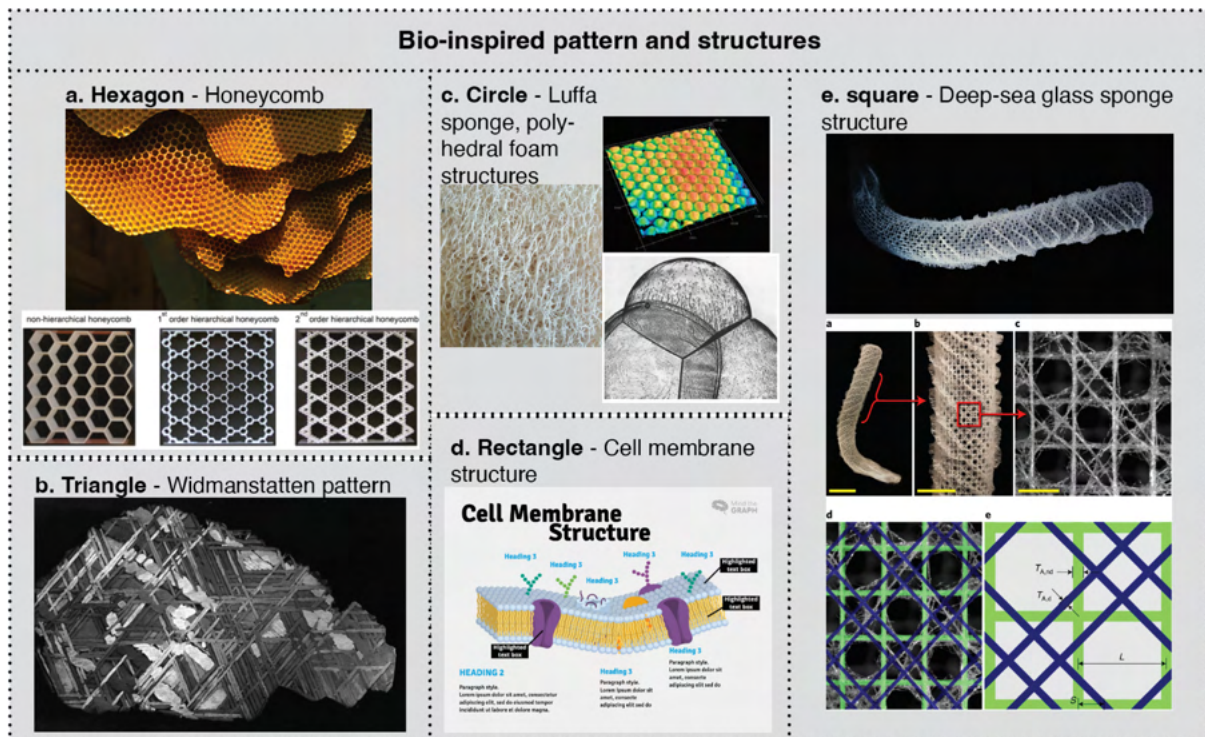
Figure 5-4 Bio-inspired patterns and structures a. hexagon (Wang, 2019), b. triangle (Brandt et al., 2013) , c. circle (Goss et al., 2020), d. rectangle (Weerasinghe et al., 2019), and e. square (Fernandes et al., 2021)

5.2.2.2 Pattern design inspiration

In textile design, the patterns are influenced by size and proportion, the interaction between patterns, and if applied in the context of clothing, the silhouette of the garment (Russell, 2021). Designers can achieve visual harmony by placing the right type and size of patterns in specific areas of garments and objects. Patterns can be utilised to create focal points or used to hide or reduce immaterial areas. Large patterns can help draw attention from a distance, meanwhile small patterns can evoke a subtle and delicate appearance. Moreover, stripes can elongate a silhouette to create a slender appearance, horizontal patterns can produce a widening appearance, and florals can help divert attention. For 4DP PTCs to effectively produce shape transformations, the pattern must be a seamless repeat pattern and the shapes within the pattern must join edge-to-edge. Hence, related literature have often cited the use of tessellating patterns (Grimmelsmann et al., 2016; Kabir et al., 2020b). In addition, when designing patterns, material type, the connectivity between shapes (in a tessellation) and its influence on shape performance must also be considered to determine the outcome of fabric design.
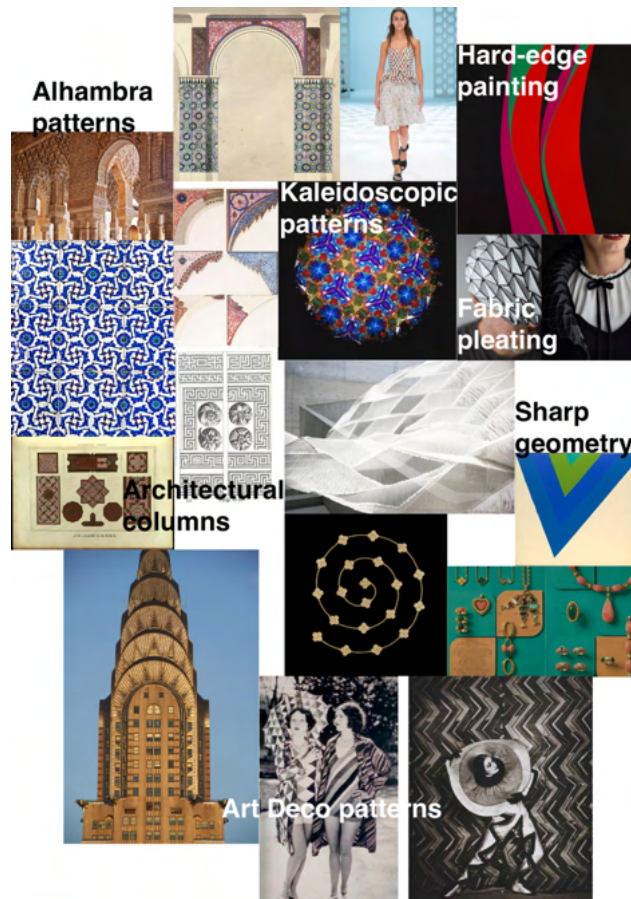
Figure 5-5 Pattern inspiration with examples from various art and design disciplines i.e., architecture, fashion, and fine art

Figure 5-5 illustrates an inspiration board with patterns deriving from various art and design disciplines i.e., architecture, fashion, and fine art. Examples include Alhambra patterns seen in architecture (Arabic patterns), kaleidoscopic patterns, bio-inspired patterns, hard-edge painting, fabric pleating, architectural columns, art deco inspired art, architecture, and jewellery design. The images cohesively demonstrate qualities i.e., sharp geometry and lines, tessellating shapes, repeat patterns, surface texture created through shapes, patterns that alternate (shape-shift i.e., kaleidoscopic patterns) between 2D and 3D forms, and patterns can be overlapped to engender new shapes and patterns. In addition, such patterns can also be used to create interesting surface relief patterns giving continuation of movement with 3D quality.

5.2.2.3 Types of tessellating patterns

There are three key types of tessellations in pattern design i) regular, ii) semi-regular, and iii) demi-regular (Boots et al., 1999). The shapes within a tessellation can be connected edge-to-edge, non-edge-to-edge, and overlapping. In addition, tessellating patterns can be classified as unary (single shape), binary (two shapes), ternary (three shapes), and quatemary (four shapes) and so on. Kaleidoscopic patterns are examples of tessellations that consist of multiple shapes. In 3DP/4DP textiles various shapes, scale, and tessellation compositions can be utilised to produce different surface designs and materials with distinctive mechanical properties. A useful tessellation requires to possess at least two key properties i) can be used to generate a seamless repeat pattern for images of any scale and ii) be decomposable into finer patterns which can collectively form a hierarchy to be used to represent spatial features of a arbitrarily fine resolution (Boots et al., 1999). **Figure 5-6** illustrates the fundamental concept of the various types of tessellation compositions in pattern design.
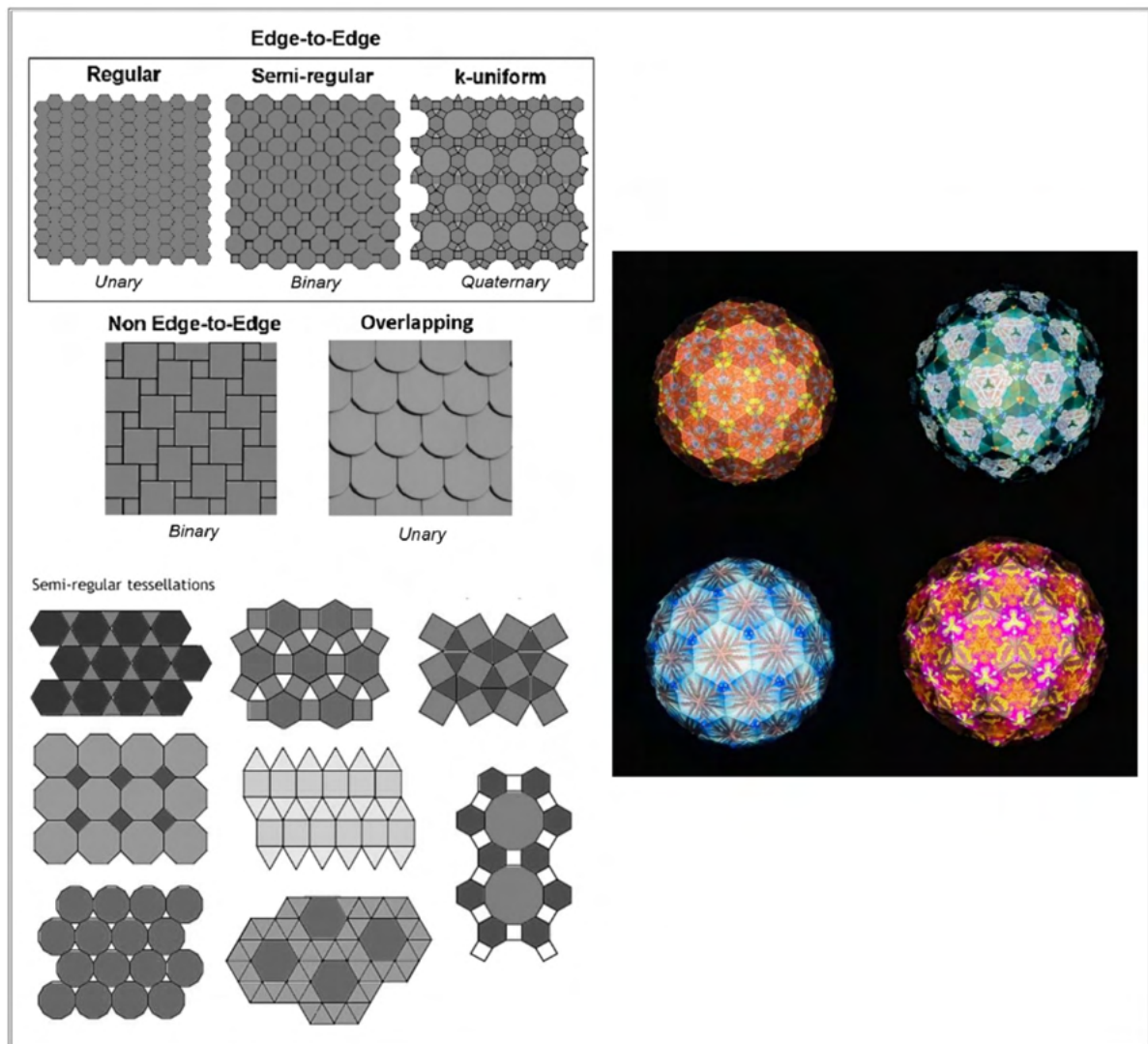
Figure 5-6 Types of tessellation compositions in pattern design (Leaden, 2023)

An overview of unary shape tessellating patterns is shown in **Figure 5-6**. In textile and other surface design disciplines, common repeat patterns that tessellate include: block repeat, full and half drop repeat, brick repeat, striped repeat, and diamond shaped repeat (Russell, 2021). Different repeat patterns can be used to design tessellations, though the shape ultimately dictates which type of repeat pattern is applicable.

5.2.2.4 Folding tessellation patterns
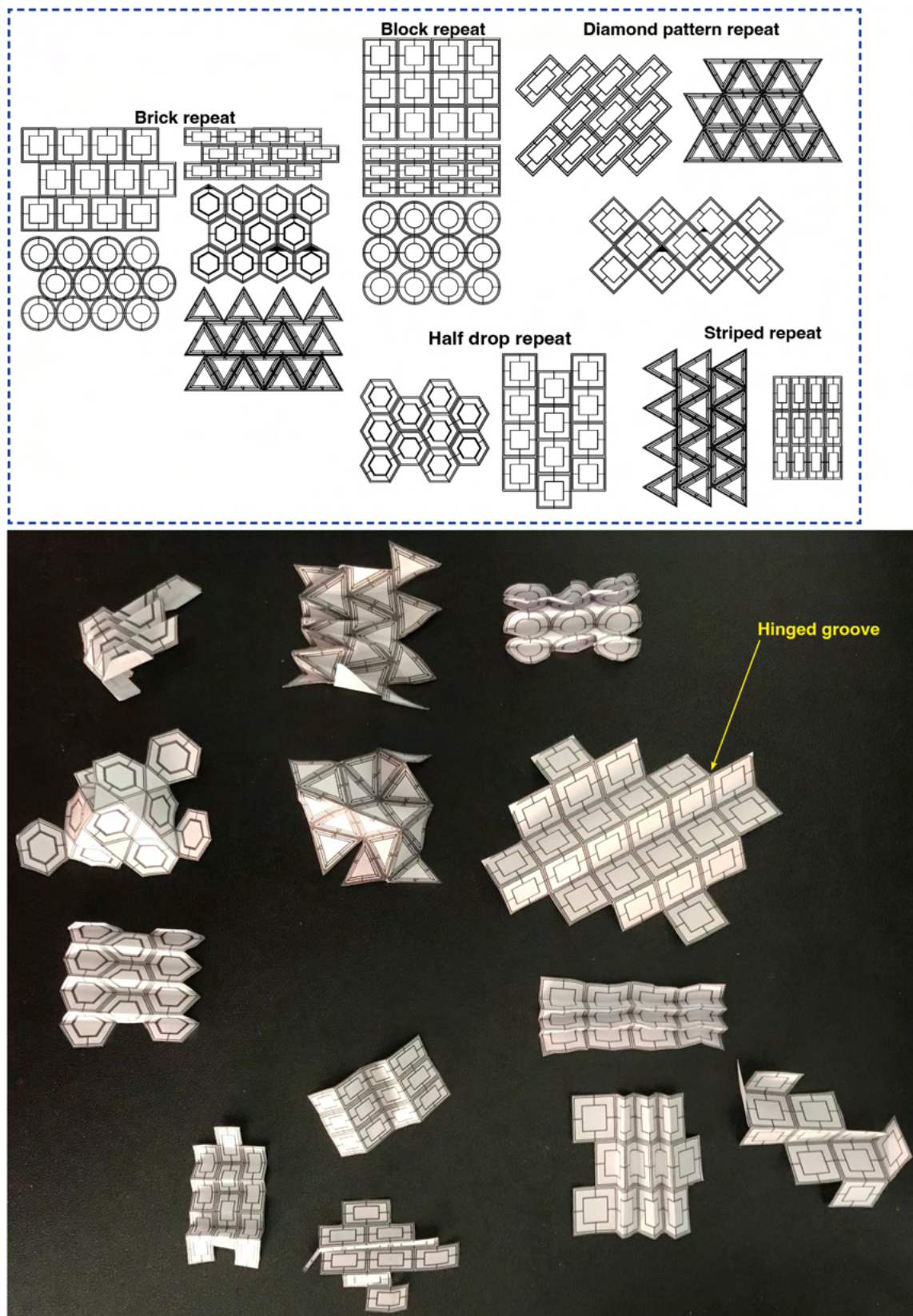
Figure 5-7 Unary tessellation patterns (top) and folding with unary tessellation patterns (bottom)

Folding paper in pleating development is a part of the pleating process (**Figure 5-7**) (Jackson, 2015). In this study, the tessellation patterns were developed using Rhino – Rhinoceros 3D version 8 (Rhinoceros, 2024), a CAD software used commercially in the design, engineering, rapid prototyping, and computer-aided manufacturing (CAM) industries. The patterns were then printed on Tyvek (a paper-like textile) with the hinged grooves scored and then folded to create pleated templates (Tyvek moulds). Tyvek is more durable and textile-like than paper. The benefit of folding Tyvek is that one can immediately visualise how the final pleated fabric may look before the pleating process which can be used for rapid generation of design ideas. Moreover, these moulds may also be used for latter thermomechanical programming processes whereby a 4DP PTC is sandwiched between two paper moulds whilst subjected to heat to program a new permanent (pleated) form.

The folding experiments resulted in various pleat forms i.e., crystal pleats, accordion pleats, and more intricate pleats i.e., knife-across accordion and hybrid pleat forms. This process of working between 2D and 3D forms provides learning opportunities to identify and differentiate the effects of pattern arrangement in 2D flat form to 3D solid form. The reversal sequence from 3D to 2D too provides opportunities to improve the tessellation pattern to achieve versatile pleated forms. Moreover, 2D/3D design processes also provide the flexibility to find your design composition, switch and or reposition materials, patterns, and shapes. Such methods have been used across industries for pattern drafting, fabric pleating (Jackson, 2015), product design, architecture, jewellery design, prototype models, machinery, video games, concept art (Pramadhiya, 2019). Furthermore, additional hinges were engineered within the shapes which enabled folding in between tessellating shapes and within each shape.

Additional hinges within shapes

Red shaded area = additional internal hinges
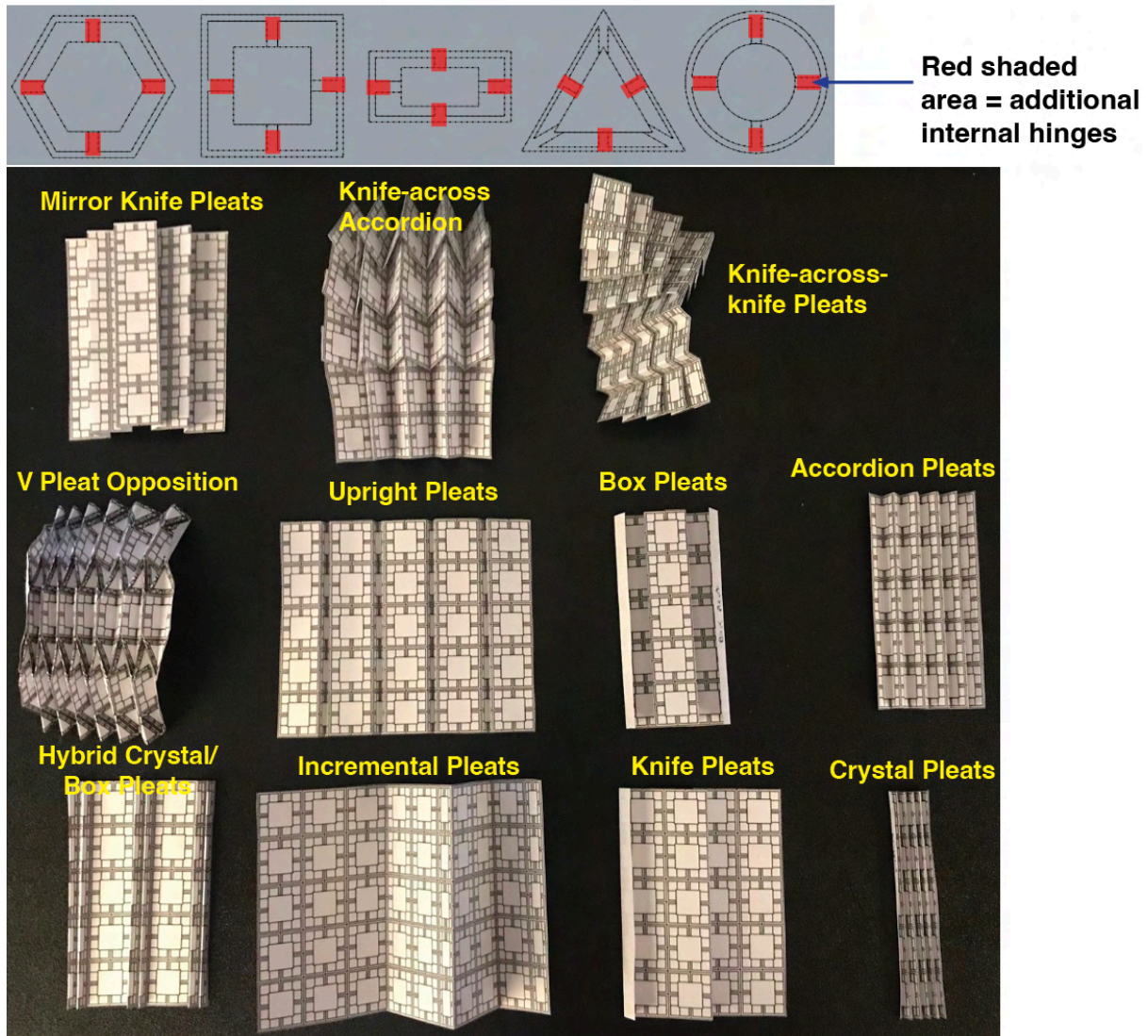
Figure 5-8 Pleating experiments with additional hinged shapes

Through pleating experiments with Tyvek, unary patterns were identified to be suited for common pleats i.e., box pleats, accordion etc, while binary and multi-shaped patterns were able to satisfy the demands of irregular shaped and sculptural pleated forms i.e., v pleat opposition (**Figure 5-8**). Multi-shaped patterns provided opportunities for more versatile pleat designs and hybrid pleating forms when desired.

5.2.2.5 Hinge mechanism for pattern

5.2.2.5.1 Structure

Designers and architects alike have utilised self-shaping mechanisms to facilitate stable structural forms for their designs (Kycia, 2022). This has resulted in more efficient designs whereby form is dictated by the self-shaping capabilities of the materials themselves. Aside from pattern's influence on shape transformation performance, hinge mechanism is also of great importance because it eases shape deformation and recovery in 4DP materials (Schmelzeisen et al., 2018). Common practices include local stiffening, textile hinge, 3DP hinge, and local adhesion. **Figure 5-9** illustrates the structural differences between a regular 4DP PTC (b) and a 4DP PTC with a SMP hinge (c).
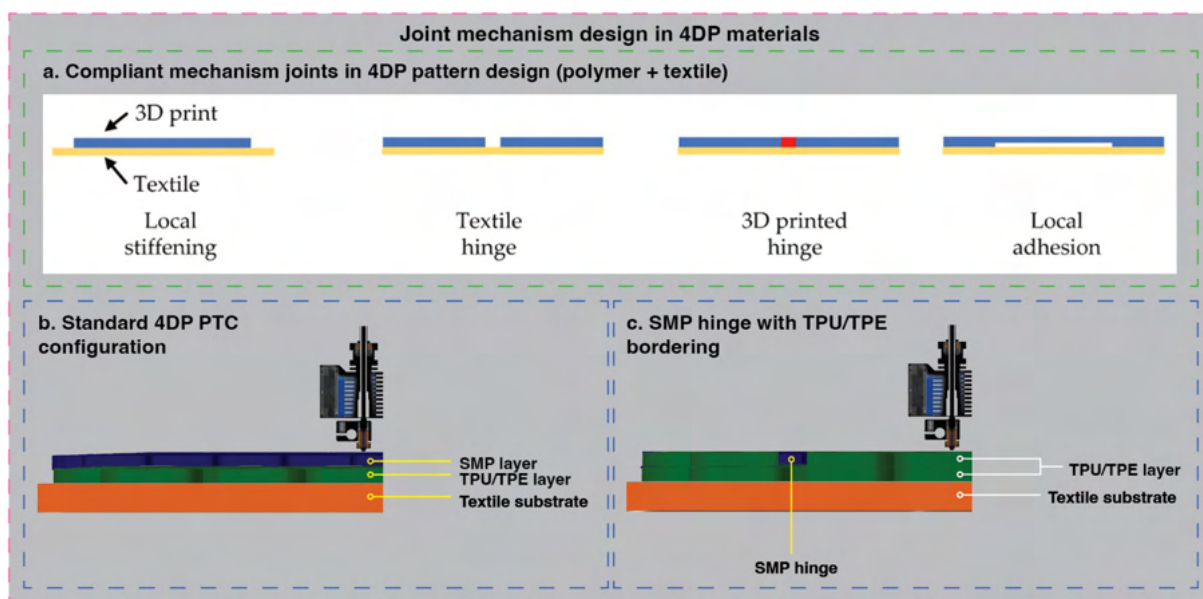
Figure 5-9 a. Compliant mechanism joints in 4DP materials (Koch et al., 2021), b. standard 4DP PTC, c. 4DP PTC with SMP hinge with TPU/TPE border

Hinged joints are customarily used by designers in exterior, and interior architecture (b, c, h), 4DP objects (f), wearable objects (a), parametric design (a, c), actuators (d, e), and furniture and millwork (g) (**Figure 5-10**) as it enables material mobility, flexibility, and elasticity. Such

joints enhance the adaptability of materials to certain shapes and forms via balancing stored energy and forces (stimuli) acting on it. Hinges facilitate bending and folding motions and is particularly effective for the design of applications that involve expansion/contract, opening/closing, and self-assembling/disassembling structures. Precedent studies have also shown hinge design (Yamamura & Iwase, 2021) and materials used (Mao et al., 2015) to influence actuation, recovery, and flexibility of the material in 4D printing .Though further experimentation is required to develop practical and functional hinge designs for 4DP PTCs.
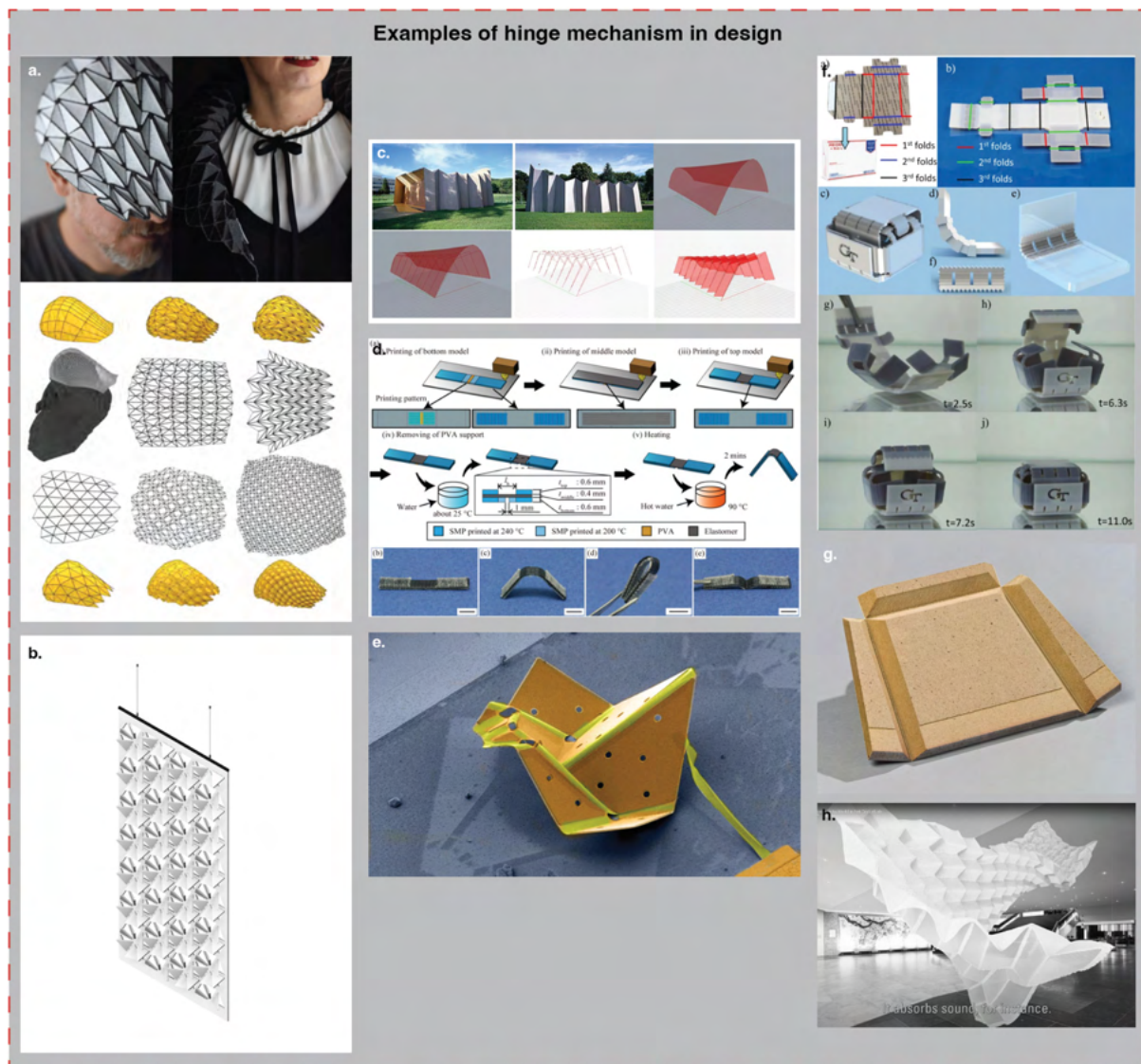
Figure 5-10 Examples of hinge mechanism in design a. Gardiner et al. (2018), b. BIMcontent (2023), c. El Khoury (2017), d. Yamamura and Iwase (2021), e. Liu et al. (2021), f. Mao et al. (2015), g. Groovfold (n.d.), h. Boon (2019)

5.2.2.5.2 3D design and modelling
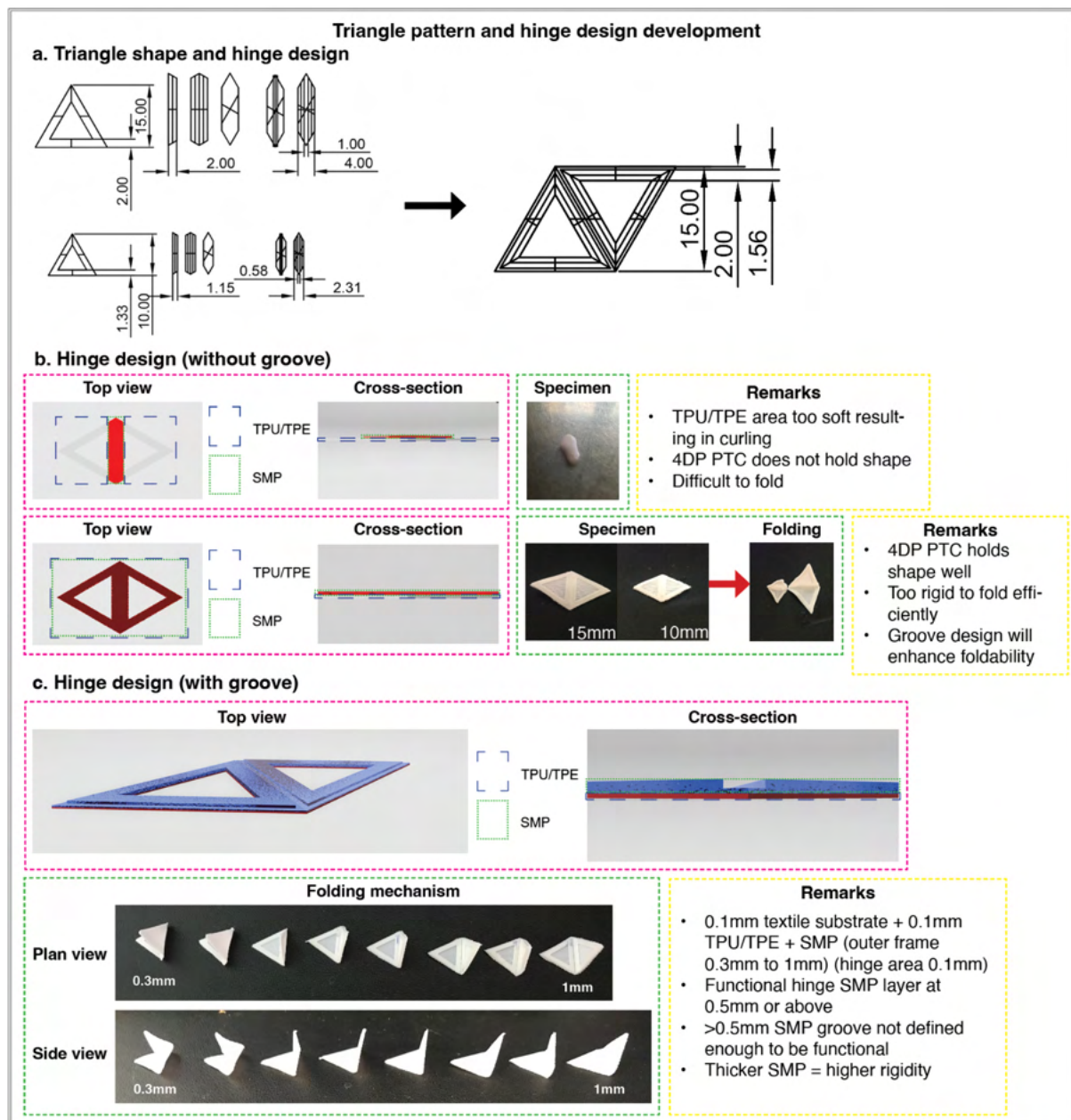
Figure 5-11 a. Triangle shape and hinge design, b. hinge design (without groove), and c. hinge design (with groove)

In the previous experiments, the SMP was deposited to overlay the TPU/TPE layer resulting in a standard shape profile consisting of 0.1 mm of SMP, TPU/TPE, and a nylon substrate. As reported in section 3.4.3, hinges have been utilised in a multitude of design applications due to its enhancement on actuation, shape recovery, flexibility, and mobility of materials. Moreover,

it can also be used to enhance aesthetics while improving functionality. In this study, a hinge design was developed to improve the adaptability of the 4DP PTCs. **Figure 5-11b** and **c** illustrates the structural differences between 4DP PTCs with hinge designs (**5-11b** without groove) and (**5-11c** with groove). However, 4DP PTCs with a SMP hinge alone was unable to hold a permanent form (**Figure 5-11b**). The developed grooved hinge can enhance the foldability of the 4DP PTCs. And to maximise the shape recovery and utility of the specimen, the hinge must be connected to an outer SMP frame. To achieve this, the polymer thickness surrounding the groove must be elevated for a well-defined groove channel (groove trough at 0.1 mm with surrounding areas at < 0.5 mm) (**Figure 5-11c**).

In preliminary experiments, specimens were printed with a SMP frame of 0.3 mm to 1.0 mm. The TPU/TPE thickness remained unchanged. It was discovered that 0.3 mm and 0.4 mm SMP frames were too fine to produce a contrast between the surrounding areas and the groove channel, resulting in the inability for hinge to function correctly. The groove hinges on specimens with a SMP frame of 0.5 mm onwards was able to fold and bend efficiently. However, towards the higher end of SMP thickness i.e., 0.7 mm onwards, the folding action was more demanding (rigid) at the cost of a well-defined groove and stronger structural form. Thus, at 0.5 mm 4DP PTCs was able to create an equilibrium between maximising hinge performance and structural form while minimising material thickness and rigidity (trough area with 0.1 mm SMP). **Figure 5-12** illustrates 3D modelling and rendering process in Rhino 8 and **Figure 5-13** shows the technical drawing (plan and side profile views) and measurements of bio-inspired shapes with a groove hinge.

Figure 5-12 3D modelling and rendering on Rhino 8
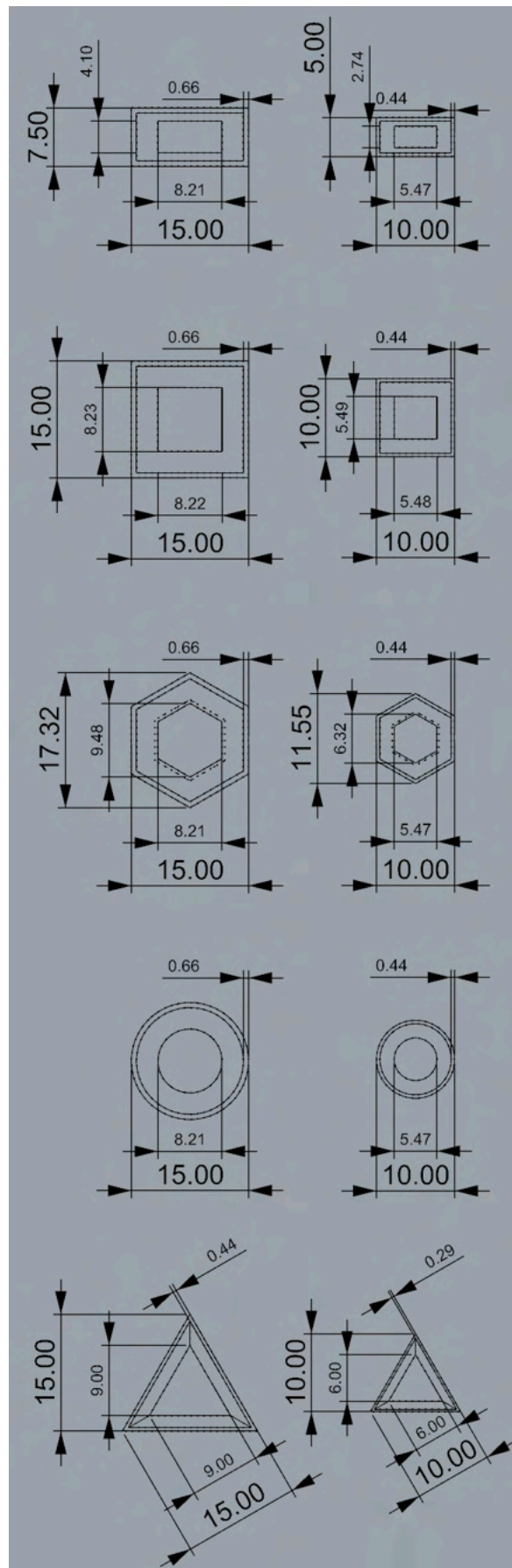
Figure 5-13 Technical drawing and measurements of shapes with hinged grooves

In addition to SMP-based hinge design, related literature has also developed hinged systems with different material compositions i.e., textile hinges, PLA hinges (Koch et al., 2021). The function of alternative hinge compositions is to facilitate simultaneous self-folding motions in both inverse and reverse directions without having to deposit polymers on both faces of the textile substrates and to improve the flexibility and mobility of 4DP PTCs for wearable applications. **Figure 5-13a**, **b**, and **c**, illustrates hinges designed with various material compositions. When the 4DP PTC is subjected to a heat stimulus the specimen self-folds to its programmed form (outer hinges, yellow arrow direction) and a reverse self-folding action (centre hinge, red angle) are simulated (**Figure 5-13**). It is observed that the reverse self-folding angle is reliant on the centre hinge's flexibility. A smaller reverse self-folding angle is generated when the centre hinge is composed of more flexible materials with textile hinges seen as the most flexible, followed by the TPU/TPE hinge, and SMP hinge as the least flexible.
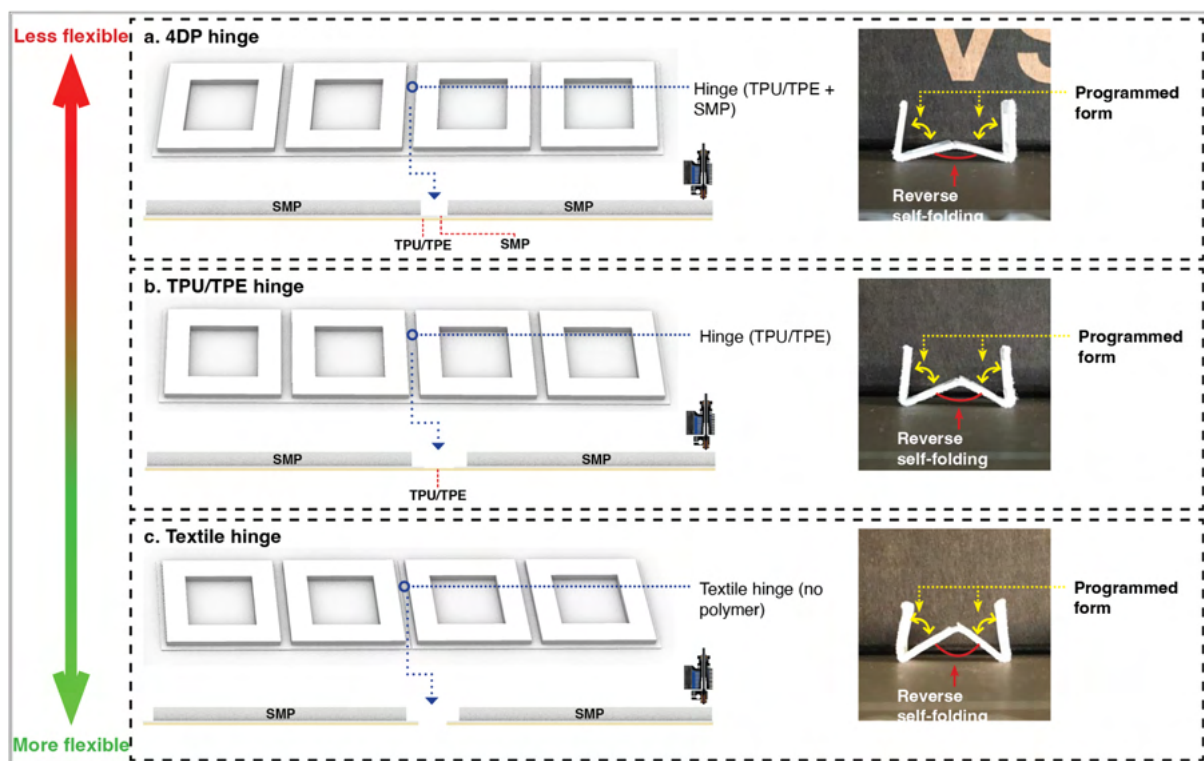
Figure 5-14 Alternative 4DP PTC hinge composition

5.2.3 Characterisation and evaluation

5.2.3.1 Mechanical performance

5.2.3.1.1 T-peel test for peel resistance

The process for this test is identical to the experiment shown in section 4.2.3.2.

5.2.3.1.2 Cross-sectional microscopic analysis

The process for this test is identical to the experiment shown in section 4.2.3.2.

5.2.3.1.3 Tensile strength and Young's modulus

Tensile strength experiments were conducted in accordance with ISO 9073-18:2008 (ISO, 2008a) to determine 4DP PTCs' maximum stress before failure with its breaking extension as an indicator of its ductility (Pal et al., 2022). The test was repeated five times resulting in average breaking load, extension, and Young's modulus results. The specimen ends were secured onto an Instron 4411 tensile tester with 25 mm fixes. The specimens (100 mm ± 1 mm x 150 mm) were cut long enough to extend beyond the clamps with 10 mm on each end (**Figure 4-4a**, **c**). The extension rate was calibrated at (300 ± 10 mm/min) with a break force range of 10% to 90% performed at full-scale force. These experiments determined 4DP PTC's mechanical properties (i.e., tensile strength, ductility, and rigidity at Tg).

5.2.3.1.4 Bursting strength

The 70A-SMP specimen with TPU printed at 210/220/230/240/250°C and 82A-SMP with TPU printed at 210/220/230/240/250°C were tested in accordance with ISO 13938-2:2019 (ISO, 2019) by using a pneumatic intelligent bursting strength tester (TruBurst 610, James H. Heal) (Heal, 2019). The extrusion temperature of SMP remained constant at 200°C. The size of the specimens was 150 mm x 150 mm x 0.3 mm in a test area of 50 cm^2, which were clamped over

the diaphragm of the bursting strength tester. Pressure was then applied onto the underside of the diaphragm in three areas across the specimen until it burst. This test provides the amount of pressure required to rupture the specimen and is used to ascertain durability, performance, and strength (**Figure 5-14**). The total average bursting strength (kPa), time (s) and height at burst (mm) were calculated with a machine.
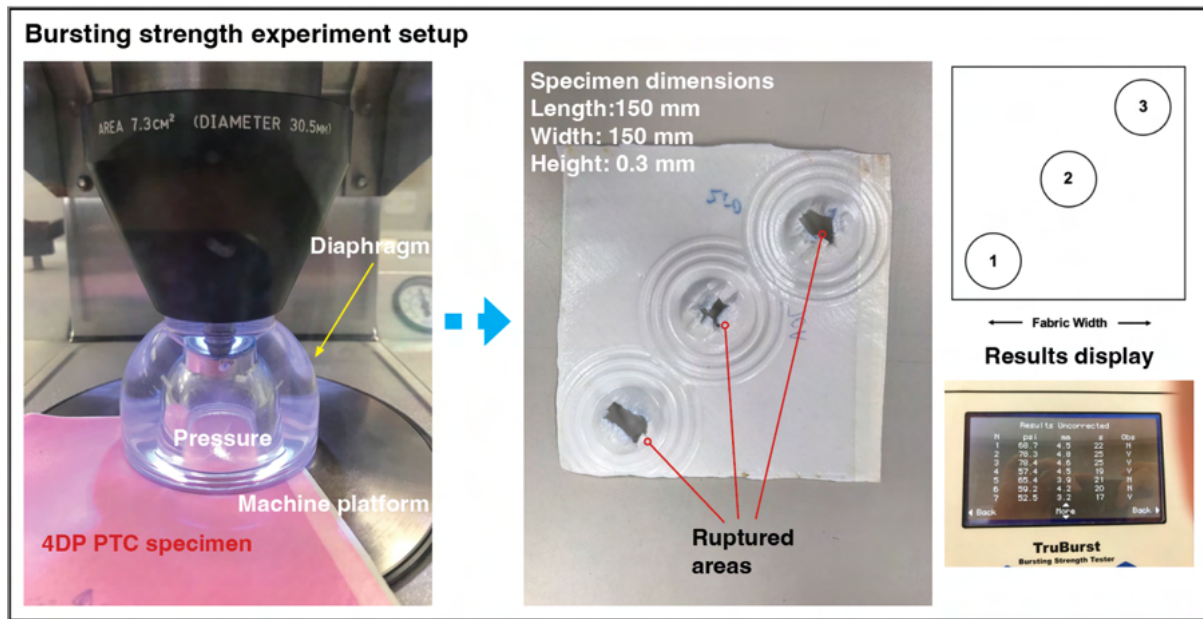
Figure 5-15 Tested areas as per ISO 13938-2:2019 (modified from (ISO, 2019))

5.2.3.2 Shape performance

5.2.3.2.1 Thermomechanical programming

4DP PTC specimens undergo a) thermomechanical programming of the 4DP PTCs and b) shape recovery evaluation. The shape performance experiments initiated with the testing of test strips with specific dimensions shown in **Figure 5-15**, to identify the optimal performing 4DP PTC material combinations. After having determined the optimum material combinations, the 4DP PTCs were printed in all five pattern shapes (honeycomb, rectangle, etc.) in small and large scaled pattern sizes (totalling 10 specimens) and were evaluated for their shape

performance. Thermo-rheological characterisation is the thermo-mechanical programming of SMP materials in a shape memory cycle (Lendlein & Gould, 2019) which occurs as an i) original (permanent) shape, ii) temporary shape, and iii) recovery (back to permanent shape) (Behl & Lendlein, 2007) (**Figure 5-16a to c**). The 4DP specimen's default permanent shape materialises as a flat structure. To program a new permanent shape (90° angled structure), the specimens were heated at above Tg (55°C – as suggested by the manufacturer (SMP, 2023)) for 90 seconds with a Lab Companion OV4-30 vacuum oven capable of heat distribution with a controlled temperature range of up to 250°C (LabCompanion, 2023). The use of controllable temperature instruments ensures an even distribution of heat used in numerous SMP studies (Agbakoba et al., 2022; Tobushi et al., 1992; Xie, 2011). During this process, the polymer is transformed from a glassy to rubbery state allowing stress to be induced onto the specimen bending it halfway to a fixed 90° right-angle ($\theta_{90°}$) and secured onto a square jig with polyimide tape. Induced stress is used to reorganise the polymer backbone structure facilitating the programming of a new permanent shape. The specimen was subsequently left to cool until it returned to its glass state.
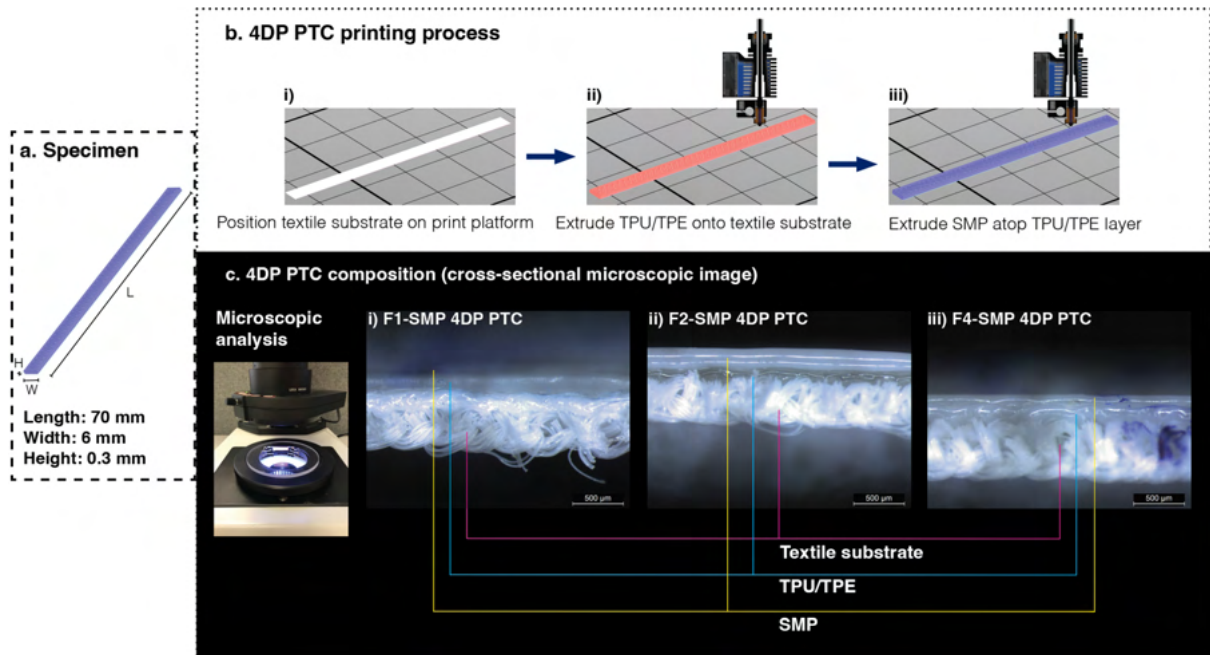
Figure 5-16 Test specimens for shape performance experiments (Cheung et al., 2024)
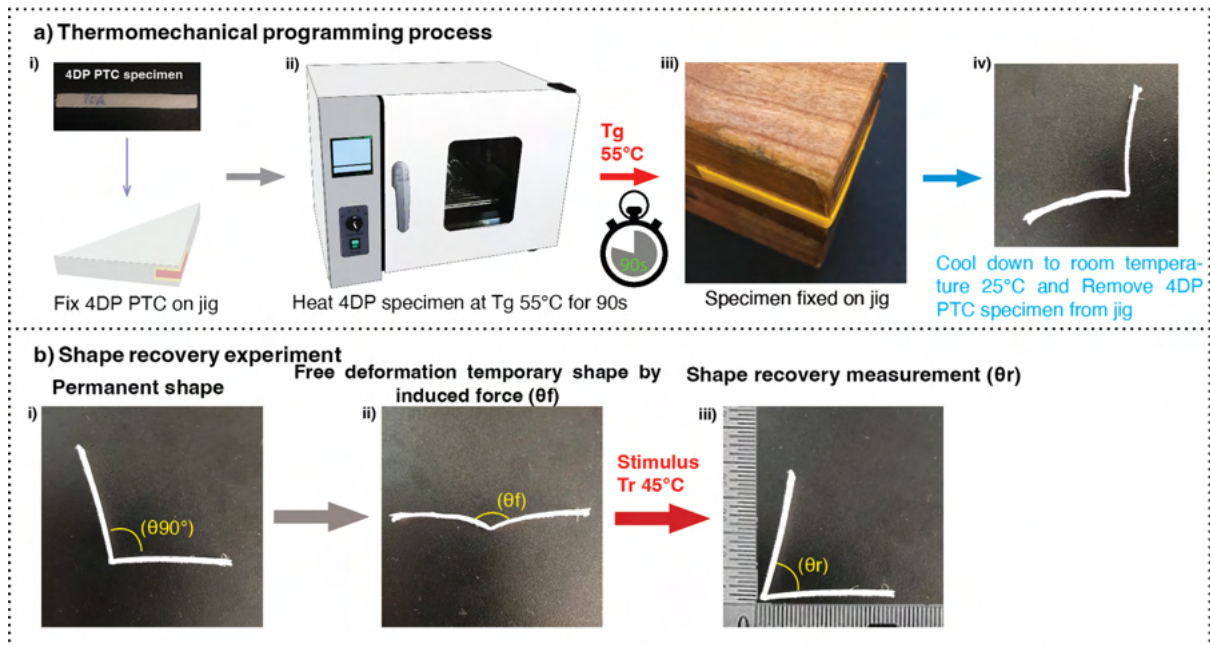
Figure 5-17 a. thermomechanical programming process and b. shape recovery experiment (Cheung et al., 2024)

5.2.3.2.2 Shape fixity and recovery

Post thermomechanical programming, the specimens (test strips and specimens with the five patterns) were subjected to an external force to flatten it to $\theta_0 = 180°$ (**Figure 5-16** and **5-17**). The external stress was removed allowing the specimen to freely deform (θ_f). Subsequently the specimens were heated at Tr = 45°C (as per manufacturer's recommendations in a Lab Companion OV4-30 oven chamber). The resulting shape recovery (θ_r) was recorded with a digital protractor that is accurate to two-decimals. Each 4DP PTC specimen was tested under five repetitions ensuring consistency and the reliability of the results (Cheung et al., 2024). The shape fixity rate (R_f) and recovery rate (R_r) was calculated as follows (modified from (Abbasi-Shirsavar et al., 2019)):

$$Rf = \frac{\theta 0 - \theta f}{\theta 0} \times 100\%$$

$$Rr = \frac{\theta 0 - \theta r}{\theta 0 - \theta 90°} \times 100\%$$

The aim of this experiment is to identify which 4DP PTC combination can achieve a shape recovery angle that is as precise to the permanent shape as possible. The results were averaged with the standard deviation (SD) calculated. For this study, 4DP PTCs were tested for self-bending, self-folding, and self- contraction shape recovery behaviours. The self-bending and folding specimens were measured with a digital protractor while self-contraction specimens were manually stretched out and then subjected to Tr stimuli. Due to the elasticity of both the polymer layers and textile substrate, the self-contraction specimens curled up when stretched and self-contracted back to its original printed form when stimulated.
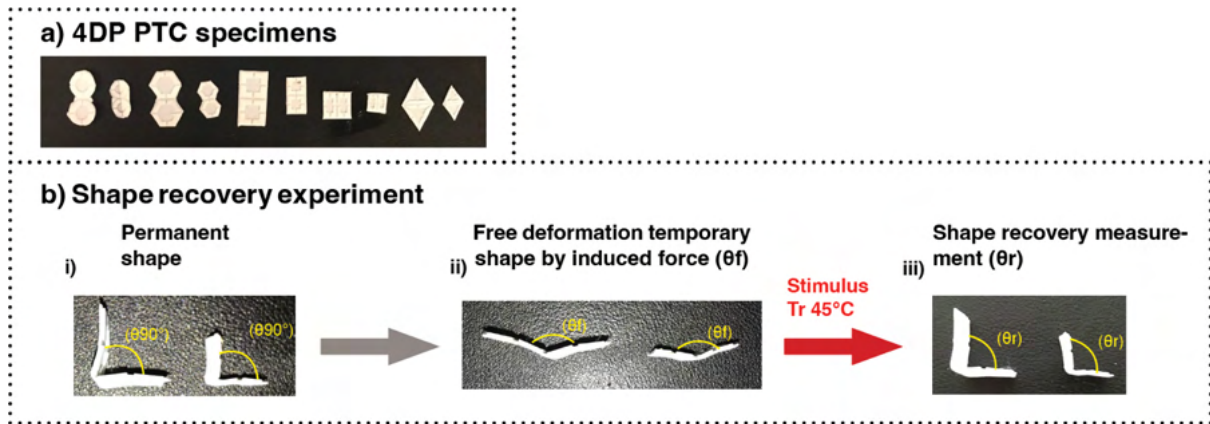
Figure 5-18 4DP PTC specimens with pattern and shape recovery experiment

5.2.3.2.3 Shape response

To test for shape response, the specimens were subjected to an external force to flatten it to $\theta_0 = 180°$. The external force was subsequently removed allowing the specimen to deform (θ_f). Then the specimens are heated at Tr triggering it to transform from its temporary shape to its permanent form. The time needed for the shape recovery to complete was recorded using an iPhone 7 stopwatch which recorded to an accuracy of two decimals. The specimens were tested under five repetitions with an averaged result and standard deviation (SD) calculated.

5.2.3.2.4 Bending rigidity and hysteresis

The pure bending tests were conducted with a KES-FB2-L Large Bending tester in a controlled environment with a regulated temperature of 23°C and a humidity of 65% in accordance with ISO291:2008 atmospheric conditions (ISO, 2008b). This device evaluates the bending rigidity, hysteresis, and texture of materials using "bending" that imitates hand movements with the sensitivity of a fingertip performed by textile practitioners (KatoTech, 2023). The KES-FB2-L can measure both large and minute bending movements and is particularly useful for measuring thick sheet materials and composites made from various materials. It executes forward and backward mechanical movements and measures the force required to bend the specimens at

150° resulting in quantitative data that reveals a material's difference in rigidity, recoverability, fullness, softness, and anti-drape stiffness. The results are depicted as B-MEAN (mean result of forward and backward movement) = bending rigidity (gf.cm^2/cm) where a higher value indicates greater stiffness and 2HB-MEAN (mean result of forward and backward movement) = bending hysteresis (gf.cm/cm) where higher values reveal poorer recoverability per unit of fabric width. The machine can measure extremely small values at 0.0001 up to an accuracy of 50 gf.cm and offers accurate data reproducibility.

The test specimens can be sized at up to 20 cm x 20 cm with a maximum thickness of 15 mm. However, for thicker or more rigid materials, the B-MEAN and 2HB-MEAN often exceeded 50 gf.cm. Hence, for evaluating such materials, the specimens are reduced in size to help retrieve results that are closer to the characteristic dimension of the material and deliver more precise data (results are computed per unit width by the device) (de Bilbao et al., 2010). This study tested specimens sized at 5 cm (h) x 10 cm (w) for warp and 10 cm (h) x 5 cm (w) for weft. The sensitivity of the bending movement was set at 5 x 1 (smallest sensitivity) for both warp and weft specimens to ensure the results stay within 50 gf.cm and the bending rate was fixed at 0.5 cm^{-1}/s. The specimens were secured onto a fixed jaw and a moving jaw by tightening the screws with a ratchet screwdriver. During the experiment, the clamp rotated around the fixed jaw ensuring a continuous curve throughout the specimen length. **Figure 5-18a** and **b**, illustrates the specimen size and test setup.
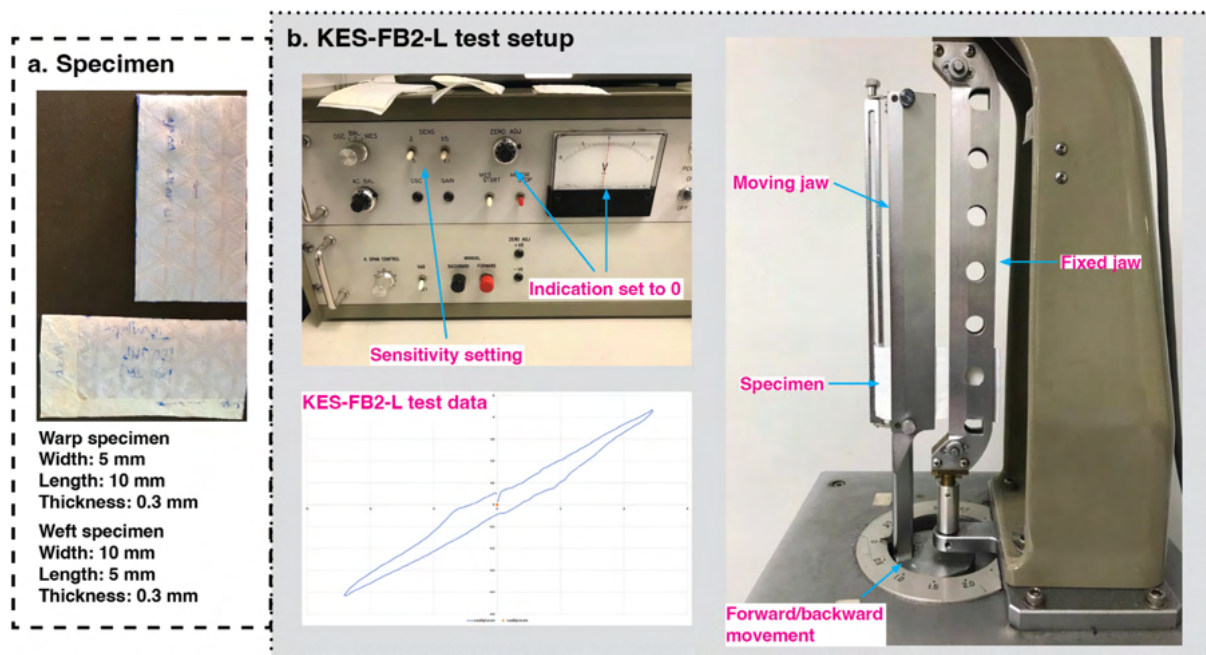
Figure 5-19 a. Specimen size and b. KES-FB2-L pure bending tester setup

In this study, five bioinspired patterns inspired by honeycomb, Widmanstätten patterns (meteorites), marine sponge skeletal structures, and luffa sponge structures were abstracted as honeycomb, rectangle, circle, triangle, and square shapes and existed in small (edge to edge diameter $\varnothing$ = 10 mm) and large ($\varnothing$ =15 mm) scales (< 10 mm shapes were too rigid to fold properly). The shapes were designed to enhance aesthetics and facilitate the opportunity to manipulate 4DP PTC's material rigidity. Two specimens derived from each type of shape (**Table 5-3** and **5-4**), totalling 10. All shapes tessellated edge-to-edge apart from the circle specimens (circular shapes cannot fully tessellate due to its geometry). The simplified structures enable an even distribution of polymers ensuing the 4DP PTCs to have uniform mechanical properties. Each individual shape within the patterns were hollowed in the middle which reduced material use and printing time (as shown in **Table 5-4**) while retaining rigidity, strength, and performance. By utilising these patterns, 4DP PTCs can be enhanced with uniform pressure distribution, excellent mechanical properties, versatile shape manipulation,

and improved mobility; also seen in other aerospace and automotive applications (Al-Dhaheri et al., 2020; Ganilova & Low, 2018).
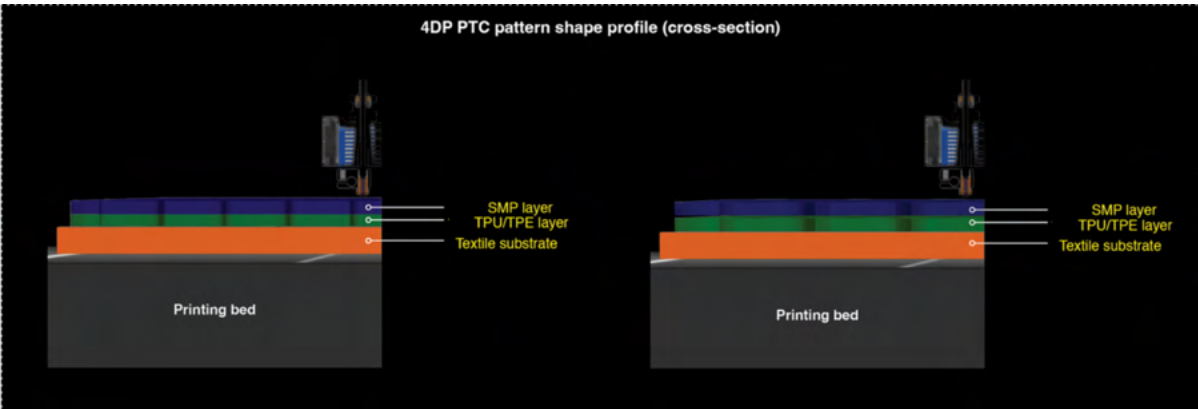
Table 5-3 Printing time and polymer usage for a 200 mm x 200 mm specimen
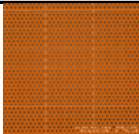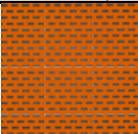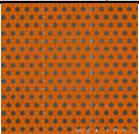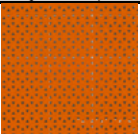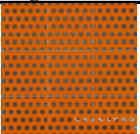
Pattern	Specimen no.	TPU pattern size	Printing time	Filament used (g)	SMP pattern size	Printing time	Filament used (g)
Honeycomb	1	(S)	1 hr 1 min	3.31	(S)	1 hr 32 min	2.94
	2	(L)	1 hr 2 min	3.81	(L)	1 hr 9 min	3.36
Rectangle	3	(S)	1 hr 6 min	4.04	(S)	1 hr 12 min	3.58
	4	(L)	51 min	3.18	(L)	55 min	2.81
Circle	5	(S)	58 min	3.49	(S)	1 hr 16 min	3.10
	6	(L)	38 min	2.46	(L)	47 min	2.18
Triangle	7	(S)	1 hr 17 min	4.74	(S)	1 hr 27 min	4.21
	8	(L)	59 min	3.68	(L)	1 hr 4 min	3.26
Square	9	(S)	1 hr 3 min	3.85	(S)	1 hr 10 min	3.41
	10	(L)	45 min	2.80	(L)	48 min	2.48

Note: - (L) = 150% ($\varnothing$ = 15 mm) large infill pattern; (S) = 100% ($\varnothing$ = 10 mm) small infill pattern; g = grams; hr = hour(s); min = minute(s)

Table 5-4 3D pattern configuration and 3D file

	Pattern shape				
Pattern size	Honeycomb *(honeycomb)*	Rectangle *(cell membrane structure)*	Circle *(Polyhedral foam structure)*	Triangle *(Widmanstätten pattern)*	Square *(Deep-sea glass sponge structure)*
Small					

Large	
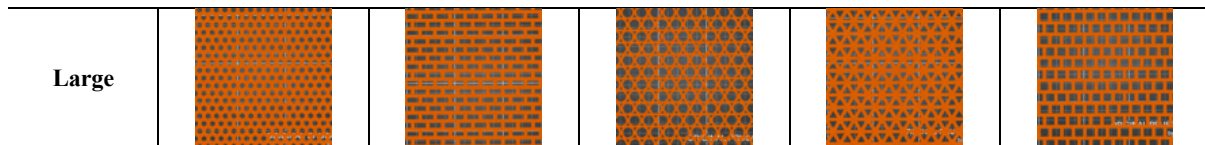
5.2.3.3 Scanning electron microscope analysis

A Hitachi TM3000 tabletop SEM (Hitachi, 2011) was used to investigate the surfaces of 4DP PTC specimens at original and programmed forms. Due to the dimension constraints of the machine, the specimens totalling 6 (F1/F2/F3-SMP 4DP PTC at original and programmed form) were sized at 8 mm x 8 mm to fit in the microscope. The experiment was conducted in an environment that adheres to the constant atmospheric conditions outlined in ISO 291:2008 (ISO, 2008b).

As the 4DP PTC specimens are not electrically conductive materials, the specimens underwent a coating process using a Hitachi E-1010 ION sputter which coated the specimen with a thin conductive film (gold or carbon) (**Figure 5-19**). The specimen is place on a copper coin and placed in a vacuum chamber which must reach 10 Pa or less for the coating process to take place. The countdown timer was set at 30 seconds and the specimens were sputtered twice totalling 60 seconds. Once the coating process is completed the specimen is placed on the SEM platform. To generate an electron beam in the SEM, the vacuum system is activated to remove the air and to create a vacuum environment. Subsequently, the measurement and analysis of the specimens are conducted using the TM3000 application. Images of the specimens were taken at various magnifications to study the 4DP PTC's polymer surface at different forms.
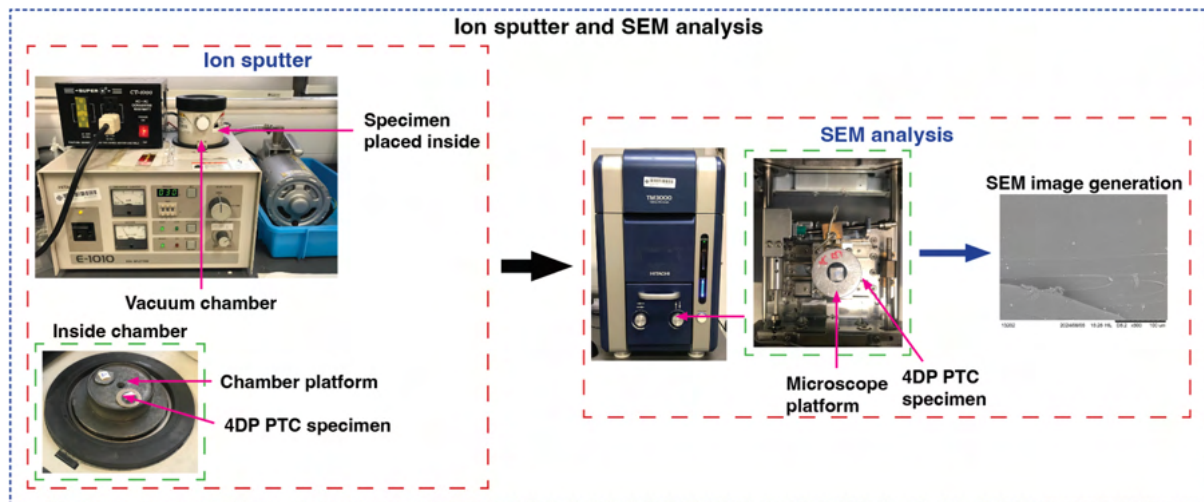
Figure 5-20 SEM analysis process

5.3 Results and discussion

5.3.1 SMP surface roughness and coefficient of friction

Table 5-5 Surface friction and roughness results (warp/weft directions)

Sample	SMD (μm)		MIU (μ)	
	Warp	*weft*	*Warp*	*weft*
SMP (warp/weft)	*0.14*	*1.40*	*0.15*	*1.54*

MIU – mean coefficient of friction; SMD – surface roughness deviation
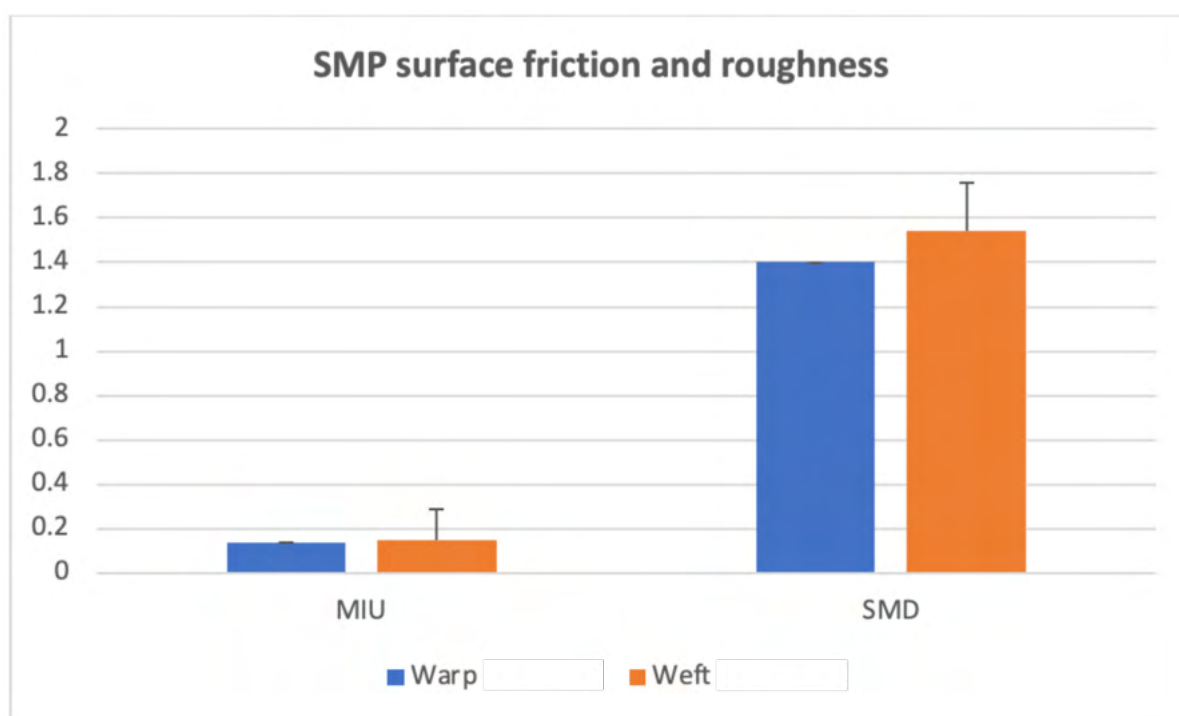
Figure 5-21 SMP surface friction and roughness results

5.3.1.1 Summary

SMP were printed at default temperatures of 200°C as recommended by the manufacturers and measured the lowest surface friction and 2nd lowest surface roughness out of all polymers after 70A TPU (**Table 5-5** and **Figure 5-20**). Warp and weft directions recorded similar MIU and SMD.

5.3.2 Mechanical performance

5.3.2.1 Peel resistance

The printing of SMP onto textile substrates has not been scientifically investigated (Koch et al., 2021) so preliminary tests of printing SMP directly onto fabric were conducted. However, the adhesion quality was often quite poor (easily peeled off), or the material did not adhere onto the fabric surface which led to the clogging of the extruder nozzle. Previous PTC experiments demonstrated that flex polymers have good adhesion without the use of any coupling agent onto synthetic knitted substrates, so the TPU/TPE polymers were used to adhere the SMPs with the textile substrates to create the 4DP PTCs. This arrangement can be used to combine polymers and textile substrates together with high durability whilst maintaining the flexibility of PTCs. A total of 15 samples (five of each combination) were printed with optimal printing parameters informed by the previous T-peel experiments and the SMP was printed at default conditions (200°C) as recommended by the manufacturer. The dimensions of the specimens were sized in accordance with ISO 11339:2022 (ISO, 2022b) (identical to the experiments in chapter four). The results of the polymer-SMP composite test strips are shown in **Table 5-6**, **Figures 5-21** and **5-22**. ISO recommends the first and last 25 mm of the test to be disregarded when examining the record curve to maximize result precision. The maximum/minimum load and average load were recorded in newtons (N), and average peel strength was presented as N/mm^2.

Table 5-6 T-peel test results in accordance with ISO 11339:2022 for TPU/TPE – SMP

Sample	Peel resistance			Peel strength
	Maximum (N)	*Average (N)*	*Minimum (N)*	*Average (N/mm^2)*
F1-SMP (70A TPU)	*140.00*	*118.00*		*22.18*
F2-SMP (82A TPU)	*87.00*	*65.30*	0	*6.81*
F3-SMP (40D TPE)	*39.20*	*29.60*		*1.39*
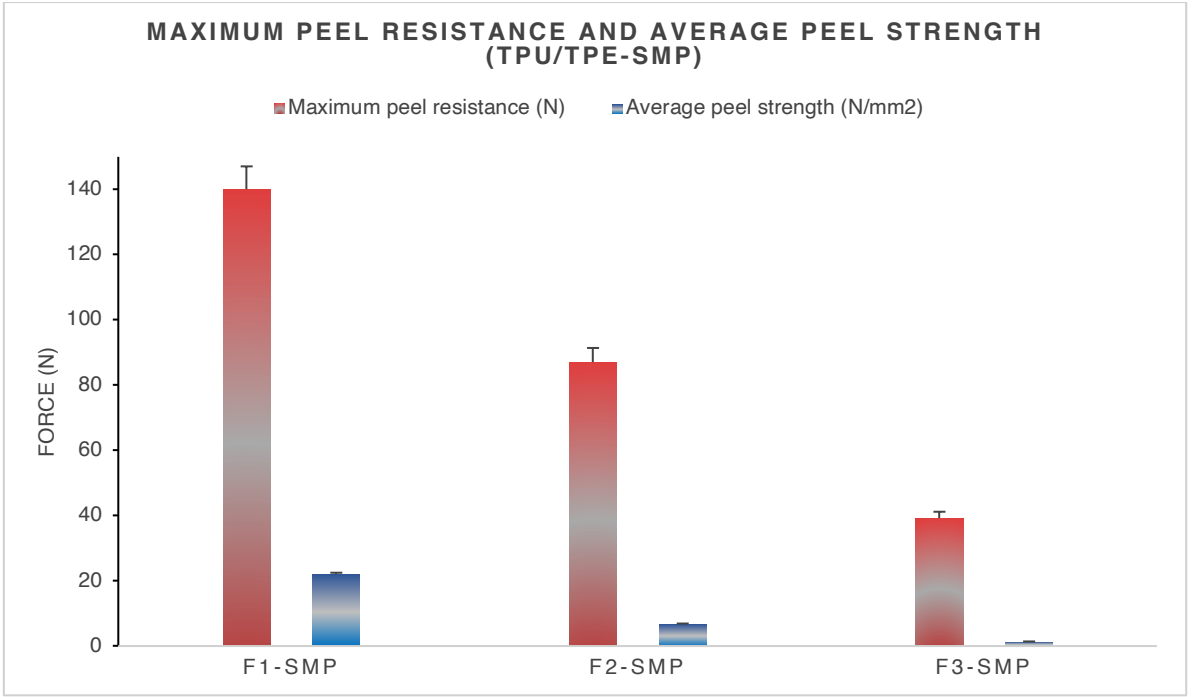
Figure 5-22 Results of T-peel tests for TPU/TPE – SMP
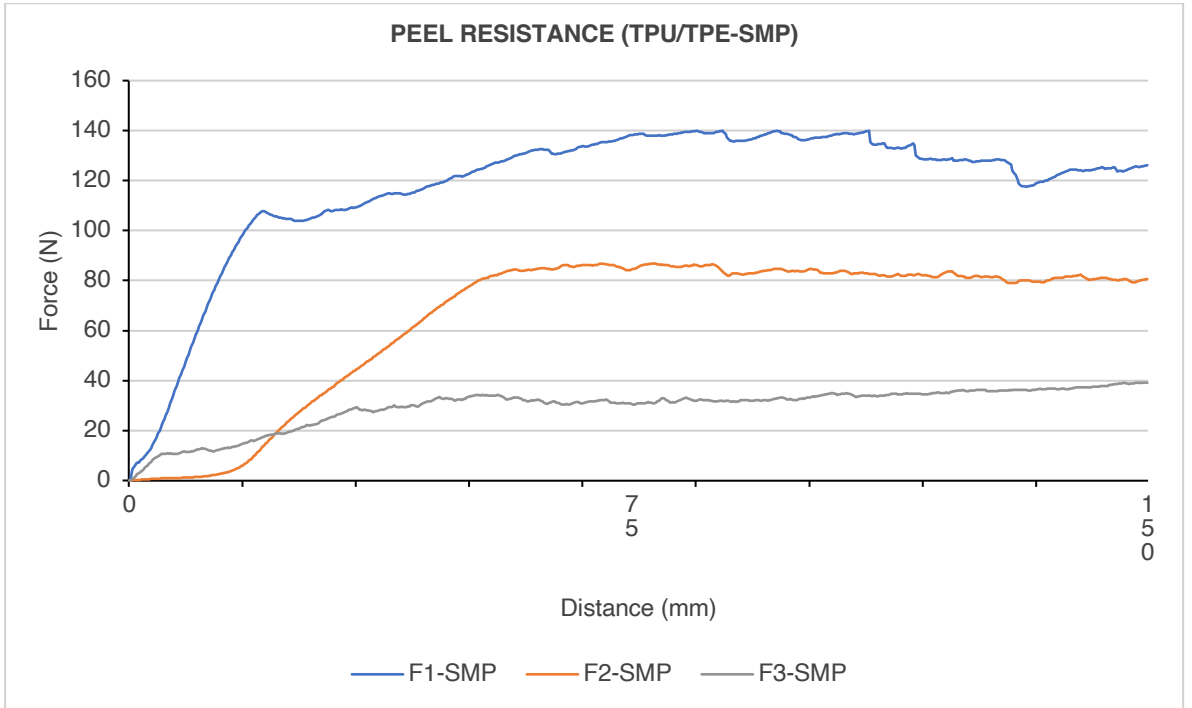
Figure 5-23 T-peel test results for TPU/TPE-SMP
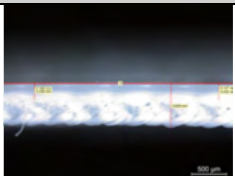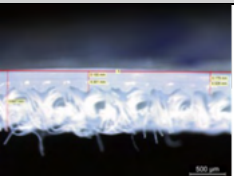
5.3.2.1.1 Summary

Flex polymer is shown to significantly influence peel resistance between TPU/TPE-SMP. F1-SMP demonstrated significantly greater peel resistance than F2-SMP (326% greater peel strength) and F3-SMP (1596% greater peel strength) (**Figure 5-21** and **5-22**). Overall, all the specimens demonstrated a consistent peel resistance which reflected the gradual separation of the flex polymer from the SMP with no damage found in either adherend. Further experiments will investigate the effects of flex polymer Shore on shape recovery.

5.3.2.2 Cross-sectional microscopic analysis

Table 5-7 shows cross-sectional microscopic images of 4DP PTCs composed of an identical nylon substrate and PU-based SMP but with a different combination of flex polymer resulting in F1/F2/F3-SMP 4DP PTCs. The polymers were printed at optimal printing temperatures: flex layer was printed at 240°C and the SMP layer at 200°C. The experimental set up is identical to the cross-sectional analysis in sections 4.3.1.2 and 4.3.2.2.

Table 5-7 Cross-sectional microscopic analysis of 4DP PTCs

	F1-SMP 4DP PTC			F2-SMP 4DP PTC			F3-SMP 4DP PTC		
	FLEX	**SMP**	**Total**	**FLEX**	**SMP**	**Total**	**FLEX**	**SMP**	**Total**
MAX	0.05 mm	0.26 mm	0.31 mm	0.04 mm	0.23 mm	0.17 mm	0.10 mm	0.20 mm	0.30 mm
MIN	0.05 mm	0.18 mm	0.23 mm	0.01 mm	0.13 mm	0.24 mm	0.18 mm	0.15 mm	0.33 mm
Total	0.75 mm			0.63 mm			0.85 mm		

MAX – maximum polymer depth; MIN – minimum polymer depth; Total – total thickness of polymer and fabric

The total thickness of the 4DP PTCs ranges from 0.63 mm to 0.85 mm with F3-SMP 4DP PTC recording the highest total thickness. And the variance between minimum/maximum depth of flex layer ranges from 0.01 mm to 0.18 mm with F3-SMP 4DP PTC recording the highest flex layer thickness ranging from 0.10 mm to 0.18 mm (minimum and maximum points). F1-SMP

4DP PTC had the least difference between minimum and maximum depth of flex layer at < 0.01 mm indicating greater consistency in polymer thickness. Moreover, the SMP layer thickness ranged from 0.13 mm to 0.26 mm with F1-SMP 4DP PTC measuring the thickest SMP layer followed by F2-SMP 4DP PTC and F3-SMP 4DP PTC. F3-SMP 4DP PTC had the least difference between minimum and maximum depth of SMP layer at 0.05 mm indicating greater consistency in polymer thickness.

5.3.2.2.1 Summary

In this experiment, the results have shown different flex layer combination to influence the thickness and consistency of the SMP layer and the total thickness of the 4DP PTC. The findings also show an increase in SMP layer thickness when a lower shore flex polymer was used with F1-SMP 4DP PTC measuring a thicker SMP layer in comparison with F2 and F3-SMP 4DP PTCs. The softer flex polymer layer enhances the fusion and covalent bond between the SMP and flex layers yielding greater peel resistance between substrates (consistent with the results shown in 5.3.2.1). This phenomenon has been shown in 3DP PTCs and 4DP PTCs (Cheung & Choi, 2022; Cheung et al., 2024; Schollenberger, 2000).

5.3.2.3 Tensile strength and Young's modulus

Polymer Shore and printing directions was shown to affect the tensile strength and modulus of 4DP PTCs (**Table 5-8**, **Figures 5-23** and **5-24**). The highest breaking load was achieved by F2-SMP 4DP PTC for both warp (652.30 N, *SD* = 20.45) and weft (665.70 N, *SD* = 83.10), followed by F1 SMP 4DP PTC with warp (582.60 N, *SD* = 56.94) and weft (629.39 N, *SD* = 47.64), and F3 SMP 4DP PTC with a significantly lower tensile strength with warp (356.85 N, *SD* = 33.89) and weft (380.43 N, *SN* = 25.08).

Table 5-8 4DP PTC's tensile strength and Young's modulus

Sample	Warp					Weft				
	Average breaking load (N)	*SD*	*Average breaking extension (%)*	*SD*	*Young's modulus (GPa)*	*Average breaking load (N)*	*SD*	*Average breaking extension (%)*	*SD*	*Young's modulus (GPa)*
F1-SMP 4DP PTC	582.60	56.94	4.38	0.71	0.11	629.39	47.64	3.99	0.69	0.16
F2-SMP 4DP PTC	652.30	20.45	7.52	0.30	0.14	665.70	83.10	5.05	0.60	0.18
F3-SMP 4DP PTC	356.85	33.89	11.41	0.60	0.11	380.43	25.08	10.86	0.59	0.17

Notes: - (N) = newtons, *SD* = standard deviation, and *(GPa)* = gigapascal
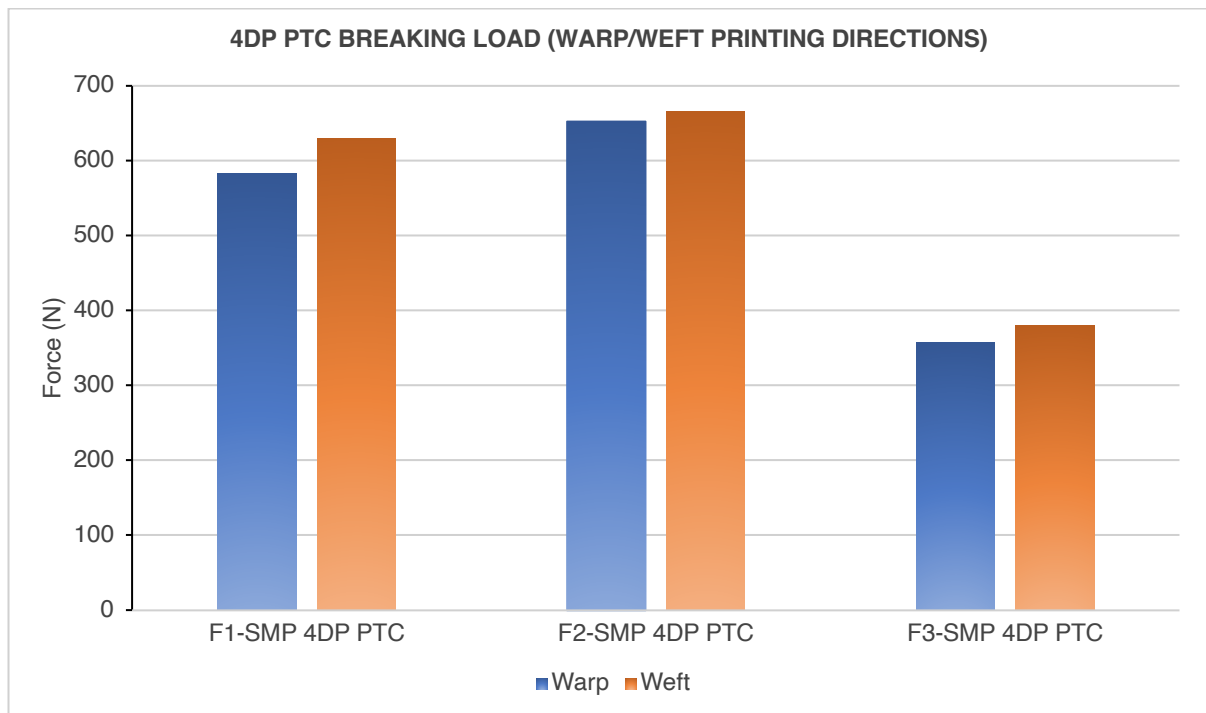
Figure 5-24 4DP PTC breaking load (warp/weft printing directions)
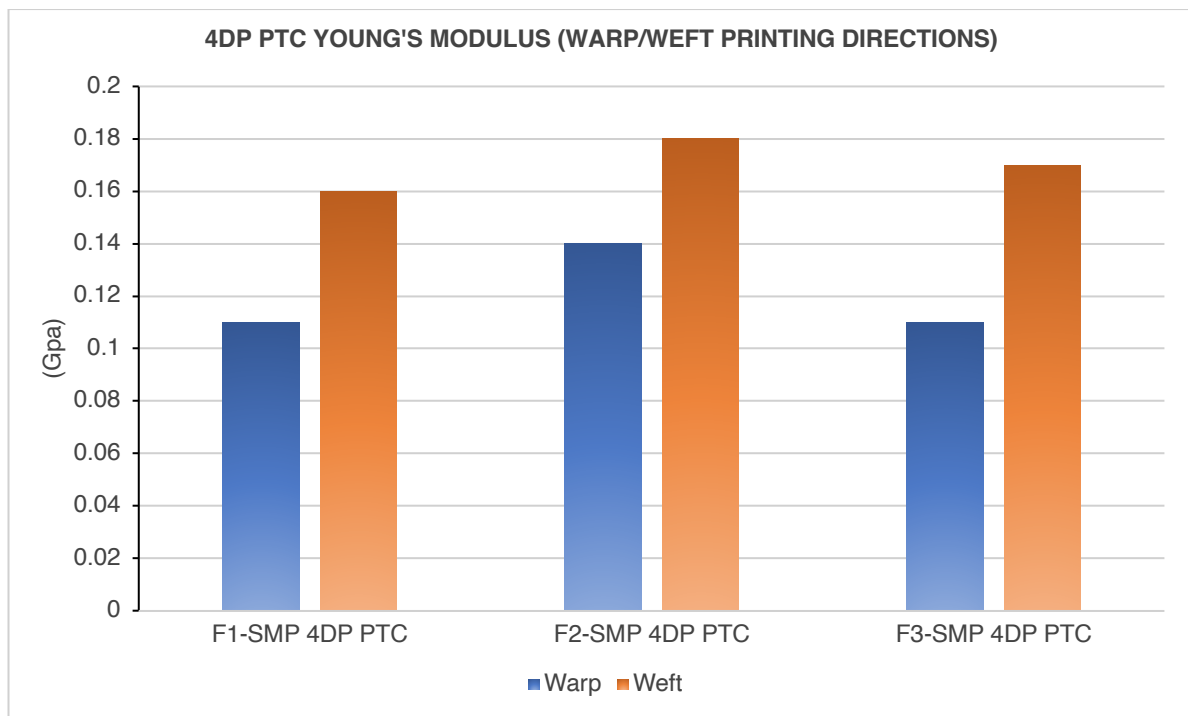
Figure 5-25 4DP PTC Young's modulus (warp/weft printing directions)

5.3.2.3.1 Summary

Though F3 had the highest Shore, harder materials are prone to being brittle which leads to the reliance of the unhardened internal material for its structural strength (in this case the 4DP PTC relies on the nylon substrate's tensile strength) (Accu, 2023). Overall, weft printing directions demonstrated higher tensile strength than specimens printed in warp. In addition, F2-SMP 4DP PTC recorded marginally higher Gpa than F1/F3 specimens with weft specimens also recording higher modulus than warp specimens which indicates its higher stiffness.

5.3.2.4 Bursting strength

Table 5-9 Bursting strength results

Sample	Temperature	*kpa*	Height at burst *(mm)*	Time at burst *(s)*
F1-SMP 4DP PTC	**210°C**	753.091	23.63	23.33
	220°C	720.272	17.60	24.00
	230°C	536.642	11.97	23.33
	240°C	591.341	18.23	18.67
	250°C	580.079	14.60	15.00
F2-SMP 4DP PTC	**210°C**	667.872	22.20	22.67
	220°C	741.876	18.40	24.67
	230°C	603.291	18.80	17.67
	240°C	666.493	17.90	21.67
	250°C	579.505	16.60	14.93
F3-SMP 4DP PTC	**210°C**	553.277	13.55	21.33
	220°C	512.551	12.37	23.00
	230°C	577.809	16.11	17.00
	240°C	491.609	14.84	18.67
	250°C	511.992	15.29	14.67

Note: - (s) = seconds; (mm) = millimetres; (kpa) = kilopascal
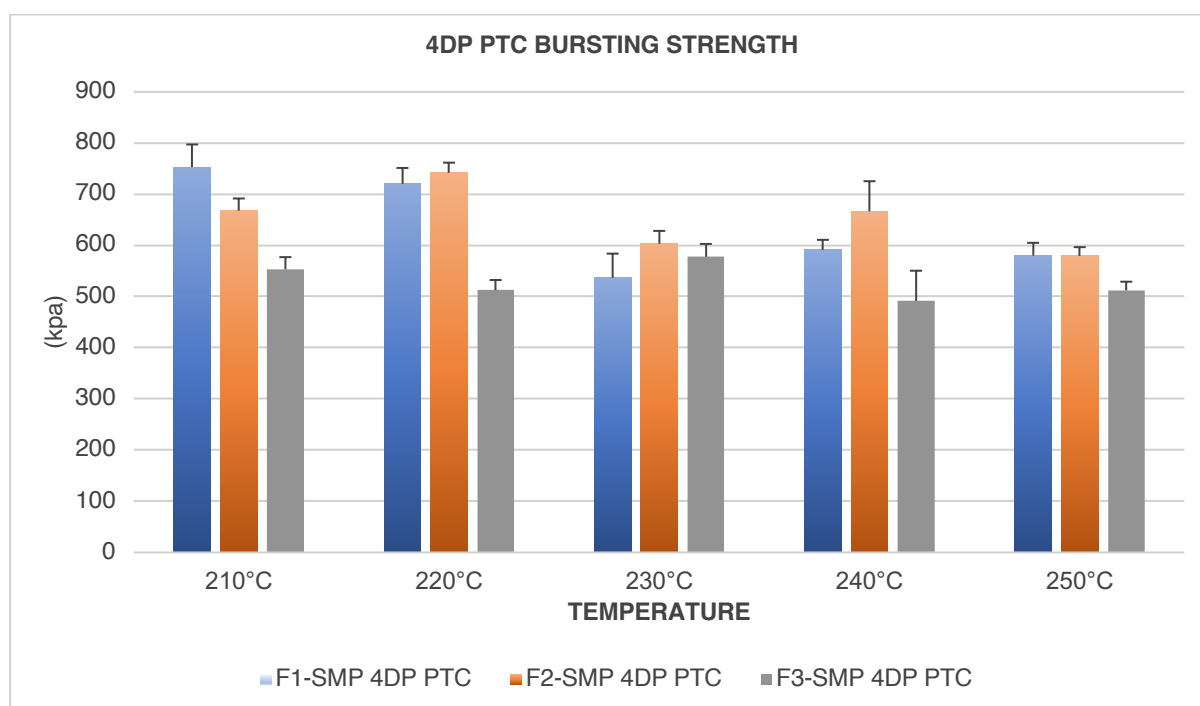
Figure 5-26 4DP PTC bursting strength

TPU extrusion temperature and TPU type was shown to affect bursting strength (**Table 5-9** and **Figure 5-25**). F1-SMP (210°C TPU) specimens measured with the highest average strength of 753.091 kpa meanwhile F3-SMP printed at 240°C TPU yielded the lowest average

at 491.609 kpa. The average burst time was also lower with F3-SMP 4DP PTC. Overall, across temperatures F1-SMP specimens measured an average of 636.285 kpa, F2-SMP at 651.810 kpa, and F3-SMP at 529.451 kpa with 220°C F2-SMP yielding the highest bursting strength of 741.876 kpa.

5.3.2.4.1 Summary

The results indicate that extrusion temperature and type of TPU to influence bursting property. Overall F2-SMP measured with an average that was slightly above F1-SMP at 651.808 kpa across temperatures with F3-SMP having the lowest resilience to bursting. The results suggest printing 70A TPU at 210°C, 82A TPU at 220°C, and 40D TPU at 230 °C.

5.3.3 Shape performance

5.3.3.1 Plain specimen

The experiments in this section are conducted on F1/F2/F3-SMP 4DP PTCs specimens with an all-over rectilinear infill but without a pattern.

5.3.3.1.1 Shape fixity and recovery

The specimens have a SMP layer thickness ranging from 0.1 mm to 1.0 mm and were examined for its ability to shape fix and recover to self-folding, self-bending, and self-contracting when subjected to a heat stimulus.

5.3.3.1.1.1 Self-folding

The specimens were subject to thermomechanical programming to a 90° angle and subsequently stimulated with Tr = 45°C under five repeated cycles. The specimens were measured using an electronic protractor to determine its ability to shape fix to a programmed

form. Higher shape fixity is demonstrated when the programmed material matches the geometry of the programmed angle.

Table 5-10 4DP PTC shape fixity and recovery for self-folding 90° angle experiments

Specimen	Tr (°C)	$\theta_{90°}$ (°)	θ_o (°)	θ_f (°)	θ_r (°)	R_f (%)	SD	R_r (%)	SD
F1-SMP 4DP PTC				10.0	94.4	94.3	2.4	95.2	1.8
F2-SMP 4DP PTC	45°C	90°	180°	10.2	97.3	94.4	3.0	91.9	3.2
F3-SMP 4DP PTC				9.5	102.2	94.7	2.6	86.4	2.5

Note: - SD: standard deviation; $\theta_{90°}$: 90° right-angle form; 180° θ_o: 180° flat form; θ_f: free deformation at flat form; θ_r: recovery; R_r: recovery ratio; R_f: fixity ratio
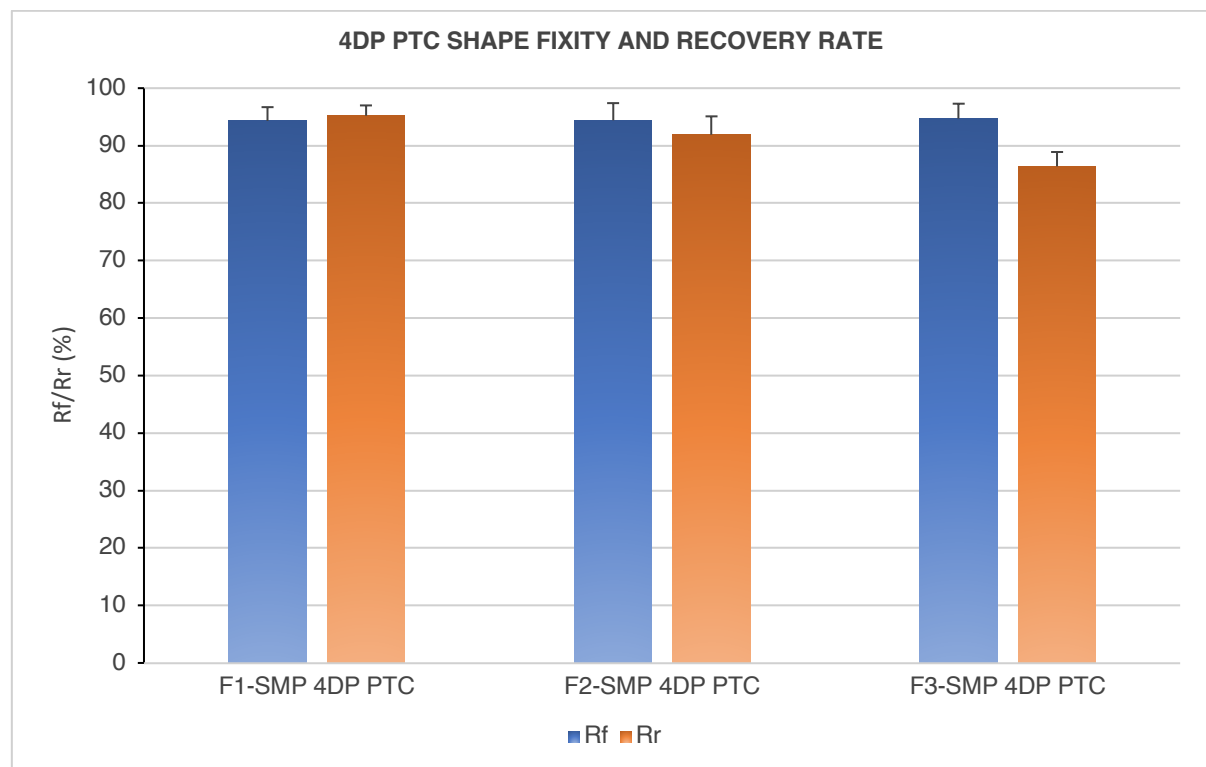
Figure 5-27 4DP PTC shape fixity and recovery rate (self-folding)

F1-SMP 4DP PTC measured an average R_f of 94.3% (*SD* = 2.4), F2-SMP 4DP PTC with 94.4% (*SD* = 3.0), and F3-SMP 4DP PTC with 94.7% (*SD* = 2.6) (**Table 5-10** and **Figure 5-26**). In addition, F1-SMP 4DP PTC measured with an average R_r of 95.2% (*SD* = 1.8), F2-SMP 4DP PTC with 91.9% (*SD* = 3.2), and F3-SMP 4DP PTC with 86.4% (*SD* = 2.5). The results indicate

F3-SMP combination to offer marginally better shape fixity performance but poorer recovery than F1/F2-SMP (F1-SMP has better shape recovery across specimens). This phenomenon is caused by its higher Shore hardness which helps with its ability to fix to a form but at the cost of its ability to transform in shape. The lower Shore polymers have better mobility when subjected to Tr (Sun et al., 2015).

5.3.3.1.1.2 Self-bending

For self-bending experiments, the specimens were subject to thermomechanical programming to a self-bending form with a 240° angle and subsequently stimulated with Tr = 45°C under five repeated cycles. The specimens were measured using an electronic protractor to determine its ability to shape fix to a programmed form. Higher shape fixity is demonstrated when the programmed material matches the geometry of the programmed angle.

Table 5-11 4DP PTC shape fixity and recovery for self-bending experiments

Specimen	Tr (°C)	$\theta_{b°}$ (°)	θ_o (°)	θ_f (°)	θ_r (°)	R_f (%)	SD	R_r (%)	SD
F1-SMP 4DP PTC				0.0	45.3	100.0	0.0	223.0	7.6
F2-SMP 4DP PTC	45°C	240°	180°	0.0	34.3	100.0	0.0	171.5	6.1
F3-SMP 4DP PTC				0.0	29.7	100.0	0.0	148.3	5.8

Note: - SD: standard deviation; $\theta_{90°}$: 90° right-angle form; 180° θ_o: 180° flat form; θ_f: free deformation at flat form; θ_r: recovery; R_r: recovery ratio; R_f: fixity ratio
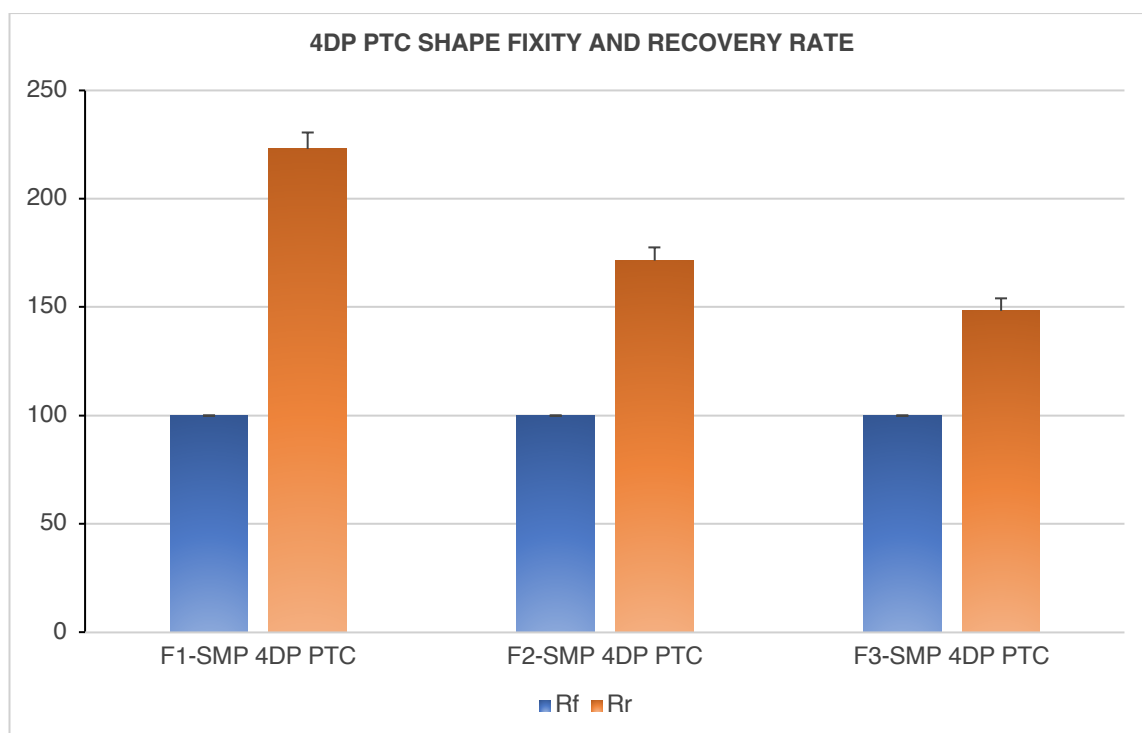
Figure 5-28 4DP PTC shape fixity and recovery rate (self-bending)

Excellent shape fixity was found across specimens with F1/F2/F3-SMP 4DP PTCs measuring an average R_f of 100.0% ($SD = 2.4$) (**Table 5-11** and **Figure 5-27**). For shape recovery, all types of specimens produced angles that were beyond its programmed angled. This occurrence is particularly beneficial for developing applications that require shape recovery beyond its programmed form i.e., sculptural forms. F1-SMP 4DP PTC measured with an average R_r of 223.0% ($SD = 7.6$), F2-SMP 4DP PTC with 171.5% ($SD = 6.1$), and F3-SMP 4DP PTC with 148.3% ($SD = 5.8$). The results indicate that lower shore specimens have higher mobility shown by its ability to self-bend beyond its programmed angle.

5.3.3.1.2 Shape response

5.3.3.1.2.1 Self-folding

F1/F2/F3-SMP 4DP PTCs were able to yield an average shape response of >11s at Tr 45°C (recommended temperature by manufacturer (KatoTech, n.d.-c)), which outperforms

previously researched thermo-responsive 4DP/SMP materials (Loh, 2021; Tibbits, 2014). The results showed quicker shape response as polymer Shore was increased with F3-SMP 4DP PTC recording the fastest average time (4.27s, SD = 0.95), while F1-SMP 4DP PTC recorded the slowest recovery (10.73s, SD = 3.60) (**Table 5-12** and **Figure 5-28**). In terms of shape response alone, F3-SMP 4DP PTC was the best performing specimen type.

Table 5-12 Shape response results for self-folding 90° angle experiments

Specimen	Tr	Time (s)	
		Average	*SD*
F1-SMP 4DP PTC		10.73	3.60
F2-SMP 4DP PTC	45°C	9.55	1.57
F3-SMP 4DP PTC		4.27	0.95

Note: - (s): seconds; *SD*: standard deviation.
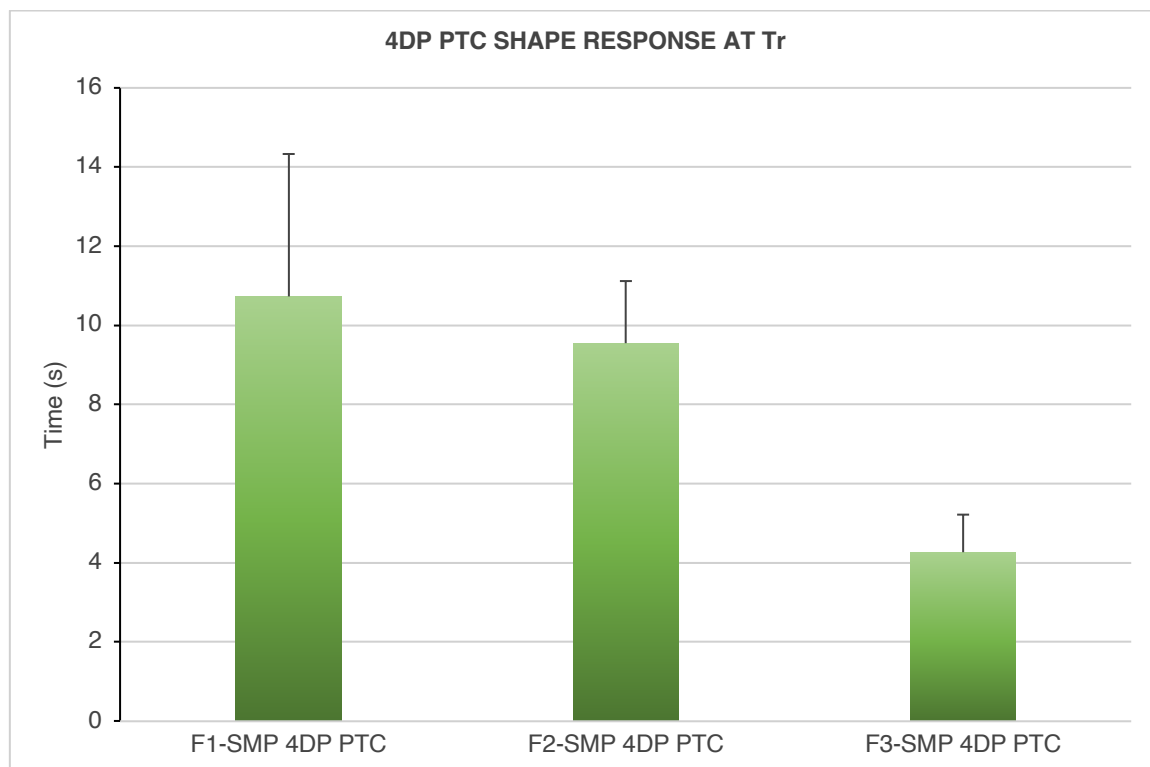
Figure 5-29 4DP PTC shape response at Tr (self-folding)

5.3.3.1.2.2 Self-bending

For self-bending experiments, F1/F2/F3-SMP 4DP PTCs were able to yield an average shape response of > 17.22s at Tr 45°C. The results showed quicker shape response as polymer Shore was increased with F3-SMP 4DP PTC recording the fastest average time (5.35s, $SD = 0.33$), while F1-SMP 4DP PTC recorded the slowest recovery (17.22s, $SD = 0.80$) (**Table 5-13** and **Figure 5-29**). Alike self-folding specimens, F3-SMP 4DP PTC was the best performing specimen type.

Table 5-13 Shape response results for self-bending experiments

Specimen	Tr	Time (s)	
		Average	*SD*
F1-SMP 4DP PTC		17.22	0.80
F2-SMP 4DP PTC	45°C	6.25	0.41
F3-SMP 4DP PTC		5.35	0.33

Note: - (s): seconds; *SD*: standard deviation.
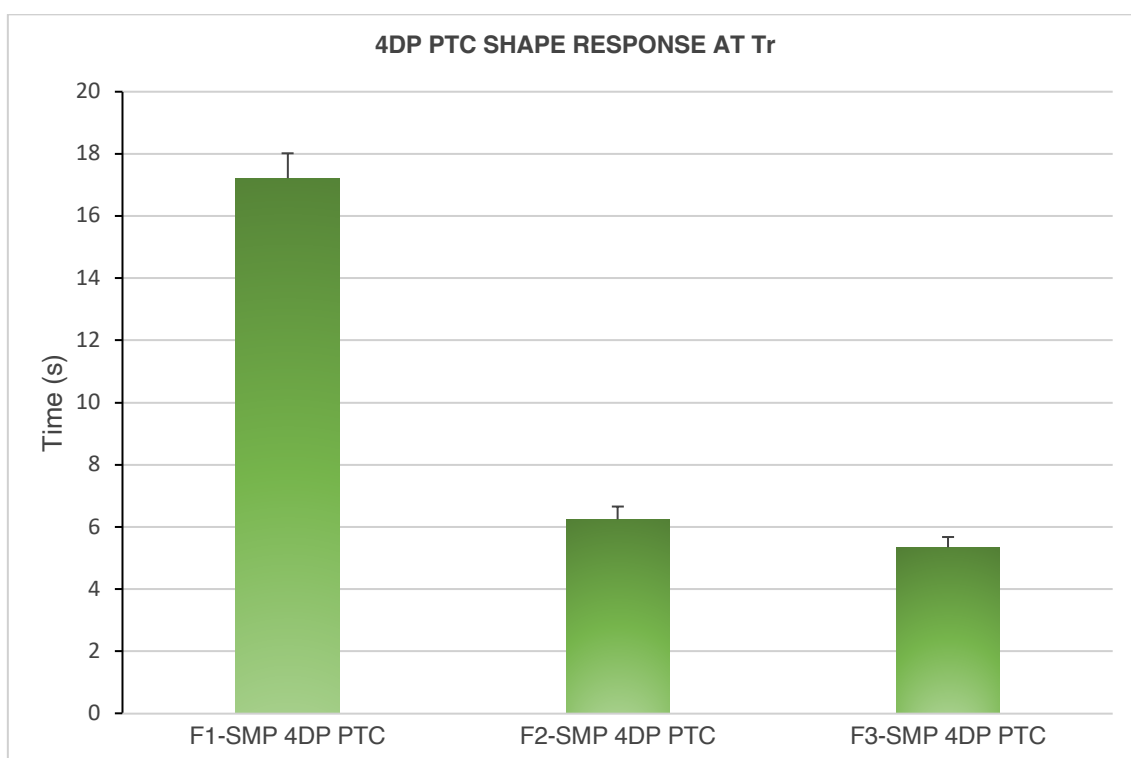
Figure 5-30 4DP PTC shape response at Tr (self-bending)

5.3.3.1.2.3 Self-contracting shape response

Self-contracting experiments were conducted to investigate how rapidly a stretched-out specimen would recover back to its permanent shape i.e., in situations when it is strained by the user. Thus, shape fixity experiments were not applicable as the printed form serves as the permanent shape. F1/F2/F3-SMP 4DP PTCs were able to yield an average shape response of > 2.67s at Tr 45°C. All specimens demonstrated comparable response speeds but F2-SMP 4PD PTC recorded marginally faster average time (2.06s, *SD* = 0.22), followed by F3-SMP 4DP PTC (2.10s, *SD* = 0.30), and F1-SMP 4DP PTC (2.67s, *SD* = 0.24) (**Table 5-14** and **Figure 5-30**).

Table 5-14 Shape response results for self-contracting experiments

Specimen	Tr	Time (s)	
		Average	*SD*
F1-SMP 4DP PTC		2.67	0.24
F2-SMP 4DP PTC	45°C	2.06	0.22
F3-SMP 4DP PTC		2.10	0.30

Note: - (s): seconds; *SD*: standard deviation.
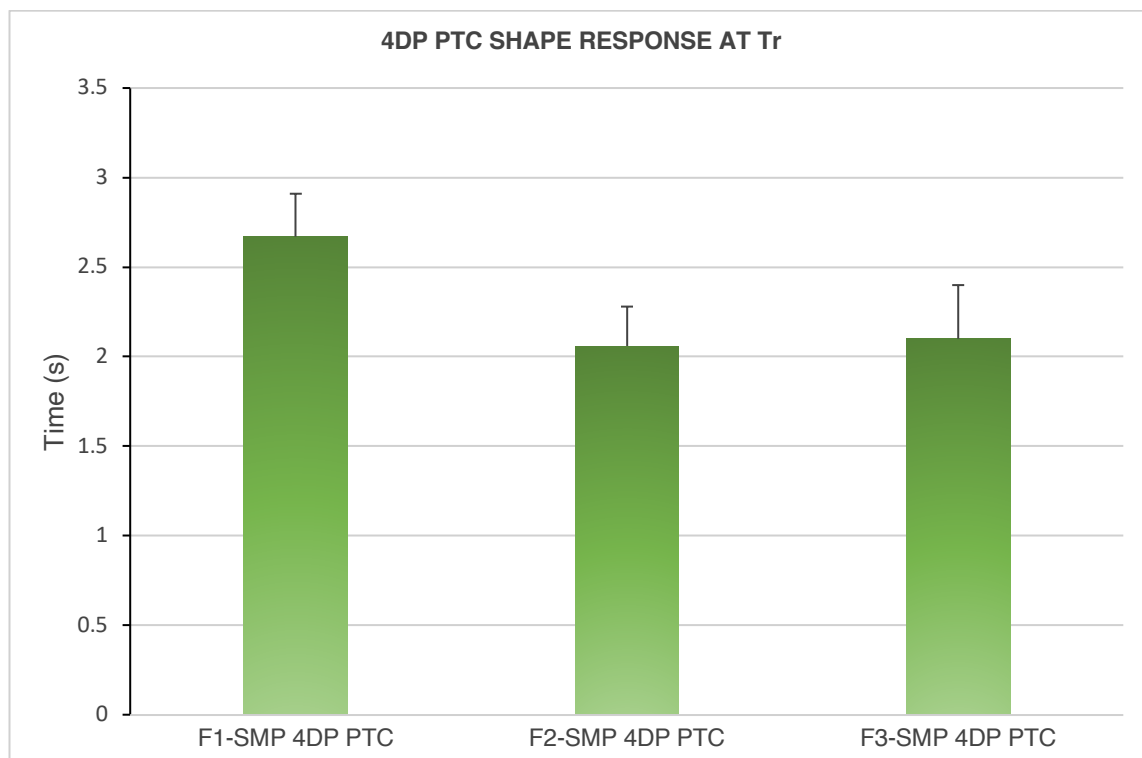
Figure 5-31 4DP PTC shape response at Tr (self-contracting)

5.3.3.1.2.4 SMP thickness on self-folding

Having identified the optimal material combination and the most consistent performing shape transformation behaviour (self-folding also used for pleating), this section investigates the effects of SMP layer thickness on shape fixity, recovery, and response. The previous shape experiments results showed F1-SMP 4DP PTCs with the default SMP thickness of 0.1 mm to achieve better overall shape fixity and recovery performance whilst the higher shore F2 and F3-SMP 4DP PTC to have quicker shape response. In this section, F1/F2/F3-SMP 4DP PTCs with a SMP layer thickness of 0.1 mm to 1 mm are tested for their shape fixity and recovery. The specimens were subject to thermomechanical programming to a 90° angle and subsequently stimulated with Tr = 45°C under five repeated cycles. The specimens were measured using an electronic protractor to determine its ability to shape fix to a programmed form. Higher shape fixity is demonstrated when the programmed material matches the geometry of the programmed angle.

Table 5-15 4DP PTC self-folding shape fixity and recovery experiments (0.1 mm to 1 mm)

SMP thickness (mm)	F1-SMP 4DP PTC		F2-SMP 4DP PTC		F3-SMP 4DP PTC	
	R_f (%)	R_r (%)	R_f (%)	R_r (%)	R_f (%)	R_r (%)
0.1	95.2	94.3	91.9	94.4	86.4	95.0
0.2	100.0	88.1	100.0	91.1	100.0	83.1
0.3	98.8	69.6	100.0	70.8	98.5	60.2
0.4	100.0	77.4	100.0	59.2	99.2	50.4
0.5	100.0	71.5	100.0	48.0	100.0	33.6
0.6	100.0	72.2	100.0	44.4	100.0	28.5
0.7	100.0	44.4	98.3	33.5	100.0	20.9
0.8	100.0	28.5	99.1	33.2	100.0	20.8
0.9	98.9	42.6	100.0	28.6	99.9	10.2
1.0	100.0	22.2	100.0	30.3	100.0	10.3

Note: - R_r: recovery ratio; R_f: fixity ratio
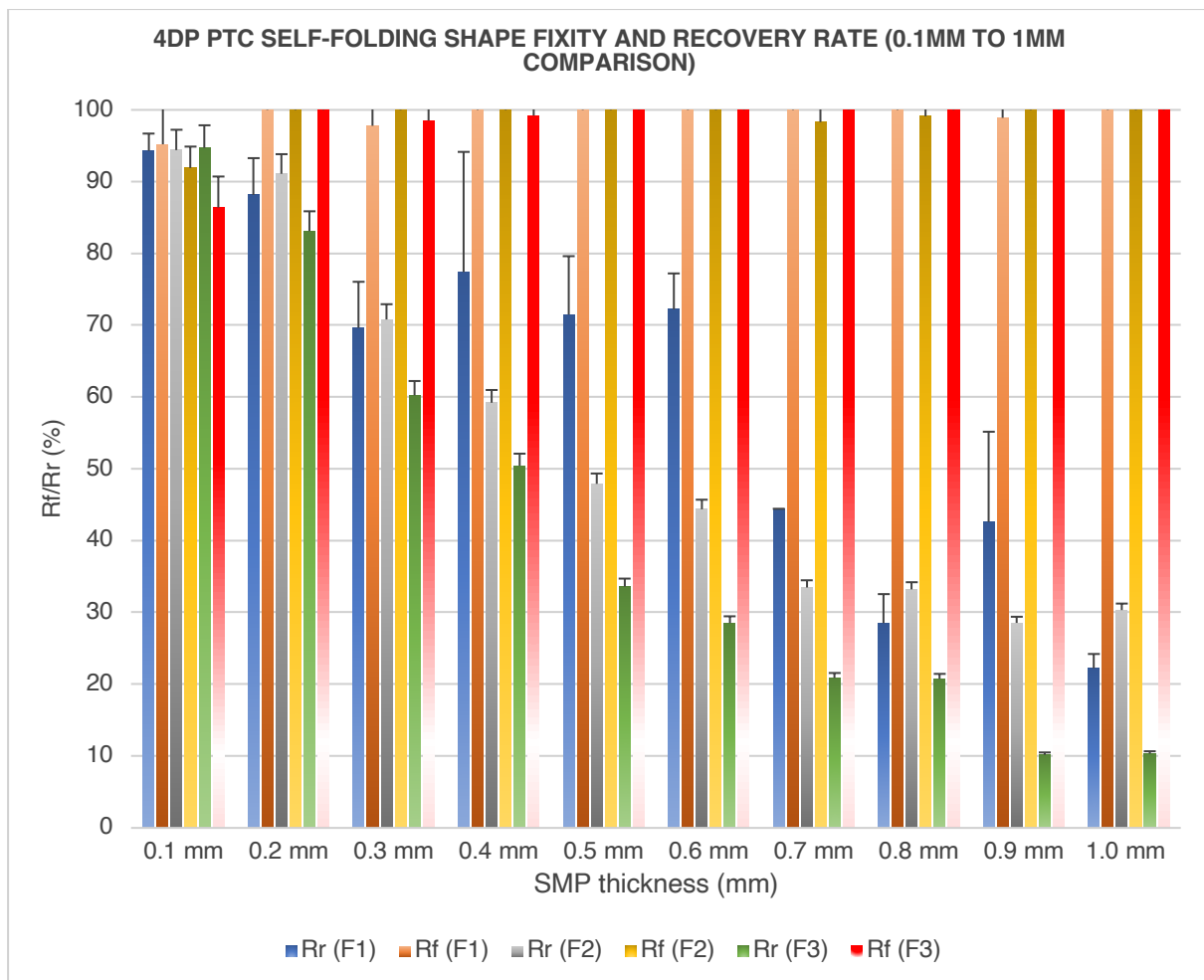
Figure 5-32 4DP PTC self-folding shape fixity and recovery rate (0.1 mm to 1 mm comparison)

The results indicated SMP layer thickness to have negligible effects on shape fixity for all three types of 4DP PTCs (**Table 5-15** and **Figure 5-31**). The shape fixity ranged from 86.4% to 100.0% with F1-SMP 4DP PTC averaging 99.19%, F2-SMP 4DP PTC at 98.93%, and F3-SMP 4DP PTC at 98.41%. On the other hand, SMP thickness had a significant influence on shape recovery with ratios ranging from 10.2% to 95.0% across specimens. The overall results indicated a decrease in shape recovery capabilities as SMP thickness was increased with the optimal performing specimens (0.1 mm and 0.2 mm SMP) achieving 83.1% to 95.0% shape recovery ratio. This decrease in shape recovery as SMP thickness is increased is caused by the thicker polymer layer which caused greater strain and constrained 4DP PTC's ability to

perform transformation when subject to Tr. The higher strain caused by the thicker SMP at a glass state reduced 4DP PTC's flexibility and ability to achieve elastic deformation and recovery. Fiber elasticity has been shown in related studies as a fundamental influence for the fixity and recovery of polymer composites (Nishikawa et al., 2012).

5.3.3.1.2.5 SMP thickness on self-folding response

Table 5-16 Shape response results for self-folding 90° angle experiments

SMP thickness (mm)	F1-SMP 4DP PTC		F2-SMP 4DP PTC		F3-SMP 4DP PTC	
	Time (s)					
	Average	SD	Average	SD	Average	SD
0.1	10.73	3.60	9.55	1.33	4.27	0.39
0.2	8.86	0.94	7.73	1.75	5.60	0.99
0.3	8.31	0.94	8.82	0.99	4.82	1.03
0.4	8.47	1.33	8.03	2.01	6.01	1.37
0.5	7.82	1.88	7.77	1.22	5.21	0.77
0.6	6.92	0.54	7.78	1.03	4.33	0.85
0.7	8.32	0.71	8.43	2.55	4.05	1.01
0.8	8.47	1.17	8.01	1.89	5.06	1.22
0.9	8.97	3.77	9.03	1.01	4.98	0.85
1.0	7.22	0.99	8.86	1.11	6.02	0.91

Note: - (s): seconds; *SD*: standard deviation.
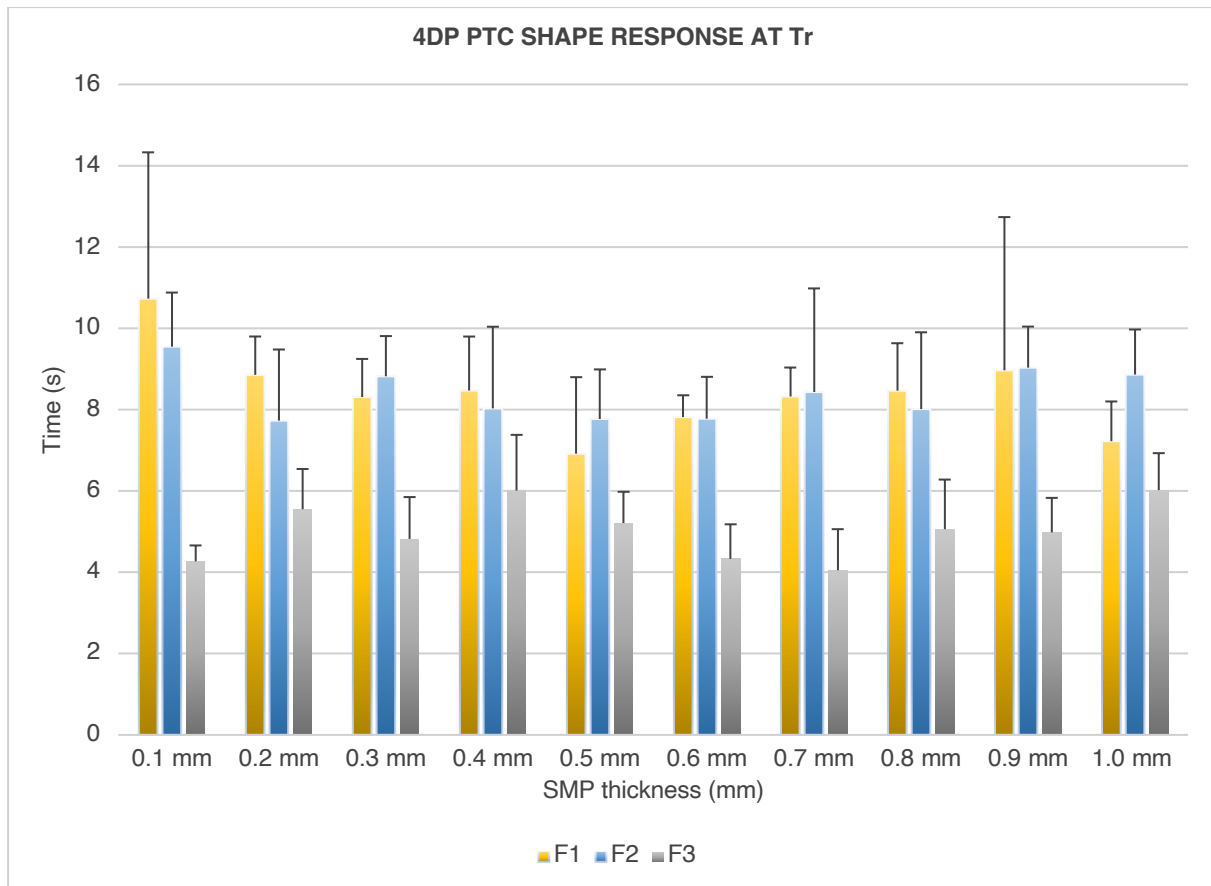
Figure 5-33 4DP PTC self-folding shape response (0.1 mm to 1 mm comparison)

The shape response of 4DP PTC specimens with 0.1 mm to 1 mm SMP layer ranged from 4.27s to 10.73s. F3-SMP 4DP PTC, on average responded the quickest at 5.03s, F2-4DP PTC at 8.40s, and F1-SMP 4DP PTC at 8.41s when subject to Tr. The overall results did not show any patterns between SMP thickness and shape response. The response rate was varied and sporadic across all specimens (**Table 5-16** and **Figure 5-32**).

5.3.3.1.3 Overall summary

Through shape recovery experiments, the following phenomena was observed:

Self-folding

1. F1-SMP 4DP PTC showed the quickest response meanwhile F3-SMP 4PP PTC was the slowest.

2. F3-SMP 4DP PTC showed highest shape fixity but lowest recovery, meanwhile F1-SMP 4DP PTC showed the best shape recovery rate.

Self-bending

1. F3-SMP 4DP PTC showed the quickest response meanwhile F1-SMP 4DP PTC was the slowest.

2. All specimens showed 100% shape fixity and the ability to self-bend beyond its programmed angle with F1-SMP 4DP PTC producing a larger angle.

Self-contracting

1. F2-SMP 4DP PTC showed a marginally quicker response in comparison with F3 and F1-SMP 4DP PTCs.

SMP thickness

1. 4DP PTCs with 0.1 mm SMP thickness were the optimal performing 4DP PTCs in terms of shape fixity and recovery at up to 100% and 95.0% respectively.

2. SMP thickness did not have a significant influence on shape response.

The results suggest that different polymer combinations have their own merits and should therefore be selected according to the application requirements where different aspects should be considered i.e., material flexibility, response speed required, and level of shape recovery required. In the subsequent chapter, different 4DP PTC patterns will be developed, and further experiments will be conducted.

5.3.3.2 Specimens with pattern

The manipulation of textiles through folding is particularly valuable for the development of pleated textile surfaces. This is supported by the previous shape performance results which have indicated F1-SMP 4DP PTC with SMP layer at 0.1 mm performing self-folding transformation as the most consistent overall. Hence, this chapter focuses on the evaluation of 4DP PTC's shape performance with the honeycomb, rectangle, circle, triangle, and square patterns in small (edge to edge diameter $\varnothing$ = 10 mm) and large ($\varnothing$ =15 mm) that are programmed with self-folding capabilities. Such specimens have a trough area of 0.1 mm with the surrounding area at 0.5 mm (technical drawing shown in **Figure 5-12**).

5.3.3.2.1 Shape fixity and recovery

The specimens were subject to thermomechanical programming to a 90° angle and subsequently stimulated with Tr = 45°C under five repeated cycles. The specimens were measured using an electronic protractor to determine its ability to shape fix to a programmed form. Higher shape fixity is demonstrated when the programmed material matches the geometry of the programmed angle.

Table 5-17 4DP PTC shape fixity and recovery for self-folding 90° angle experiments

Pattern	Pattern Size	Tr (°C)	$\theta_{90°}$ (°)	θ_o (°)	θ_f (°)	θ_r (°)	R_f (%)	SD	R_r (%)	SD
Honeycomb	S				5	80.4	97.1	3.2	89.3	4.1
	L				10	87.1	94.3	2.9	96.8	3.3
Rectangle	S				4	85.3	97.7	3.0	94.8	2.8
	L				2	82.1	98.7	4.3	91.2	5.0
Circle	S	45°C	90°	180°	2	82.1	98.6	3.4	91.2	3.7
	L				5	80.3	97.2	3.2	89.3	2.9
Triangle	S				5	86.7	97.0	3.2	96.3	3.6
	L				6	85.4	96.6	2.7	94.9	5.2
Square	S				5	81.0	97.1	4.9	90.0	6.1
	L				5	78.8	96.8	4.1	87.5	3.2

Note: - SD: standard deviation; $\theta_{90°}$: 90° right-angle form; 180° θ_o: 180° flat form; θ_f: free deformation at flat form; θ_r: recovery; R_r: recovery ratio; R_f: fixity ratio
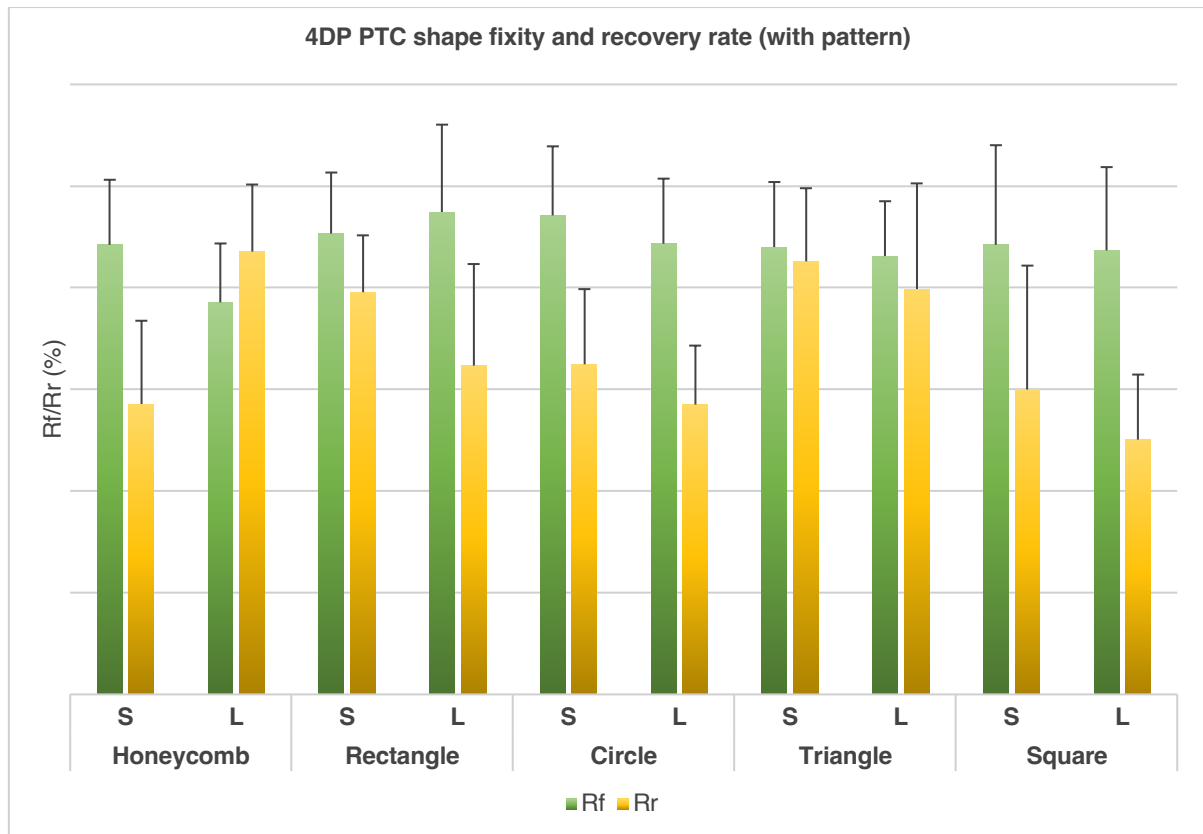
Figure 5-34 4DP PTC shape fixity and recovery (with pattern)

The specimens yielded an average R_f between 94.3% ($SD = 2.9$) to 98.7% ($SD = 4.3$) with Large rectangular pattern yielding marginally higher shape fixity in comparison with other shaped patterns and scale (**Table 5-17** and **Figure 5-33**). In addition, the specimens measured an average R_r between 87.5% ($SD = 3.2$) to 96.8% ($SD = 3.3$) with large honeycomb pattern yielding marginally better shape recovery in comparison with other shaped patterns and scale. Overall, the results indicated smaller scaled patterns to yield marginally greater shape fixity and recovery. Hence, smaller scaled patterns can be utilised to improve the shape performance of 4DP PTCs.

5.3.3.2.2 Shape response

To test for shape response, the specimens were subjected to an external force to flatten it to $\theta_0 = 180°$. The external force was subsequently removed allowing the specimen to deform (θ_f).

Then the specimens are heated at Tr triggering it to transform from its temporary shape to its permanent form. The time needed for the shape recovery to complete was recorded using an iPhone 7 stopwatch which recorded to an accuracy of two decimals. The specimens were tested under five repetitions with an averaged result and SD calculated.

Table 5-18 Shape response results for self-folding 90° angle experiments

Pattern	Pattern Size	Tr	Time (s)	
			Average	*SD*
Honeycomb	S		3.29	0.53
	L		3.32	0.45
Rectangle	S		3.12	0.41
	L	45°C	3.51	0.69
Circle	S		4.16	0.22
	L		4.09	0.91
Triangle	S		4.01	1.10
	L		4.24	1.54
Square	S		5.64	0.75
	L		4.84	0.11

Note: - (s): seconds; *SD*: standard deviation.
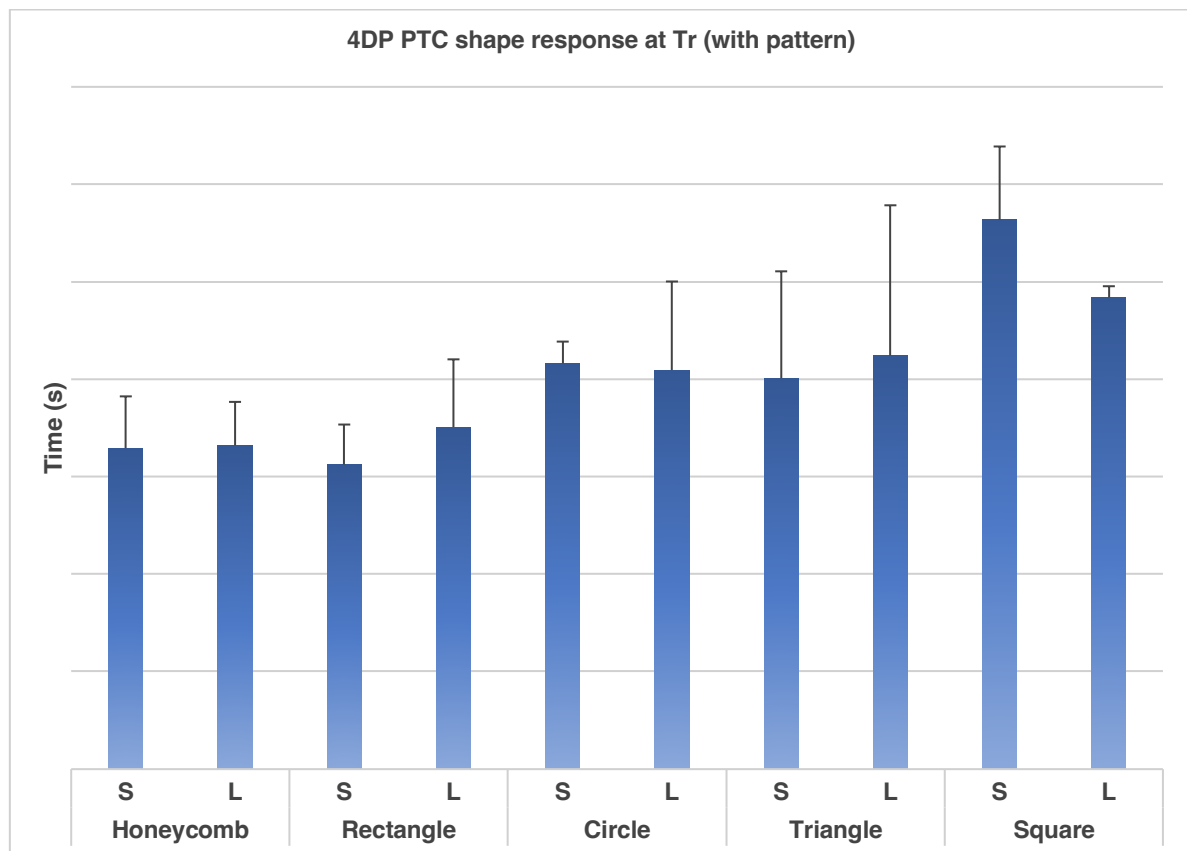
Figure 5-35 4DP PTC shape response at Tr (with pattern)

For self-folding experiments, all specimens yielded an average shape response of > 5.64s at Tr

45°C (**Table 5-18** and **Figure 5-34**). Pattern shape and scale were shown to influence the shape

response rate, with larger scaled shapes yielding marginally slower response rates. Honeycomb

patterns yielded the quickest response at 3.29s ($SD = 0.53$) for small-scaled pattern and 3.32s

($SD = 0.45$) for larger scaled pattern. On the other hand, square shaped specimens yielded the

slowest response at 5.64s ($SD = 0.75$) for small-scaled pattern and 4.84s ($SD = 0.11$) for larger

scaled pattern. Though the overall results show pattern to influence shape response, the effects

are not significant.

5.3.3.2.3 Summary

Pattern shape and size was shown to influence shape fixity, recovery, and response in 4DP

PTCs. However, the effects were insignificant, thus different shapes may be used based on

aesthetic motivations.

5.3.3.3 Bending rigidity and hysteresis

The following sections shows the bending rigidity and hysteresis of 4DP PTCs with various

patterns at $\varnothing = 10$ mm and $\varnothing = 15$ mm scales.

5.3.3.3.1 Honeycomb

Table 5-19 Bending rigidity and hysteresis of honeycomb patterns

Specimen	Warp		Weft	
	B-MEAN (gf.cm2/cm)	2HB-MEAN (gf.cm/cm)	B-MEAN (gf.cm2/cm)	2HB-MEAN (gf.cm/cm)
Small pattern	0.1338	0.0534	0.0322	0.0444
Large pattern	0.0515	0.0812	0.0084	0.0786

Note: - results for 0.1 mm SMP thickness
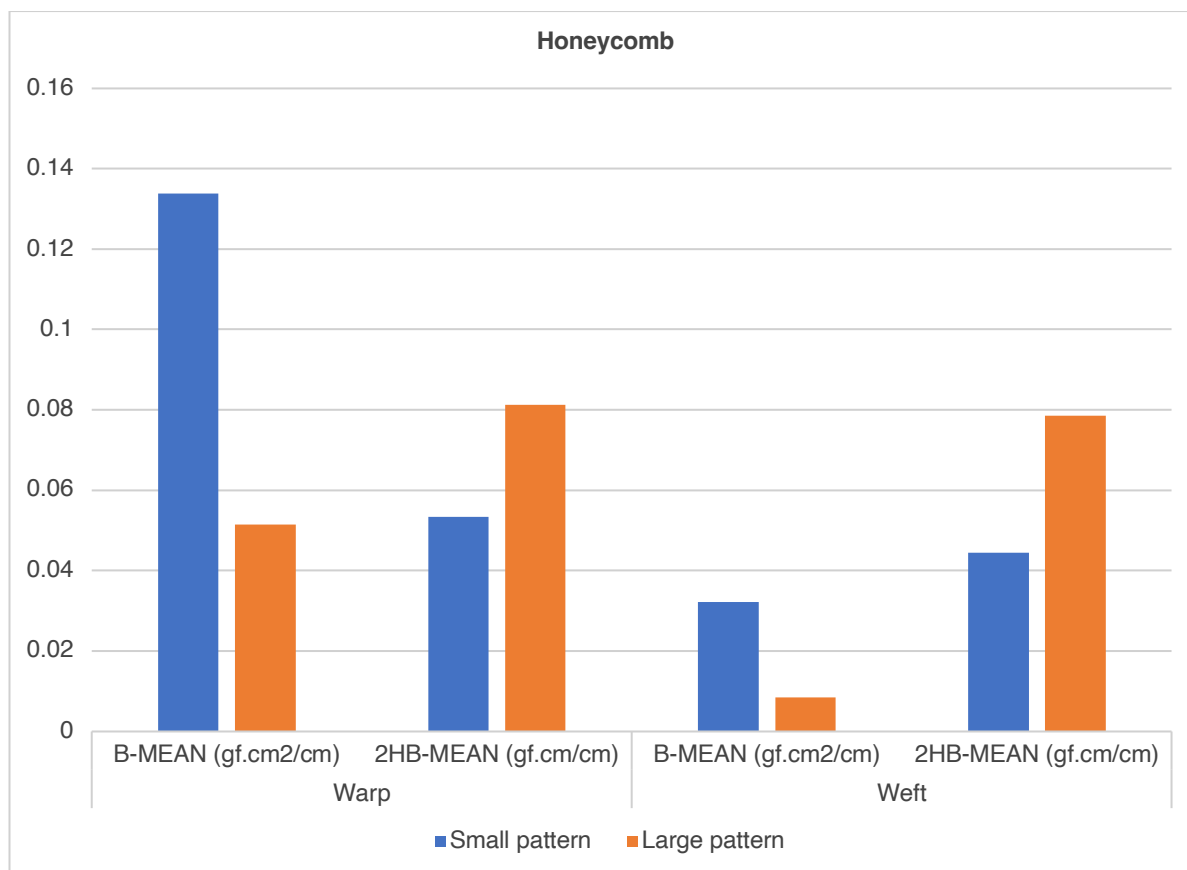
Figure 5-36 Bending rigidity and hysteresis of honeycomb patterns

The B-MEAN of honeycomb pattern specimens in warp ranges from 0.0515 to 0.1338 gf.cm^2/cm and in weft 0.0084 to 0.0322 gf.cm^2/cm (**Table 5-19** and **Figure 5-35**). The 2HB-MEAN of honeycomb specimens in warp ranged from 0.0534 to 0.0812 gf.cm/cm and in weft 0.0444 to 0.0786 gf.cm/cm. The results showed small, patterned specimens to possess greater rigidity and better recoverability. Overall, the results suggest the scale and type of repeat pattern can influence bending rigidity and hysteresis for honeycomb patterns.

5.3.3.3.2 Rectangle

Table 5-20 Bending rigidity and hysteresis of rectangle patterns

Specimen	Warp		Weft	
	B-MEAN (gf.cm2/cm)	*2HB-MEAN (gf.cm/cm)*	*B-MEAN (gf.cm2/cm)*	*2HB-MEAN (gf.cm/cm)*
Small pattern	0.0479	0.0597	0.0627	0.1293
Large pattern	0.0456	0.0811	0.1123	0.1497

Note: - results for 0.1 mm SMP thickness
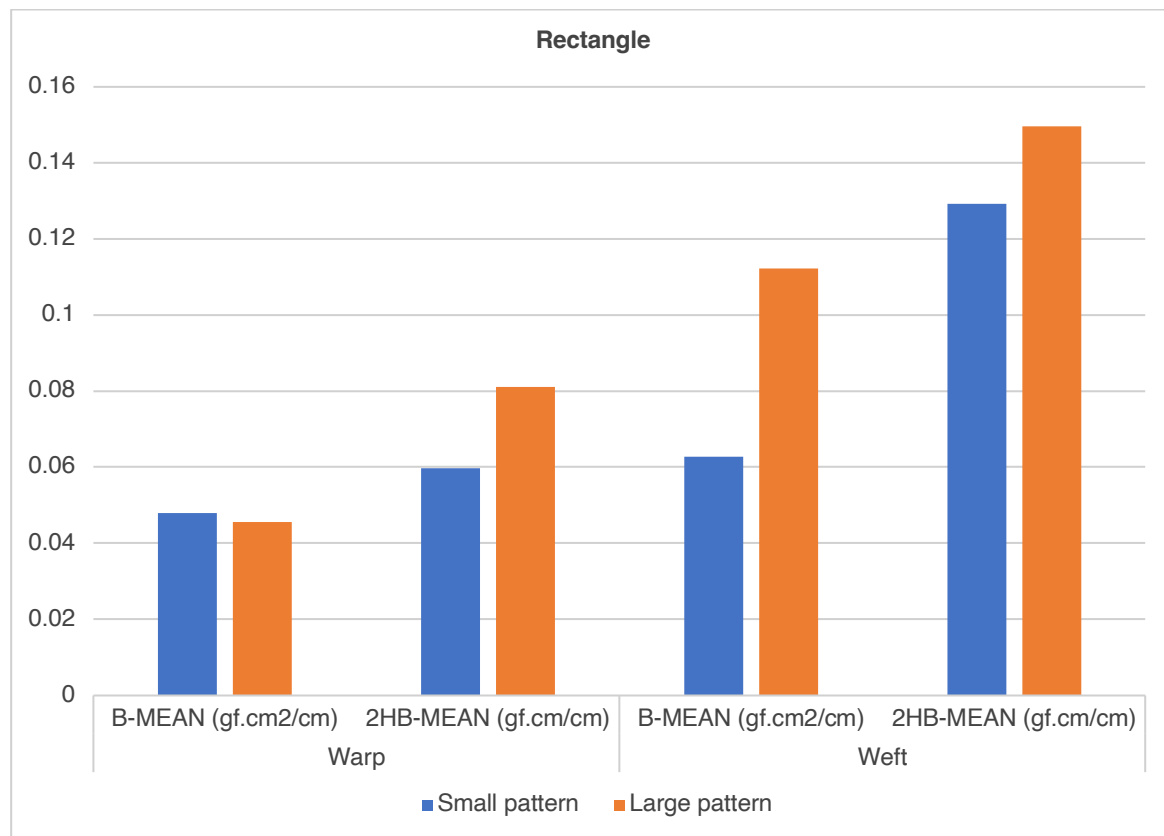
Figure 5-37 Bending rigidity and hysteresis of rectangle patterns

The B-MEAN of rectangle pattern specimens in warp ranged from 0.0456 to 0.0479 gf.cm^2/cm and in weft 0.0627 to 0.1123 gf.cm^2/cm (**Table 5-20** and **Figure 5-36**). The 2HB-MEAN of honeycomb specimens in warp ranges from 0.0597 to 0.0811 gf.cm/cm and in weft 0.1293 to 0.1497 gf.cm/cm. The results showed larger patterned specimens to possess greater rigidity but

poorer recoverability. Alike honeycomb patterns, the results too suggest the scale and type of repeat pattern can influence bending rigidity and hysteresis for rectangle patterns.

5.3.3.3.3 Circle

Table 5-21 Bending rigidity and hysteresis of circle patterns

Specimen	Warp		Weft	
	B-MEAN (gf.cm2/cm)	2HB-MEAN (gf.cm/cm)	B-MEAN (gf.cm2/cm)	2HB-MEAN (gf.cm/cm)
Small pattern	0.0531	0.0371	0.0342	0.0415
Large pattern	0.0381	0.0389	0.0396	0.0632

Note: - results for 0.1 mm SMP thickness
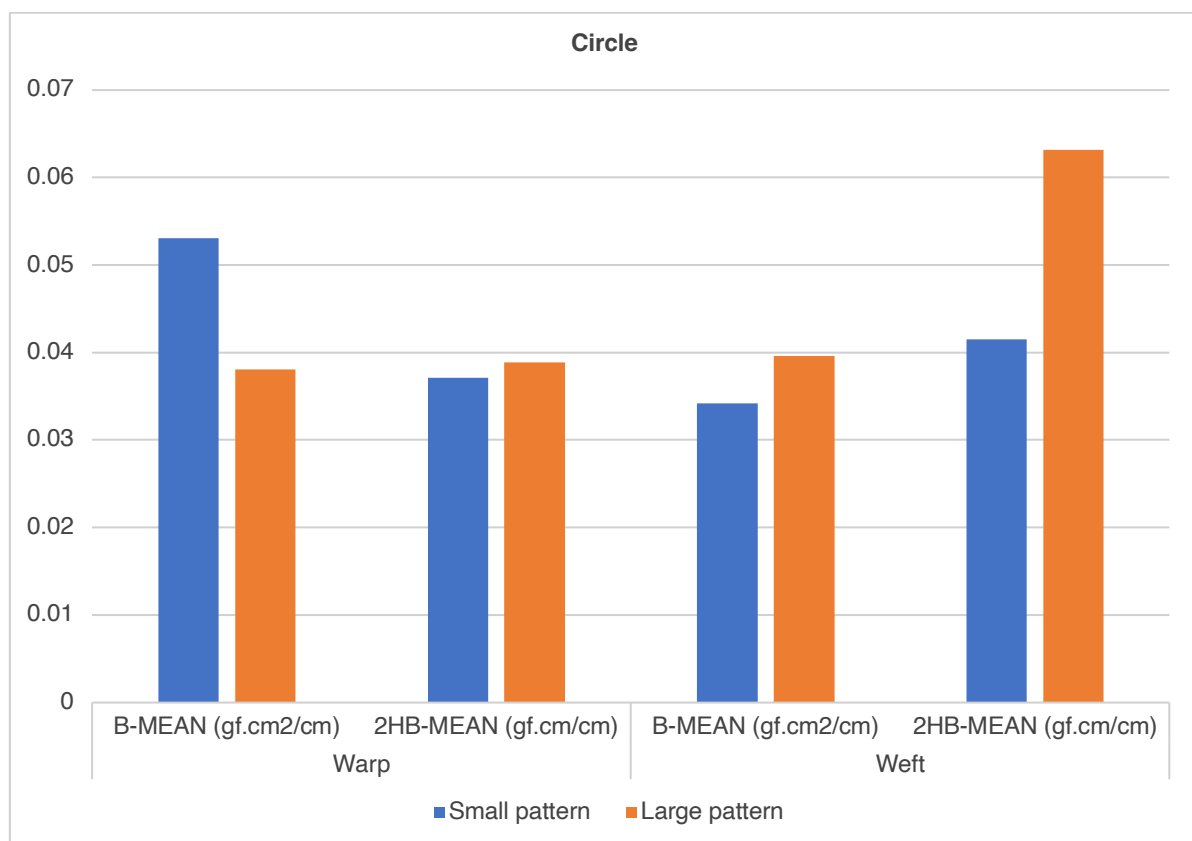
Figure 5-38 Bending rigidity and hysteresis of circle patterns

The B-MEAN of circle pattern specimens in warp ranged from 0.0381to 0.0531 gf.cm^2/cm and in weft 0.0342 to 0.396 gf.cm^2/cm (**Table 5-21** and **Figure 5-37**). The 2HB-MEAN of

honeycomb specimens in warp ranges from 0.0389 to 0.1371 gf.cm/cm and in weft 0.0415 to 0.0632 gf.cm/cm. The results showed smaller patterned specimens to possess greater rigidity and better recoverability. Overall, the results suggest the scale and type of repeat pattern can influence bending rigidity and hysteresis for circle patterns.

5.3.3.3.4 Triangle

Table 5-22 Bending rigidity and hysteresis of triangle patterns

Specimen	Warp		Weft	
	B-MEAN (gf.cm2/cm)	2HB-MEAN (gf.cm/cm)	B-MEAN (gf.cm2/cm)	2HB-MEAN (gf.cm/cm)
Small pattern	0.0959	0.0753	0.0903	0.0988
Large pattern	0.0905	0.1047	0.0435	0.1646

Note: - results for 0.1 mm SMP thickness
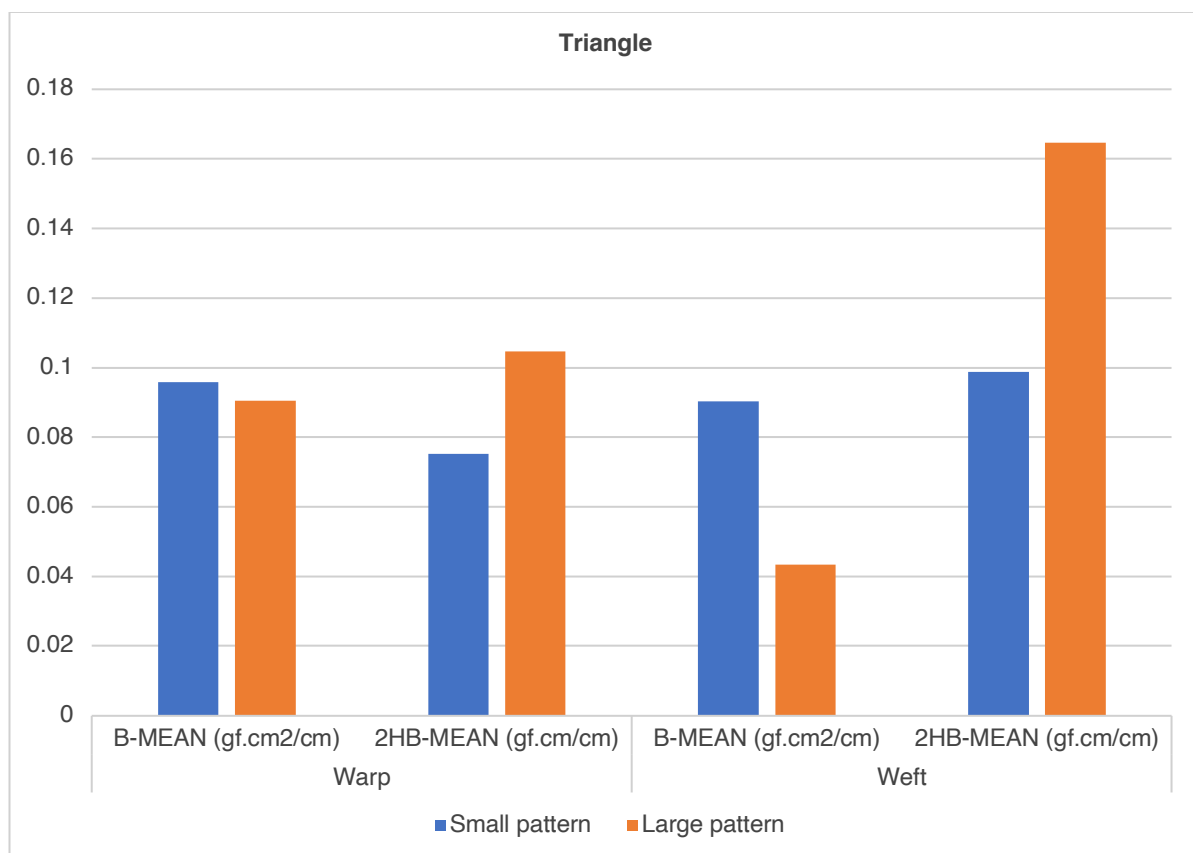
Figure 5-39 Bending rigidity and hysteresis of triangle patterns

The B-MEAN of triangle pattern specimens in warp ranged from 0.0905 to 0.0959 gf.cm²/cm and in weft 0.0435 to 0.0903 gf.cm²/cm (**Table 5-22** and **Figure 5-38**). The 2HB-MEAN of triangle specimens in warp ranged from 0.0753 to 0.1047 gf.cm/cm and in weft 0.0988 to 0.1646 gf.cm/cm. The results showed smaller patterned specimens to possess greater rigidity and better recoverability. Overall, the results suggest the scale and type of repeat pattern can influence bending rigidity and hysteresis for triangle patterns.

5.3.3.3.5 Square

Table 5-23 Bending rigidity and hysteresis of square patterns

Specimen	Warp		Weft	
	B-MEAN (gf.cm2/cm)	*2HB-MEAN (gf.cm/cm)*	*B-MEAN (gf.cm2/cm)*	*2HB-MEAN (gf.cm/cm)*
Small pattern	0.0591	0.0425	0.0544	0.0541
Large pattern	0.1069	0.1359	0.1423	0.1706

Note: - results for 0.1 mm SMP thickness
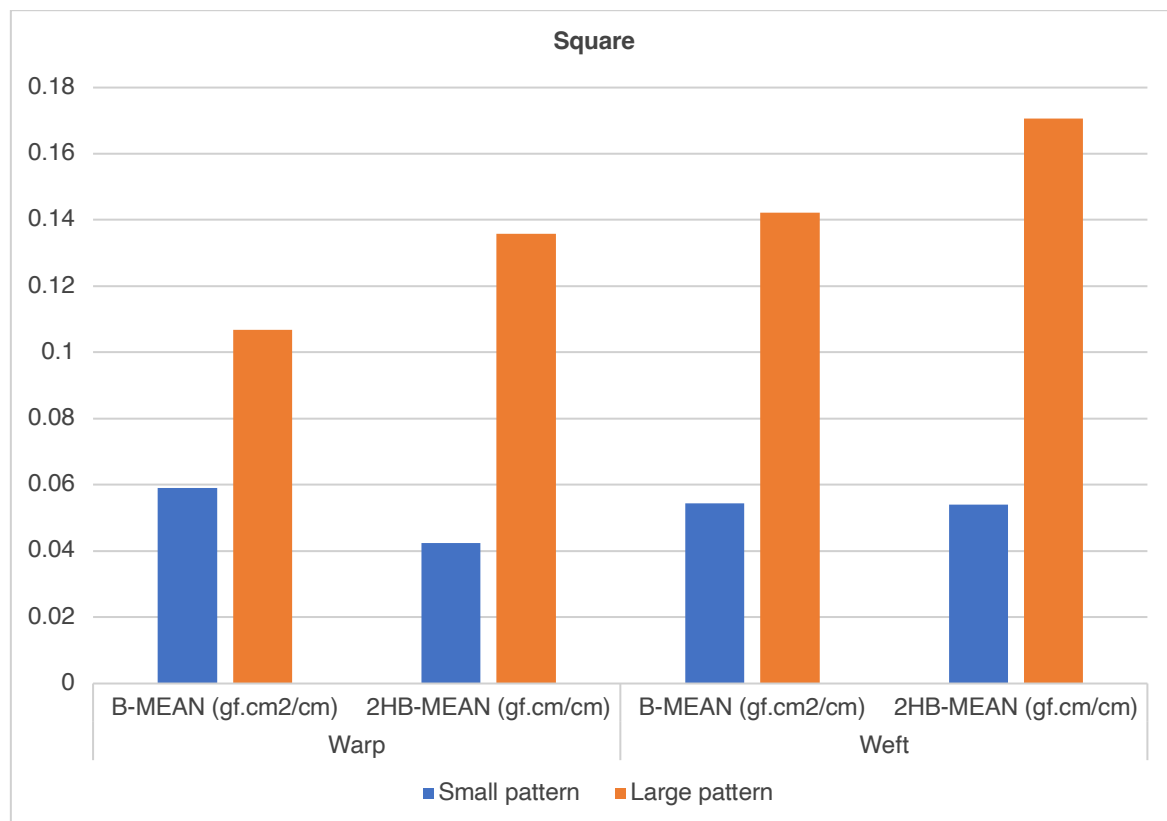
Figure 5-40 Bending rigidity and hysteresis of square patterns

The B-MEAN of square pattern specimens in warp ranged from 0.0591 to 0.1069 gf.cm^2/cm and in weft 0.0544 to 0.1423 gf.cm^2/cm (**Table 5-23** and **Figure 5-39**). The 2HB-MEAN of honeycomb specimens in warp ranges from 0.0425 to 0.1359 gf.cm/cm and in weft 0.0541 to 0.1706 gf.cm/cm. Alike rectangle specimens, the results showed larger patterned specimens to possess greater rigidity but poorer recoverability. Overall, the results suggest the scale and type of repeat pattern can influence bending rigidity and hysteresis for circle patterns.

5.3.3.3.6 Overall summary

Table 5-24 Average bending rigidity and hysteresis (all shapes)

Shape	Warp		Weft	
	B-MEAN (gf.cm2/cm)	2HB-MEAN (gf.cm/cm)	B-MEAN (gf.cm2/cm)	2HB-MEAN (gf.cm/cm)
Honeycomb	0.09265	0.06730	0.02030	0.06150
Rectangle	0.04675	0.07040	0.08750	0.13950
Circle	0.04560	0.03800	0.03690	0.05235
Triangle	0.09320	0.09000	0.06690	0.13170
Square	0.08300	0.08920	0.09835	0.11235

Note: - results for 0.1 mm SMP thickness
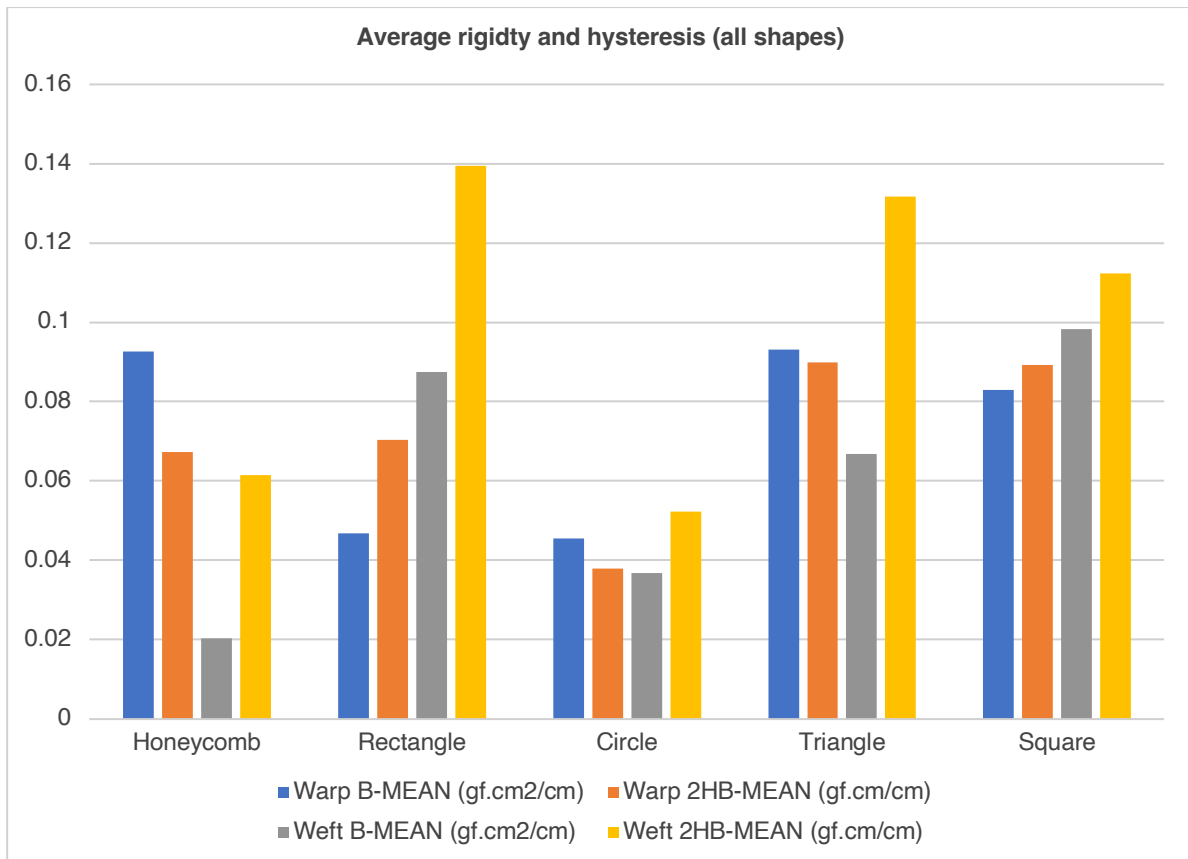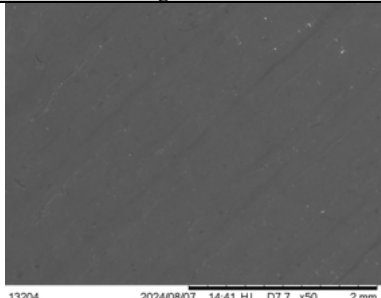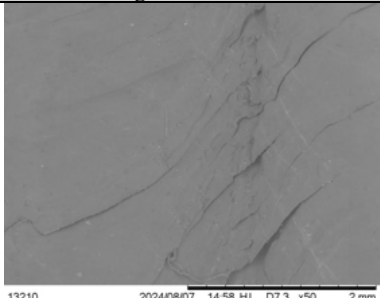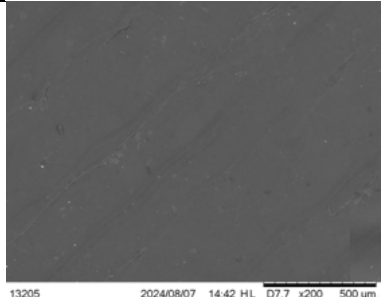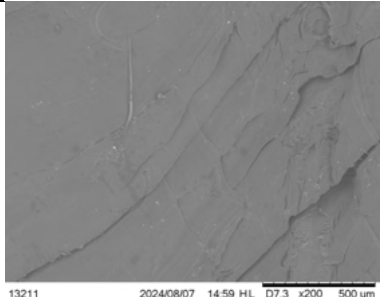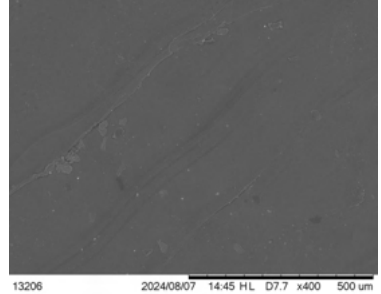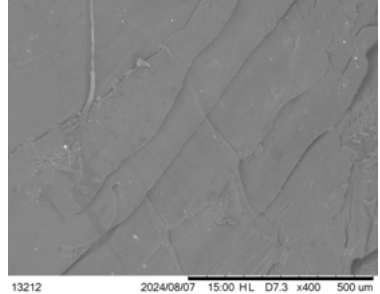
Figure 5-41 Average bending rigidity and hysteresis (all shapes)
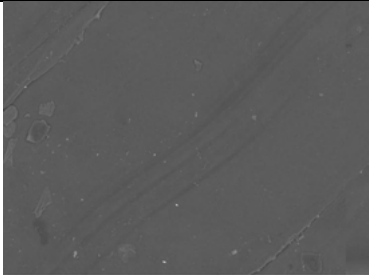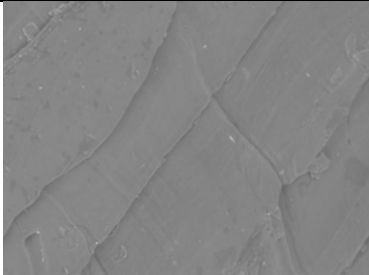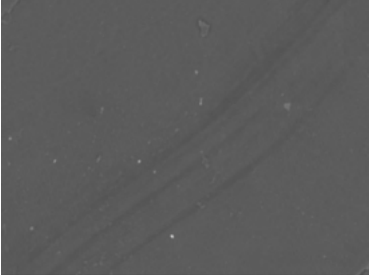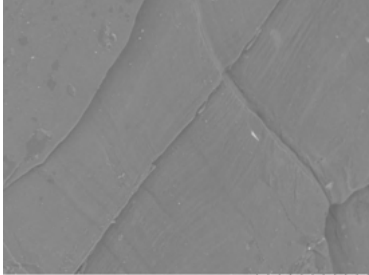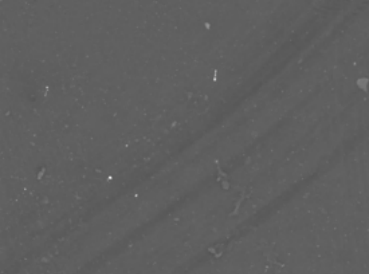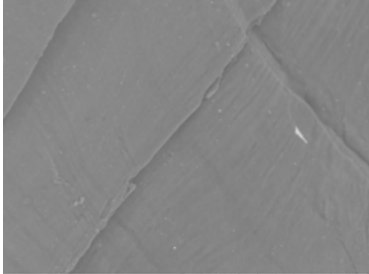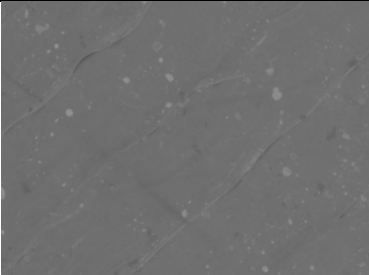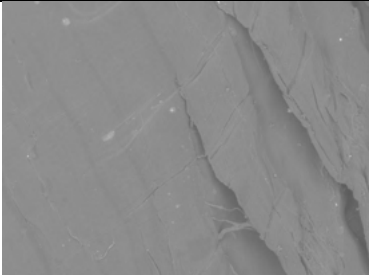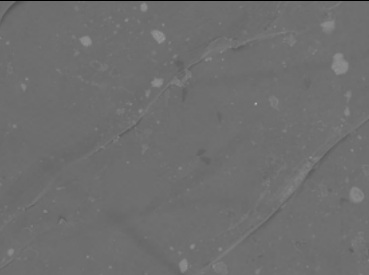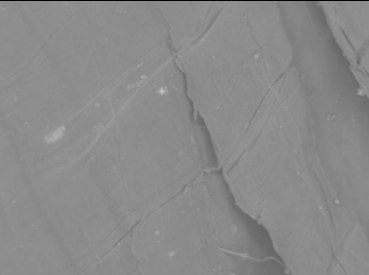
Overall, the results suggest the scale and type of repeat pattern to influence bending rigidity and hysteresis for all shaped patterns (**Table 5-24** and **Figure 5-40**). The results inclusive of all pattern type and scale combinations indicates triangle and honeycomb patterns to possess the highest bending rigidity in both warp and weft directions. In addition, the results also indicate smaller shaped patterns to yield greater bending rigidity due to it being a more densely packed with polymer (lesser fabric only areas). Moreover, higher hysteresis was generally found when 4DP PTC possessed greater rigidity, thus suggesting rigidity to influence the bending recoverability of the material. In previous shape recovery experiments, specimens that were printed with higher shore specimens yielded greater shape performance, thus pattern and its arrangement can be used to selectively stiffen the material for greater shape fixity and recovery.
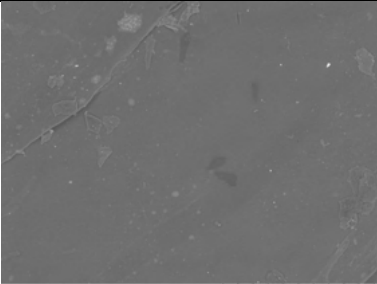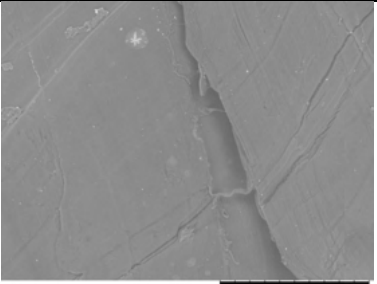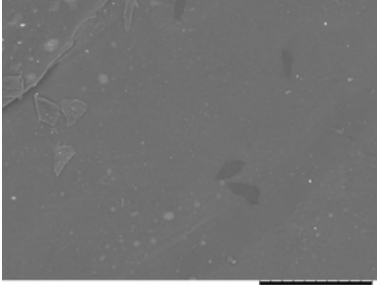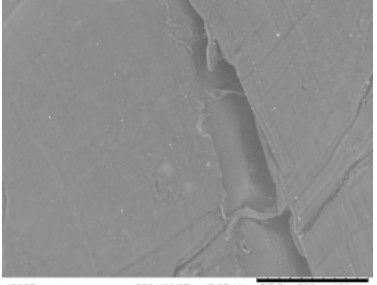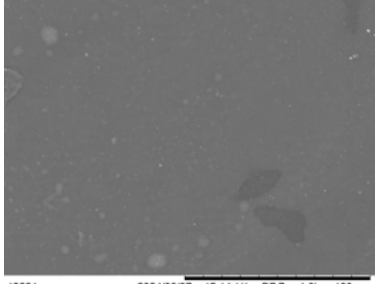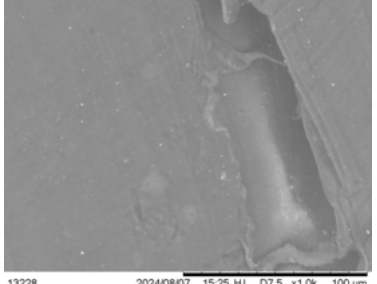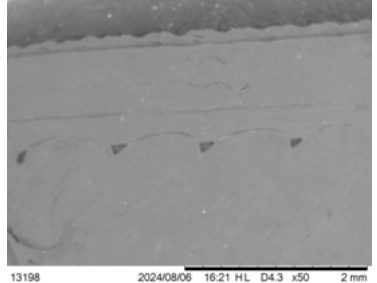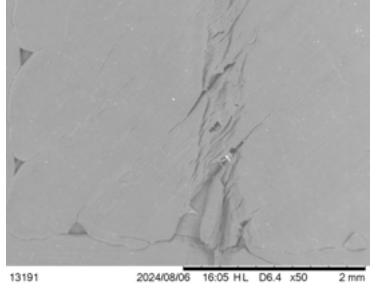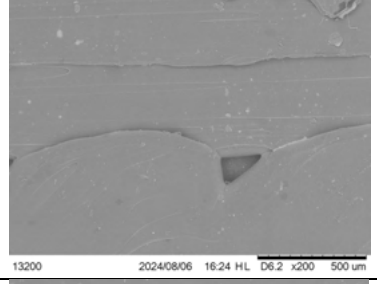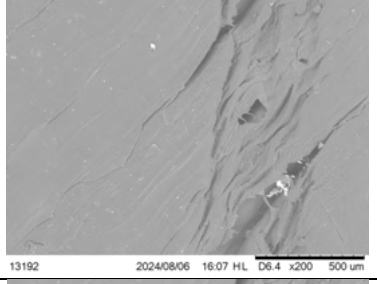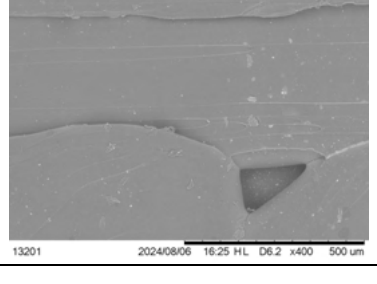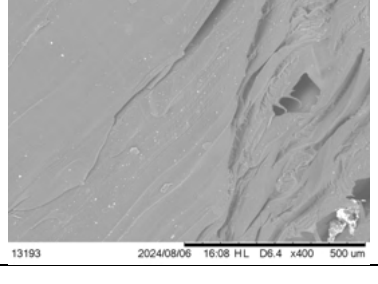
5.3.3.4 Scanning electron microscope analysis
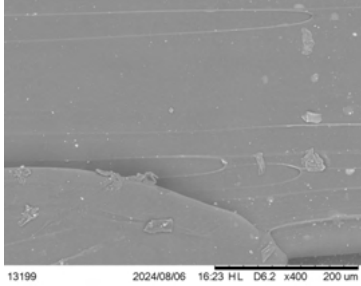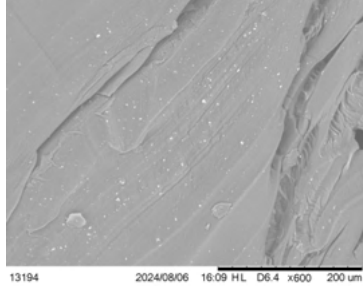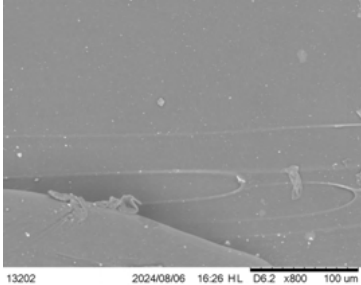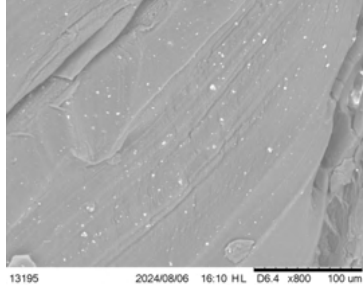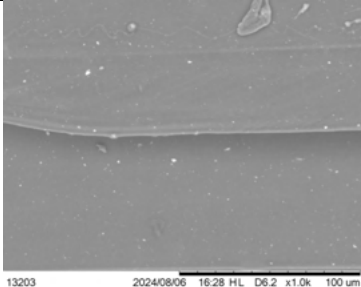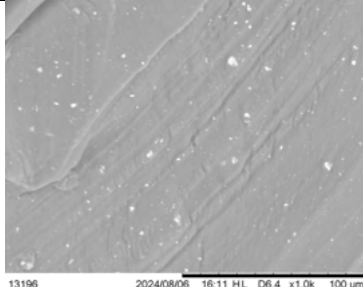
SEM images of the 4DP PTC specimens were taken at various magnifications i.e., x50 (default zoom), x200, x400, x600, x800, and x1000 to study the 4DP PTC's polymer surface at different states i.e., original printed form and programmed form. The larger magnification intervals were used as smaller intervals showed insignificant difference between images. During this experiment, 3 types of specimens (F1/F2/F3-SMP 4DP PTC) were used which resulted in a total of 36 SEM images at various states and magnification (**Table 5-25**).

Table 5-25 4DP PTC SEM analysis

Specimen	Magnification	Original form	Programmed form
F1-SMP 4DP PTC	50		
	200		
	400		

	600	13207 2024/08/07 14:47 HL D7.7 x600 200 um	13213 2024/08/07 15:01 HL D7.3 x600 200 um
	800	13208 2024/08/07 14:48 HL D7.4 x800 100 um	13214 2024/08/07 15:02 HL D7.3 x800 100 um
	1000	13209 2024/08/07 14:50 HL D7.7 x1.0k 100 um	13215 2024/08/07 15:03 HL D7.3 x1.0k 100 um
F2-SMP 4DP PTC	50	13216 2024/08/07 15:09 HL D7.7 x50 2 mm	13223 2024/08/07 15:21 HL D7.5 x50 2 mm
	200	13217 2024/08/07 15:10 HL D7.7 x200 500 um	13224 2024/08/07 15:22 HL D7.5 x200 500 um
	400	13218 2024/08/07 15:11 HL D7.7 x400 500 um	13225 2024/08/07 15:23 HL D7.5 x400 500 um

	600		
	800		
	1000		
F3-SMP 4DP PTC	50		
	200		
	400		

600	13199 2024/08/06 16:23 HL D6.2 x400 200 um	13194 2024/08/06 16:09 HL D6.4 x600 200 um
800	13202 2024/08/06 16:26 HL D6.2 x800 100 um	13195 2024/08/06 16:10 HL D6.4 x800 100 um
1000	13203 2024/08/06 16:28 HL D6.2 x1.0k 100 um	13196 2024/08/06 16:11 HL D6.4 x1.0k 100 um

F1-SMP 4DP PTC

The images at the original printed form overall show an even surface with miniscule parallel slanting lines which show the extrusion direction during the 3D printing process (**Table 5-25**). The width of these lines averaged 200 μm. In addition, minute white spots were also observed in the images which was caused by the coating from the ion sputter process. At 100 μm scale, minor surface irregularities can be seen across the image, however these spots all measure at < 10 μm which cannot be perceived by the human eye or touch. Meanwhile the programmed form images show a surface crease caused by the programming of a folded form with minute hairline fissures extending from the principal folding crease. In the imaged area, the principal crease measures at < 200 μm, while the fissures measure at width ranging from 1 μm to 2 μm. These fissures appear to be the extrusion direction during the 3D printing process that were

distorted due to folding and thermomechanical programming. Minor white spots are also observed in the images caused by the coating from the sputter process.

F2-SMP 4DP PTC

Alike F1-SMP 4DP PTC, the images at the original printed form overall show an even surface with miniscule parallel slanting lines which show the extrusion direction during the 3D printing process (**Table 5-25**). The width of these lines averaged 200 μm. In addition, minute white spots were also observed in the images which was caused by the coating from the ion sputter process. At 100 μm scale, minor surface irregularities can be seen across the image, however these spots all measure at < 10 μm. Like F1-SMP 4DP PTC, the programmed form images show a surface crease caused by the programming of a folded form with minute hairline fissures extending from the principal folding crease. The distance between the fissures however appears to be more uniform than the F1-SMP 4DP PTC specimen. In the imaged area, the principal crease measures at < 200 μm, while the fissures measure at width ranging from 1 μm to 2 μm.

F3-SMP 4DP PTC

F3-SMP 4DP PTC also show similar characteristics with F1 and F2-SMP 4DP PTC. The images at the original printed form overall show an even surface with miniscule parallel slanting lines which show the extrusion direction during the 3D printing process (**Table 5-25**). However, towards the edges of the specimen, small indentations of < 100 μm is observed. In addition, minute white spots were also observed in the images which was caused by the coating from the ion sputter process. At 100 μm scale, minor surface irregularities can be seen across the image, however these spots all measure at < 10 μm which cannot be perceived by the human eye or touch. Alike F1 and F2-SMP 4DP PTCs, the F3-SMP 4DP PTC programmed form images also show surface creases caused by the programming of a folded form with minute

hairline fissures extending from the principal folding crease. These creases appear to be more pronounced in comparison with the other 4DP PTCs. In the imaged area, the principal crease measures at < 500 μm, while the fissures measure much wider at width ranging from 20 μm to 30 μm. From the images, it is observed that these fissures are surface fractures caused by the folding process during thermomechanical programming due to its larger width. Minor white spots are also observed in the images caused by the coating from the sputter process.

5.3.3.4.1 Summary

In this experiment, a change in surface topography and composition was observed across all 4DP PTC specimens at original and programmed forms. Through the SEM images, it is evident that the surface composition changes under stress during thermomechanical programming. Across all samples, F3-SMP 4DP PTC appears to be the most affected by the induced stress during programming as indicated by the larger surface irregularities. Though these surface fissures are all < 100 μm and cannot be perceived by human eye or touch and therefore does not affect the appearance of the textile material.

5.4 4DP PTC functionality

5.4.1 Comparative analysis of results

The experimental results have shown 4D printing conditions i.e., material combinations, printing parameters, and pattern design to influence 4DP PTC performance. In this chapter, all findings of this study are visualised and compared via tabular format which provides an overview of 4DP PTC's performance. Through comparative analysis, one can visualise the performance of 4DP PTCs designed under specific conditions (i.e., material combinations, printing parameters, and pattern design). The results can be used as an indication of what design decisions to make when designing 4DP PTC. The comparative analysis workflow in shown in **Figure 5-41**.
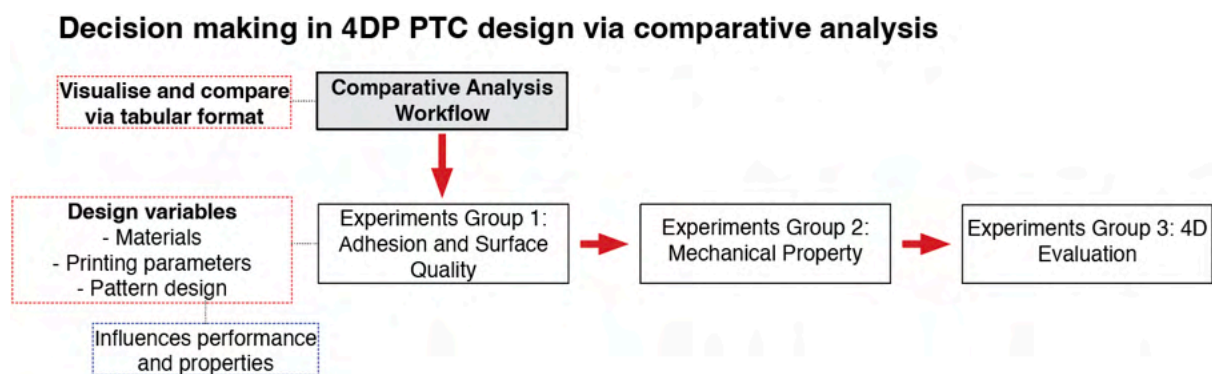
Figure 5-42 Experimental results comparative analysis workflow

5.4.1.1 Adhesion and surface quality

In comparison bar charts, lengthier bars indicate better performance. Result insights are presented in the end of each sub-chapter and answers to the research questions of this study.
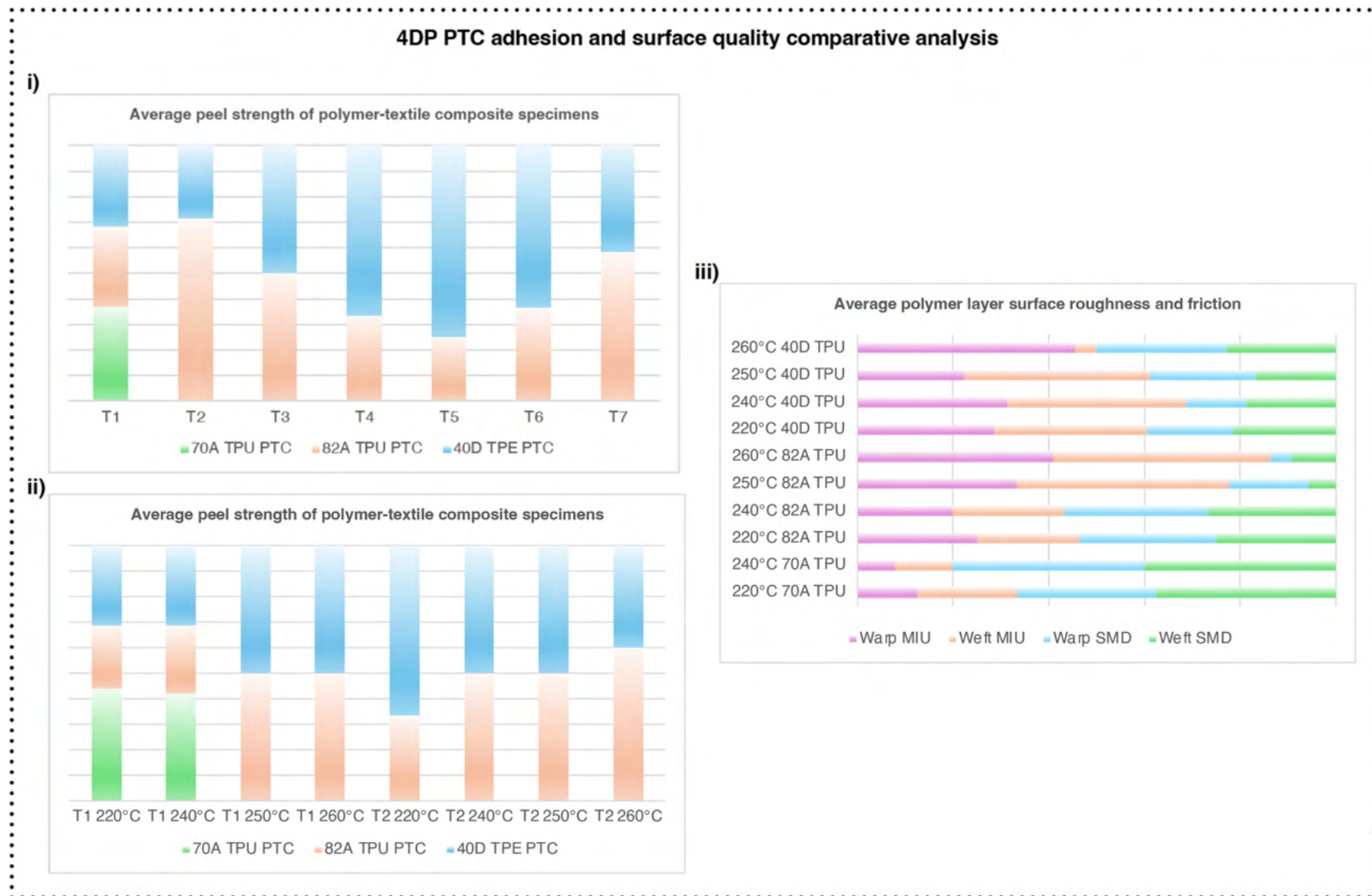
Figure 5-43 i) Material's effects on adhesion, ii) and iii) printing parameter's effects on adhesion and on surface quality

Insights:

- o The results indicate T1 fabrics to yield the most consistent peel resistance performance with all polymer types (**Figure 5-42**).

- o Higher peel resistance was found in 82A and 40D PTC specimens when the polymers were extruded at higher temperature ranges.

- o Higher surface quality was found when polymers were extruded at higher temperature ranges however a lower dimensional accuracy was found.

- o Overall materials and printing parameters were shown to affect 4DP PTC adhesion and surface quality.

5.4.1.2 Mechanical performance
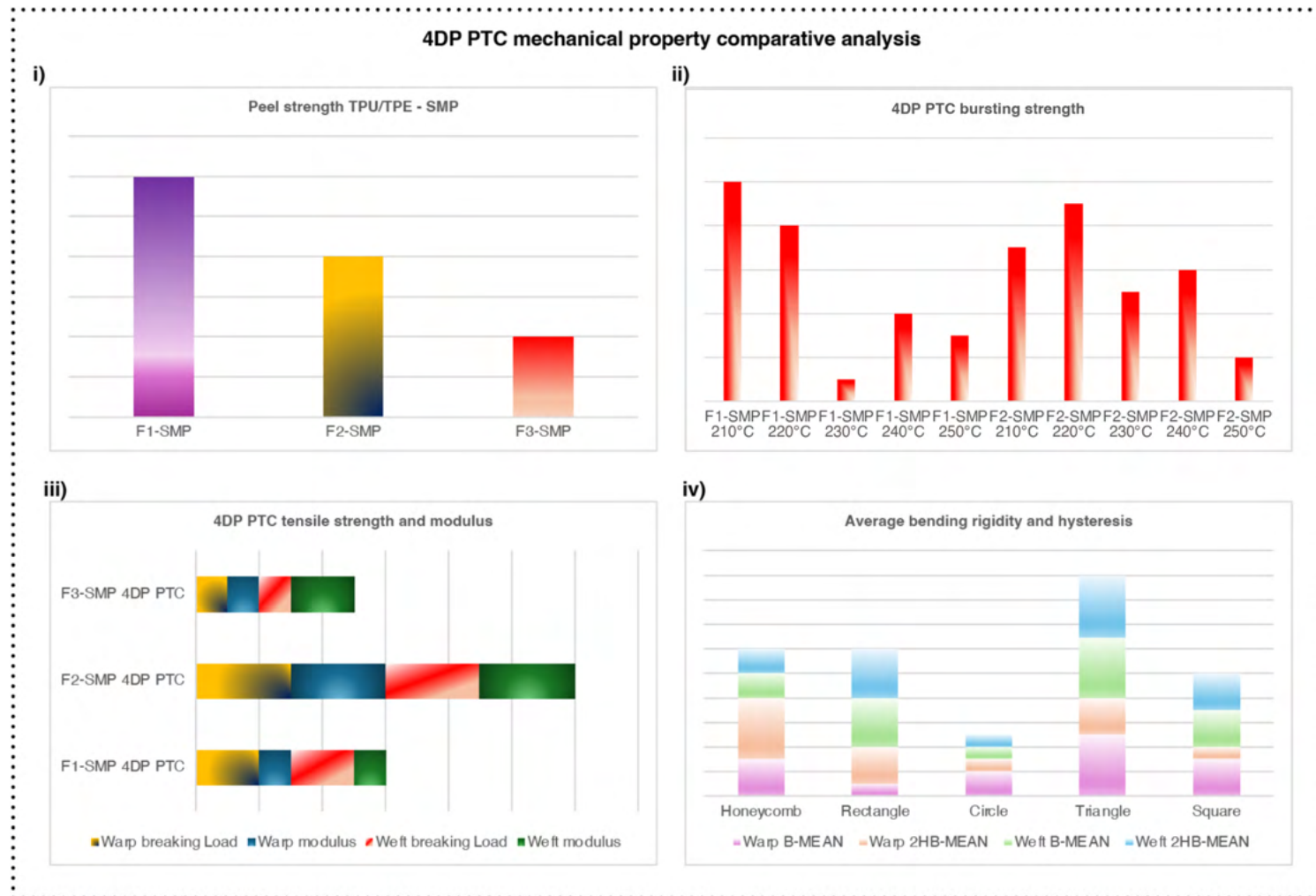
Figure 5-44 i) Material's effects on adhesion (TPU/TPE – SMP), ii) printing parameter's effects on bursting strength, iii) material's effects on tensile strength and modulus, and iv) pattern's effects on bending rigidity and hysteresis

Insights:

- o The results indicate F1-SMP material combinations to yield the highest peel strength. (**Figure 5-43**).

- o Specimens tended to have higher bursting strength when extruded at lower temperature ranges.

- o Material was shown to influence tensile strength and modulus with F2-SMP 4DP PTC recording the highest in tensile strength and modulus.

- o Pattern scale and shape was shown to influence bending rigidity and hysteresis (recoverability) with triangle pattern yielding the highest in both warp and weft directions.

- o Overall, material, printing parameter, and pattern design were shown to influence 4DP PTC's mechanical properties.

5.4.1.3 Shape performance
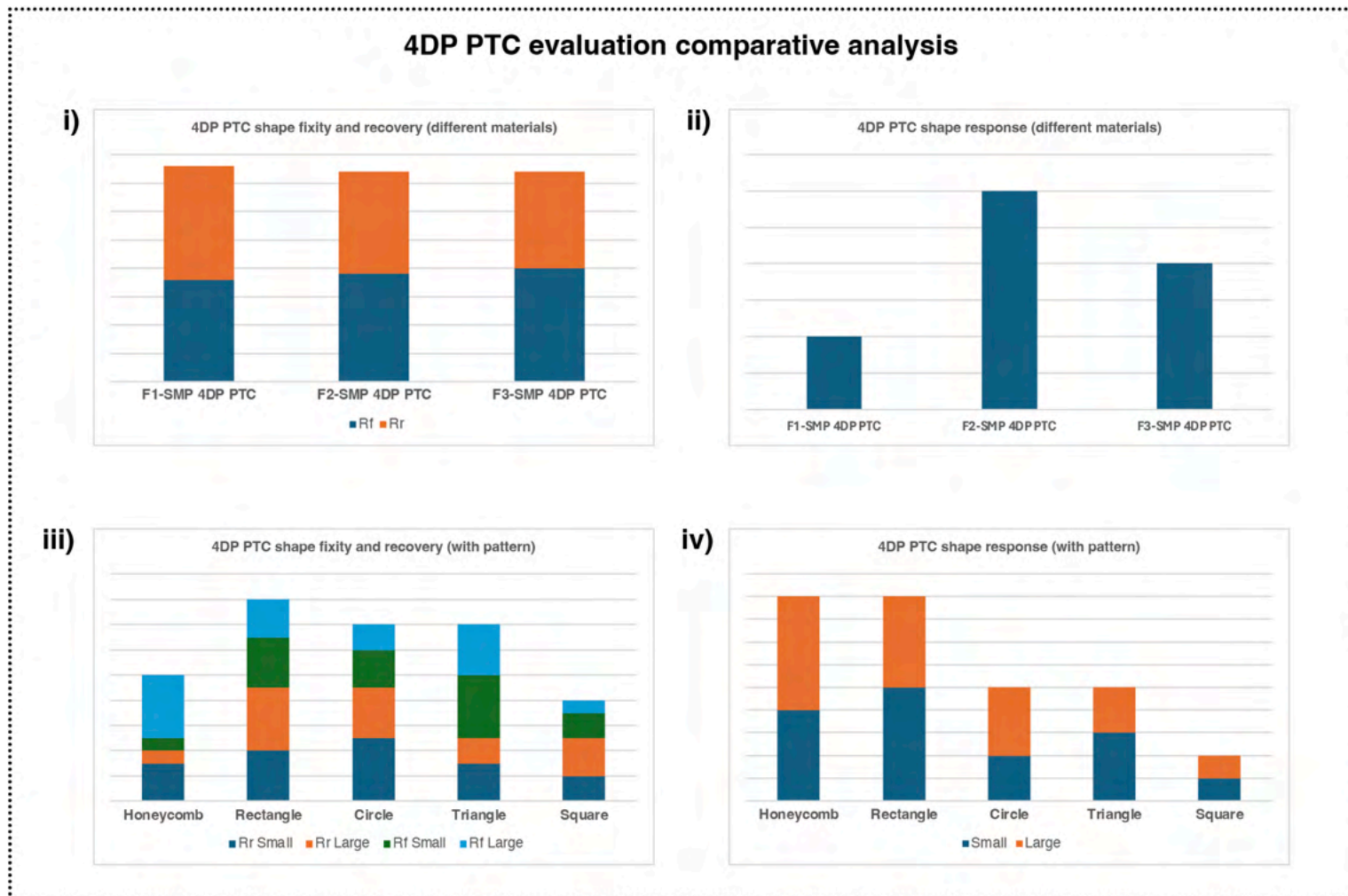
Figure 5-45 i) material's influence on shape fixity and recovery, ii) material's influence on shape response, iii) pattern's influence on shape fixity and recovery, and iv) pattern's influence on shape response

Insights:

- The overall results suggest polymer shore to influence 4DP PTC shape response, fixity, and recovery (**Figure 5-44**).

- The results indicate F1-SMP 4DP PTCs to have the highest shape response and recovery rate.

- Pattern shape and size were also shown to influence 4DP PTC shape performance.

- Though the effects were negligible, thus different shapes may be used based on aesthetic motivations.

5.4.2 Postproduction thermomechanical programming and shape recovery
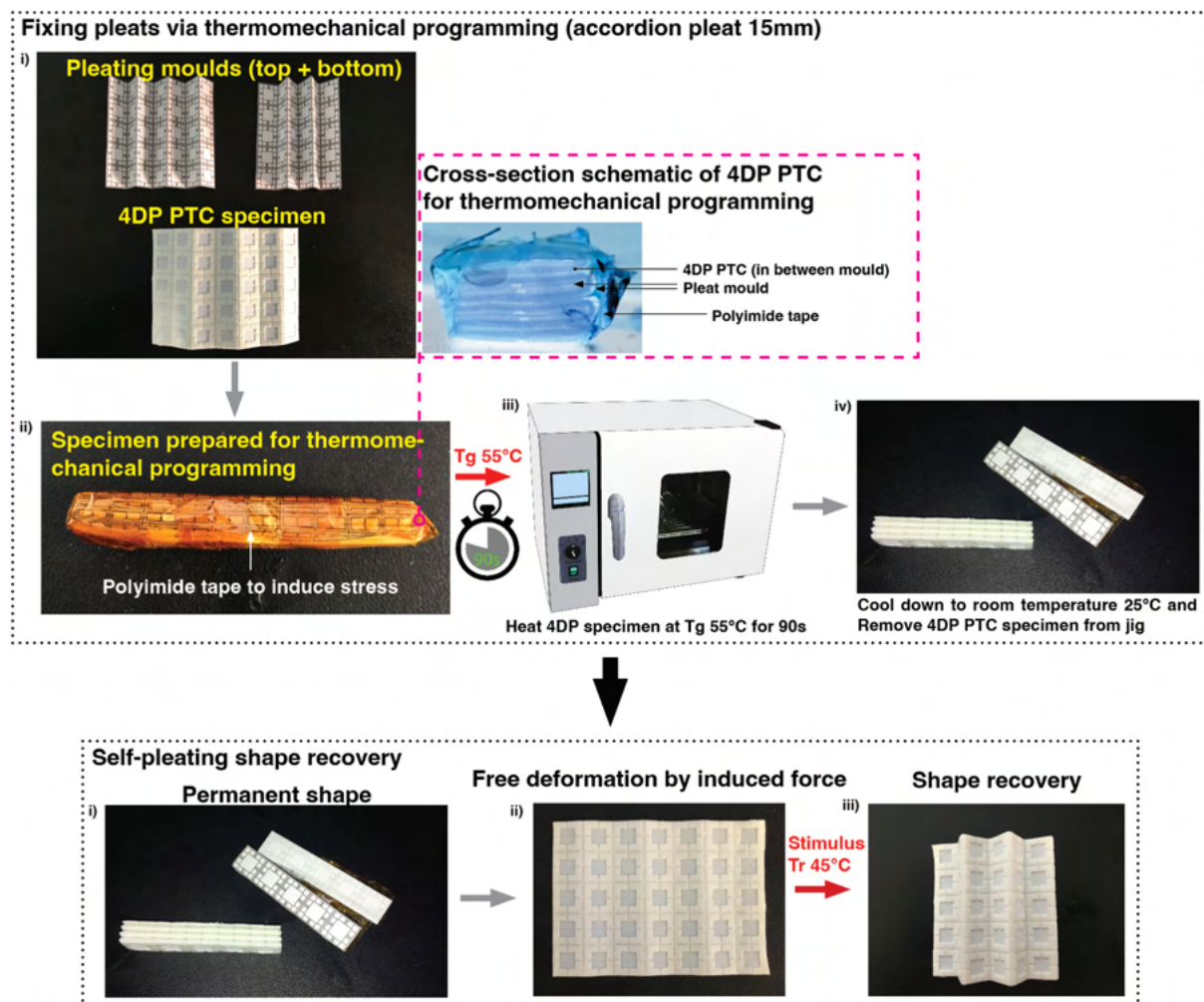
Figure 5-46 Fixing pleats via thermomechanical programming process (accordion pleat 15 mm) and shape recovery

The following section highlights the programming of 15 mm and re-programming of 7.5 mm width accordion pleats on a 4DP PTC specimen with square tessellating pattern to demonstrate 4DP PTC's re-programmability. To program or fix the fabric to an accordion pleated pattern of 15 mm, the 4DP PTC undergoes a thermomechanical programming process (same as chapter 5.1.2). Instead of fixing the 4DP PTC onto a jig, the textile specimen can be folded and encased in between pleating moulds (top + bottom pieces) alike conventional heat setting to pleat fabrics in the textile industry. Polyimide tape is used to secure the 4DP PTC to the pleated form. The specimen is then subjected to Tg for 90s (much quicker than conventional heat setting which takes between 25 – 30 minutes) in a Lab Companion OV4-30 vacuum oven. During thermomechanical programming, the SMP transforms from a glassy to rubbery state allowing stress to be induced onto the specimen for shape fixing to the pleated form. The specimen is then left to cool down to room temperature (**Figure 5-45**). Due to its excellent shape fixity properties, the specimen can be used at this stage without further modifications. Though, alike conventional pleating, there is the need to spread open the fabric for both practicality reasons and to see the results of the pleating. In addition, for shape recovery to happen, the specimen can be stimulated with Tr = 45°C to trigger shape transformation. Due to the innate strain of the inverse and reverse folds in accordion pleats, it was not possible to achieve the same level of shape recovery shown in inverse only specimens (in previous experiments). Though as shown in **Figure 5-45**, a pleated form with an even distribution of inverse/reverse folds can be achieved.
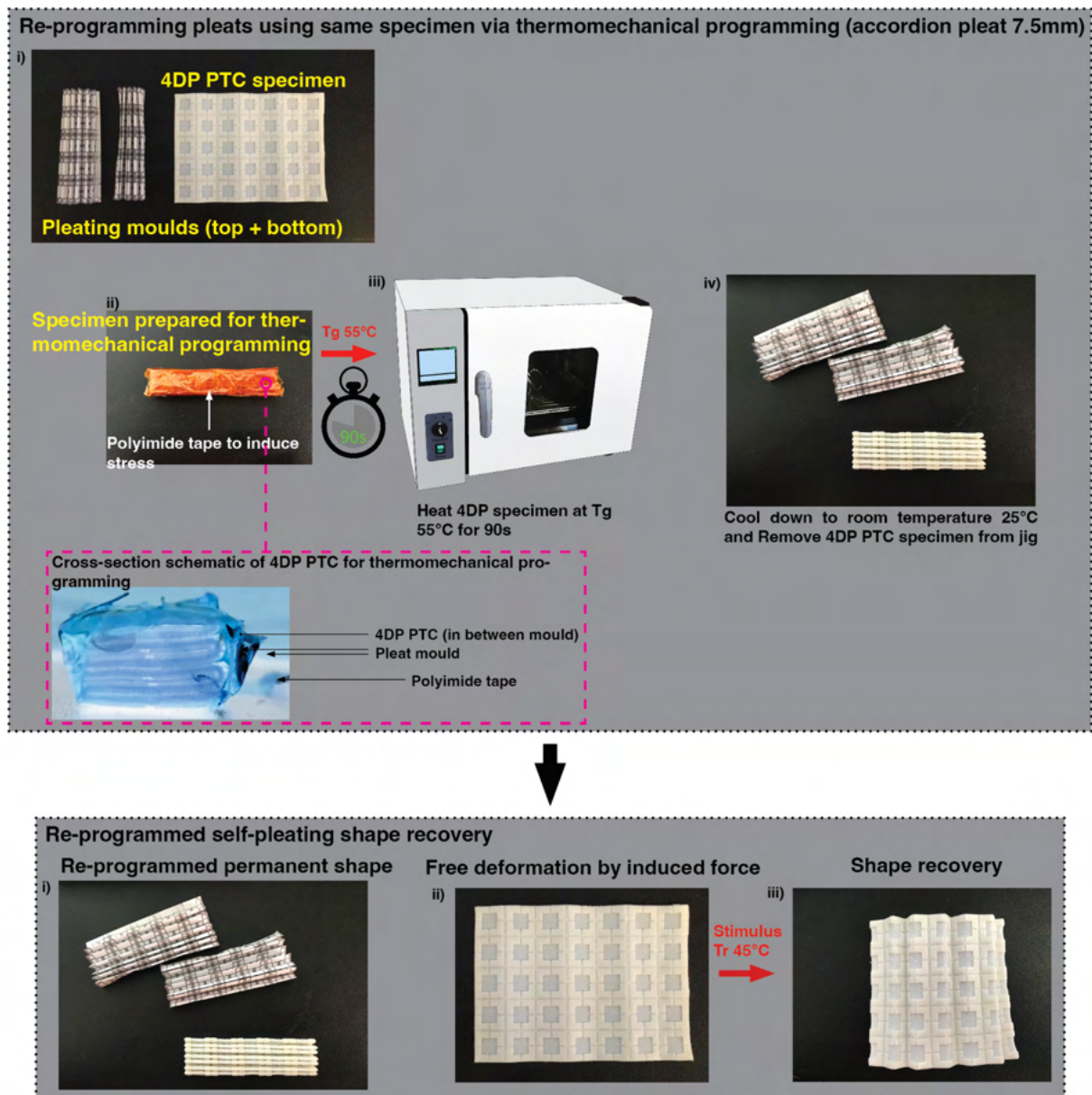
Figure 5-47 Re-programming pleats using same specimen via thermomechanical programming (accordion pleat 7.5 mm) and shape recovery

The SMP components of 4DP PTCs enables re-programming or "re-pleating" of a different permanent form. The re-programming of pleats is challenging with conventional fabrics because during heat setting the polyester fibres are melted into the pleats resulting in a permanent pleated form (Jackson, 2015). Though natural fibres can be re-pleated, they have poor shape fixing ability. As shown in prior experiments, 4DP PTCs have high shape fixity, recovery, and repeatability averaging < 90%. To re-program a new permanent form (in this

case an accordion pleat 7.5 mm), the same 4DP PTC specimen was used. The 4DP PTC undergoes an identical process as shown in **Figure 5-45**. Alike **Figure 5-45**, the specimens can be used right after the thermomechanical process without further modifications or can be stimulated with Tr = 45°C to trigger shape transformation. And again, due to the innate strain of the inverse and reverse folds in accordion pleats, it was not possible to achieve the same level of shape recovery shown in inverse only specimens (in previous experiments). Like **Figure 5-45**, a pleated form with an even distribution of inverse/reverse folds can also be achieved.

5.4.3 Discussion

The comparative analysis in sections 5.4.1.1, 5.4.1.2, and 5.4.1.3 have provided valuable insights to assist with decision making when designing 4DP PTCs. The results showed F1 flexible polymers extruded at 240°C to yield the highest peel strength in combination with T1 substrate and PU-based SMPs (extruded at 200°C). F1-SMP 4DP PTC possessed the highest bursting strength but marginally lesser tensile strength than F2-SMP 4DP PTC. And for shape recovery performance, F1-SMP 4DP PTC also held best overall performance in response, shape fixity, and recovery. Furthermore, for pattern design, triangle, rectangle, square, and honeycomb shapes possessed comparable rigidity and hysteresis, facilitating enhanced shape fixity, response, and recovery which are imperative for fixing pleats and shapeshifting. 4DP PTCs were also able to self-fold at high fixity, response, and recovery rates indicating its effectiveness for the development of self-pleating/re-pleatable materials. The overall results validate the fact that the shape and mechanical performance of 4DP PTCs can be fine-tuned via material choice, printing conditions, and pattern design for different applicational needs accordingly.
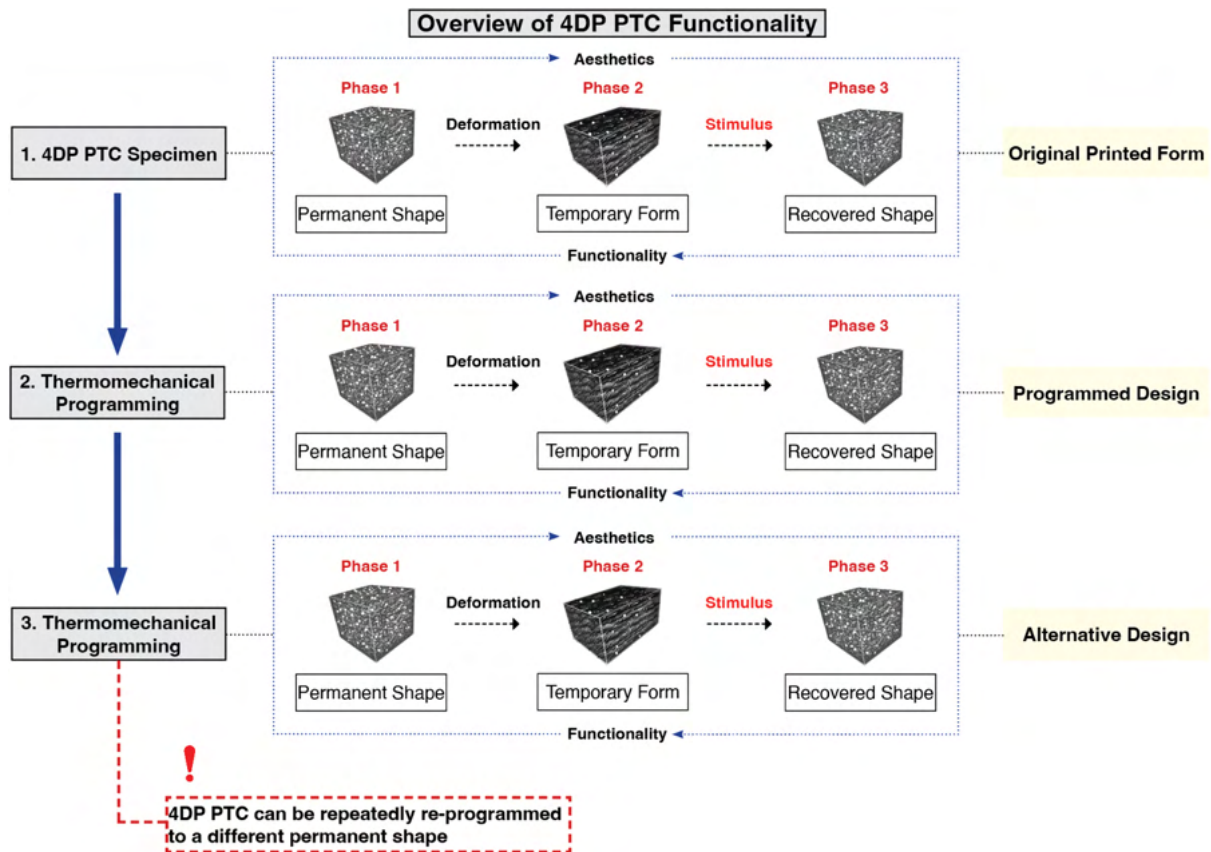
Figure 5-48 Overview of 4DP PTC functionality

The shape performance experiments have shown 4DP PTC specimens to possess excellent shape fixity and recovery capabilities. In addition, it has also shown variables i.e., material and pattern type to influence bending rigidity and hysteresis which also impacts shape performance. Due to the functionality of 4DP PTCs, such materials can be used for creating applications that are highly adaptable. **Figure 5-47** illustrates an overview of the functionality of 4DP PTCs. 4DP PTCs are capable of shape transformation when subjected to a stimulus in accordance with its original printed form, programmed form, and re-programmed forms. In addition, 4DP PTCs can be repeatedly re-programmed through thermomechanical programming to a different permanent shape. Design applications can exploit 4DP PTC's excellent shape fixity and/or recovery properties according to different purposes.

Chapter 6: RESULTS ANALYSIS AND DESIGN APPLICATIONS

6.1 Introduction
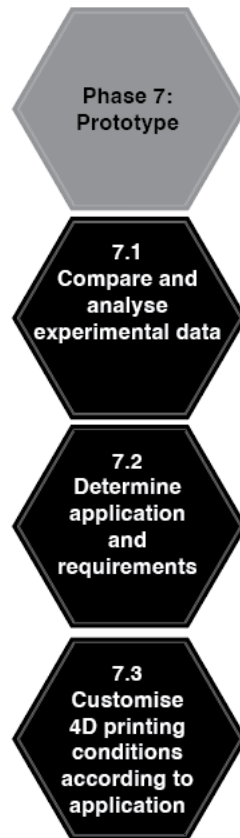
Figure 6-1 4DP PTC design framework (showing chapter 6 experiments)

Figure 6-1 illustrates the experiments conducted in chapter six. This chapter presents the creative design practices for 4DP PTCs and discusses the manipulation of 4D printing conditions to fine-tune 4DP PTC's mechanical properties for various applications. A collection of re-programmable pleated textile prototypes aimed for garments, accessories, and interior textiles will be presented. The specifications of such prototypes are presented in detail allowing for reproduction. In addition, a re-sizable/re-shapable concept facemask will be developed to demonstrate 4DP PTC's functionality. To conclude, the advantages of 4DP PTCs in terms of aesthetics and functionality based on comparative analysis and observations and other potential applications of 4DP PTCs are also presented.

6.2 Development of 4DP PTC prototypes

Chapter five has shown 4DP PTCs to possess excellent shape transformation capabilities. Therefore, when designing garments, accessories, or other objects one can utilise its shape transformation properties individually or a combination of all these properties. For example, shape fixity can be used for the development of materials that can be permanently shaped but also allows re-programming to new permanent forms (shown in **Figure 5-46**). One can make use of 4DP PTC's high shape fixity rate to create permanent pleats that can be repeatedly re-pleated. Applications that solely use shape fixity include re-pleatable textiles, re-shapable light shades, or re-sizable wearables i.e., facemasks. On the other hand, by utilising 4DP material's innate shape recovery properties, objects with high adaptability and transformability can also be developed i.e., adaptable footwear, garments, or interactive wall design etc. Shape recovery can also be used for the development of flexible fitting garments that can be triggered by a stimulus.

6.2.1 Design process

In fashion design, textiles and garments have a synergistic relationship with each other which requires deliberation (Gale & Kaur, 2004). Preceding experiments with 4DP PTCs have evidently shown the need for integrating design thinking that considers structural functionality, surface and dimensional quality, and mechanical properties, with shape recovery performance. In addition to these characteristics, surface design too has an intrinsic link with such qualities. Textiles are commonly designed to suit specific aesthetic needs but often with in-built functions i.e., houndstooth patterns (woven with higher resistance to twisting), sharkskin fabrics (wrinkle-resistant with shiny surface), spacer fabrics (high performance appearance with odour resistance) (Sinclair, 2014). The pattern or structural design is an amalgamation of aesthetics and unique mechanical properties.

Figure 6-2 shows an overview of the design and development process for creating 4DP PTCs. This design process explores the relationship between surface pattern design with shape recovery to produce novel 4DP PTC creations through practice-driven making. The pattern design process consists of four stages, including design research, practice-led making, design optimisation, and fabrication. This design process reflects the necessity for multidisciplinary thinking around art, design, and technology to develop aesthetic and functional 4DP PTCs.
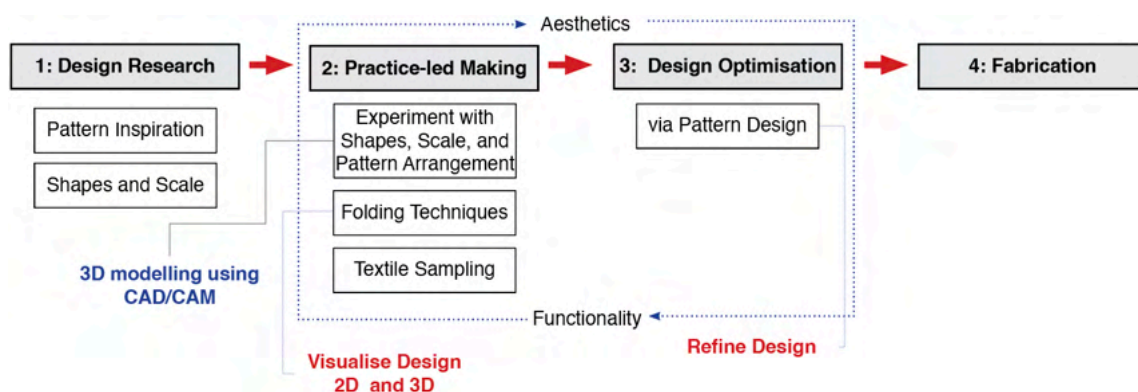
Figure 6-2 4DP PTC creation process

6.2.2 Pattern design principles
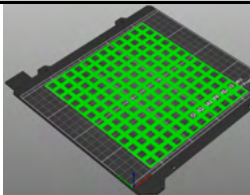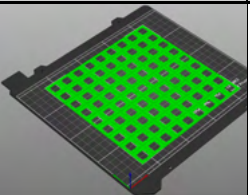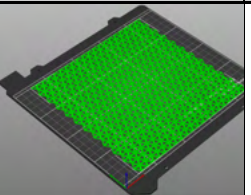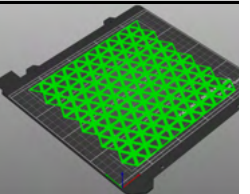
4DP PTC's creation process is based upon all prior design experiments and findings. This chapter explores the physical prototyping of 4DP PTCs using unary and other multi-shaped tessellating patterns. In pattern design, key principles to focus on include, gradation, direction, contrast, repetition, among other principles (Russell, 2021). By adhering to such principles, a wide array of patterns can be created. Due to the technical requirements of 4DP PTCs, tessellating patterns must be used to facilitate SM behaviour, thus geometrical patterns with straight edges conjoined together is vital for optimising 4DP PTC performance.
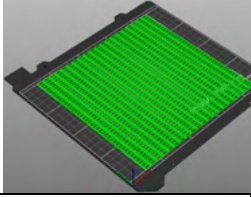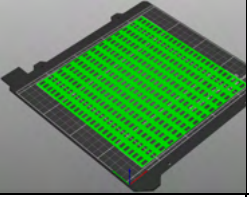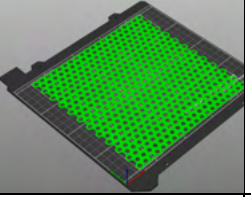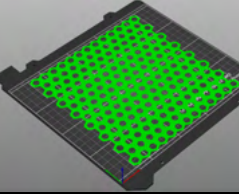
6.2.3 Design results and discussion

The 4DP PTCs in this study are divided into two main groups with one designed with unary tessellation and the other with multi-shaped tessellating patterns (i.e., binary, ternary etc). They are further classified according to the size of the shapes used. The tessellation patterns were developed using Rhino – Rhinoceros 3D version 8 (Rhinoceros, 2024). The specifications of the resulting 4DP PTC prototypes are presented and discussed in detail.

6.2.3.1 Unary tessellation pattern

Table 6-1 4DP PTC with unary tessellation

Prototype no:	S1	S2	T1	T2
3D model:				
Geometry/shape:	Square	Square	Triangle	Triangle
Dimensions:	200 mm x 200 mm (original form)	200 mm x 200 mm (original form)	200 mm x 200 mm (original form)	200 mm x 200 mm (original form)
Fabric:	80% NY 20% EA	80% NY 20% EA	80% NY 20% EA	80% NY 20% EA
Filament:	70A TPU PU SMP	70A TPU PU SMP	70A TPU PU SMP	70A TPU PU SMP
Printing Temp:	TPU – 240°C SMP – 200°C	TPU – 240°C SMP – 200°C	TPU – 240°C SMP – 200°C	TPU – 240°C SMP – 200°C

Printing Speed:	20 mm/s	20 mm/s	20 mm/s	20 mm/s
Infill %/pattern:	15% rectilinear	15% rectilinear	15% rectilinear	15% rectilinear
Polymer thickness:	0.1 mm TPU 0.2 mm SMP	0.1 mm TPU 0.2 mm SMP	0.1 mm TPU 0.5 mm SMP	0.1 mm TPU 0.5 mm SMP
Comments:	10 mm triangle	15 mm square	10 mm triangle	15 mm triangle
Prototype no:	**R1**	**R2**	**H1**	**H2**
3D model:				
Geometry/shape:	Rectangle	Rectangle	Honeycomb	Honeycomb
Dimensions:	200 mm x 200 mm (original form)	200 mm x 200 mm (original form)	200 mm x 200 mm (original form)	200 mm x 200 mm (original form)
Fabric:	80% NY 20% EA	80% NY 20% EA	80% NY 20% EA	80% NY 20% EA
Filament:	70A TPU PU SMP	70A TPU PU SMP	70A TPU PU SMP	70A TPU PU SMP
Printing Temp:	TPU – 240°C SMP – 200°C	TPU – 240°C SMP – 200°C	TPU – 240°C SMP – 200°C	TPU – 240°C SMP – 200°C
Printing Speed:	20 mm/s	20 mm/s	20 mm/s	20 mm/s
Infill %/pattern:	15% rectilinear	15% rectilinear	15% rectilinear	15% rectilinear
Polymer thickness:	0.1 mm TPU 0.2 mm SMP	0.1 mm TPU 0.2 mm SMP	0.1 mm TPU 0.2 mm SMP	0.1 mm TPU 0.2 mm SMP
Comments:	10 mm rectangle	15 mm rectangle	10 mm honeycomb	15 mm honeycomb

There are eight unary tessellating patterned prototypes composed of square, triangle, rectangle, and honeycomb shapes as shown in **Table 6-1**. They are further categorised as S1 (square), T1 (triangle), R1 (rectangle), and H1 (honeycomb) (10 mm shape size), and S2, T2, R2, and H2 (15 mm shape size) specimens. All the shapes in each pattern fully tessellate edge-to-edge. Circle pattern that was shown in chapter five was not carried forward because they are unable to tessellate edge-to-edge which is important for facilitating SM behaviour in 4DP PTCs. The specimens were fabricated with F1 fabric, 70A TPU, with a PU SMP and measured 200 mm x 200 mm in its original printed form. The polymer thickness, infill pattern, and print speed remained constant across samples identical to previous experiments.
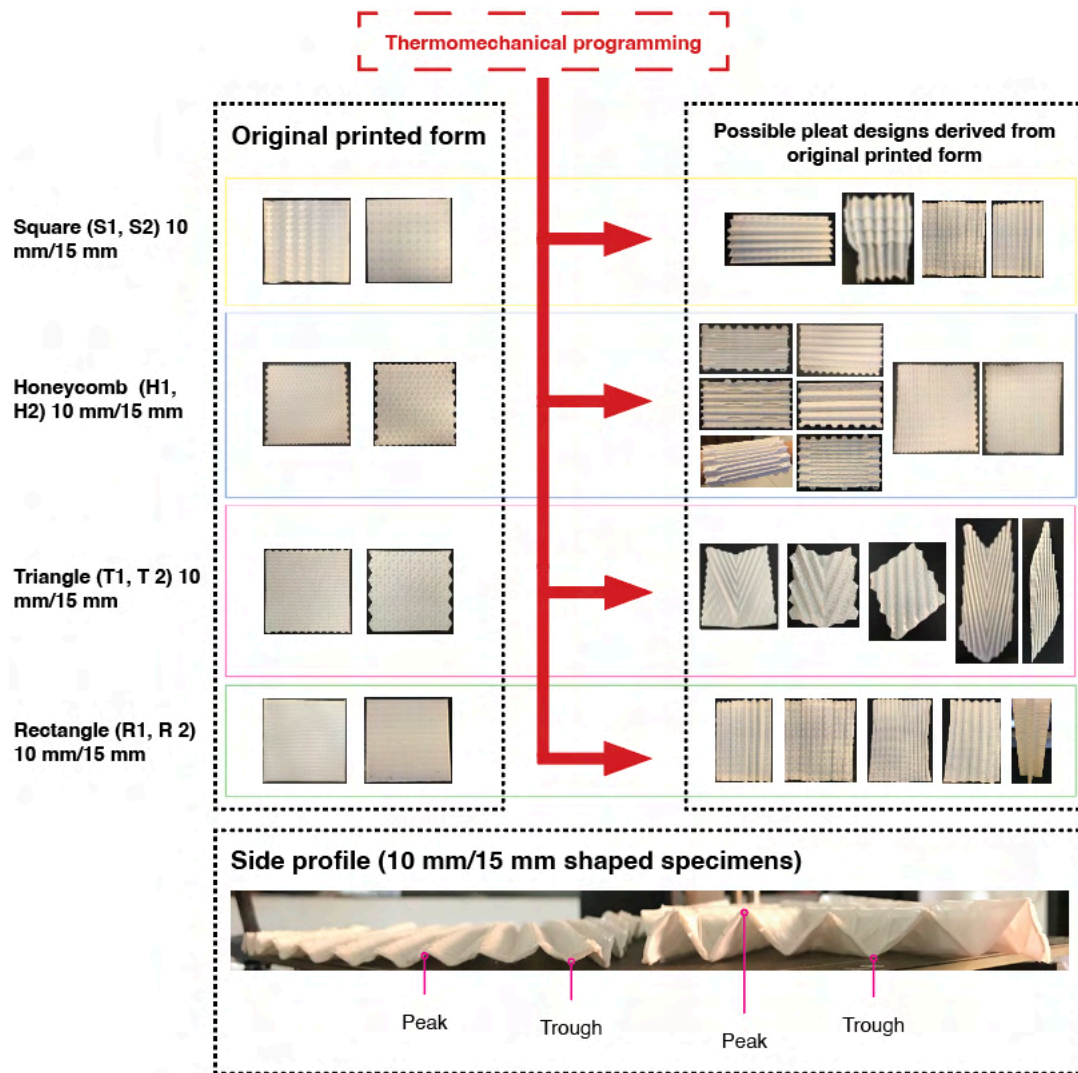
Figure 6-3 Unary tessellating 4DP PTC's shapeability and side profile
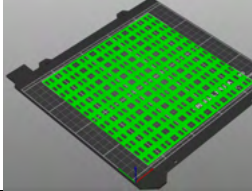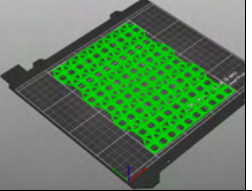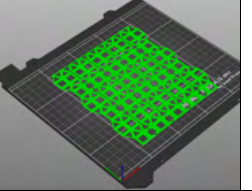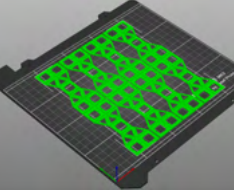
Unary tessellating 4DP PTCs demonstrate high levels of shapeability as shown in **Figure 6-3**. Such specimens can be folded to different pleated forms and shape fixed via thermomechanical programming to a new permanent form. The hinge joint developed in section 5.2.2.5.2, enhances the foldability and shapeability of the 4DP PTCs. By exploiting the hinge mechanism, multiple pleat designs can be pre-embedded in the unary specimens and can be easily folded by the user to different pleated forms when desired. After the folding process, the specimens can be fixed to these pleated forms via a thermomechanical process shown in chapter five and can be repeatedly reprogrammed by the user to alternative pleated designs. The different
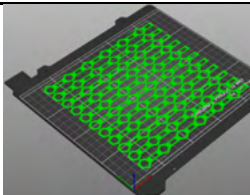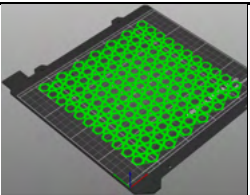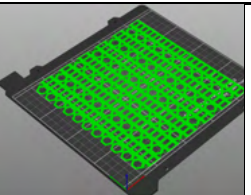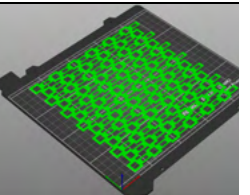
pleated forms create various surface designs with different alternations and undulations alike conventional pleated fabrics. Depending on the type and scale of pattern, different types of pleats can be created i.e., crystal and box pleats, grid folding variations, and chevron pleats etc.

Pattern shape size, folding direction and, intervals were shown to influence the surface design of 4DP PTCs. The specimens with larger shaped patterns resulted in surfaces with larger peaks and troughs and the specimens with smaller shaped patterns resulted in surface with smaller peaks and troughs and pleats that were more densely packed together due to its smaller shapes. Larger folding intervals also created a more exaggerated three-dimensional (surface convolutions and texture) effect with a slight reduction in surface area.

6.2.3.2 multi-shaped tessellation pattern

Table 6-2 4DP PTC with multi-shaped tessellation

Prototype no:	R1S1	S1T1v1	S1T1v2	S2T2
3D model:				
Geometry/shape:	Rectangle, square	Square, triangle	Square, triangle	Square, triangle
Dimensions:	200 mm x 200 mm (original form)	200 mm x 150 mm (original form)	180 mm x 150 mm (original form)	200 mm x 190 mm (original form)
Fabric:	80% NY 20% EA	80% NY 20% EA	80% NY 20% EA	80% NY 20% EA
Filament:	70A TPU PU SMP	70A TPU PU SMP	70A TPU PU SMP	82A TPU PU SMP
Printing Temp:	TPU – 240°C SMP – 200°C	TPU – 240°C SMP – 200°C	TPU – 240°C SMP – 200°C	TPU – 240°C SMP – 200°C
Printing Speed:	20 mm/s	20 mm/s	20 mm/s	20 mm/s
Infill %/pattern:	15% rectilinear	15% rectilinear	15% rectilinear	15% rectilinear
Polymer thickness:	0.1 mm TPU 0.5 mm SMP	0.1 mm TPU 0.5 mm SMP	0.1 mm TPU 0.5 mm SMP	0.1 mm TPU 0.5 mm SMP
Comments:	10 mm rectangle and square	10 mm square and triangle	10 mm square and triangle with textile hinges	15 mm square and triangle
Prototype no:	H2R2	H2T1	H2T1R2	R2S2

3D model:				
Geometry/shape:	Hexagon, rectangle	Hexagon, triangle	Hexagon, triangle, rectangle	Rectangle, square
Dimensions:	200 mm x 200 mm (original form)	200 mm x 200 mm (original form)	200 mm x 200 mm (original form)	200 mm x 200 mm (original form)
Fabric:	80% NY 20% EA	80% NY 20% EA	80% NY 20% EA	80% NY 20% EA
Filament:	70A TPU PU SMP	70A TPU PU SMP	70A TPU PU SMP	70A TPU PU SMP
Printing Temp:	TPU – 240°C SMP – 200°C	TPU – 240°C SMP – 200°C	TPU – 240°C SMP – 200°C	TPU – 240°C SMP – 200°C
Printing Speed:	20 mm/s	20 mm/s	20 mm/s	20 mm/s
Infill %/pattern:	15% rectilinear	15% rectilinear	15% rectilinear	15% rectilinear
Polymer thickness:	0.1 mm TPU 0.5 mm SMP	0.1 mm TPU 0.5 mm SMP	0.1 mm TPU 0.5 mm SMP	0.1 mm TPU 0.5 mm SMP
Comments:	15 mm hexagon and rectangle	15 mm hexagon and 10 mm triangle	15 mm hexagon and rectangle and 10 mm triangle	15 mm rectangle and square

Based on the findings of unary patterned specimens, the multi-shaped tessellating specimens investigated the interrelation between different shapes. The tessellation patterns were developed using Rhino – Rhinoceros 3D version 8 (Rhinoceros, 2024). The specifications of 4DP PTCs with multi-shaped tessellating patterns are shown in **Table 6-2**. Each pattern design contained at least two or more shapes. Due to the versatile nature of the geometrical shapes, endless shape combinations could be generated to form patterns. However, it would not be practical to explore all imaginable combinations, thus the experiment focused on narrowing down patterns that could be folded to common pleats seen in textile design. The selection of shapes is driven by prior findings on shape performance, mechanical property experiments, and the feasibility of connecting shapes together to form edge-to-edge tessellations which is a prerequisite for 4DP PTC to perform shape transformations. Bending rigidity and hysteresis, and shape performance experiments indicated that shape performance can be enhanced via the use of different shape combinations i.e**.,** honeycomb with triangle to maximise shape fixity (H2T1), honeycomb with rectangle to maximise shape response (H2T1R2), and rectangle with square (R2S2v1 and v2) to maximise hysteresis (shape recovery). Moreover, different types of

hinges (shown in **Figure 5-12**) were also adopted in some specimens (i.e., H2R2, R2S2) to increase flexibility and to vary surface aesthetics. Both small and larger scaled shapes were used independently and in combination with each other for both functional and aesthetic purposes. Moreover, the pleating experiments showed various types of pleats i.e., crystal and box hybrid pleats, variations of v-pleat oppositions, and pleated 3D structural forms were conceivable by folding the multi-shaped tessellating 4DP PTCs (**Figure 6-4**). All the specimens were fabricated with F1 fabric, 70A TPU, with a PU SMP, and the specimens varied in dimensions due to the figure of the tessellating pattern. The polymer thickness, infill pattern, and print speed remained constant across samples identical to previous experiments.
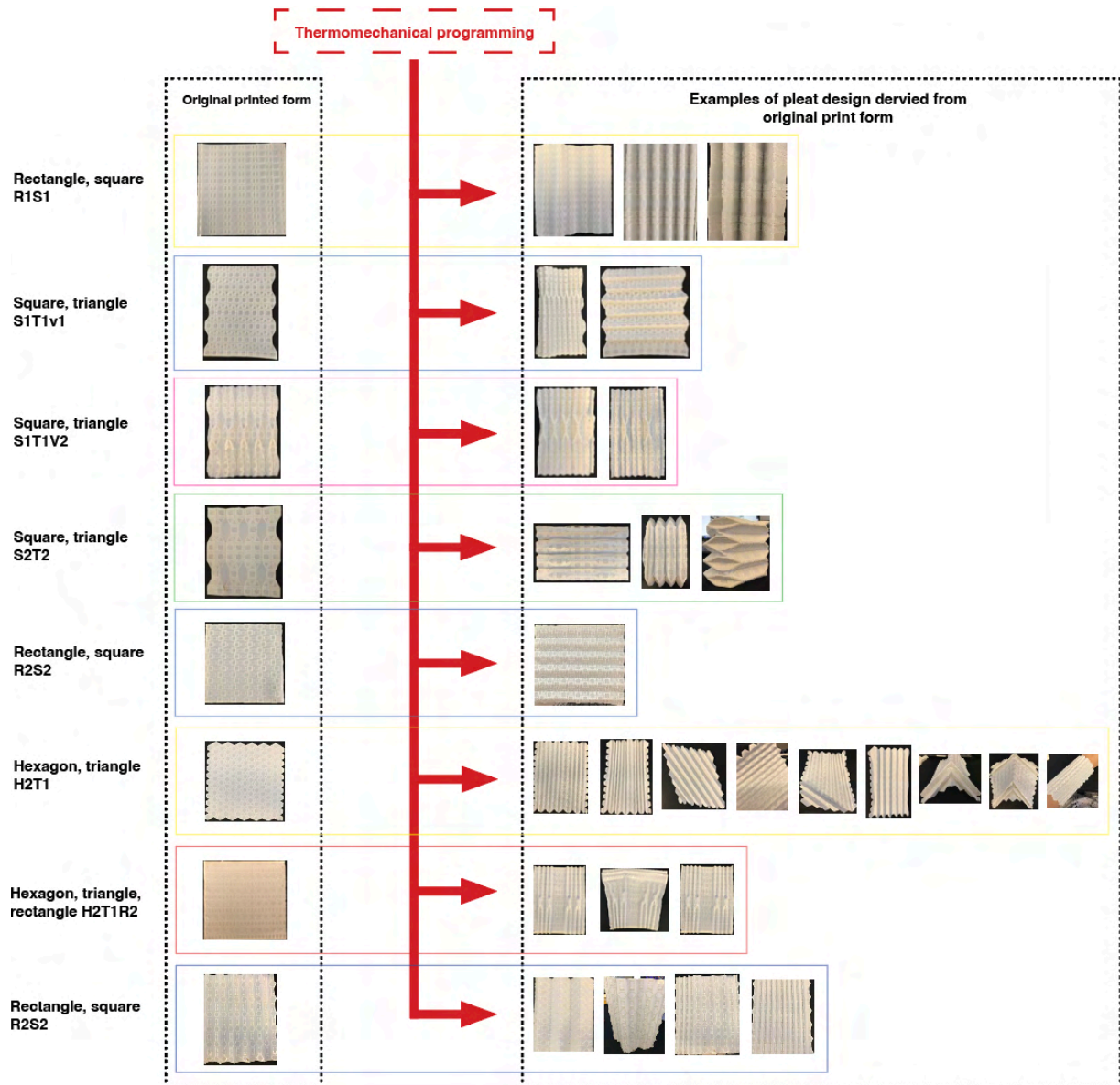
Figure 6-4 multi-shaped tessellating 4DP PTC's shapeability

Pattern shape size, folding direction and, intervals were shown to influence the surface design of 4DP PTCs. The specimens with larger shaped patterns resulted in surfaces with larger peaks and troughs and the specimens with smaller shaped patterns resulted in surface with smaller peaks and troughs and pleats that were more densely packed together due to its smaller shapes. Larger folding intervals also created a more exaggerated three-dimensional (surface convolutions and texture) effect with a slight reduction in surface area.

6.2.3.3 Summary

Eight 4DP PTC prototypes including unary and multi-shaped tessellating patterns were evaluated for their shape performance. The selection criteria are based on the results from section 5.3.3.2, where the results indicated that triangle, honeycomb, and rectangle recording the highest recovery rate, and honeycomb, rectangle, and triangle to record the quickest shape recovery. The selected prototypes were designed with tessellating patterns containing these individual shapes (unary) or a combination (multi-shaped) of these shapes. As shown in sections 6.2.3.1 and 6.2.3.2, all types of specimens showed excellent shape fixity capabilities after thermomechanical programming and can be shape fixed to various pleated forms when subjected to subsequent programming processes. In this section, the prototypes are tested for their shape recovery from flat to their programmed form (**Table 6-3**).

Table 6-3 Summary of prototype performance

Prototype	Tessellation	Transformation	Observations
R1	*Unary*	Flat → box pleat	Strong shape fixity, curling, and folding
R2	*Unary*	Flat → box pleat	Strong shape fixity, curling, and folding
T1	*Unary*	Flat → crystal pleat	Insignificant shape changes due to strong shape fixity but with signs of curling on the edges
T2	*Unary*	Flat → chevron pleat	Insignificant shape changes due to strong shape fixity but with signs of curling on the edges
H1	*Unary*	Flat → box pleat	Slight contraction
H2	*Unary*	Flat → box pleat	Slight contraction, curling, and folding
S2T2	*Multi*	Flat → 3D accordion structure	Contraction and folding
H2T1R2	*Multi*	Flat → surface accordion	Slight contraction and curling on the edges

The experimental setup is identical to the experiments in section 5.3.3. The 4DP PTC prototypes are subjected to external stress to flatten and then left to free deformation before subjecting to Tr (45°C). Due to the high level of shape fixity, most of the prototypes were unable to be flattened back to its original printed form. **Table 6-3** outlines the summary of observations during the experiment. The shape recovery process is captured using and iPhone 7, and **Figure 6-5** shows video captures of the shape recovery process.

During the experiment, the following phenomenon was observed: the shape response ranged from 10.11s to 19.09s, prototypes that had higher levels of shape fixity had insignificant change in shape, several specimens i.e., R1, R2, T1, T2, H2, H2T1R2 displayed curling on the edges when subjected to Tr, and R1, R2, H2, and S2T2 showed larger folding capabilities. The curling phenomenon was caused by the Tr, however when cooled down and placed on a flat surface, the curling was no longer observed. This experiment enables designers and practitioners to use the findings as a reference for developing further shape transformations or the design of shape shifting structures for various applications. The subsequent sections discuss the potential applications of 4DP PTC materials.
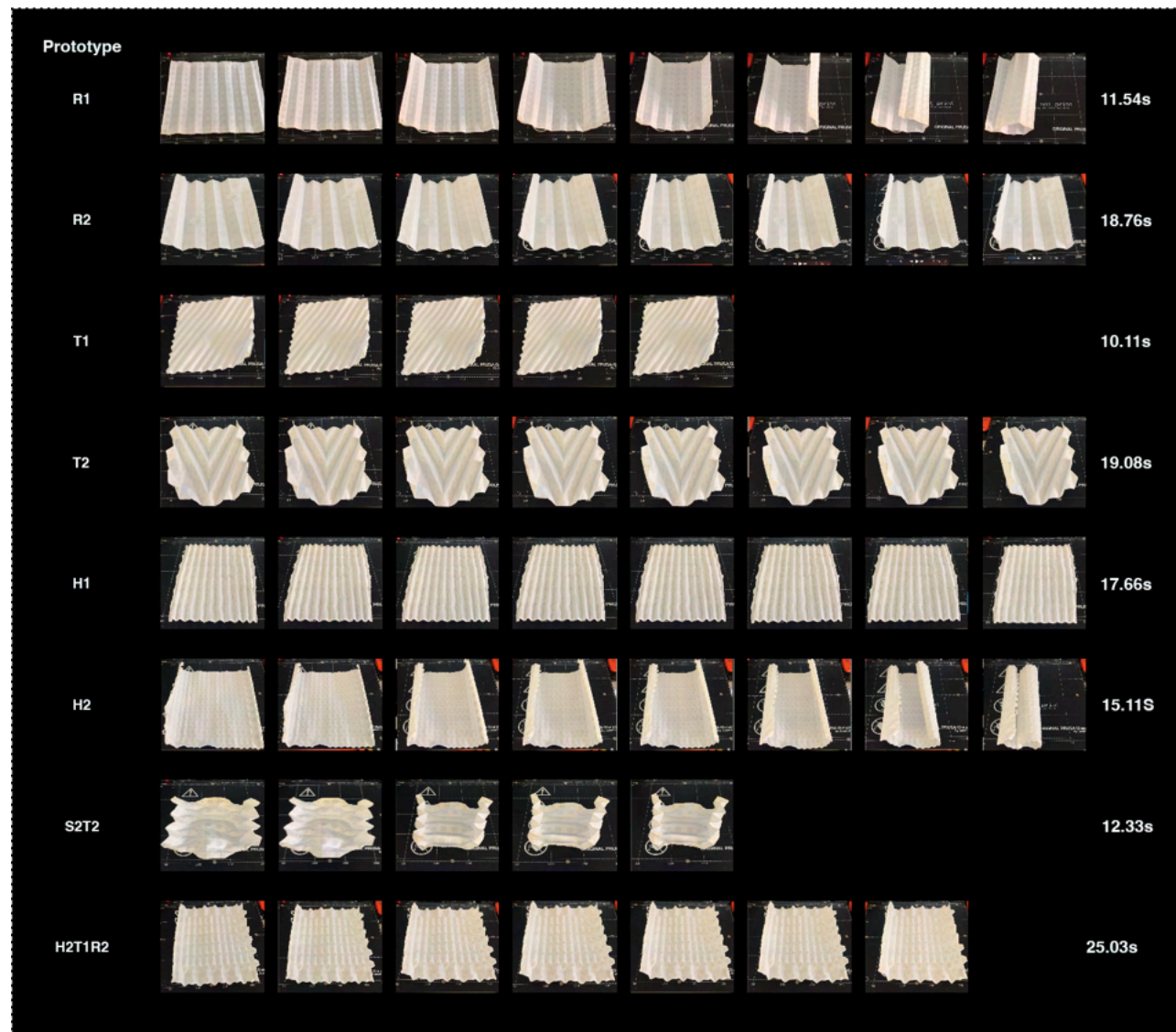
Figure 6-5 Video captures of 4DP PTC prototypes' shape recovery

6.3 Potential applications of 4DP PTC

4DP textiles have been discussed in existing literature as having potential to be adopted in a wide range of application in various fields i.e., automotive applications in dashboards, seating, side-panels, individual production of components with personal logos or brands, and functional sport textiles with reinforced parts (muscle support/kinesio tapes) (Loh, 2021; Mayer, 2022; Tibbits et al., 2014). In this study, 4DP PTCs with the five basic shapes have shown excellent shape fixity (up to 98.7%) and recovery properties (up to 96.8%) which can be used for the development of adaptable and versatile products that combines aesthetics with functionality (**Figure 6-5**). For example, shape fixity can be used for the design of re-pleatable textiles and applications that can be re-sized or re-shaped. The ability to be re-programmed repeatedly to shape fix with high consistency to different permanent forms cannot be realised with conventional textiles. 4DP PTCs can also be exploited for its shape recovery property for the development of dynamic and transformative garments. This chapter will demonstrate the potentials of 4DP PTCs in three design concepts:- 1) re-pleatable textiles for garments, accessories, and textile-based products, 2) adaptable facemask, and 3) re-shapable lampshade.
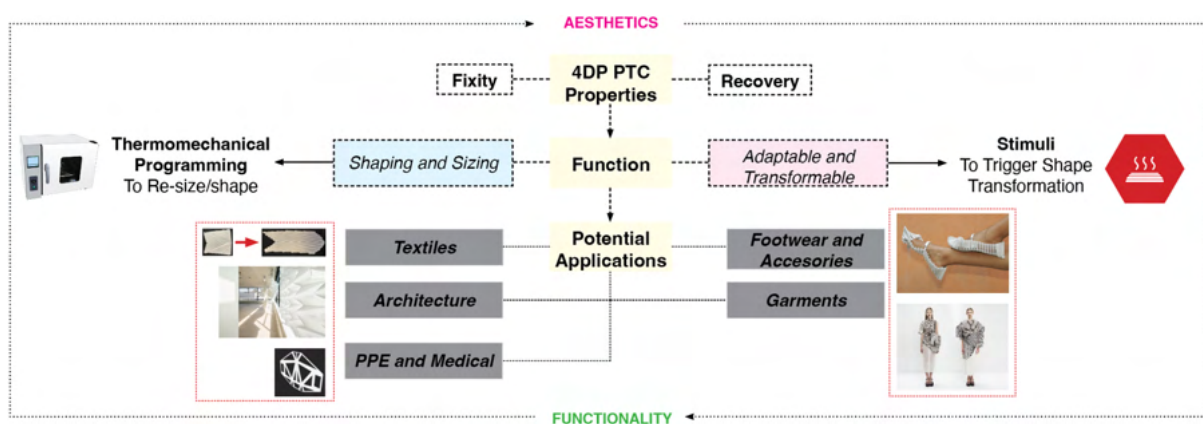
Figure 6-6 4DP PTC applications according to property

The unary and multi-shaped tessellation specimen experiments indicated that numerous pleated surfaces can be realised via different folding methods. The design experiments indicated that the pattern shape, size, folding direction, interval, and degree of fold to influence the surface aesthetics and structure of the specimens. Unary, square and rectangle patterned specimens can be folded to produce simple horizontal and vertical pleats, while hexagon and triangular patterned specimens can be used to produce pleats that were angled i.e., V-shaped pleats. The combination of shapes produced further visually interesting surfaces.

6.3.1 Re-pleatable textiles

4DP PTC's post-manufacture programmability offers unprecedented personalisation for textile products. One such use for 4DP PTCs would be the development of fabrics that can be re-pleated with high shape fixity (**Figure 6-6**). Its high shapeability, enables designers to develop versatile design objects that can be re-shaped/re-sized/re-purposed for different scenarios or occasions. Suitable types of applications include adaptable garments, accessories, and interior textile products, and textile products that can be temporarily flat packed to optimise storage or shipping and stimulated back to its permanent form. 4DP PTCs can be strategically used to provide flexible, adaptable, and modifiable textile products.
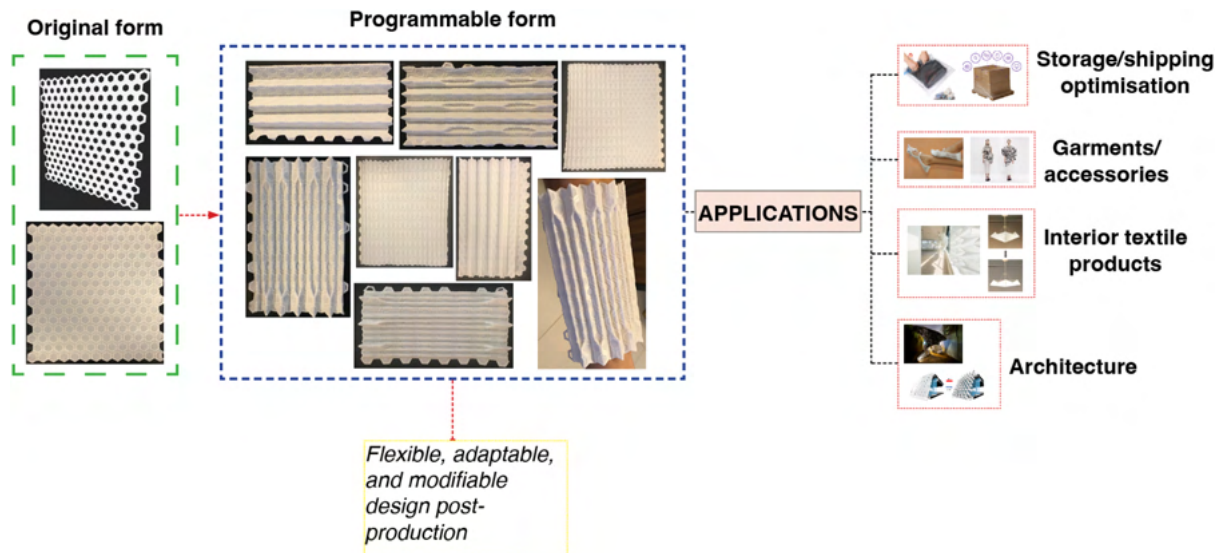
Figure 6-7 4DP PTC re-pleatable textiles

6.3.1.1 Development of re-pleatable textiles

The process for developing re-pleatable textiles is identical to the steps shown in **Figure 6-2**. The textile development process consists of four stages, including design research, practice-led making, design optimisation, and fabrication. Such steps reflect the importance of multidisciplinary thinking around art, design, and technology to develop aesthetic and functional 4DP PTCs.

6.3.1.2 Functionality of re-pleatable textiles

The 4DP PTC re-pleatable textiles utilises its innate transformation capabilities for re-shaping or to create dynamic visual transformation effects. Its functionality include:

1. The surface design of 4DP PTCs can be repetitively re-shaped by the user via a straightforward folding and consequent thermomechanical process to adapt to the user's needs and environment.

2. Applications that will benefit from 4DP PTC's shape fixity capabilities include the development of fabrics with re-pleatable surfaces for interior textile products i.e., lamp shades, room dividers or garments and accessories with adaptable surface aesthetics.

3. 4DP PTC's shape recovery properties can also be exploited for developing applications with surface and/or shape transformation capabilities i.e., soft robotics, self-assembly products, or intelligent sun shelters. **Figure 6-5** shows video screen captures of the shape transformation of various 4DP PTC specimens. As shown in the images, SMPs can be strategically extruded in target areas (resulting in different pattern designs) to attain shape transformation in specific zones to achieve aesthetic and functional goals.

4. 4DP PTC's shape fixity property can also be used to temporarily pleat fabrics to optimise storage or shipping i.e., (flat packing). The key advantage of re-pleatable textiles is its ability to be modified and adapted post-production for both aesthetic and/or functional purposes. **Figure 6-8** demonstrates the shapeability of various 4DP PTC specimens.
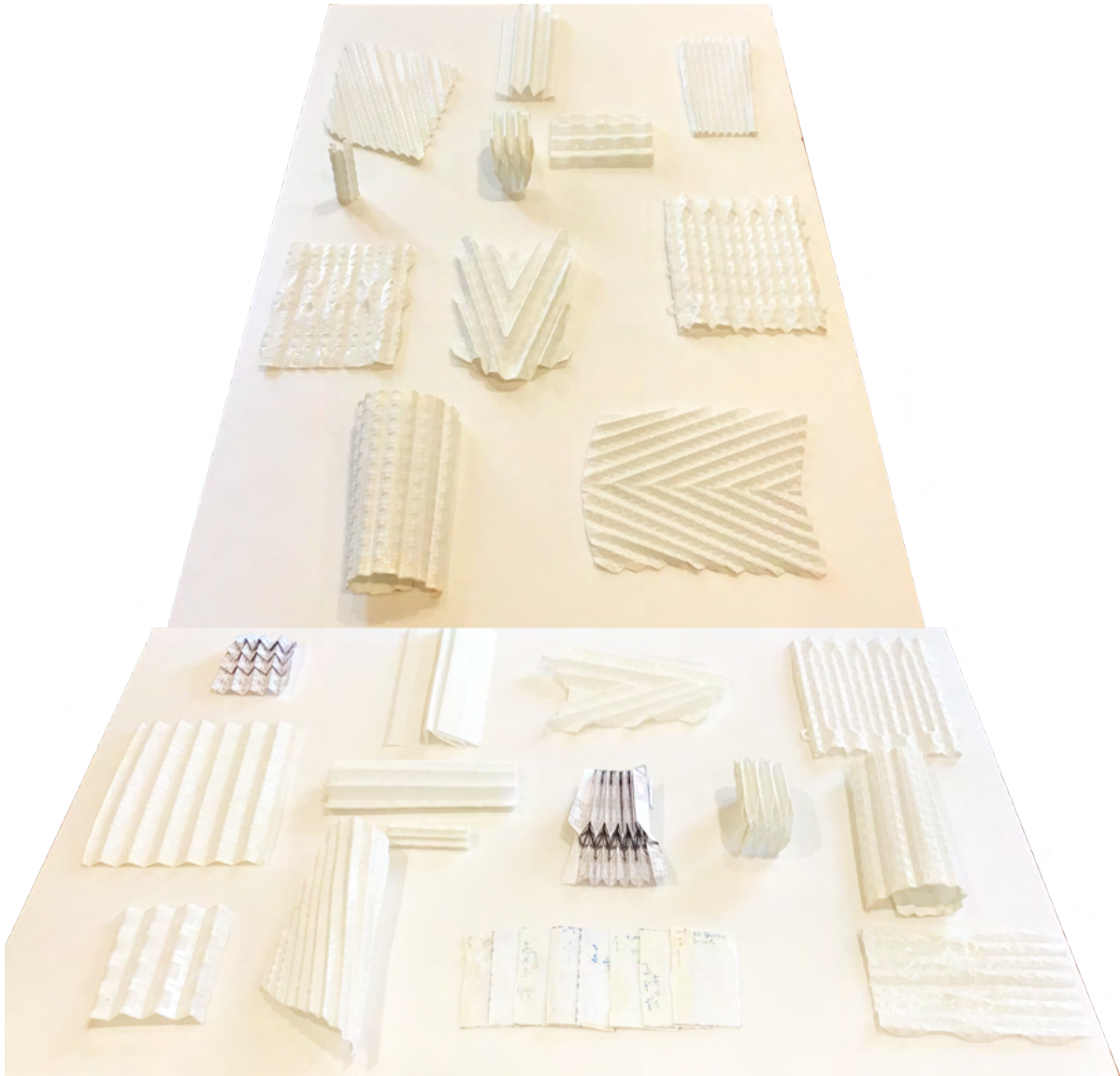
Figure 6-8 4DP PTC fabric specimens

6.3.2 Flexible sizing facemask

Aside from utilising a 4DP material's shape transformation property which delivers eye-catching novelty, 4DP PTC's high level of shapeability can also be taken advantage of to design smaller-scaled wearable applications with flexible sizing mechanisms i.e., facemasks or other personal protective equipment. Its highly efficient shapeability, enables designers to develop wearables that can be re-shaped/re-sized/re-purposed for different individuals or scenarios. Although there are offerings of customisable masks in the market, their design and

manufacturing processes are often highly complicated and expensive. In addition, the design process is often intrusive to the consumer as it requires 3D facial scans and the use of complicated software to simulate auto-fitting. Furthermore, they cannot be re-adjusted or re-fitted post-manufacturing. 4DP PTC's shape transformation capabilities can overcome these limitations as it offers post-production adjustments. Facemasks can be custom shaped and fitted by the user at the comfort of their homes. Other advantages of using 4DP PTCs for facemasks include custom fixing around nose bridge and cheek areas for perfect seal with face resulting in better protection, reducing pressure points to face during prolonged wear for maximum comfort, has high shape recovery even post stretching or shaping, and 4D printing polymers are lightweight, hypoallergenic, and can be extruded on a wide range of fabrics and materials (**Figure 6-9**). In addition, the materials used for producing 4DP PTCs are also relatively low in cost and are readily available in the market.
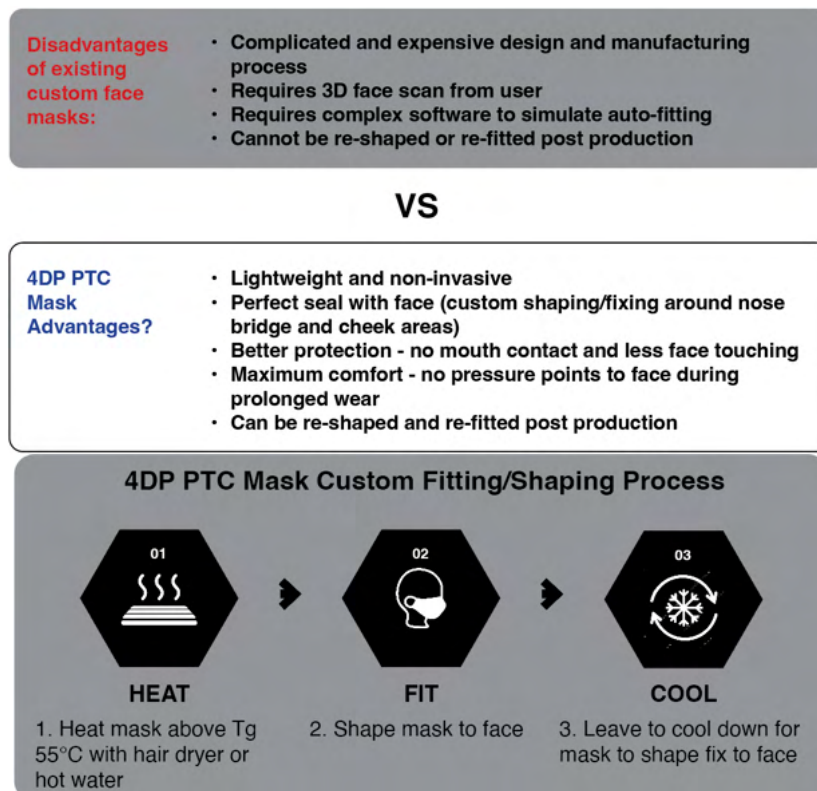
Figure 6-9 4DP PTC mask advantages and custom fitting/shaping process

6.3.2.1 Development of flexible sizing facemask

The design process starts with an overall sketch of a facemask silhouette using Rhino 8 (Rhinoceros, 2024). This silhouette functions as a general shape for the mask and is inspired by the Asaro head which was developed by John Asaro in 1976, with the goal to simplify the human head to different planes to understand how light and shadows fall on a head (Büsken, 2021). The practice of viewing human body parts as planes or as tessellating patterns are now widely used in 3D modelling and the design of customized garments and shoes and is also (Ulerich et al., 2023; Xu et al., 2019). To visualise how the facemask silhouette would appear three-dimensionally, folding experiments were conducted which identified where hinges are required to be added to enhance the shapeability of the facemask (**Figure 6-10**, number 1).

Figure 6-10 (number 2) illustrates the technical sketches for the 4DP PTC facemask that are designed using Asaro's principle. The internal planes of the mask are designed in accordance with the planar structure of the human face. Such planes are connected via 4DP hinged grooves which can be folded or bended to shape. Due to the flexibility of the hinges, 4DP PTC facemasks focuses on the three-dimensionality of the human face for optimising comfort and fit (**Figure 6-10**, number 3). The foldable hinges facilitate as shaping and sizing mechanisms. And to improve the appearance and fitting of 4DP PTC facemasks, various prototypes with different planal structures were developed and underwent thermomechanical programming to see its shapeability (**Figure 6-10**, number 4).
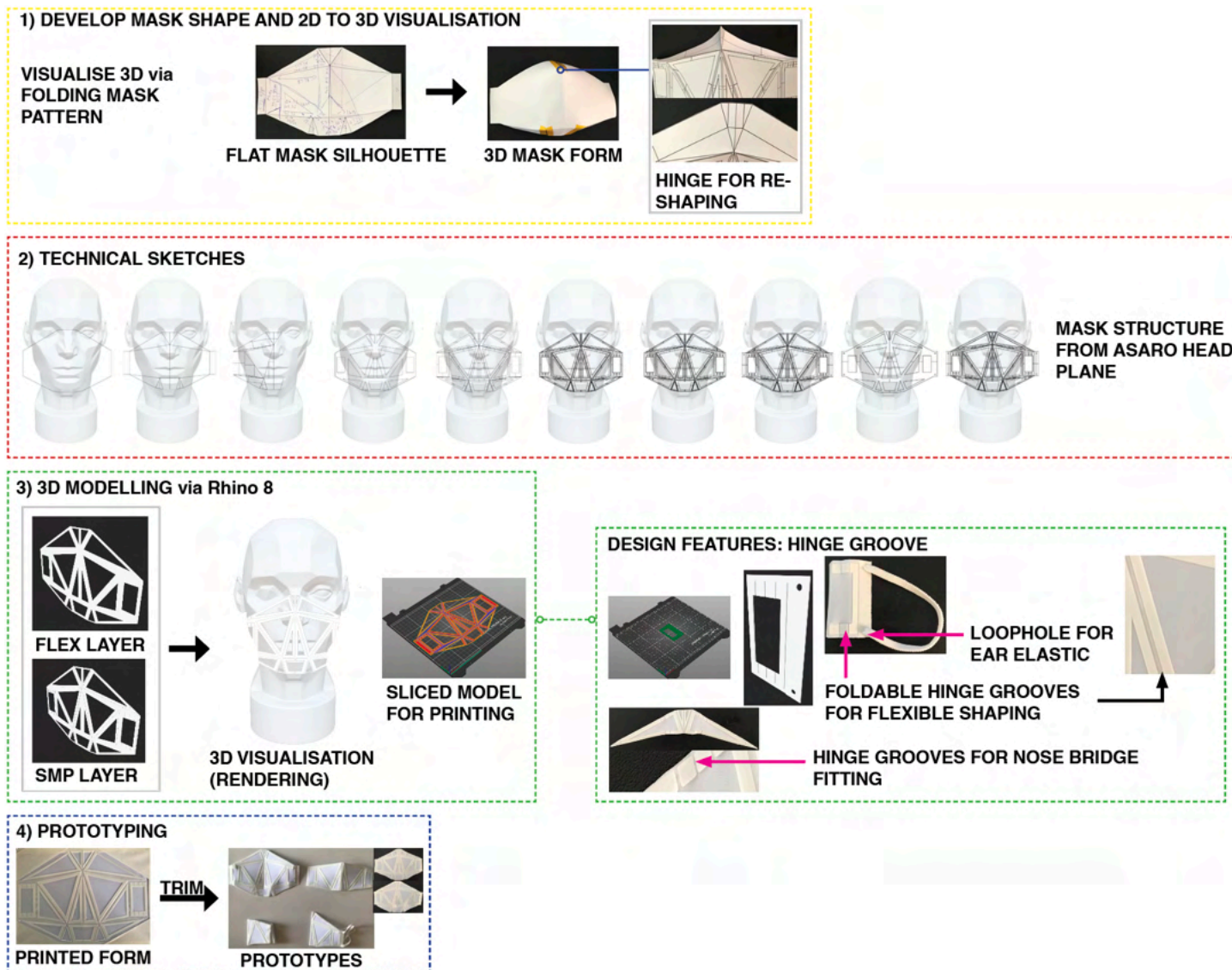
Figure 6-10 4DP PTC facemask development
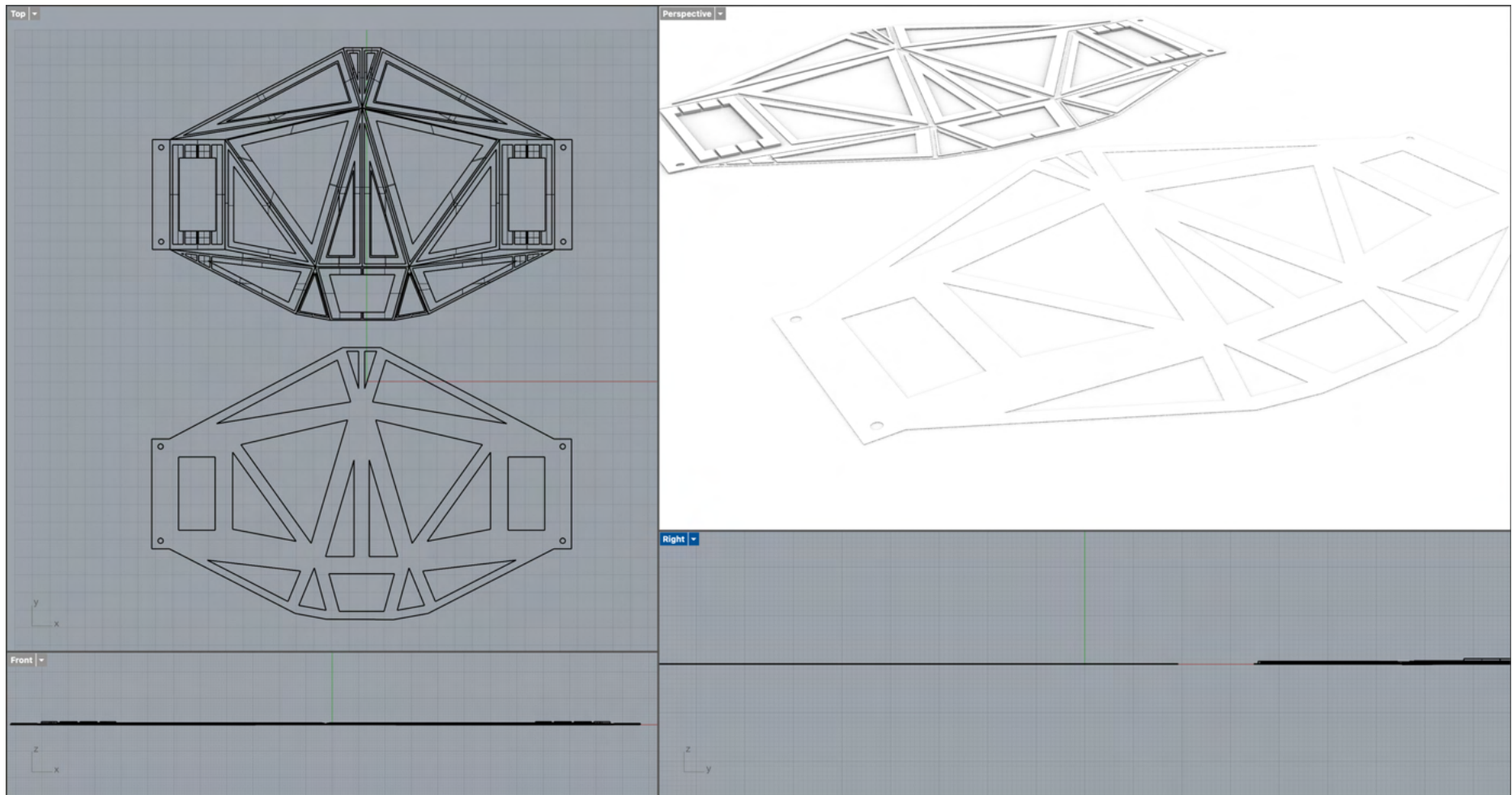
Figure 6-11 3D modelling and rendering on Rhino 8

6.3.2.2 Functionality of flexible sizing facemask

The 4DP PTC facemask utilises its innate transformation capabilities for re-shaping or to create dynamic visual transformation effects. Its functionality include:

1. 4DP PTC's excellent shapeability, facilitates mass customisation, where wearable products focus on users and can be adapted post-manufacturing. This design strategy facilitates product design that reflects the choice of individuals at a low production cost and flexible process.

2. A facemask developed using 4DP PTCs can be easily programmed to shape individual faces in the domestic environment by heating the mask from a glassy to rubbery state which will allow the mask to be moulded or folded to a desired form. Once cooled down to room temperature, the facemask returns to a glassy state and is fixed to the new programmed shape. This process can be repeated to achieve the desired shape.

3. 4DP PTC facemasks can be re-shaped to adapt to the user's face shape and they can also be depended upon for its excellent elastic recovery post stretching or shaping via repetitive wear.

4. Design features can be implemented into 4DP PTC facemasks to facilitate flexible shaping/sizing (**Figure 6-10**), i.e., foldable hinge grooves on the edges of the mask and nose bridge for form-fitting and varying polymer thickness to increase or reduce rigidity to achieve comfort and improved shaping.

5. **Figure 6-11** illustrates the facemask in various programmed forms and when worn.
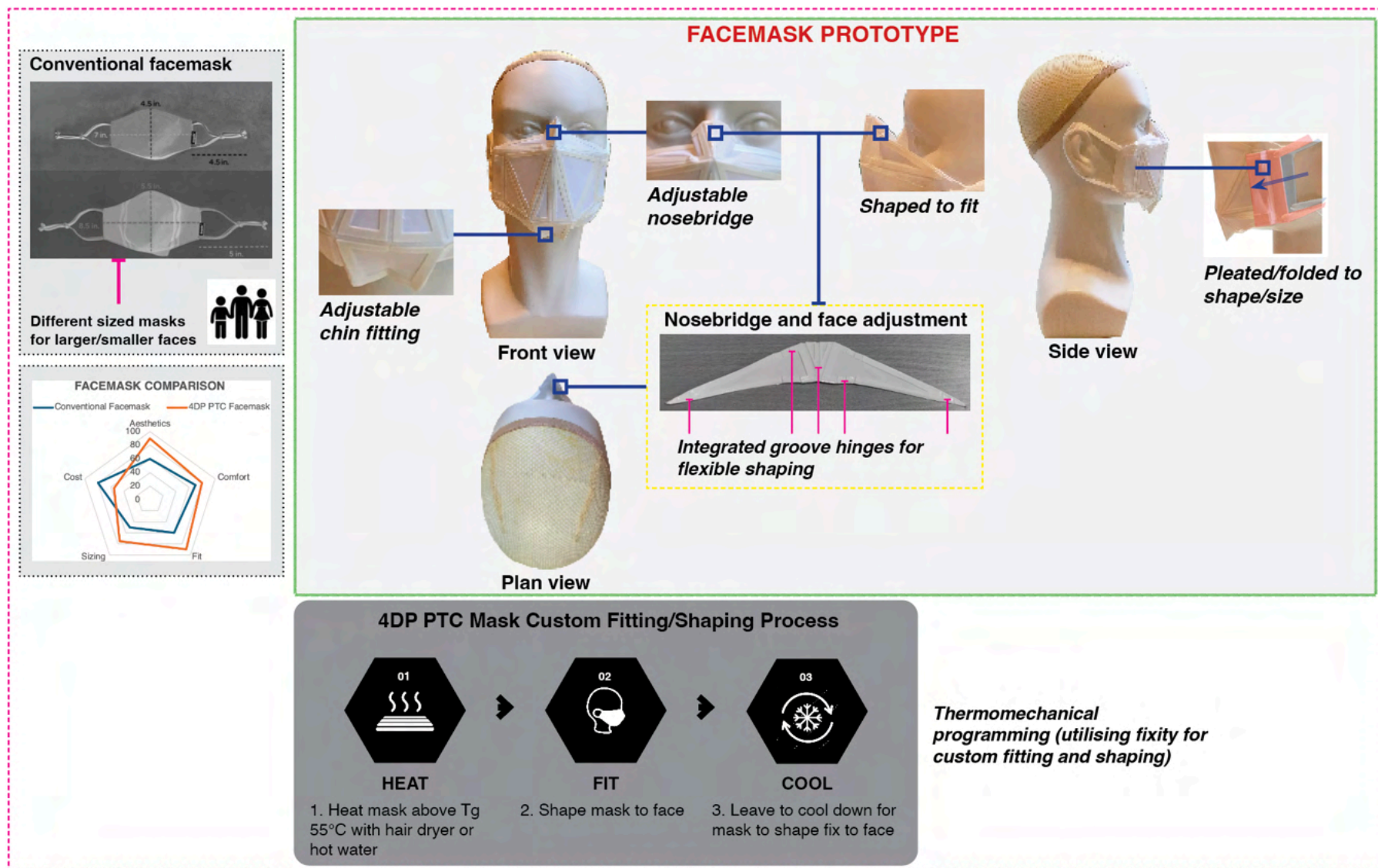
Figure 6-12 4DP PTC facemask functionality

6.3.3 Re-shapable lampshade

By utilising 4DP PTC's efficient shapeability, textile products such as re-shapable lampshades can also be developed. 4DP PTC's highly efficient shape fixity allows lampshade to be shaped by the user to different designs and occasions to suit different moods. There is currently a lack of home textile products that possess the capability to be transformed by the user. Products designed with 4DP PTCs possess the capability to transform into multiple shapes for aesthetic purposes, blend into different environments and rooms, and are easily re-shaped.

6.3.3.1 Development of re-shapable lampshade

The process for developing the material for re-shapable lampshade is identical to the process for developing re-pleatable textiles (**Figure 6-13** and **Figure 6-14**). The textile development process consists of four stages, including design research, practice-led making, design optimisation, and fabrication. Such steps reflect the importance of multidisciplinary thinking around art, design, and technology to develop aesthetic and functional 4DP PTCs. A simple lamp shade is created by fabricating a 4DP PTC material that can be shaped to a cylindrical design. This design emphasises on the surface pleat manipulation and can be folded by the user between different forms. In addition, to lampshades, 4DP PTC materials can be used for designing table lamps, chandelier shades, wall lighting, and re-shapable space sound absorbers (Sakagami et al., 2020). The shape performance experiment results have suggested several pattern combinations i.e., hexagon with triangle, square with triangle, rectangle with square (R2, S2), and triangle with honeycomb to achieve higher shape fixity which can improve the design and shapeability of the re-shapable lampshade.

6.3.3.2 Functionality of re-shapable lampshade

The 4DP PTC re-shapable lampshade utilises its innate transformation capabilities for re-shaping or to create dynamic visual transformation effects (**Figure 6-13**). Its functionality include:

1. The possibility to create DIY lampshade designs. Users can unleash their creativity by transforming the 4DP PTC multi-shaped lampshade into various shapes via thermomechanical programming which shape fixes the material to a new programmed form. Its innovative material, tessellating structure, and hinge mechanism enable the adjacent polymer structure to be re-shaped and fixed (once it cools down to a glassy state) to a desired shape. By simply programming the material to your desired shape via folding and thermomechanical programming, users can decorate their space in different styles with a single light pendant.

2. The lampshade can be transformed into different designs to blend into different décor styles. It can also be programmed as ceiling light shade or as lighting fixtures for different interiors including living and dining rooms, bedrooms, kitchen, hotel, restaurants, café, bars clubs, office, galleries, or showrooms.

3. The lampshades are constructed of premium quality materials with unique surface designs and are constructed using temperature resistance materials. In addition, the 4DP PTC materials have been evaluated in accordance with industry standards for tensile and bursting strength, and peel resistance ensuring durability.

4. Due to the shapeability of the 4DP PTCs, the lampshade can be re-shaped to fit most bulb holders. In addition, LED candles can also be used as a light source which requires no electrical installation and does not interfere with the shape change of 4DP PTCs.

5. The lampshades are also lightweight and can be flat packed to optimise storage or shipping and can be stimulated back to its permanent form when required.
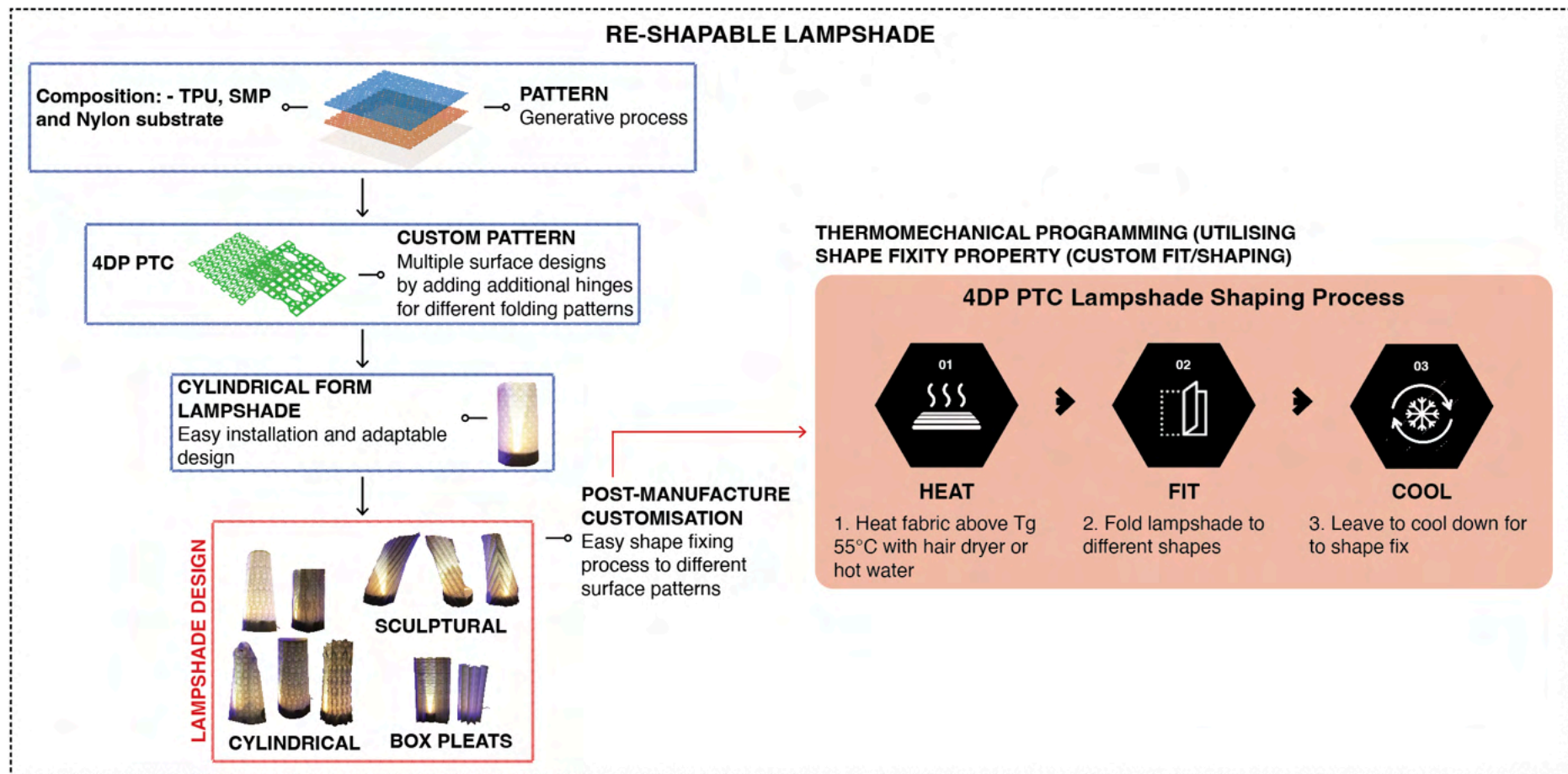
Figure 6-13 4DP PTC re-shapable lampshade
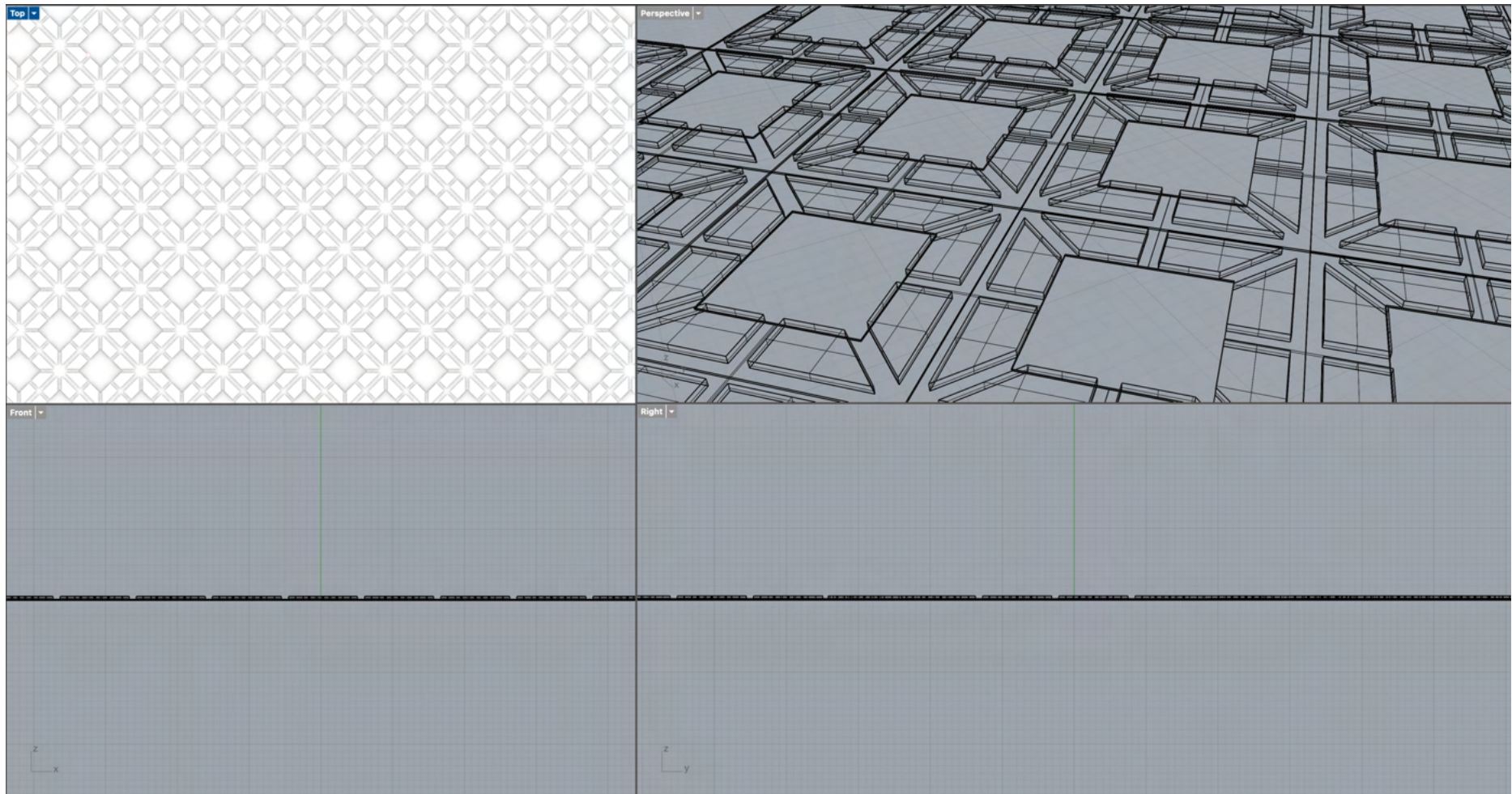
Figure 6-14 3D modelling and rendering on Rhino 8

6.4 Discussion

In this study, the thermo-responsive 4DP PTCs have demonstrated both aesthetic and technical advantages and have been substantiated through various design experiments. A systematic approach of design and evaluation was used to develop 4DP PTCs which differs from existing shape transformative material design and manufacturing. 4DP PTC's novelty also lies in its technical and aesthetic advantages in comparison with conventional textile materials.

6.4.1 Aesthetic advantages

Thermo-responsive 4DP PTC's can be summarised as adaptable, flexible, and modifiable. 4D printing technologies enable designers to completely rethink their approach towards designing textile products. It enables them to develop mass produced articles with functional elements and offers post-manufacturing customisation by utilising its shape transformation properties. 4DP PTCs unparallel level of versatility propositions the development of textile products with high adaptability and flexibility. Its foremost advantage includes the production of textiles with highly flexible surface design that can be customised during the design process and post manufacturing by using a straightforward thermomechanical programming process. Post-process customisation affords users the opportunity to alter the surface appearance of textile products to combine and create different ensembles and synthesise different elements onto one surface. 4DP PTCs can be developed to accommodate to the changing dynamics of the user's lifestyle or environment. Garments and wearables can be designed with flexible sizing (i.e., flexible sizing masks or shoes) and textile products with shape transformation capabilities can change its structural form for aesthetic and functional purposes (i.e., re-shapable lampshade or room divide. Users can also utilise 4DP PTC's transformation capability to conveniently store articles. The application of 4DP PTCs in textile products will assist in the further development and evolution of sustainable design.

6.4.2 Technical advantages

This study has demonstrated the technical advantages of 4DP PTCs based on material characterisation and design experiments. As shown in **Figure 6-7** and **6-8**, 4DP PTCs possess high shapeability and can be re-shaped to multiple different surface designs via a straightforward folding and thermomechanical process. By folding the material in different directions and at different intervals, multiple forms can be created with a slight modification in size and structure. 4DP PTC's versatility and adaptability anticipates users to buy and own less products. Moreover, 4D printing approach to developing adaptable materials promotes sustainability and makes us more environmentally conscious.

4DP PTC's development has an overall a low carbon footprint (both material and energy saving) and maximises flexibility and efficiency in manufacturing customised products. The digital visualisation process pre-manufacture enables the ease for modifying the design to reduce production steps, material use and printing time. Base patterns, textures, and materials can be modified to optimise designs to respond to individual user requirements. The use of FDM/FFF technologies also provides high speed and affordable printing over a vast surface area. Sustainability can also be viewed from the perspective of longer-lasting items i.e., wear resistant shoes or sports garments with reinforced areas for stress areas. Polymer extrusion onto these areas can enhance aesthetics, functionality, increase tensile strength, and extend service life.

6.5 Summary

In comparison with conventional materials, 4DP PTCs distinguishes itself due to its potential for personalisation and shapeability both pre-manufacture and post-production. In this chapter, a series of unary and multi-shaped tessellating 4DP PTCs and its specifications are presented.

Such specimen's alternative forms which are created via a folding and thermomechanical process are also shown and examined. To demonstrate the functionality and feasibility of applying 4DP PTCs in real-world applications, the 4DP PTCs were used to design a collection of re-pleatable textiles and re-shapable facemask. The construction techniques, characteristics, and design elements, i.e., pattern type and size, folding direction, and intervals of the prototypes are also discussed in detail. 4DP PTC's high adaptability allows different forms to be produced by using a few simple but highly versatile pattern designs anticipating users to buy and own less items. To conclude, 4DP PTCs bridges together two emerging AM research fields (4D printing and PTCs) where existing theoretical contributions are fragmented and limited. This chapter provides an efficient design procedure with visually interesting outcomes. It also demonstrates the implement of suitable design strategies for specific designs and applications which aims to rouse further innovation and developments in this emerging field.

Chapter 7: CONCLUSIONS AND RECOMMENDATIONS

7.1 Conclusions

Chapter seven concludes on the explorative study of thermo-responsive four-dimensional printed polymer-textile composites. An overall summary of the foundations and development of this design concept is discussed. The practical knowledge obtained from the studio and lab-based experiments has led to the development of a 4DP PTC model. This model encompasses the design, development, and evaluation process, the properties and performance of the resulting prototypes, and the creative and functional significance of 4DP PTC design applications. To conclude, the study limitations, and recommendations for further works are also presented.

This study is committed to add to the current literature on 4DP PTCs by developing a novel textile material with high customisability and shapeability. The amalgamation of theoretical study and practical experimentation has led to the establishment of a systematic design, development, and evaluation process for engineering active textile materials with customisable mechanical and shape performance with high adaptability. The objectives of this study have been accomplished which includes: i) the establishment of a 4DP PTC design concept and theoretical model, ii) the development of PTCs and 4DP PTCs under various material combinations and printing variables, iii) the evaluation of such material's mechanical and shape performance to ascertain optimal performing combinations, and iv) demonstrate the potential applications of 4DP PTCs in design. The following sections recapitulates on the practical experiments, the applications for 4DP PTC in design, and the contribution of the design theories established in this study. **Table 7-1** summarises the experiments that were carried out in this study to meet the objectives.

Table 7-1 RQ and objectives

	RQ	Objective	Chapter/section
1	*What are the optimal material combinations and printing parameters for maximising peel resistance between TPU/TPE and textile substrate?*	To examine material partners and extrusion temperatures for maximising peel resistance.	4.3.1, 4.3.2, 5.3.2.1
2	*What the optimal material combinations and printing parameters for maximising surface quality of polymers?*	To examine material partners and extrusion temperatures for maximising surface quality.	4.2.2.3.3, 4.2.2.3.4
3	*What the optimal material combinations and printing parameters for maximising tensile strength of 4DP PTCs?*	To examine material partners and extrusion temperatures for maximising the tensile strength of 4DP PTCs.	5.3.2.3, 5.3.2.3.1
4	*What the optimal material combinations/printing parameters for maximising bursting strength of 4DP PTCs?*	To examine material partners and extrusion temperatures for maximising the bursting strength of 4DP PTCs.	5.3.2.4, 5.3.2.4.1
5	*How does material and pattern design influence bending rigidity and recoverability?*	To experiment with different shaped patterns and its influence on bending rigidity and hysteresis.	5.3.3.3, 5.3.3.3.1 – 5.3.3.3.6
6	*What do we have to consider when making design decisions for fabricating 4DP PTCs?*	To identify and establish a systematic process through practical experimentation and theoretical study for the design, development, and evaluation of 4DP PTCs.	3.6, 7.1.1
7	*What processes and equipment are used to program a permanent shape into 4DP PTCs?*	To experiment and establish a feasible process for thermomechanical programming 4DP PTCs.	5.4.2
8	*How does bending rigidity and recoverability influence the shape recovery of 4DP PTCs?*	To investigate the relationship between bending rigidity and hysteresis of 4DP PTCs and its influence on shape performance.	5.4.1
9	*How can we fine-tune 4D printing conditions to manipulate the performance (i.e., fixity, recovery, and response rate) of 4DP PTCs?*	To determine the optimal conditions for optimising 4DP PTC performance via using comparative analysis methods for examining all experimental results.	5.3.3
10	*What are the potentials and limitations of 4DP PTCs using FDM/FFF printing technologies? What applications would benefit from thermo-responsive 4DP PTCs?*	To demonstrate the potentials of 4DP PTCs in design via several applications and to identify the limitations of the materials.	6.3, 6.4, 6.5

7.1.1 Design concept and 4DP PTC model

The 4DP PTC design concept originated from existing literature (chapter two), which revealed the advantages of FDM/FFF technologies, the wide range of available materials, and how such materials can be used in combinations with other substrates that are manufactured using traditional methods i.e., woven and knitted substrates to create a novel class of material composites. In addition, practitioners can use 4D printing methods to develop active materials with high shapeability and shape transformation capabilities. Such materials have showed substantial potential for a wide range of applications and industries calling for further study (Cheung et al., 2024; Koch et al., 2021; Tibbits et al., 2014). However, current literature shows

insufficient exploration of 4DP PTCs that combines SMPs with textile substrates via FDM/FFF processes to create textile-based composite materials with unique mechanical properties and efficient shape transformation.

The design concept of 4DP PTCs was proposed in chapter three based on the critical analysis of existing literature. The design challenges are identified via reviewing existing fabrication methods, materials, and the rigorous performance and design requirements for various textile-related applications. In addition, the textile characterisation methods that are used to facilitate the evaluation of 4DP PTC performance are identified. Industry standard evaluation methods for mechanical and shape performance provides data that can help optimise the design and development of 4DP PTCs. Through examining existing theoretical frameworks, three key design variables i.e., material combinations, printing parameters, and surface design was found to influence the performance of 4DP PTCs. The fundamental design principles and processes for creating 4DP PTCs are also presented which begins with the development and characterisation of PTCs and the subsequent addition of a SMM to this composite material resulting in a 4DP PTC.

A 4DP PTC concept model is established based on theoretical and practical investigation and guides the design and development of 4DP PTCs (**Figure 7-1**). This model illustrates the interaction between PTCs and 4DP PTCs and can be used to develop both types of materials. It also shows the different design variables and their relationship with each other. Other design considerations and processes are also provided in this model. The type of application and its requirements determine which materials, patterns, structures, and printing parameters are used for developing PTC/4DP PTC materials. The model reveals three fundamental design variables for developing PTC/4DP PTC materials including material selection (fabric and polymer), 3D

modelling and slicing (pattern and structure design), and FDM/FFF printing (printing parameters). Such variables can be fine-tuned to meet the diverse requirements of the final application i.e., material profile, rigidity, surface aesthetics etc. Industry standard evaluation methods can be used to characterise the fabric specimens to provide feedback that can help optimise material design. Through experimentation, it was identified that PTCs served an important role in the development of 4DP PTCs. PTCs must serve it purpose as the base material for 4DP PTCs and requires good covalent bond with SMP to facilitate consistent and efficient shape and mechanical performance. And as mentioned previously, the key design variables can be adjusted to benefit different applications. This systematic design model comprises of design, development, and evaluation processes and has been validated and supported with practical experimentation and quantitative data and can be used for the development of PTCs, 4DP PTCs, and related applications. It also integrates advance technological processes and materials and combines aesthetics with functionality.
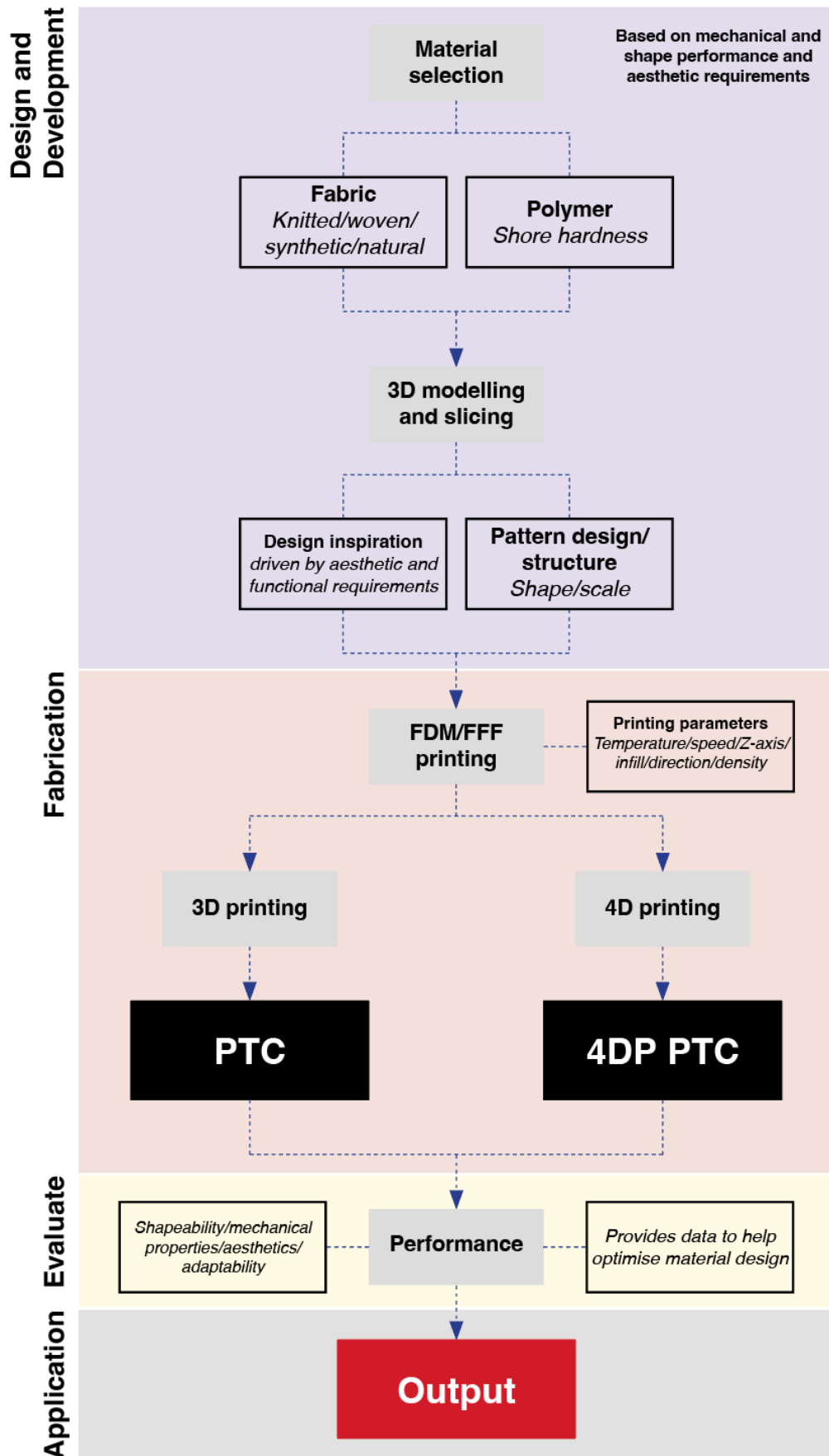
Figure 7-1 4DP PTC model

7.1.2 Practical experiments

As shown in **Figure 7-1**, this study is based on two core exploratory experiments: PTC and 4DP PTC. These experiments along with its results are presented in chapters four and five, respectively. The data-driven results are critically analysed, and the investigations have led to the identification of changing principles that occur between design variables and its influence on surface design, material properties and performance. The functional features and the highly adaptable aesthetics of 4DP materials have proven immense potential for developing novel textile-based products and wearables. The design principles, 4DP PTC prototypes, and systematic study of the different design parameters all serve as a comprehensive reference towards further works and design applications for 4DP PTCs. The empirical nature of the study adds to the current literature and can also lead to further work in fashion and textiles, and other design related research fields and industries. It also helps capture the interest of practitioners from other fields i.e., soft robotics and architecture.

7.1.2.1 PTC

The experiments conducted in chapter four revealed the optimal material partners and printing parameters to maximise the surface quality of the polymer surface and the peel resistance between substrates in PTC materials. The PTC experiments serve as the groundwork for the further development of 4DP PTCs. Seven types of textile substrates including knitted, woven, synthetic, and natural fibres and three types of flexible polymers including TPU/TPE with varying shore hardness were used in the experiments. The findings indicated that both material combinations and extrusion temperature to have significant influence over the surface quality of the polymer layer and the peel resistance between substrates. These properties were comprehensively examined under industry standards.

It was observed that synthetic knitted textiles (T1) were able to achieve greater peel resistance with all types of polymers regardless of shore hardness due to its ability to achieve greater polar interactions resulting in stronger covalent bonds and peel resistance. The structure of knitted fabrics also allowed polymers to penetrate the structure, however penetration depth was not correlated with peel resistance. Moreover, the lower shore hardness polymers i.e., 70A and 82A were also able to achieve greater peel resistance due to its polymeric structure. Extrusion temperature was also demonstrated to have significant effects on both peel resistance and surface quality. Even though higher ranging temperatures of 250°C and 260°C enhanced the peel resistance between polymer and textile substrates, it had negative effects on the surface and dimensional quality of the polymer layers. The overall results revealed the preferable material choice and printing parameter to choose when developing PTCs to optimise print quality and peel resistance which are necessary to move onto developing 4DP PTCs.

7.1.2.2 4DP PTC

Chapter five explores the development of 4DP PTCs by using the findings in chapter four as a reference point. 4DP PTCs are synthesised based on a PTC. A SMP is extruded atop the PTC giving it shape transformative capabilities. The shape performance experiments have shown 4DP PTCs to possess great potential for creating adaptable forms for aesthetic and functional purposes with the potential to be embraced by a wide variety of applications. In addition, 4DP PTCs also showed excellent mechanical performance which is imperative if they are to repetitively re-programmed and re-shaped which requires endurance.

The optimal performing PTC in terms of material combination and printing parameters is used as a foundation for developing 4DP PTCs. A SMP is added to this PTC resulting in F1-SMP, F2-SMP, and F3-SMP 4DP PTCs. Such materials undergo peel resistance tests to determine its

compatibility with the SMP. In addition, they are subjected to tensile and bursting strength tests to determine the optimal performing 4DP PTC. The modulus results deriving from the tensile tests also indicate the material's rigidity which is important for shape fixity. The shape performance experiments encompass shape fixity, recovery, and response and are used to determine the optimal performing 4DP PTC when subjected to common actuation movements i.e., self-bending, self-folding, and contraction. The overall results indicated F1-SMP to be the most consistent and were carried forward for further experiments which examined 4DP PTCs with 10 patterns consisting of tessellations with different shapes and sizes. The findings indicated that tessellating pattern shape and size can be used to selectively stiffen the 4DP PTC for greater shape fixity and recovery.

7.1.3 Applications

The results of the practical experiments have showed 4DP PTC materials to satisfy the potential requirements i.e., mechanical strength and flexibility of various applications. It was indicated in the findings that the mechanical and shape performance of the materials were fine tuneable via the material, printing parameters, and pattern variables. As such, this study utilised this knowledge to demonstrate the potential applications of 4DP PTCs by developing concept prototypes: re-pleatable textiles, flexible sizing facemask, and re-shapable lampshade (in chapter six). These prototypes were designed by adhering to the material selection framework and design model which reflected the feasibility of these design systems. Whilst developing the concept prototypes, the design aesthetics and technical feasibility were considered. Other factors that were considered included shape fixity, material rigidity and hysteresis, and mechanical performance which altogether influenced the design's adaptability and shapeability.

The prototypes were designed to exploit 4DP PTC's excellent shape fixity capabilities. For example, re-pleatable textiles utilised 4DP PTC's post-manufacture shape fixing to different permanent forms which facilitated the re-pleating to various surface designs, flexible sizing facemask by utilising shape fixity properties to transform to various sizes and forms, and re-shapable lampshade that transforms under the same concept as the re-pleatable textiles to create different design forms for aesthetic purposes. These designs can transform to alternative forms and sizes via a thermomechanical programming process which helps fix it to its new permanent form. Shape fixity ensures the material to fix to its programmed form, and when the material loses its programmed shape due to free deformation, it can transform back to this form whenever it is subjected to a stimulus. In contrast with existing 4DP material research that commonly exploit 4DP material's shape recovery only, which often yields inconsistent results and is used for eye-catching novelty, this study utilises 4DP PTC's highly efficient shape fixity which is validated with experimental data (though it also possesses efficient shape recovery and response). The versatility of 4DP PTCs can be further realised in multi-functional products that adapts to different occasions and needs.

7.2 Recommendations

This study serves as groundwork for using FDM/FFF processes to develop novel shape transformative materials that can be programmed post-manufacturing. Such materials are highly adaptable and can be applied in a wide range of applications. In this study, the 4DP PTC design concept is validated through theoretical and practical developments in contrast with existing studies that are mostly theoretical. And this process has proven to be both an effective and a novel approach supported with quantitative data and analysis to developing shape transformative materials with consistent performance. Though this study is innovative in various aspects including the establishment of a systematic design and evaluation process for

4DP PTCs, development of a material selection framework, and the creation of a novel material using extrusion processes, the 4DP PTC research scope can be extended.

7.2.1 Limitations

Although this study is novel in many aspects, it possesses a few limitations.

1. In this study, 7 types of textile substrates and 4 types of polymers (1 being a thermo-responsive SMP) were used in the experiments. Though this is representative of the types of materials that are readily available (including fabric structure, fibre, and polymer shore). This study would benefit from exploring additional types of SMPs for creating 4DP PTCs. However, due to the obtainability of other SMPs for FDM/FFF processes and the technical difficulties working with such materials, they have not been included in this study. Further studies must therefore identify other appropriate materials or processes or synthesise other types of SMPs with different properties i.e., actuation temperature, type of stimulus or shore hardness that are suitable for extrusion processes.

2. The specimens in this study were printed with rectilinear infill at 15% density. Such conditions were fixed to ensure consistent results across all experiments. In FDM/FFF printing, there are other types of infill and density that can be explored. Both these variables in theory, have the capacity to influence both the mechanical and shape performance of the 4DP PTCs which can provide additional knowledge on how infill and density can be used to fine-tune 4DP PTC mechanical and shape performance.

3.   Ten tessellating patterns deriving from five bio-inspired shapes were explored in this study. The experiments have shown pattern shape and scale to influence the mechanical and shape performance of 4DP PTCs. There are endless potentials to develop more complex tessellating patterns. It is anticipated that further experimentation with pattern design can provide a further understanding on how pattern shape, scale, and arrangement can improve both the aesthetics and functionality of 4DP PTC materials so they can be used in a wider range of applications.

4.   The results from the mechanical and shape performance experiments have showed 4DP PTCs to fulfil the requirements i.e., mechanical strength and flexibility of various potential applications ranging from wearable applications to textile-based products. This study demonstrates the potential of such materials via the development of concept prototypes i.e., re-pleatable textiles, flexible sizing facemask, and re-shapable lampshade. Such prototypes were designed by following the material selection framework and design process and utilises 4DP PTC's excellent shape fixity capabilities for post-manufacture shaping, sizing, and pleating in contrast with existing studies that commonly exploit 4DP material's shape recovery for eye-catching novelty. However, as these prototypes are intended for real-world use, user-centred research methodologies can be used to provide feedback that can enhance the design ergonomics. In addition, though the 4DP PTC specimens are much larger than most 4DP materials, the maximum size remains at 250 mm x 210 mm. Larger sized printers should be sourced to widen 4DP PTC's potential applications into other fields i.e., architecture and robotics or alternative methods of joining 4DP PTCs together must be developed.

7.2.2 Future work

In this study, 4DP PTC materials using extrusion processes and multi-material printing have demonstrated the potential to be used in a wide range of applications due to its high customisability, adaptability, and shapeability. There is potential to extend the scope of research into various 4D printing areas. Recommendations for further research works are outlined below.

1. As mentioned in the limitations, though the materials used in this study are representative of the types of materials that are readily available for 4DP PTC development. In future studies, practitioners could explore working with other types of SMMs i.e., hydrogels to develop 4DP PTCs using extrusion methods. Further studies may also wish to explore the feasibility of synthesising SMPs with different shore hardness for extrusion processes. Furthermore, there is also the potential to develop SMPs that have two-way or multiple-way shape memory capabilities for 4DP PTCs which will open more opportunities for 4DP materials to be used in robotics etc.

2. FDM/FFF printing is prevalently used in 4D printing fields due to its wide material compatibility and possibility to print on different materials. With advances made in extrusion technologies, further research can experiment with smaller nozzle sizes to enhance the resolution and quality of the printed surface. In addition, printing with alternative nozzle sizes can be used to fine-tune the mechanical property of 4DP materials. Practitioners can also use pellet-based extruders in place of filament extruding methods for 4D printing which are capable of higher output making it ideal for larger-scaled objects.

3. The shapes used in this study were selected due to their ability to fully tessellate. However, there are endless potentials to develop different types of patterns and structures using textile design principles. In future studies, practitioners may wish to experiment with different types of tessellations with different types of shapes, scales, and profile. Preliminary findings have already indicated pattern design to influence the performance of 4DP PTCs. Via further exploration of pattern design, practitioners can develop functional materials that combines aesthetics with functionality.

4. Further research can explore the development of 4DP products that integrates using user-centred research methodologies i.e., card sorting, interviews and questionnaires, usability testing, and A/B testing to provide feedback that can enhance the design. By involving end-users into the research and design process, we can procure data that can enhance the usability of products and respond effectively to user requirements. Machine learning can be used to analyse this big data and can efficiently structure and classify usable information that helps improve the design. Via introducing automated processes into the design framework we can streamline 4D printing design and manufacturing processes.

APPENDIX

Chapter 4

Surface roughness and coefficient of friction of textiles in (warp/weft) direction

ID	Test 1		Test 2		Test 3		Average	
	MIU (μ)	SMD (μm)	MIU (μ)	SMD (μm)	MIU (μ)	SMD (μm)	MIU (μ)	SMD (μm)
T1	0.41/0.42	1.04/5.47	0.39/0.41	1.02/5.58	0.37/0.41	1.09/5.54	0.39/0.41	1.05/5.53
T2	0.19/0.15	7.66/11.50	0.18/0.14	7.73/11.50	0.19/0.15	7.98/11.72	0.18/0.15	7.79/11.57
T3	0.25/0.18	3.24/3.84	0.24/0.17	3.23/3.00	0.24/0.15	2.82/3.79	0.24/0.17	3.10/3.54
T4	0.31/0.20	1.91/1.44	0.27/0.20	1.99/1.49	0.24/0.19	2.12/1.59	0.27/0.20	2.01/1.51
T5	0.23/0.16	2.11/8.03	0.22/0.16	2.00/7.98	0.22/0.15	1.98/9.23	0.22/0.16	2.03/8.41
T6	0.30/0.19	1.78/1.71	0.30/0.18	2.23/1.65	0.31/0.18	1.99/1.70	0.30/0.18	2.00/0.17
T7	0.27/0.24	0.74/1.95	0.25/0.24	0.69/1.90	0.24/0.24	0.74/1.84	0.25/0.24	0.72/1.90

MIU – mean coefficient of friction; SMD – surface roughness deviation

Surface friction and roughness results (warp/weft directions)

Sample	Test 1		Test 2		Test 3		Average	
	MIU (μ)	SMD (μm)	MIU (μ)	SMD (μm)	MIU (μ)	SMD (μm)	MIU (μ)	SMD (μm)
220-TPU 70A (warp/weft	0.75/0.78	1.44/1.43	0.85/0.95	1.40/1.50	0.99/0.96	1.44/1.40	0.86/0.90	1.43/1.44
240-TPU 70A (warp/weft	0.91/0.71	1.14/1.23	1.00/0.99	1.30/1.31	0.96/1.02	1.30/1.48	0.96/0.91	1.25/1.34
220-TPU 82A (warp/weft)	0.40/0.52	1.67/1.83	0.41/0.51	1.67/1.66	0.43/0.52	1.55/1.84	0.41/0.52	1.63/1.78
240-TPU 82A (warp/weft)	0.45/0.48	1.62/2.34	0.44/0.48	1.14/1.23	0.49/0.55	1.32/1.40	0.46/0.50	1.36/1.66
250-TPU 82A (warp/weft)	0.44/0.46	3.64/1.40	0.45/0.56	4.52/2.76	0.48/0.50	2.20/5.99	0.46/0.51	3.45/3.38
260-TPU 82A (warp/weft)	0.40/0.47	3.23/4.10	0.25/0.49	4.16/5.36	0.24/0.44	4.17/3.59	0.30/0.47	3.85/4.35
220-TPE 40D (warp/weft)	0.32/0.31	2.26/1.87	0.41/0.33	2.29/2.22	0.41/0.36	2.42/2.23	0.38/0.33	2.30/2.11
240-TPE 40D (warp/weft)	0.40/0.47	3.00/4.23	0.46/0.44	4.58/2.94	0.48/0.46	3.38/2.95	0.45/0.46	3.70/3.37
250-TPE 40D (warp/weft)	0.44/0.50	2.40/2.69	0.49/0.55	3.25/2.44	0.50/0.48	2.60/3.04	0.48/0.51	2.80/2.72
260-TPE 40D (warp/weft)	0.48/0.53	2.23/2.00	0.53/0.50	1.90/1.88	0.47/0.47	1.78/2.79	0.49/0.50	2.00/2.22
SMP (warp/weft)	0.14/0.15	1.41/1.69	0.14/0.15	1.19/1.69	0.14/0.15	1.59/1.23	0.14/1.40	0.15/1.54

MIU – mean coefficient of friction; SMD – surface roughness deviation

Chapter 5

Bursting strength results

Sample	Extrusion temperature	kpa				Height at burst (mm)				Time at burst (s)			
		Test 1	Test 2	Test 3	Mean	Test 1	Test 2	Test 3	Mean	Test 1	Test 2	Test 3	Mean
F1-SMP 4DP PTC	210°C	797.723	765.318	692.233	753.091	23.60	24.20	23.10	23.63	25	25	20	23.33
	220°C	676.376	741.186	743.255	720.272	17.70	17.40	17.60	17.60	22	25	25	24.00
	230°C	519.175	489.528	601.223	536.642	12.50	9.70	13.70	11.97	22	23	25	23.33
	240°C	598.465	610.876	564.681	591.341	17.70	18.00	19.00	18.23	19	20	17	18.67
	250°C	606.739	546.754	586.744	580.079	13.40	15.80	14.70	14.60	16	13	16	15.00
F2-SMP 4DP PTC	210°C	686.718	682.581	634.318	667.872	22.10	23.20	21.40	22.20	25	25	18	22.67
	220°C	716.365	744.634	764.629	741.876	17.50	19.00	18.70	18.40	24	25	25	24.67
	230°C	637.765	579.16	592.949	603.291	20.00	19.90	16.50	18.80	19	17	17	17.67
	240°C	654.313	743.944	601.223	666.493	17.60	17.50	18.60	17.90	21	25	19	21.67
	250°C	573.991	602.602	561.923	579.505	15.30	18.10	16.40	16.60	14	16	15	14.93
F3-SMP 4DP PTC	210°C	499.872	603.298	556.661	553.277	10.89	12.55	17.21	13.55	20	21	23	21.33
	220°C	480.225	511.337	546.091	512.551	15.00	11.22	10.90	12.37	18	23	28	23.00
	230°C	615.225	558.117	560.085	577.809	11.17	17.89	19.27	16.11	17	15	19	17.00
	240°C	463.152	500.939	510.766	491.609	14.31	18.53	11.68	14.84	20	17	19	18.67
	250°C	473.281	561.598	501.097	511.992	13.08	17.55	15.24	15.29	15	14	15	14.67

Note: - (s) = seconds; (mm) = millimetres; (kpa) = kilopascal

REFERENCES

Abbasi-Shirsavar, M., Baghani, M., Taghavimehr, M., Golzar, M., Nikzad, M., Ansari, M., & George, D. (2019). An experimental–numerical study on shape memory behavior of PU/PCL/ZnO ternary blend. *Journal of Intelligent Material Systems and Structures*, *30*(1), 116-126.

Accu. (2023). *Strength, Rigidity & Hardness - What's the difference?* Retrieved 4 October from https://www.accu.co.uk/p/111-strength-rigidity-hardness-difference

Agbakoba, V. C., Hlangothi, P., Andrew, J., & John, M. J. (2022). Mechanical and Shape Memory Properties of 3D-Printed Cellulose Nanocrystal (CNC)-Reinforced Polylactic Acid Bionanocomposites for Potential 4D Applications. *Sustainability*, *14*(19), 12759.

Agkathidis, A., Berdos, Y., & Brown, A. (2019). Active membranes: 3D printing of elastic fibre patterns on pre-stretched textiles. *International Journal of Architectural Computing*, *17*(1), 74-87.

Agkathidis, A., & Varinlioglu, G. (2022). 4D Printing on Textiles: developing a file to fabrication framework for self-forming, composite wearables. In *Advances in Product Design Engineering* (pp. 61-81). Springer.

Akiyama, M. M., Brewer, W. F., & Shoben, E. J. (1979). The yes—no question answering system and statement verification. *Journal of Verbal Learning and Verbal Behavior*, *18*(3), 365-380.

Al-Dhaheri, M., Khan, K., Umer, R., Van Liempt, F., & Cantwell, W. (2020). Process-induced deformation in U-shaped honeycomb aerospace composite structures. *Composite Structures*, *248*, 112503.

Alshebly, Y. S., Mustapha, K. B., Zolfagharian, A., Bodaghi, M., Mohamed Ali, M. S., Almurib, H. A., & Nafea, M. (2022). Bioinspired pattern-driven single-material 4D printing for self-morphing actuators. *Sustainability*, *14*(16), 10141.

Ayachit, S., & Thakur, M. (2017). Functional Clothing for The Diferently Abled. *Indian Journal of Public Health*, *8*(4), 905.

Ballast, D. K. (2002). *Interior design reference manual*. Professional Publications Incorporated.

Banerjee, P. K. (2014). *Principles of fabric formation*. CRC press.

Behl, M., & Lendlein, A. (2007). Shape-memory polymers. *Materials today*, *10*(4), 20-28.

Bertaux, E., Lewandowski, M., & Derler, S. (2007). Relationship between friction and tactile properties for woven and knitted fabrics. *Textile Research Journal*, *77*(6), 387-396.

Berzowska, J., & Coelho, M. (2005). Kukkia and vilkas: Kinetic electronic garments. Ninth IEEE International Symposium on Wearable Computers (ISWC'05),

BIMcontent. (2023). *Screen Acoustic AutexAU Cascade Folding F3*. Retrieved 25 Dec from https://bimcontent.com/download/screen-acoustic-autexau-cascade-folding-f3/

Biswas, M. C., Chakraborty, S., Bhattacharjee, A., & Mohammed, Z. (2021). 4D printing of shape memory materials for textiles: Mechanism, mathematical modeling, and challenges. *Advanced Functional Materials*, *31*(19), 2100257.

Boon, S. (2019). *Self-folding Fabric*. Retrieved 25 December from https://www.samiraboon.com/archi-folds

Boots, B., Okabe, A., & Sugihara, K. (1999). Spatial tessellations. *Geographical information systems*, *1*, 503-526.

Brandt, M., Sun, S. J., Leary, M., Feih, S., Elambasseril, J., & Liu, Q. C. (2013). High-value SLM aerospace components: from design to manufacture. *Advanced Materials Research*, *633*, 135-147.

BritishPlasticsFederation. (n.d.). *Shape Memory Polymer - A Complete Guide*. BPF. Retrieved 1 August from https://www.bpf.co.uk/plastipedia/applications/shape-memory-polymer.aspx

Büsken, D. (2021). *The Asaro Head: How To Master The Planes Of The Head*. https://bueskenart.com/asaro-head/

Capdevila, F., Carrera-Gallissà, E., Escusa, M., & Rotela, M. (2020). Canonical analysis of the Kawabata and sliding fabric friction measurement methods. *The Journal of The Textile Institute*, *111*(6), 890-896.

Chen, X. (2015). *Advances in 3D textiles*. Elsevier.

Cheung, T. C., & Choi, S. Y. (2022). Evaluation of the influence of three-dimensional printing conditions on peel resistance and surface roughness of flexible polymer-textile composites. *Textiles Research Journal*. https://doi.org/10.1177/00405175221133841

Cheung, T. C., Choi, S. Y., & Jiang, S. (2024). Influence of Thermoplastic Polyurethane and Elastomer Polymers on Self-folding Behaviour of 4D-printed Polymer-textile Composites. *Additive Manufacturing*, *79*, 103909. https://doi.org/https://doi.org/10.1016/j.addma.2023.103909

Chi, Y., Li, Y., Zhao, Y., Hong, Y., Tang, Y., & Yin, J. (2022). Bistable and multistable actuators for soft robots: Structures, materials, and functionalities. *Advanced Materials*, *34*(19), 2110384.

Choi, J., Kwon, O.-C., Jo, W., Lee, H. J., & Moon, M.-W. (2015). 4D printing technology: a review. *3D Printing and Additive Manufacturing*, *2*(4), 159-167.

Christopher, B. (2018). *The Elephants of Materials Science: SMAs Never Forget Their Shape*. COMSOL. Retrieved 1 August from https://www.comsol.com/blogs/the-elephants-of-materials-science-smas-never-forget-their-shape/

Correa, D., Menges, A., Menges, A., Sheil, B., & Glynn, R. (2017). Fused filament fabrication for multi-kinematic-state climate-responsive aperture. *Fabricate*, 190-195.

Craftech. (2013). The Ultimate Guide to Grades of Nylon. In. New York: Craftech Industries, Inc.

Da-Silva-Júnior, P. F., Serres, A. J. R., Freire, R. C. S., de Freitas Serres, G. K., Gurjão, E. C., de Carvalho, J. N., & Santana, E. E. C. (2018). Bio-inspired wearable antennas. *Wearable Technologies*, *219*.

de Bilbao, E., Soulat, D., Hivet, G., & Gasser, A. (2010). Experimental study of bending behaviour of reinforcements. *Experimental Mechanics*, *50*, 333-351.

Ding, Z., Yuan, C., Peng, X., Wang, T., Qi, H. J., & Dunn, M. L. (2017). Direct 4D printing via active composite materials. *Science advances*, *3*(4), e1602890.

Dragoni, E., & Ciace, V. A. (2021). Mechanical design and modelling of lightweight additively manufactured lattice structures evolved from regular three-dimensional tessellations. *Proceedings of the Institution of Mechanical Engineers, Part C: Journal of Mechanical Engineering Science*, *235*(10), 1759-1773.

Drobny, J. G. (2014). *Handbook of thermoplastic elastomers*. Elsevier.

El Khoury, C. (2017). Folding: A Parametric Model To Support The Creative Stage Of Architectural Project. *Architecture and Planning Journal (APJ)*, *23*(3), 7.

Ellinwood, J. G. (2021). *Fashion by design*. Fairchild Books.

Elsasser, V. H. (2010). Textiles: Concepts and principles.

FastRadius. (n.d.). *Why does 3D printing layer height matter?* Fast Radius. Retrieved 18 August from https://www.fastradius.com/resources/why-3d-printing-layer-height-matter/#:~:text=Key%20considerations%20for%203D%20printer%20layer%20height.-,When%20deciding%20your&text=When%20printing%20a%20part%20via,mm%20being%20the%20most%20common.

Fernandes, M. C., Aizenberg, J., Weaver, J. C., & Bertoldi, K. (2021). Mechanically robust lattices inspired by deep-sea glass sponges. *Nature materials*, *20*(2), 237-241.

Fields, G. (2018). *Self Forming Structures: An Exploration into 3D Printing on Pre-stretched Fabric*. Retrieved 25 September from https://n-e-r-v-o-u-s.com/blog/?p=8011

Filatech. (2022). *Filatech*. Retrieved 10 March from https://fila-tech.com/

Foo, E. W., Lee, J. W., Ozbek, S., Compton, C., & Holschuh, B. (2019). Iterative design and development of remotely-controllable, dynamic compression garment for novel haptic experiences. Proceedings of the 23rd International Symposium on Wearable Computers,

Funk, D., & Ndubisi, N. O. (2006). Colour and product choice: a study of gender roles. *Management research news*.

Gale, C., & Kaur, J. (2004). *Fashion and Textiles: An Overview*. Berg Publishers. https://books.google.com.hk/books?id=y5-FKtWbta0C

Gandhi, M. V., & Thompson, B. (1992). *Smart materials and structures*. Springer Science & Business Media.

Ganilova, O. A., & Low, J. J. (2018). Application of smart honeycomb structures for automotive passive safety. *Proceedings of the Institution of Mechanical Engineers, Part D: Journal of Automobile Engineering*, *232*(6), 797-811.

Gardiner, M., Aigner, R., Ogawa, H., & Hanlon, R. (2018). Fold mapping: parametric design of origami surfaces with periodic tessellations. *Origami*, *7*, 105-118.

Ge, Q., Sakhaei, A. H., Lee, H., Dunn, C. K., Fang, N. X., & Dunn, M. L. (2016). Multimaterial 4D printing with tailorable shape memory polymers. *Scientific reports*, *6*(1), 1-11.

Goehrke, S. (2015). *"It's Love" 4D Printed Lamp from DC for Life*. Retrieved 15 Dec from https://3dprint.com/63399/its-love-4d-printed-lamp/

Gök, M. O., Bilir, M. Z., & Gürcüm, B. H. (2015). Shape-memory applications in textile design. *Procedia-Social and Behavioral Sciences*, *195*, 2160-2169.

Gokarneshan, N., & Alagirusamy, R. (2009). Weaving of 3D fabrics: A critical appreciation of the developments. *Textile Progress*, *41*(1), 1-58.

Goncu-Berk, G., Karacan, B., & Balkis, I. (2020). Embedding 3D Printed Filaments with Knitted Textiles: Investigation of Bonding Parameters. *Clothing and Textiles Research Journal*, *40(3)*, 171-186. https://doi.org/https://doi.org/10.1177/0887302X20982927

Gorlachova, M., & Mahltig, B. (2021). 3D-printing on textiles – an investigation on adhesion properties of the produced composite materials. *Journal of Polymer Research*, *28*, 207-216. https://doi.org/https://doi.org/10.1007/s10965-021-02567-1

Goss, D., Mistry, Y., Niverty, S., Noe, C., Santhanam, B., Ozturk, C., Penick, C. A., Lee, C., Chawla, N., & Grishin, A. (2020). Bioinspired honeycomb core design: An experimental study of the role of corner radius, coping and interface. *Biomimetics*, *5*(4), 59.

Grimmelsmann, N., Meissner, H., & Ehrmann, A. (2016). 3D printed auxetic forms on knitted fabrics for adjustable permeability and mechanical properties. IOP Conference Series: Materials Science and Engineering,

Groeger, D., Chong Loo, E., & Steimle, J. (2016). Hotflex: Post-print customization of 3d prints using embedded state change. Proceedings of the 2016 CHI Conference on Human Factors in Computing Systems,

Groovfold. (n.d.). *Miter Folding*. Retrieved 23 December from https://groovfold.com/Miterfolding.html

Guberan, C., Clopath, C., & Tibbits, S. (2016). *Active Shoes*. Retrieved 28 July from http://www.selfassemblylab.net/activeShoes.php.

Guberan, C., Clopath, C., & Tibbits, S. (n.d.). *Active Shoes*. Retrieved 28 July from http://www.selfassemblylab.net/activeShoes.php.

Heal, H. J. (2019). *TruBurst INTELLIGENT BURSTING STRENGTH TESTER*. Retrieved 2 April from https://vvc.eu/wp-content/uploads/2019/11/truburst.pdf

Hitachi. (2011). Hitachi Tabletop Microscope TM3000. In.

Hosmer, K. (2014). *Innovative Fashion Collection Designed with 3D Printing Technology*. https://mymodernmet.com/noa-raviv-3d-printing-fashion-hard-copy/

Hsiang Loh, G., Pei, E., Gonzalez-Gutierrez, J., & Monzón, M. (2020). An overview of material extrusion troubleshooting. *Applied Sciences*, *10*(14), 4776. https://doi.org/https://doi.org/10.3390/app10144776

Hu, J. (2007). *Shape memory polymers and textiles*. Elsevier.

Hu, J., & Lu, J. (2014). Smart polymers for textile applications. In *Smart polymers and their applications* (pp. 437-475). Elsevier.

Hu, J., Meng, H., Li, G., & Ibekwe, S. I. (2012). A review of stimuli-responsive polymers for smart textile applications. *Smart Materials and Structures*, *21*(5), 053001.

Imani, M., Donn, M., & Balador, Z. (2018). Bio-inspired materials: Contribution of biology to energy efficiency of buildings. In (pp. 1-24): Springer International Publishing: Cham.

Instron. (1996). *Instron Series 4400 Testing Systems*. Instron Corporation.

ISO. (2008a). BS EN ISO 9073-18:2008 Textiles —Test methods for nonwovens — Part 18: Determination of breaking strength and elongation of nonwoven materials using the grab tensile test. In: BSI Britrrish Standard.

ISO. (2008b). *ISO 291:2008(en) Plastics — Standard atmospheres for conditioning and testing*. BSI Standards Limited.

ISO. (2010). *ISO 11339: 2010 Adhesives — T-peel test for flexible-to-flexible bonded assemblies*. Retrieved 25 March from https://www.iso.org/standard/52890.html

ISO. (2019). *ISO 13938-2:2019(en) Textiles — Bursting properties of fabrics — Part 2: Pneumatic method for determination of bursting strength and bursting distension*. ISO. Retrieved 6 November from https://www.iso.org/obp/ui/#iso:std:iso:13938:-2:ed-2:v1:en

ISO. (2022a). *ISO 10365:2022*. BSI Standards Limited 2022.

ISO. (2022b). *ISO 11339:2022 Adhesives — T-peel test for flexible-to-flexible bonded assemblies*. BSI Standards Limited.

Jackson, P. (2015). *Complete Pleats: Pleating Techniques for Fashion, Architecture, Design*. Laurence King Publishing.

Jose, S., George, J. J., Siengchin, S., & Parameswaranpillai, J. (2020). Introduction to shape-memory polymers, polymer blends and composites: State of the art, opportunities, new challenges and future outlook. *Shape Memory Polymers, Blends and Composites*, 1-19.

Kabir, S., Kim, H., & Lee, S. (2020a). Characterization of 3D printed auxetic sinusoidal patterns/nylon composite fabrics. *Fibers and Polymers*, *21*(6), 1372-1381. https://doi.org/https://doi.org/10.1007/s12221-020-9507-6

Kabir, S., Kim, H., & Lee, S. (2020b). Physical property of 3D-printed sinusoidal pattern using shape memory TPU filament. *Textile Research Journal*, *90*(21-22), 2399-2410.

Kadolph, S. J. (2012). *Textiles: basics*. Pearson Higher Ed.

Kapsali, V. (2015). Biomimetic approach to the design of textiles for sportswear applications. In *Textiles for Sportswear* (pp. 77-94). Elsevier.

Kars, I. (2021). *'Inaccessibility is a collective problem': the promise and limits of adaptive fashion*. The Guardian. Retrieved 24 September from

https://www.theguardian.com/fashion/2021/aug/20/inaccessibility-is-a-collective-problem-the-promise-and-limits-of-adaptive-fashion

KatoTech. (2023). *KES-FB2-A Pure Bending Tester*. Retrieved 12 August from https://english.keskato.co.jp/archives/products/kes-fb2-a

KatoTech. (n.d.-a). *KES-FB4-A surface tester*. Retrieved 15 May from https://english.keskato.co.jp/archives/products/kes-fb4-a

KatoTech. (n.d.-b). *KES-FB4-A surface tester*. Retrieved 15 May from https://english.keskato.co.jp/archives/products/kes-fb4-a

KatoTech. (n.d.-c). *SMP*. Retrieved 21 August from https://english.keskato.co.jp/

Kawabata, S., & Niwa, M. (1991). Objective measurement of fabric mechanical property and quality:: its application to textile and clothing manufacturing. *International Journal of Clothing Science and Technology*.

Khamkar, P. (2021). *4D Printing: Emerging Trends in Healthcare and Future Directions*. Retrieved 15 December from https://amchronicle.com/insights/4d-printing-emerging-trends-in-healthcare-and-future-directions/

Khoo, Z. X., Teoh, J. E. M., Liu, Y., Chua, C. K., Yang, S., An, J., Leong, K. F., & Yeong, W. Y. (2015). 3D printing of smart materials: A review on recent progresses in 4D printing. *Virtual and Physical Prototyping*, *10*(3), 103-122.

Koch, H. C., Schmelzeisen, D., & Gries, T. (2021). 4D textiles made by additive manufacturing on pre-stressed textiles—An overview. Actuators,

Kohli, R., & Krishnamurti, R. (1987). A heuristic approach to product design. *Management Science*, 1523-1533.

Kong, D., & Xiao, X. (2016). High cycle-life shape memory polymer at high temperature. *Scientific reports*, *6*(1), 1-10.

Korger, M., Glogowsky, A., Sanduloff, S., Steinem, C., Huysman, S., Horn, B., Ernst, M., & Rabe, M. (2020). Testing thermoplastic elastomers selected as flexible three-dimensional printing materials for functional garment and technical textile applications. *Journal of Engineered Fibers and Fabrics*, *15*, 1-10. https://doi.org/https://doi.org/10.1177/1558925020924599

Kozior, T., Döpke, C., Grimmelsmann, N., Juhász Junger, I., & Ehrmann, A. (2018). Influence of fabric pretreatment on adhesion of three-dimensional printed material on textile substrates. *Advances in Mechanical Engineering*, *10(8)*, 1-8. https://doi.org/https://doi.org/10.1177/1687814018792316

Kuang, X., Chen, K., Dunn, C. K., Wu, J., Li, V. C., & Qi, H. J. (2018). 3D printing of highly stretchable, shape-memory, and self-healing elastomer toward novel 4D printing. *ACS applied materials & interfaces*, *10*(8), 7381-7388.

Kuang, X., Roach, D. J., Wu, J., Hamel, C. M., Ding, Z., Wang, T., Dunn, M. L., & Qi, H. J. (2019). Advances in 4D printing: materials and applications. *Advanced Functional Materials*, *29*(2), 1805290.

Kycia, A. (2022). *Self-shaping Textiles: Form-finding of Tensile Surface Structures Through 3D Printing on Pre-stressed Fabric* Technische Universität Berlin].

LaBat, K. L., & Sokolowski, S. L. (1999). A three-stage design process applied to an industry-university textile product design project. *Clothing and Textiles Research Journal*, *17*(1), 11-20.

LabCompanion. (2023). *OV4-30 Vacuum Oven*. Retrieved 25 September from https://labcompanionshop.com/product/ov4-30-vacuum-oven

Lagoudas, D. C. (2008). *Shape memory alloys: modeling and engineering applications*. Springer.

Leaden, C. (2023). *You Can Step Inside The World's Largest Kaleidoscope In Upstate NY*. Retrieved 17 January from https://secretnyc.co/worlds-largest-kaleidoscope-ny/

Leenders, M. (2011). *Shape memory textiles*. Retrieved 2 August from https://marielleleenders.nl/work/shapememorytextiles/

Lendlein, A., & Gould, O. E. (2019). Reprogrammable recovery and actuation behaviour of shape-memory polymers. *Nature Reviews Materials*, *4*(2), 116-133.

Lerche, L. (2012). *Quantitative Methods*. Elsevier.

Lin, J., Zhou, J., & Koo, H. (2015). Enfold: clothing for people with cerebral palsy. Adjunct Proceedings of the 2015 ACM International Joint Conference on Pervasive and Ubiquitous Computing and Proceedings of the 2015 ACM International Symposium on Wearable Computers,

Lipson, H., & Kurman, M. (2013). *Fabricated: The new world of 3D printing*. John Wiley & Sons.

Liu, C., Qin, H., & Mather, P. (2007). Review of progress in shape-memory polymers. *Journal of materials chemistry*, *17*(16), 1543-1558.

Liu, Q., Wang, W., Reynolds, M. F., Cao, M. C., Miskin, M. Z., Arias, T. A., Muller, D. A., McEuen, P. L., & Cohen, I. (2021). Micrometer-sized electrically programmable shape-memory actuators for low-power microrobotics. *Science Robotics*, *6*(52), eabe6663.

Loh, G. H., Sotayo, A., & Pei, E. (2021). Development and testing of material extrusion additive manufactured polymer–textile composites. *Fashion and Textiles*, *8*(1), 1-21. https://doi.org/https://doi.org/10.1186/s40691-020-00232-7

Loh, H. H. (2021). *4D printing of shape-changing thermo-responsive textiles* Brunel University London].

Mahnke, F. H. (1996). Color, environment, and human response. *Detroit: Van Nostrand Reinhold*.

Mao, Y., Yu, K., Isakov, M. S., Wu, J., Dunn, M. L., & Jerry Qi, H. (2015). Sequential self-folding structures by 3D printed digital shape memory polymers. *Scientific reports*, *5*(1), 13616.

Markl, X. (2017). *A Technical Perspective The Flexure Revolution, Compliant Mechanisms applied to Watchmaking*. Retrieved 9 January from https://monochrome-watches.com/technical-perspective-flexure-revolution-compliant-mechanisms-applied-watchmaking/

Mather, P. T., Luo, X., & Rousseau, I. A. (2009). Shape memory polymer research. *Annual Review of Materials Research*, *39*(1), 445-471.

Matmatch. (n.d.). *What is the Coefficient of Friction?* Retrieved 28 Aug from https://matmatch.com/learn/property/coefficient-of-friction

Mayer, K. (2022). *3D Print on Textile*. Retrieved 5 May from https://www.karlmayer.com/html/textile-makerspace/applications_for_rapid_textile/

McIntyre, J. E. (2005). *Synthetic fibres: nylon, polyester, acrylic, polyolefin*. Taylor & Francis US.

McKnight. (2016). *Fashion label Threeasfour unveils two 3D-printed dresses for Biomimicry collection*. Dezeen. Retrieved 12 August from https://www.dezeen.com/2016/02/17/3d-printed-dresses-threeasfour-new-york-fashion-week-2016/

Miachalovic, M. (2022). *Thermoplastic Elastomers*. Polymer Science Learning Center. Retrieved 18 May from https://pslc.ws/macrog/exp/rubber/sepisode/tpe.htm

Microsystems, L. (n.d.). *Leica Application Suite* In (Version Version 4) https://www.leica-microsystems.com/products/microscope-software/p/leica-application-suite/

Mondal, I. H. (2021). *Fundamentals of Natural Fibres and Textiles*. Woodhead Publishing.

Mpofu, N. S., Mwasiagi, J. I., Nkiwane, L. C., & Njuguna, D. (2019). Use of regression to study the effect of fabric parameters on the adhesion of 3D printed PLA polymer onto

woven fabrics. *Fashion and Textiles*, *6*(1), 1-12.
https://doi.org/https://doi.org/10.1186/s40691-019-0180-6

Mu, T., Liu, L., Lan, X., Liu, Y., & Leng, J. (2018). Shape memory polymers for composites. *Composites Science and Technology*, *160*, 169-198.

Naficy, S., Gately, R., Gorkin III, R., Xin, H., & Spinks, G. M. (2017). 4D printing of reversible shape morphing hydrogel structures. *Macromolecular Materials and Engineering*, *302*(1), 1600212.

Nam, S., & Pei, E. (2020). The influence of shape changing behaviors from 4D printing through material extrusion print patterns and infill densities. *Materials*, *13*(17), 3754.

NervousSystem. (2013). *Kinematics*. Retrieved 25 September from https://n-e-r-v-o-u-s.com/projects/sets/kinematics/

Neuß, J., Kreuziger, M., Grimmelsmann, N., Korger, M., & Ehrmann, A. (2016). Interaction between 3D deformation of textile fabrics and imprinted lamellae. Proceedings of Aachen-Dresden-Denkendorf International Textile Conference,

Ngo, T. D., Kashani, A., Imbalzano, G., Nguyen, K. T., & Hui, D. (2018). Additive manufacturing (3D printing): A review of materials, methods, applications and challenges. *Composites Part B: Engineering*, *143*, 172-196.
https://doi.org/https://doi.org/10.1016/j.compositesb.2018.02.012

NinjaTek. (2022). *NinjaFlex*. Retrieved 30 March from www.ninjatek.com

Nishikawa, M., Wakatsuki, K., Yoshimura, A., & Takeda, N. (2012). Effect of fiber arrangement on shape fixity and shape recovery in thermally activated shape memory polymer-based composites. *Composites Part A: Applied Science and Manufacturing*, *43*(1), 165-173.

Otsuka, K., & Ren, X. (1999). Recent developments in the research of shape memory alloys. *Intermetallics*, *7*(5), 511-528.

Pal, T., Pramanik, S., Verma, K. D., Naqvi, S. Z., Manna, P., & Kar, K. K. (2022). Fly ash-reinforced polypropylene composites. *Handbook of Fly Ash*, *9*, 243-270.

Paul, R. (2019). *High performance technical textiles*. John Wiley & Sons.

Pei, E., Shen, J., & Watling, J. (2015). Direct 3D printing of polymers onto textiles: experimental studies and applications. *Rapid Prototyping Journal*, *21(5)*, 556-571.
https://doi.org/https://doi.org/10.1108/RPJ-09-2014-0126

Persson, N. K., Martinez, J. G., Zhong, Y., Maziz, A., & Jager, E. W. (2018). Actuating textiles: next generation of smart textiles. *Advanced materials technologies*, *3*(10), 1700397.

Pramadhiya, A. (2019). *Mixing 2D & 3D in Concept Art Article Review*. Retrieved 4 February from https://medium.com/@alvinpramadya/mixing-2d-3d-in-concept-art-article-review-56bfc3e92170

Prusa3d. (2022). *Layer height*. Prusa3d. Retrieved 30 August from https://help.prusa3d.com/article/layers-and-perimeters_1748

Prusa, J. (2021a). *3D printing handbook. User manual for 3D printers: Original Prusa i3 MK3+*. Prusa3D.

Prusa, J. (2021b). *First Layer Calibration (i3)*. Prusa Research. Retrieved 28 August from https://help.prusa3d.com/article/first-layer-calibration_112364

Rahman, O., & Gong, M. (2016). Sustainable practices and transformable fashion design– Chinese professional and consumer perspectives. *International Journal of Fashion Design, Technology and Education*, *9*(3), 233-247.

Recreus. (2021). *Direct extrusion vs. bowden type*. Recreus. Retrieved 21 March from https://recreus.com/gb/noticias/learn-with-recreus/direct-extrusion-vs-bowden-type

Recreus. (2022a). *Filaflex*. Recreus. Retrieved 10 March from https://recreus.com/gb/

Recreus. (2022b). *Filaflex 70A*. Retrieved 14 October from https://recreus.com/gb/filaments/6-filaflex-70a.html

Rhinoceros. (2024). https://www.rhino3d.com

Rivera, M. L., Moukperian, M., Ashbrook, D., Mankoff, J., & Hudson, S. E. (2017). Stretching the bounds of 3D printing with embedded textiles. Proceedings of the 2017 CHI conference on human factors in computing systems,

Roueche, J., & Shirley, L. (2012). *Elements and Principles of Design*. https://digitalcommons.usu.edu/cgi/viewcontent.cgi?article=2503&context=extension_curall

Russell, A. (2021). *The Fundamentals of Printed Textile Design*. Bloomsbury Academic. https://books.google.com.hk/books?id=-f1aEAAAQBAJ

Sakagami, K., Okuzono, T., Suzuki, H., Koyanagi, N., & Toyoda, M. (2020). Application of paper folding technique to three-dimensional space sound absorber with permeable membrane: case studies of trial productions. *Int J Acoust Vib*, *25*(2), 243-247.

Sanatgar, R. H., Campagne, C., & Nierstrasz, V. (2017). Investigation of the adhesion properties of direct 3D printing of polymers and nanocomposites on textiles: Effect of FDM printing process parameters. *Applied Surface Science*, *403*, 551-563. https://doi.org/https://doi.org/10.1016/j.apsusc.2017.01.112

Satami. (n.d.). *Memory wire*. Retrieved 3 August from https://satami.com.hk/memory-wire-video/

Schmelzeisen, D., Koch, H., Pastore, C., & Gries, T. (2018). 4D textiles: hybrid textile structures that can change structural form with time by 3D printing. In *Narrow and Smart Textiles* (pp. 189-201). Springer.

Schollenberger, C. S. (2000). Thermoplastic polyurethane elastomers. In *Handbook of elastomers* (pp. 405-434). CRC Press.

Schwarz, I., & Kovačević, S. (2017). Textile application: from need to imagination. In *Textiles for advanced applications*. IntechOpen.

Seymour, S. (2019). Functional aesthetics. In *Functional Aesthetics*. Ambra Verlag.

Shaqour, B., Abuabiah, M., Abdel-Fattah, S., Juaidi, A., Abdallah, R., Abuzaina, W., Qarout, M., Verleije, B., & Cos, P. (2021). Gaining a better understanding of the extrusion process in fused filament fabrication 3D printing: A review. *The International Journal of Advanced Manufacturing Technology*, *114*(5), 1279-1291. https://doi.org/https://doi.org/10.1007/s00170-021-06918-6

Shin, D.-G., Kim, T.-H., & Kim, D.-E. (2017). Review of 4D printing materials and their properties. *International Journal of Precision Engineering and Manufacturing-Green Technology*, *4*(3), 349-357.

Sinclair, R. (2014). *Textiles and fashion: materials, design and technology*. Elsevier.

Sitotaw, D. B., Ahrendt, D., Kyosev, Y., & Kabish, A. K. (2020). Additive manufacturing and textiles—state-of-the-art. *Applied Sciences*, *10*(15), 5033.

SMP. (2023). INTELLIGENT MATERIAL. In S. T. Inc. (Ed.).

Spahiu, T., Canaj, E., & Shehi, E. (2020). 3D printing for clothing production. *Journal of Engineered Fibers and Fabrics*, *15*, 1-8. https://doi.org/https://doi.org/10.1177/1558925020948216

Spahiu, T., Grimmelsmann, N., Ehrmann, A., Piperi, E., & Shehi, E. (2017). Effect of 3D printing on textile fabric. *Engineering and Entrepreneurship*, *1*(1), 1-7.

Spencer, D. J. (2001). *Knitting technology: a comprehensive handbook and practical guide* (Vol. 16). CRC press.

Staszczak, M., Nabavian Kalat, M., Golasiński, K. M., Urbański, L., Takeda, K., Matsui, R., & Pieczyska, E. A. (2022). Characterization of Polyurethane Shape Memory Polymer and Determination of Shape Fixity and Shape Recovery in Subsequent Thermomechanical Cycles. *Polymers*, *14*(21), 4775.

Störmer, J., Görmer, D., & Ehrmann, A. (2021). Influence of washing on the adhesion between 3D-printed TPU and woven fabrics. *Communications in Development and Assembling of Textile Products*, *2*(1), 34-39. https://doi.org/https://doi.org/10.25367/cdatp.2021.2.p34-39

Strzelec, K., Sienkiewicz, N., & Szmechtyk, T. (2020). Classification of shape-memory polymers, polymer blends, and composites. In *Shape Memory Polymers, Blends and Composites* (pp. 21-52). Springer.

Sun, J., Liu, Y., & Leng, J. (2015). Mechanical properties of shape memory polymer composites enhanced by elastic fibers and their application in variable stiffness morphing skins. *Journal of Intelligent Material Systems and Structures*, *26*(15), 2020-2027.

Sydney Gladman, A., Matsumoto, E. A., Nuzzo, R. G., Mahadevan, L., & Lewis, J. A. (2016). Biomimetic 4D printing. *Nature materials*, *15*(4), 413-418.

Tadaki, T., Otsuka, K., & Shimizu, K. (1988). Shape memory alloys. *Annual Review of Materials Science*, *18*(1), 25-45.

Tadesse, M. G., Dumitrescu, D., Loghin, C., Chen, Y., Wang, L., & Nierstrasz, V. (2018). 3D printing of NinjaFlex filament onto PEDOT: PSS-coated textile fabrics for electroluminescence applications. *Journal of Electronic Materials*, *47*(3), 2082-2092. https://doi.org/https://doi.org/10.1007/s11664-017-6015-6

Tanaka, H., Mizuki, M., & Keisuke, S. (2020). From 4D-Printing to Contextual 4D-Design. 4D Printing & Meta Materials Conference,

Thakur, S. (2017). Shape memory polymers for smart textile applications. *Textiles for advanced applications*, 323-336.

Tibbits, S. (2014). 4D printing: multi-material shape change. *Architectural Design*, *84*(1), 116-121.

Tibbits, S., McKnelly, C., Olguin, C., Dikovsky, D., & Hirsch, S. (2014). 4D printing and universal transformation.

TIME. (2006). *Best inventions of 2006*. TIME magazine. Retrieved 3 August from http://content.time.com/time/specials/packages/article/0,28804,1939342_1939424_1939705,00.html

Tobushi, H., Hashimoto, T., Ito, N., Hayashi, S., & Yamada, E. (1998). Shape fixity and shape recovery in a film of shape memory polymer of polyurethane series. *Journal of Intelligent Material Systems and Structures*, *9*(2), 127-136.

Tobushi, H., Hayashi, S., & Kojima, S. (1992). Mechanical properties of shape memory polymer of polyurethane series: basic characteristics of stress-strain-temperature relationship. *JSME international journal. Ser. 1, Solid mechanics, strength of materials*, *35*(3), 296-302.

Ulerich, O., Cananau, S., Prisecaru, D. A., Mărgăritescu, M., & Negrea, C.-S. (2023). Design of Customized Shoe Soles Using Lattice Structures Fabricated by Additive Manufacturing. International Conference on Intelligent Systems in Production Engineering and Maintenance,

Uysal, R., & Stubbs, J. B. (2019). A New Method of Printing Multi-Material Textiles by Fused Deposition Modelling (FDM). *Tekstilec*, *62*(4). https://doi.org/https://doi.org/10.14502/Tekstilec2019.62.248-257

Venkatraman, P. (2015). Fabric properties and their characteristics. *Materials and technology for sportswear and performance apparel*, 53-86.

Vivanco, T., Valencia, A., & Yuan, P. F. (2020). 4D printing: Computational Mechanical Design of Bi-dimensional 3D Printed Patterns over Tensioned Textiles for Low-energy Three-dimensional Volumes.

Wagner, M., Chen, T., & Shea, K. (2017). Large shape transforming 4D auxetic structures. *3D Printing and Additive Manufacturing*, *4*(3), 133-142.

Wang, Y., & Li, X. (2021). 4D printing reversible actuator with strain self-sensing function via structural design. *Composites Part B: Engineering*, *211*, 108644.

Wang, Z. (2019). Recent advances in novel metallic honeycomb structure. *Composites Part B: Engineering*, *166*, 731-741.

Watkin, H. (2016). *3D Printed Patterned Landscapes of Cyprus*. Retrieved 9 January from https://all3dp.com/3d-printed-patterned-landscapes-cyprus/

WBLFabrics. (2022). Retrieved 30 March from https://www.whaleys-bradford.ltd.uk/

Weerasinghe, D., Perera, S., & Dissanayake, D. (2019). Application of biomimicry for sustainable functionalization of textiles: review of current status and prospectus. *Textile Research Journal*, *89*(19-20), 4282-4294.

Wexner, L. B. (1954). The degree to which colors (hues) are associated with mood-tones. *Journal of applied psychology*, *38*(6), 432.

WGSN. (2022). *Top Trends for 2023 & Beyond*. WGSN. Retrieved 8 December from https://www-wgsn-com.ezproxy.lb.polyu.edu.hk/fashion/article/6361cafe031be9c1d670d794

WilsonCollegeofTextiles. (n.d.). *Kawabata Evaluation System*. Retrieved 28 Aug from
https://textiles.ncsu.edu/tpacc/comfort-performance/kawabata-evaluation-system/

Wolfe, G. M. (2016). *Fashion!* (Vol. 7th edition). The Goodheart-Willcox Company, Inc.

Xie, T. (2011). Recent advances in polymer shape memory. *Polymer*, *52*(22), 4985-5000.

Xu, Y., Yang, S., Sun, W., Tan, L., Li, K., & Zhou, H. (2019). 3d virtual garment modeling
from rgb images. 2019 IEEE international symposium on mixed and augmented
reality (ISMAR),

Yamamura, S., & Iwase, E. (2021). Hybrid hinge structure with elastic hinge on self-folding
of 4D printing using a fused deposition modeling 3D printer. *Materials & Design*,
203, 109605.

Yao, L., Ou, J., Cheng, C.-Y., Steiner, H., Wang, W., Wang, G., & Ishii, H. (2015).
BioLogic: natto cells as nanoactuators for shape changing interfaces. Proceedings of
the 33rd Annual ACM Conference on Human Factors in Computing Systems,

Yao, L., Ou, J., Wang, G., Cheng, C.-Y., Wang, W., Steiner, H., & Ishii, H. (2015). bioPrint:
A liquid deposition printing system for natural actuators. *3D Printing and Additive
Manufacturing*, *2*(4), 168-179.

Yi, H. (2022). 4D-printed parametric façade in architecture: prototyping a self-shaping skin
using programmable two-way shape memory composite (TWSMC). *Engineering,
Construction and Architectural Management*, *29*(10), 4132-4152.

Zaytseva, T., Koroleva, L., & Slesarchuk, I. (2021). Inclusiveness in clothing design. IOP
Conference Series: Materials Science and Engineering,

Zhang, M., & Mak, A. (1999). In vivo friction properties of human skin. *Prosthetics and
orthotics International*, *23*(2), 135-141.

Zhao, Q., Qi, H. J., & Xie, T. (2015). Recent progress in shape memory polymer: New
behavior, enabling materials, and mechanistic understanding. *Progress in Polymer
Science*, *49*, 79-120.

Zolfagharian, A., Kaynak, A., & Kouzani, A. (2020). Closed-loop 4D-printed soft robots.
Materials & Design, *188*, 108411.